VIBRATIONS OF VISCOELASTICALLY DAMPED LAMINATED STRUCTURES

by

BAHADUR CHAND NAKRA

B.Sc.(Engg.), M.Tech

Thesis presented for the degree of
Doctor of Philosophy of the University of London
and Diploma of Imperial College

Department of Mechanical Engineering,
Imperial College of Science and Technology,
London,S.W.7.

August, 1966

ABSTRACT

The equations describing the flexural vibrations of a number of configurations of laminated beams, incorporating elastic and viscoelastic laminates, have been derived. Solutions for vibration response have been obtained for the laminated beams, subjected to harmonic excitations and damping action due to strains in viscoelastic layers in each system is evaluated. In general, the solutions are limited to beams with simply supported end conditions, though for the 3 layered configuration, the procedure is outlined for other end conditions also. The theory given for the 3 layered case is applicable to any unsymmetrical configuration, without limitation on the frequency range of application. Detailed analysis of this configuration includes determining the solutions for displacement and stress responses, studying the influence of various geometrical and physical parameters on vibration damping effectiveness of the system, behaviour at high frequencies and the effect of non-linearity due to amplitude dependence of viscoelastic material properties. Other configurations, with higher number of layers have been analysed, the viscoelastic layers being placed alternately or adjacently. The equations of each system have been programmed on the Atlas digital computer for computations based on the theoretical an lys .

The effect of important parameters has been investigated and the applicability of each configuration determined from point of view of increased damping and improved frequency response of the system.

Vibration response tests have been carried out on a few samples of laminated beams, in order to verify the results obtained theoretically. Experimental work has also been done to determine the dynamic properties in shear, of a few viscoelastic materials, including those used in making the laminated beams for vibration response tests.

ACKNOWLEDGEMENTS

The author is deeply grateful to his supervisor, Dr.P.Grootenhuis, for having suggested the problem and for his helpful advice and encouragement, at every stage of the work.

Thanks are also due to Mr.A.E.Turner of Imperial Chemical Industries, for having arranged to supply a number of samples of viscoelastic materials. The help of the College laboratory staff, in particular that of Mr. Ray Gunn, during experimental work is acknowledged with thanks and appreciation. The author is indebted to his several colleagues at the College, for stimulating discussions.

Finally, the author owes gratitude to the British Council and the Indian Institute of Technology, New Delhi for making all the necessary arrangements, including the award of a Fellowship for the present work.

CONTENTS

Terminology

t_i	=	Thickness of layer 'i'.
E_i	=	Young's modulus of layer 'i' (in-phase component for a viscoelastic layer)
E_{ii}	=	Quadrature component of Young's modulus for viscoelastic layer 'i'.
G_i	=	Shear modulus of layer 'i' (in-phase component for a viscoelastic layer).
G_{ii}	=	Quadrature component of shear modulus for viscoelastic layer 'i'.
L	=	Length of the beam.
b	=	Width of the beam.
ρ_i	=	Mass density of layer 'i' per unit volume.
ρ	=	Mass density of sandwich, per unit length.
n	=	Modal number.
p	=	Circular frequency, radians/second.
η_i	=	Material loss factor of layer 'i' in shear.
β_i	=	Material loss factor of layer 'i' in direct strain.
η_s	=	Sandwich loss factor or system loss factor.
t	=	Time variable.
x	=	Space variable in beam longitudinal direction.
z	=	Space variable in beam transverse direction.
'	=	Differentiation with respect to 'x'.
.	=	Differentiation with respect to 't'.

u = Longitudinal displacement.

u_i Longitudinal displacement in layer 'i'.

w = Transverse displacement.

w_i - Transverse displacement in layer 'i'.

ζ - Flexural angle.

$\bar{u}_i, \bar{\alpha}, \bar{\beta}$ and $\bar{\gamma}$ = Angles of rotation of the normal to a section, in different layers, as indicated in various configurations.

k_i = Shear coefficient of layer 'i'.

γ_i Shear strain in layer 'i'.

ν_i Poisson's ratio of layer 'i'.

E_i^* - $E_i/(1-\nu_i^2)$.

Z_i = $\nu_i E_i/(1-\nu_i^2)$.

$f(x)$ = Intensity of dynamic loading.

x_o - Amplitude of harmonic vibration of beam ends.

DRE Displacement response effectiveness.

SRE - Stress response effectiveness.

$\alpha_{j.p}$ E_j/E_p

$\theta_{j.p}$ - t_j/t_p

$\phi_{j.p}$ - $G_j / E_p t_p^2 (\frac{n\pi}{L})^2$ - Shear parameter.

$\gamma_{i.j}$ G_i/G_j

φ $\dfrac{G_2}{E_3(t_1\ t_3)^2(\frac{n\pi}{L})^2}$ = Shear parameter as used in section III.A.

S $\dfrac{G_2}{\Gamma_3 t_3\ \bar{L})^2}$ = Shear factor for minimizing peak displacement response.

Y $= \sqrt{\dfrac{\rho p^2}{(\frac{\pi}{L})^4 E_3 t_3^3}}$ Frequency factor for minimizing peak displacement response.

K = Generalized dynamic rigidity of sandwich.

K_R = Generalized dynamic rigidity of reference system.

k = K/K_R.

E_s and t_s = Young's modulus and thickness respectively, of the solid reference system.

Q_i = $\dfrac{G_i}{(\frac{n\pi}{L})^2}$

F_n = nth. mode frequency.

T^R = Ratio of amplitude of relative transverse motion (with respect to ends) of middle of the beam, to the motion of the ends.

T^A = Ratio of amplitude of absolute transverse motion of middle of the beam, to the motion of the ends.

W^R = Relative transverse motion (with respect to ends) of any point on the beam, at any instant.

W^A = Absolute transverse motion of any point on the beam, at any instant.

$W_o{}^A$ = Amplitude of motion W^A.

$W_o{}^R$ = Amplitude of motion W^R.

θ^R = Phase difference between W^R and beam end motion.

θ^A = Phase difference between W^A and beam end motion.

i) Remaining notations denoting various algebraic expressions, are given in individual Chapters.

ii) In a 3 layered sandwich beam, the middle layer has been referred to as the 'core and the outer layers as the 'faces.

CHAPTER I:

I.A. INTRODUCTION:

Conventional approach for controlling vibrations in mechanical systems has been to avoid resonance, due to coincidence of excitation frequency and any natural frequency of the system. This is usually achieved by changing the mass or stiffness of the system. Some other methods include use of tuned vibration absorber to change the natural frequency, reducing level of excitation at the source by proper balancing etc. These approaches are no longer of any practical use when vibration excitations occur over a wide frequency range, as in aircraft and missile practice, motor car etc. In addition, the trend towards light weight, high performance systems requires the obvious use of damping, to control resonant response, which might otherwise result in structural fatigue failure, equipment malfunctioning, noise radiation and discomfort.

The materials of the structures usually chosen from point of view of strength and rigidity are in practice not found to have appreciable internal damping. A bibliography of various techniques for damping is given in [1 - 3].* Apart from material damping, damping occurs

---

* Numbers enclosed in brackets [ ] are the numbers of references, given at the end.

in structures at contact surfaces due to interfacial slip [2] or it may be introduced at supports of beams and plates by using viscoelastic adhesive at the interfaces [4], the axial and rotational motion at the joint dissipating energy in the viscoelastic material. None of these methods gives high damping, which would be required in intense noise and vibration environments. However, the use of laminated structures, involving elastic and viscoelastic layers offers a useful promise. In these structures, the energy dissipation occurs in viscoelastic layers due to their shear and/or direct strains.

Laminated (or sandwich) structures incorporating viscoelastic layers are finding practical applications [5-8]. In [5] an instance is given regarding the use of laminated construction in design of a circular bulkhead for a missile and its mountings. Other examples include circuit boards and mounting platforms for electronic instruments. Commercially, damping tapes [6] are available for application on a solid structure, required to be damped. These are composed of a stiff metal foil and a thin layer of viscoelastic adhesive. Structural sections have also been damped by the use of viscoelastic layers [8]. The development of plastics for use as viscoelastic laminates is a useful step in this direction.

Vibration response analysis of structures, having any number of elastic and viscoelastic layers bonded together, is thus desirable. Since flexural vibrations of beams and plates result in large displacement and stress responses, it is necessary to carry out analysis under these conditions. Equations of motion and expressions for boundary conditions for various end conditions for multilayered configurations are required for resonant response and wave propagation studies. From the solution, it is desired to know the influence of various geometrical and physical parameters of the laminated structure, on damping effectiveness. In addition to dynamic considerations of high damping over a broad frequency range, static stiffness of the system also usually has an important influence, at design stage. Previous studies of a three layered unsymmetrical sandwich configuration have been limited in scope and application. Analysis of such a configuration, without restrictions on the relative properties of various layers and meant for general application at both low and high modes of vibrations in structures, has not been reported. It is also necessary to carry out analysis of other unsymmetrical sandwich configurations, with higher number of layers, the viscoelastic layers being placed alternately or adjacently.

The properties of viscoelastic materials are known to depend upon the frequency, temperature and strain amplitude. This causes complications not only in theoretical analysis but also in the choice of viscoelastic materials for a specific need. The stress-strain laws for viscoelastic materials are known from the theory of viscoelasticity. For a linear viscoelastic material, there are various methods of specifying the properties, namely by using complex modulus, creep function, stress relaxation function, differential operator form or representing the stress strain relations by a hypothetical model, composed of an array of springs and dashpots etc. All these forms can be related to one another [9-12]. For sinusoidal vibration conditions, the complex modulus is a useful way of expressing the dynamic properties of viscoelastic materials, e.g. complex modulus in shear may be expressed as

$$G = G_1 + i\, G_{11} = G_1(1 + i\eta_1)$$

where G_1 and G_{11} are the elastic (or inphase) and loss (or quadrature) parts respectively. $\eta_1 = G_{11}/G_1$ is the material loss factor. A similar terminology is used for corresponding modulus, under direct strain conditions. In practice, G_1 and G_{11} are dependent upon frequency, temperature and strain. For a given frequency and temperature, their appropriate values may be used in

linear theory. However, inclusion of strain effect in a system makes the problem a non-linear one.

I.B: LITERATURE SURVEY:

At first, a review of work done on the vibrations of sandwich structures, made up of elastic layers only will be given. Later, work on damped sandwich configurations will be reviewed.

Enough work has been reported on the static analysis (bending and buckling) of sandwich structures, review of which is available in [14-17]. Work on the dynamic analysis of such structures has been reported only recently. A complete survey may be found in [15].

Kimel et al [18] and Raville et al [19] have determined natural frequencies of vibrations of 3 layered sandwich beams with simply supported and fixed ends respectively and verified the theoretical results experimentally. The faces (i.e. outer layers) used are thin compared to the core (i.e. middle layer), which is assumed to take up shear only. Y-Yuan Yu [20,21] gave an accurate theory for 3 layered elastic symmetrical sandwich (both faces being similar). There is no restriction on the ratio of face to core parameters and all inertia terms are included. In [22], using above mentioned theory, natural frequencies of vibrations of infinite and simply supported plates are determined and in [24], it is indicated how forced flexural vibrations of sandwich plates may be analysed for time dependent

boundary conditions. In [23], the equations are reduced to simplified form, for cases involving thin faces and low frequencies. The theory is later [25] extended to take into account the geometrical non-linearity, i.e. for large displacements.

Frankland [26], in a discussion to work by Yi-Yuan Yu points out the need for high frequency analysis of sandwich structures. The thickness shear and stretch modes, which normally occur at very high frequencies for homogeneous plates, may occur at lower frequencies for sandwich plates and might cause coupling with simple forms of extensional and flexural vibrations. Bolotin [27] has derived equations for vibrations of elastic rigid and soft laminates arranged alternately, taking into account only the shear effect in soft laminates and bending in rigid laminates. Tangential inertia terms are neglected and free vibrations are analysed. Chang and Fang [28] and Bieniek and Freudenthal [29] have derived the equations of motion of a conventioanal 3 layered sandwich plate, with faces taken as thin compared to the core, in order to carry out frequency response analysis. In [28], the faces are taken as membranes only and not assumed to take bending and shearing. Various families of modes, including those which are predominantly of flexural or shear types are discussed.

In [29], it is indicated how material damping for various layers may be taken account of by using complex moduli, in place of elastic ones, taking the damping as frequency and amplitude independent.

The work on viscoelastic damping of structures appears to have started with the work of Oberst [30] and Lie'nard [31]. The configuration analysed is a 2-layered one, obtained by applying a layer of viscoelastic damping material to a metal plate. This is known as unconstrained or extensional damping treatment and the damping is due to direct strains induced in the viscoelastic layer, as the plate bends. Experimental work on this type of damping was also reported by Itterbeck and Myncke [32], who used a thin layer of bitumen emulsion containing Schist powder on steel plates and measured the damping in a temperature range of $-20^{o}C$ to $80^{o}C$. Further theoretical and experimental work by Oberst, Lie'nard and Mead [33] showed that damping depends upon the stiffness and loss factor of the viscoelastic material and its thickness. A review of this work is given in [2 and 59]. Schwarzl [34] pointed out that in an arbitrary 2 layered beam, flexural and extensional vibrations are coupled and analysed the forced vibrations of such a beam, both layers being viscoelastic and having different damping properties.

Work on the development of viscoelastic materials, to fulfil the requirements for high damping, has also been reported [35].

A 3 layered sandwich configuration, in which the middle layer i.e. the core is viscoelastic is known as constrained layer configuration. In this case, shearing motion is predominant in the core and is responsible for the damping action as the structure vibrates in bending. Plass [36] analysed such a configuration, in which both the faces were considered very thin (only membranes) and shear effect in the core was included. A stress strain law for linear viscoelastic material, corresponding to a 3 element model was used for the core, and decay of free vibrations of the structure was analysed.

Kerwin [37] analysed the damping of vibrations of a 3 layered configuration, with different faces, due to shear motion of the viscoelastic core. The results are applicable to cases where loss factor of the material of the core is small and bending stiffness of one of the faces is small with respect to that of the other face. Later, general analysis was given in [38,39,60], which includes both shear and extensional damping effect. Expressions for loss factor of the system are given and optimised with respect to various parameters [60].

Shear damping is shown to depend on the mode of vibration. The results are given for the case when extensional stiffness of core and that of one of the faces are less than the stiffness of the third layer. The loss factor of the system is taken as the ratio of imaginary to real part of complex stiffness of the system. The expression for complex stiffness is obtained by firstly regarding all layers as elastic, determining the neutral axis by elastic analysis and taking moments about the neutral axis. Later, the moduli of viscoelastic layers are changed to complex values. Actually, in an arbitrary 3 layered plate, involving viscoelastic laminates, there is no fixed fibre which remains unstrained at all instants, in a similar way to an arbitrary 2-layered configuration analysed by Schwarzl [34]. So, the dynamic analysis of any arbitrary 3 layered sandwich involves consideration of coupled extensional and bending vibrations. Such equations are not derived in [37-39,60] and no response studies are given.

The relation between natural frequency and wave number of vibration, assumed in [60] is valid only for a solid beam and not for a laminated beam. Although the error involved due to this may be small for taped structures, such a relation cannot be used for sandwich structures. Further, the analysis in [60] involves an

assumption regarding the stress strain relation for the middle layer in terms of longitudinal force at middle of one of the faces. This is valid only when extensional effect of the middle layer is neglected. However in [60], this stress strain relation is employed even when the extensional effect of core is included. In the above mentioned analysis, all layers are assumed to experience bending vibrations, with sinusoidal variation along length. The effect of boundary conditions is discussed later in [43], on the basis of energy dissipation near and away from boundaries. Experimental work has also been carried out on taped structures for determining system loss factor but the properties of viscoelastic materials used are not accurately known, as reported in [60] and thus a precise verification of the theory is lacking.

It has been shown in [39 and 44] that shear damping in a 3 layered constrained configuration is more effective and useful than the extensional damping in a 2-layered unconstrained case. However, unconstrained configuration is easier to achieve on an existing structure, analysis is simple and the damping achieved is not dependent on mode of vibration. But the viscoelastic material is exposed in the unconstrained case and the environmental effect due to humidity, chemicals etc. may be adverse. Also, to achieve high damping, it may be necessary to use very thick layers in practice in this case.

The damping in both constrained and unconstrained configurations may be increased by the use of a stiff spacer between the plate to be damped and viscoelastic layer, thus magnifying the shear motion of the latter [41,42]. The foregoing analysis of 3 layered case has also been extended to multiple damping tapes [40] and it was shown that use of multiple damping tapes on the same side of the plate to be damped, gives same damping as a single tape with viscoelastic material thickness same as in one of the tapes, but foil thickness equal to sum of those of individual single tapes. An alternate method of determining loss factors of composite structures is given in [45 and 46], by defining the loss factor in terms of energy concepts and the energy storage and dissipative mechanisms in the structure are taken in accordance with those in arrays of viscoleasitc springs.

Kurtze et al [53 and 54] have carried out analysis of propagation of transverse waves and the effect of damping in sandwich configuration. Whittier [47] analysed theoretically and experimentally the case of sinusoidal excitation of a sandwich cantilever, made up of a thin layer of viscoelastic layer, a spacer, the beam to be damped and a constraining cover, the object being the evaluation of damping derived. The inertia force terms are neglected, cover stiffness is assumed

much less than that of the beam to be damped and neutral axis of the composite structure is taken at the centre of the beam to be damped. Also, the equations are applicable only to a Cantilever. Yi-Yuan Yu [48] analysed free flextural vibrations of symmetrical sandwich plates, taking complex moduli for each layer in the equations derived by treating all layers as elastic, which was done earlier [20]. Log decrement was taken as the measure of damping, taking the moduli as frequency independent.

Mead [49] pointed out that flexural loss factor is not in itself a sufficient criterion for assessment of damping effectiveness of any system, since damping treatment changes the stiffness and the mass of the structure. Since the resonant response of displacement, acceleration, stresses etc. depends on stiffness and mass as well, separate criteria are required for assessing reductions of each of these responses. These are derived for single degree freedom system for harmonic and random displacement, velocity, acceleration, inertia force and bending stress responses [49]. It is seen from [50 and 61] that resonant response of a continuous system, in a normal mode, is damping controlled in the same way as a lumped parameter spring mass system. Thus, the various criteria given in [49] are applicable to sandwich configurations. These have been applied by Mead [51, 52] to a symmetrical

sandwich plate, with viscoelastic core. Equations of motion have been derived for the sandwich plate, subjected to harmonic excitation, taking account of direct stresses in faces, shear stresses in core and transverse inertia terms. The solution is obtained for simply supported plate. The various damping effectiveness criteria have been optimised and several design studies were reported. Experimental work was done on symmetrical sandwich beams, having thin and soft viscoelastic core, in order to determine dynamic stiffness and loss factor of the system for a few modes under harmonic excitation, for comparisons with theory. Some experiments were also done for random vibrations. Like the experimental work of Ross, Ungar and Kerwin [60], the dynamic properties of viscoelastic materials used were not determined in separate tests but were those supplied by the manufacturers.

Yildiza [57] has derived the equations for the two dimensional case of a 3 layered plate, which correspond to those of Kerwin [37] for one dimensional case. No solution or damping studies were given.

Experimental work on vibration damping of 3 layered sandwich structures has been done by Ruzicka [55] and Parfitt and Lambeth [56]. In the former investigation, no comparisons with any theoretical work were done, but in the latter, comparisons with the theoretical work of [60] were done and a lot of discrepancy was observed for

stiff damping layers.

Recently flexural vibrations of symmetrically arranged multi-layered cantilevers, with elastic and viscoelastic layers occurring alternately, have been analysed [59]. The solution for displacement response for harmonic excitation was obtained by solving equations of motion by finite differences and was verified experimentally by tests on 3 and 5 layered symmetrical cantilevers. The properties of viscoelastic materials used, were separately determined in shear test, taking into account the effect of frequency, temperature and strain. These effects were allowed for in the solution. Design study has also been reported on above mentioned configurations.

In a recent paper [58], a 3 layered beam with a soft core has been analysed taking into account the effect of shear in core and direct stresses in faces together with the transverse inertia terms of the sandwich. Complex modulus is employed for the viscoelastic core in the equations in order to study free vibrations i.e. to determine natural frequency of vibration corresponding to various modes and their decay, giving damping of the system. It is indicated that the relation between loss factor and natural frequency for a normal mode is independent of boundary conditions but is dependent on geometrical and physical properties of the layers. No formal solution appears in the paper but it is pointed

out that in order to evaluate damping, natural frequency may first be calculated on a digital computer. The results are expected to correspond to those of [60] for simply supported beams. Strictly speaking, it is not correct to use complex modulus for viscoelastic material for analysing free vibrations, since complex modulus can only be employed for sinusoidal excitation conditions and free vibrations are not expected to be sinusoidal in this case. The correct form of stress strain law to be used in such a case is the operator form for linear viscoelastic materials. However, the conclusions regrading dependence of loss factor as discussed in [58] should remain valid if studies are made under sinusoidal excitation conditions, using complex modulus for viscoelastic core and evaluating system damping loss factor at the resonant frequency corresponding to each mode, which would be excited if generalized dynamic loading for the mode is employed.

Some further examples on the erroneous use of complex modulus for free vibrations, which are not sinusoidal, have been pointed out in [62 - 64]. The theory of linear viscoelasticity is reasonably complete to find applications and several problems have been solved in viscoelastic continua mechanics. Review of these appear in [9, 64 - 68].

I.C· SCOPE AND OUTLINE OF PRESENT WORK

It may be seen from Literature Survey given in previous section that work on the vibration analysis of laminated structures, with viscoelastic damping has so far been restricted to a few types of configurations. Derivation and solution of equations governing flexural vibrations of an arbitrary 3 layered unsymmetrical beam with viscoelastic core, without any restrictions on the ratio of geometrical or physical parameters of the layers, do not appear to have been done. Detailed dynamic analysis of such a configuration, with a view to understanding the damping behaviour, is desirable. Also in most cases up till now, the equations of motion have been limited in application to low frequencies because of neglect of axial and rotational inertia terms. The effect of inclusion of these on the vibration analysis of above mentioned configuration is not known.

Shear damping in a constrained treatment has been found to be frequency dependent and is maximum only under certain optimum conditions. These optimum conditions change in practice due to excitations occurring over a wide frequency range resulting in excitation of different modes and also due to change of viscoelastic material properties with frequency and temperature. The use of increased number of layers suitably arranged,

using different damping materials is expected to increase damping over a wide frequency range. There is lack of work on vibrations of laminated structures, with increased number of layers. The various layers in a multilayered configuration may be arranged either by placing the elastic and viscoelastic layers to occur alternately or the viscoelastic layers may be placed adjacent to each other, being constrained by elastic layers. The latter type will be called a "multi-cored configuration". Vibration analysis of multi-layered configurations, with parameters of any layer different from those of any other layer in the arrangement, and the effect of various geometrical and physical parameters is desirable.

The properties of viscoelastic materials are known to be dependent on the strain amplitudes. The effect of this non-linearity on resonant response forlarge values of strains, may be of importance and has been included in very few cases, as cited in "Literature Survey".

Much of the experimental work done for verification of theoretical work tends to be uncertain because of lack of sufficiently accurate properties of viscoelastic materials, which are dependent on frequency, temperature and strain. It is necessary to take account of each of these effects in comparison of theoretical and experimental work of laminated structures.

With above points in mind, the present work was outlined, as given below. Chapter II deals with the derivation of equations of flexural vibrations of a three layered unsymmetrical beam, using energy principles. In analysis I given in section II.C, the outer faces are assumed to bend like Bernoulli-Euler beams, while in analysis II given in II.D, there is no such restriction. In both cases, shear and extensional effects of core and all inertia terms of the sandwich are included. Thus, the equations are applicable for high frequencies as well. The boundary conditions for various end conditions are stated in terms of assumed displacements. Series solutions for dynamic response are given for simply supported end conditions and use of approximate variational methods is discussed for cases involving other end conditions.

In Chapter III, effect of various geometrical and physical parameters of a three layered configuration with viscoelastic core, is determined on the system damping, displacement and stress response effectiveness of the system. In addition, static stiffness is also determined for three layered unsymmetrical configuration, with same total thickness but different face thickness ratios. Comparisons are made between results of analysis I and II and also with those obtained from results of other authors. Influence of core extensional terms is determined.

Solutions for vibration response are obtained, with both ends of simply supported sandwich beam subjected to sinusoidal motion of same amplitude and phase and resonance curves are plotted. Damping effectiveness and resonant response studies are correlated in order to determine the validity of the former studies. Effect of axial and rotational inertia terms on dynamic response is determined. Solution for an assumed non-linearity in stress strain law, due to amplitude dependence, is derived by approximate variational method.

Further multi-layered configurations analysed in Chapter IV are five and seven layered unsymmetrical laminated beams, with elastic and viscoelastic layers arranged alternately. Two types of multi-cored configurations are analysed in Chapter V. In each case, the equations of motion together with expressions for boundary conditions for various end conditions are obtained and solutions for dynamic response for beams with simply supported ends are given. Effect of important system parameters is studied in each case and applicability and usefulness of each configuration are indicated.

Experimental work reported in Chapter VI deals with measurement of dynamic properties, in shear, of a number of viscoelastic materials and vibration response tests on three layered unsymmetrical, five layer unsymmetrical

and four layered double cored configurations. The dynamic properties are measured for different frequencies, temperature and shear strain amplitudes. These are used in theoretical computation of displacement response of the layered configurations tested experimentally, for comparison of theoretical and experimental results. The vibration response tests on multi-layered beams were carried out by subjecting both ends of simply supported beams to sinusoidal displacement excitation of same amplitude and phase. At various frequencies, the displacement response and phase of various locations on the beams, were measured. Finally in Chapter VII, some general conclusions and points for further work are discussed.

CHAPTER II

3 LAYERED UNSYMMETRICAL BEAM -- EQUATIONS OF MOTION -- DERIVATION AND SOLUTION

II.A: Introduction to procedure employed

The equations of flexural vibrations of a 3 layered beam, all the layers having different properties and subjected to dynamic loading, with any distribution along the length, are derived. The differential equations of motion are derived from equilibrium considerations, treating all layers as elastic, the stress-strain law not involving any functions of the time variable (denoted as the elastic case). These differential equations may be used to obtain the governing equations for the laminated beam, involving viscoelastic layers by using the appropriate stress strain laws for the viscoelastic layers, these laws involving functions of the time variable (denoted as the viscoelastic case). Subsequently, a solution to these governing equations may be determined. For sinusoidal excitations, however, it is simpler to follow an alternative procedure for linear viscoelastic materials, based on the correspondence principle [9]. Due to this, the solution for viscoelastic case may be obtained from that for the corresponding elastic case, by replacing the appropriate moduli

of elasticity in the latter solution, by complex ones. This procedure is followed in the present Chapter. However for non-linear viscoelastic materials, the stress strain law is used during the formulation itself and the solution is determined later, as given in Chapter III.

Assumptions made for the derivation of equations of motion are discussed in section II.B. Two forms of assumptions are used separately in Analysis I and Analysis II which are given in sections II.C and II.D respectively, for the 3 layered unsymmetrical case. For the derivations, energy method (Hamilton's Principle) has been employed. The same equations could be derived by considering the equilibrium of forces and moments. However, the former method is preferred because of a number of reasons, notably

i) By minimization of energy integral, both differential equations of motion and boundary conditions are obtainable for the given formulation.

ii) It is easier to include or ignore effects like bending, shearing etc. of any laminate, in a multilayered case.

iii) If exact solution of the differential equations is tedious in certain cases, an approximate solution may be obtained by minimizing the energy integral itself approxi-

mately, by variational methods, e.g. Ritz method etc.

II.B: Assumptions

II.B.1 : Assumptions for analysis I

The following assumptions have been made for deriving the equations of motion in Analysis I given in section II.C.

1) Both the faces 1 and 3 (Fig.II-1a) are assumed to bend according to Bernoulli-Euler's theory, i.e. the transverse section of the layer, originally plane, remains plane and normal to the longitudinal fibres of the beam after bending.

2) At a section, the transverse displacement 'w' remains constant, throughout the thickness of the beam.

3) The longitudinal displacements 'u' at a transverse section are assumed to vary as shown in Fig.II-1(b). The variation is linear across the thickness in each layer, the slope being 'ζ' in each face but different in the core.

4) All displacements are assumed small, as in linear elasticity theory.

5) There is perfect continuity at the interfaces and no slip occurs there while the beam is bending.

6) The viscoelastic material of the core is linear i.e. its characteristics are strain independant.

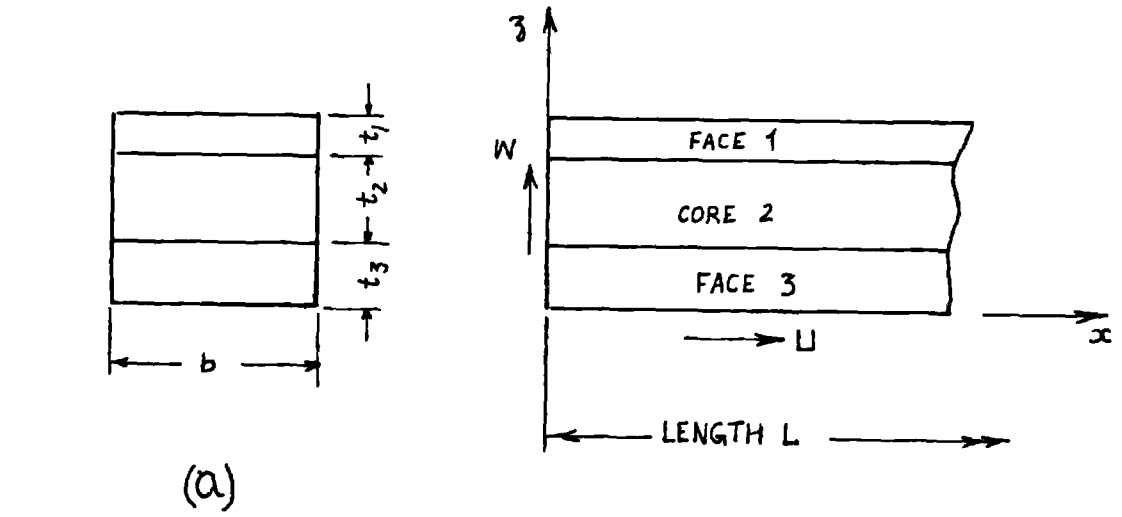

(a)

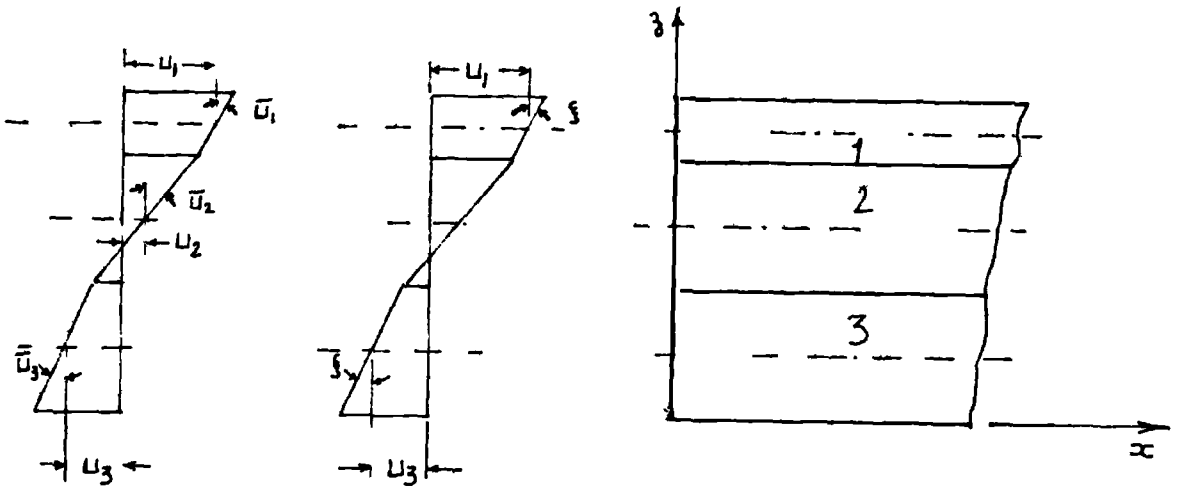

(c) (b)

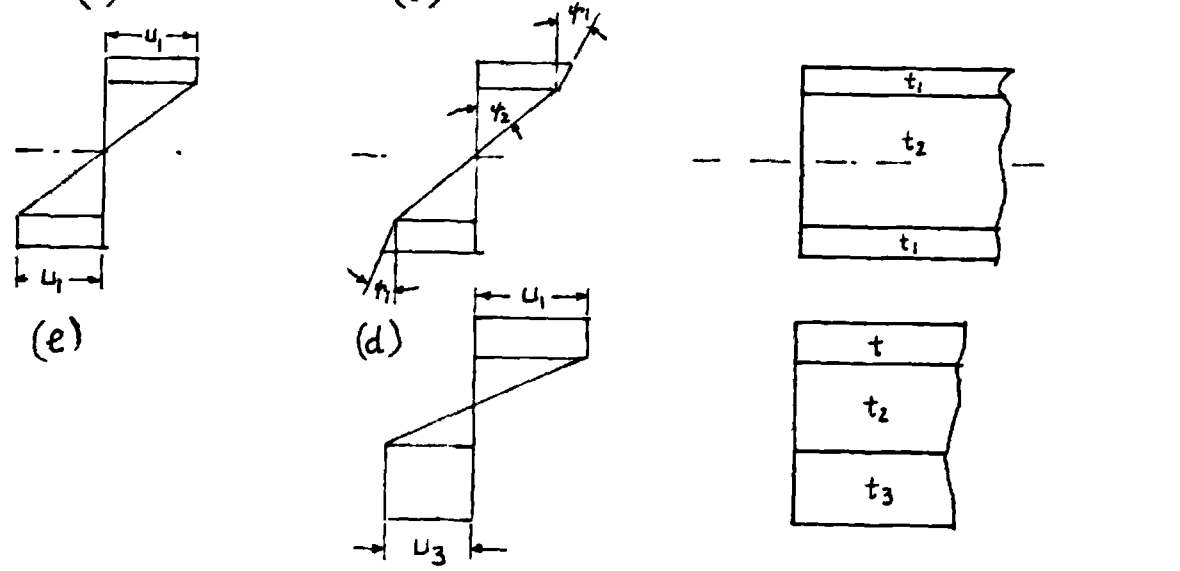

(e) (d) (f)

FIG II-1

The influence of non-linearity will be introduced in Chapter III later.

II.B.2: Assumptions for analysis II

For analysis II given in section II.D, assumptions 4), 5) and 6) of analysis I discussed in section II.B.1, hold. However, the remaining assumptions are as under:

i) The shear effect in each face has also been taken into account. This effect is of importance for thick faces and for high modes of vibrations.

ii) The equations derived do not assume a constant transverse displacement at a transverse section, but it is assumed to vary linearly through each layer thickness. Although this assumption is involved when the equations are derived, it is relaxed when the equations are used in the present work.

iii) The longitudinal displacements are assumed to vary across the thickness of the sandwich as shown in Fig. II-1(c). In analysis I, the transverse section in each face is assumed to rotate through an angle ζ, the flexural angle. However, in analysis II, such an angle is assumed different for layer 1 and layer 3, being $\bar{u}_1$ in the former layer and $\bar{u}_3$ in the latter layer.

The assumptions made for analysis II are more general than those for analysis I and the equations so derived should be more accurate for any 3 layered configuration,

each layer being quite different from the others. A comparison of the results given by both the analyses will be given in Chapter III.

II.B.3: Assumptions by other authors

The assumptions made by other authors, while analysing sandwich structures under static or dynamic conditions are as under:

In all cases, the transverse displacement 'w' is assumed constant at a section. Regarding longitudinal displacements, the assumptions are different in each case. Yu Yi Yuan 20 ha treated the case of symmetrical face sandwich (Fig.II-1d), with face and core having any general properties.

In a simplified version [23], he derived the equations for a symmetrical sandwich plate, taking the faces as membranes and not taking bending and shearing. A plot of 'u' displacements across thickness, corresponding to this is given in Fig.II-1(e). In another simplified case given in [23], he assumed the faces as thin membranes, with the core assumed existing up to middle of the faces. The same version was used by Hoff [16 and 17] for the static analysis of symmetrical sandwich structures. In addition, the bending effect of faces about their own axes was allowed for. Chang and Fang [28] assumed the variation of 'u' displacements s shown

in Fig.II-1(f) and the faces were not assumed to take any bending or shear. The displacement patterns assumed in [18 and 19] and 51] are similar to those in Fig.II-1(b). A detailed review of these references has already been given in Chapter I.

II.C: Analysis I

II.C.1: Equations of motion - derivation

According to Hamilton's principle [79], the stationary value of functional $\bar{\varphi}$ is equivalent to the equilibrium problem, where

$$\bar{\varphi} = \int_{t_1}^{t_2} (T-U+V)\, dt$$

T is the kinetic energy of the system

U is the strain energy

and V is potential energy of time dependent forces.

$$\text{or} \quad \bar{\varphi} - 0 \quad - \int_{t_1}^{t_2} (\delta T - \delta U - \delta V)\, dt \qquad \text{(II.1)}$$

With the assumed form of displacements, expressions for strain energy, kinetic energy and potential energy will be derived. The longitudinal displacements assumed at a section are shown in Fig.II-2(a). These are measured from a reference line, and vary across thickness of each layer due to bending and shearing effects.

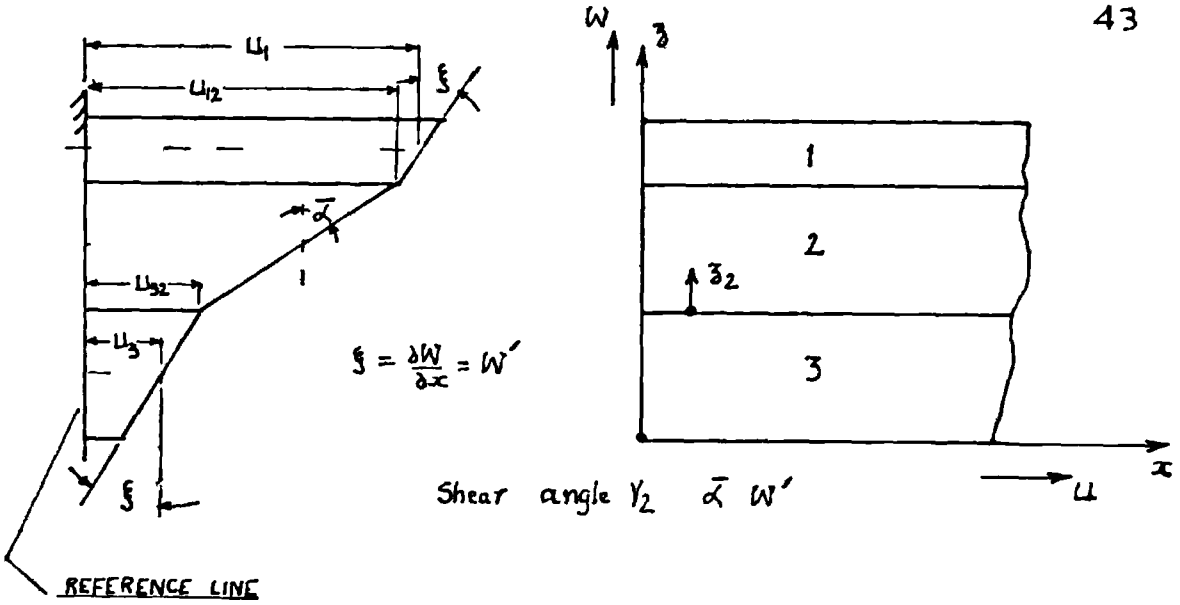

(a)

$\gamma = \frac{\partial u}{\partial z} + \frac{\partial W}{\partial x}$

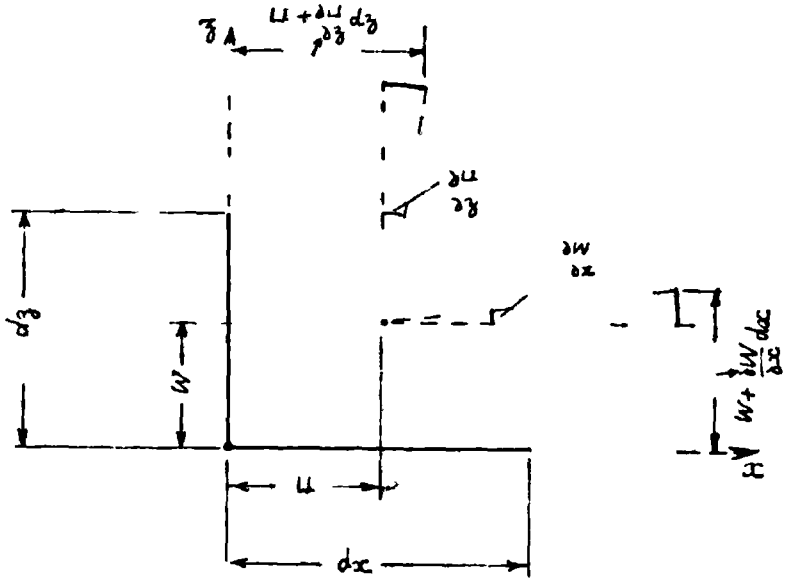

(b)

(c)

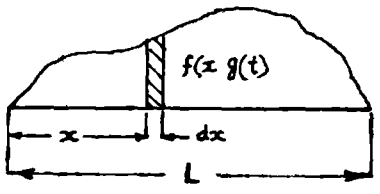

FIG. II-2

The transverse displacement at the section is w. The formulation will be done in terms of displacements u_1, u_3 and w. Using these it is possible to get the displacements and strains of any fibre in the system. Under specified conditions, solution of equations of motion will determine the magnitude and signs of these displacements and hence the position of neutral axis of the sandwich. The position of neutral axis is left to be determined in any given case from the solution to equations of motion, since its position varies from instant to instant in the viscoelastic case [34]. Subsequently, the equations derived in this section for elastic case, will be converted to be used for viscoelastic case.

The expression for γ_2, the shear strain in core i.e. layer 2 will be written down, keeping in view the sign convention as given in Fig.II-2(b).

$$\gamma_2 = \bar{\alpha} - \zeta$$

$$= \frac{(u_1 - \zeta \frac{t_1}{2}) - (u_3 + \zeta \frac{t_3}{2})}{t_2} - \zeta$$

$$= \frac{u_1 - u_3}{t_2} - \zeta \frac{a}{t_2} \quad \text{where } a = t_2 + \frac{t_1 + t_3}{2}$$

$$= \frac{u_1 - u_3}{t_2} - w' \frac{a}{t_2} \quad (\text{since flexural angle } \zeta = w') \tag{II.2}$$

The total strain energy of the sandwich is the sum of membrane energy of the faces, energy due to bending of the faces

about their own axes, shear and extensional energy of the core.

Strain energy contribution of face (1)

$$= \tfrac{1}{2} E_1 b t_1 \int_0^L \left(\frac{\partial u_1}{\partial x}\right)^2 dx + \frac{E_1 b t_1^3}{24} \int_0^L \left(\frac{\partial^2 w}{\partial x^2}\right)^2 dx \qquad \text{(II.3)}$$

Similarly, strain energy due to face (3)

$$= \tfrac{1}{2} E_3 b t_3 \int_0^L \left(\frac{\partial u_3}{\partial x}\right)^2 dx + \frac{E_3 b t_3^3}{24} \int_0^L \left(\frac{\partial^2 w}{\partial x^2}\right)^2 dx \qquad \text{(II.4)}$$

Shear strain energy in core (2)

$$= \tfrac{1}{2} G_2 b t_2 k_2 \int_0^L \gamma_2^2 dx \qquad \text{(II.5)}$$

where γ_2 is given by equation (II.2)

and k_2 is shear coefficient, due to non-uniform distribution of shear in layer 2.

$$\text{Core Extensional Energy} = \tfrac{1}{2} b E_2 \int_0^{t_2} \int_0^L \left\{u'_{32} + \frac{u'_{12} - u'_{32}}{t_2} z_2\right\}^2 dx\, dz_2$$

where ' denotes partial differentiation,

With respect to x, u_{12} and u_{32} are shown on Fig.II-2(a) and z_2 is a dummy coordinate in the core.

On simplifying

$$\text{Core Extensional Energy} = \frac{b E_2 t_2}{6} \int_0^L \left[u'^2_{12} + u'^2_{32} + u'_{12} u'_{32}\right] dx \qquad \text{(II.6)}$$

From Fig.II-2(a),

$$u_{12} = u_1 - w' \frac{t_1}{2}$$
$$u_{32} = u_3 + w' \frac{t_3}{2} \qquad \text{(II.7)}$$

After substituting eqn. II.2 in eqn. II.5 and eqn. II.7 in eqn. II.6, and adding up all the strain energy expressions,

Total strain Energy 'U' of sandwich

$$= s \int_0^L \left\{\frac{u_1-u_3}{t_2} - w' \frac{a}{t_2}\right\}^2 dx + r_1 \int_0^L u_1'^2 dx + r_3 \int_0^L u_3'^2 dx$$
$$+ q_1 \int_0^L (w'')^2 dx + q_3 \int_0^L (w'')^2 dx$$
$$+ c_2 \int_0^L \left\{u_1'^2 + u_3'^2 + u_1'u_3' + \frac{w''^2}{4}(t_1^2 + t_3^2 - t_1t_3)\right.$$
$$\left. + u_1'w''\left(\frac{t_3}{2} - t_1\right) + u_3'w''\left(t_3 - \frac{t_1}{2}\right)\right\} dx \qquad \text{(II.8)}$$

where $s = \frac{1}{2} b G_2 t_2 k_2$

$$\left.\begin{aligned} q_i &= \frac{b}{24} E_i t_i^3 \\ r_i &= \frac{b}{2} E_i t_i \end{aligned}\right| \quad (i=1,3)$$

$$c_2 = b E_2 t_2 / 6$$

Now, kinetic energy due to longitudinal displacements in a layer 'i', with middle displacement equal to u_i and rotation about middle = $\bar{u}_i$, is given as

$$\int_{-\frac{t_i}{2}}^{+\frac{t_i}{2}} \int_0^L \frac{b t_i \rho_i}{2} (\dot{u}_i + \dot{\bar{u}}_i z_i)^2 \, dx \, dz_i$$

$$= \frac{b\rho_i}{2}\int_0^L (\dot{u}_i^2 t_i + \dot{\bar{u}}_i^2 \frac{t_i^3}{12})\,dx \qquad (II.9)$$

ρ_i is mass density of layer 'i' per unit volume

t_i is thickness of layer 'i'.

Hence, total kinetic energy of sandwich, due to transverse and longitudinal displacements

$$= \tfrac{1}{2}\rho\int_0^L (\dot{w})^2 dx + \sum_{i=1}^{3}\int_0^L \frac{b\rho_i}{2}(\dot{u}_i^2 t_i + \dot{\bar{u}}_i^2 \frac{t_i^3}{12})dx \qquad (II.10)$$

where $\rho = b(\rho_1 t_1 + \rho_2 t_2 + \rho_3 t_3)$.

Now, Rotation $\bar{u}_1 = \bar{u}_3 = w'$

From Fig.II-2(a)

$$\text{Rotation } \bar{u}_2 = \frac{u_1 - u_3}{t_2} - \frac{w'\epsilon_2}{t_2}$$

Displacement u_2 of mid fibre of layer 2

$$= \frac{u_1+u_3}{2} + w'\epsilon_1$$

where $\epsilon_2 = \frac{t_3+t_1}{2}$

$$\epsilon_1 = \frac{t_3-t_1}{4}$$

Substituting these in eqn. II.10,

$$\text{Total kinetic energy} = \int_0^L [(\dot{w})^2 \frac{\rho}{2} + \frac{b\rho_1 t_1}{2}\dot{u}_1^2 + \frac{b\rho_3 t_3}{2}\dot{u}_3^2 + \dot{w}'^2(\frac{\rho_1 t_1^3 + \rho_3 t_3^3}{24})b + \frac{b\rho_2 t_2}{2}(\frac{\dot{u}_1+\dot{u}_3}{2} + \dot{w}'\epsilon_1 + \frac{b\rho_2 t_2}{24}(\dot{u}_1 - \dot{u}_3 - \dot{w}'\epsilon_2)^2]dx \qquad (II.11)$$

T

Potential energy 'V' due to forcing function of intensity (per unit length) f(x) g(t) as in Fig.II-2(c)

$$= \int_0^L f(x)\, g(t)\, w\, dx \qquad \text{(II.12)}$$

Now, equations II.8, II.11 and II.12 are to be substituted in eqn. II.1.

Equation II.1 is

$$\int_{t_1}^{t_2} (\delta T - \delta U - \delta V)\, dt = 0$$

The variations of U, T and V will be done term by term, in Appendix 1, where the details are given. On combining the various terms, the equations of motion are obtained as below, for arbitrary virtual displacements δw, δu_1 and δu_3. Also, the end point conditions, i.e. the boundary conditions are derived.

$$(2q+c_2^*)\, w^{IV} - 2s\left(\frac{a}{t_2}\right)^2 w'' + \frac{2sa}{t_2^2}\, u_1' + c_2^{**}\, u_1''' - \frac{2sa}{t_2^2}\, u_3' + c_2^{**}\, u_3''' =$$

$$f(x)g(t) - \rho \ddot{w}^{\cdot} \; b[\rho_2 t_2(\epsilon_3 \ddot{u}^{\cdot}_1 + \epsilon_4 \ddot{u}^{\cdot}_3) + \ddot{w}'' \epsilon_5] \qquad \text{(II.13)}$$

$$-\frac{2sa}{t_2^2}\, w' - c_2^{**}\, w''' + \frac{2s}{t_2^2} u_1 - u_1''(2r_1+2c_2) - \frac{2s}{t_2^2}\, u_3 - c_2 u_3''$$

$$= -b\left[\rho_1 t_1 \ddot{u}_1^{\cdot} + \rho_2 t_2\left(\frac{\ddot{u}_1^{\cdot}}{3} + \frac{\ddot{u}_3^{\cdot}}{6} + \ddot{w}^{\cdot}\epsilon_3\right)\right] \qquad \text{(II.14)}$$

$$\frac{2sa}{t_2^2}\, w' - c_2^{**} w''' \frac{2s}{t_2^2} u_1 - c_2 u_1'' \quad \frac{2s}{t_2^2}\, u_3 - u_3''(2r_3+2c_2)$$

$$= -b\left[\rho_3 t_3 \ddot{u}_3^{\cdot} + \rho_2 t_2\left(\frac{\ddot{u}_1^{\cdot}}{6} + \frac{\ddot{u}_3^{\cdot}}{3} + \ddot{w}^{\cdot}\epsilon_4\right)\right] \qquad \text{(II.15)}$$

where $q = \frac{b}{24}(E_1 t_1^3 + E_3 t_3^3)$

$r_1 = \frac{1}{2} b E_1 t_1$

$$r_3 = \tfrac{1}{2}bE_3t_3$$

$$s = \tfrac{1}{2}G_2bk_2t_2$$

$$c_2 = \frac{bE_2t_2}{6}$$

$$c_2^* = c_2\left(\frac{t_1^2+t_3^2-t_1t_3}{2}\right)$$

$$c_2^{**} = c_2\left(\frac{t_3}{2}-t_1\right)$$

$$c_2^{***} = c_2\left(t_3-\frac{t_1}{2}\right)$$

$$x_1 = \frac{t_3-t_1}{4}$$

$$\epsilon_2 = \frac{t_3+t_1}{2}$$

$$\epsilon_3 = \frac{t_3-2t_1}{12}$$

$$\epsilon_4 = \frac{2t_3-t_1}{12}$$

$$\epsilon_5 = \frac{\rho_1t_1^3+\rho_3t_3^3}{12}+\rho_2t_2\epsilon_1^2+\frac{\rho_2t_2}{12}\epsilon_2^2$$

ρ_1, ρ_2, ρ_3 are the mass densities per unit volume for layers 1, 2 and 3 respectively.

ρ is mass density per unit length of the sandwich

$$= b(\rho_1t_1+\rho_2t_2+\rho_3t_3)$$

The boundary conditions for simple supported ends are

$$w = 0$$

$$w'' = 0 \qquad \text{(II.16)}$$

$$u'_1 = u'_3 = 0$$

Shear coefficient 'k_2' will be determined in Section II.D.3.

II.C.2 Solution for Simply Supported Beam - Elastic Case

Firstly, this will be determined for the elastic case, i.e. when all layers are assumed as elastic. Later, the solution for a 3 layered sandwich, with visco-elastic core will be deduced from this in section II.C.3.

The dynamic response is required to be determined for a loading of intensity f(x) sin pt. Assuming the solution in the form of series

$$\left.\begin{aligned} w &= \sum_{n=1}^{\infty} w_n \sin \frac{n\pi x}{L} \sin pt \\ u_i &= \sum_{n=1}^{\infty} u_{in} \cos \frac{n\pi x}{L} \sin pt \\ u_3 &= \sum_{n=1}^{\infty} u_{3n} \cos \frac{n\pi x}{L} \sin pt \end{aligned}\right\} \qquad \text{(II.17)}$$

It can be seen that this assumed solution satisfies the boundary conditions given in (II.16) and also reduces the differential equations of motion (II.13) to (II.15), to algebraic equations. Writing the loading f(x) in the form of series $f(x) = \sum_{n=1}^{\infty} f_n \sin \frac{n\pi x}{L}$, substituting eqn. (II.17) in (II.13) to (II.15) and simplification gives

$$\left.\begin{aligned} u_{1n} f_3 + u_{3n} g_3 + w_n(h_3) &= f_n \\ u_{1n} f_1 - u_{3n} g_1 &= w_n h_1 \\ u_{1n} f_2 + u_{3n} g_2 &= -w_n h_2 \end{aligned}\right\} \qquad \text{(II.18)}$$

where $f_1 = \frac{2s}{t_2} + 2(r_1+c)(\frac{n\pi}{L})^2 - b\rho_1 t_1 p^2 - \frac{b\rho_2 t_2 p^2}{3}$

$g_1 = \frac{2s}{t_2} - c(\frac{n\pi}{L})^2 + \frac{b\rho_2 t_2 p^2}{6}$

$h_1 = \frac{2sa}{t_2} (\frac{n\pi}{L}) - c^{**}(\frac{n\pi}{L})^3 + b\rho_2 t_2 p^2 \varepsilon_3 (\frac{n\pi}{L})$

$f_2 = c(\frac{n\pi}{L})^2 - \frac{2s}{t_2} - \frac{b\rho_2 t_2 p^2}{6}$

$g_2 = \frac{2s}{t_2} + 2(r_3+c)(\frac{n\pi}{L})^2 - b\rho_3 t_3 p^2 - \frac{b\rho_2 t_2 p^2}{3}$

$h_2 = c^{***}(\frac{n\pi}{L})^3 + \frac{2sa}{t_2} (\frac{n\pi}{L}) - b\rho_2 p^2 t_2 \varepsilon_4 (\frac{n\pi}{L})$

$f_3 = c^{**}(\frac{n\pi}{L})^3 - \frac{2sa}{t_2} (\frac{n\pi}{L}) - b\rho_2 t_2 \varepsilon_3 p^2 (\frac{n\pi}{L})$

$g_3 = \frac{2sa}{t_2}(\frac{n\pi}{L}) + c^{***}(\frac{n\pi}{L})^3 - b_2 t_2 \varepsilon_4 (\frac{n\pi}{L}) p^2$

$h_3 = (2q+c^*)(\frac{n\pi}{L})^4 + \frac{2sa^2}{t_2}(\frac{n\pi}{L})^2 - \rho p^2 - b\varepsilon_5 p^2 (\frac{n\pi}{L})^2$

Elimination of u_{1n} and u_{3n} from equations (II.18) gives

$$w_n\left[h_3 - \frac{f_3(h_1 g_2 - h_2 g_1) - g_3(f_1 h_2 + f_2 h_1)}{f_1 g_2 + f_2 g_1}\right] = f_n \qquad \text{(II.19)}$$

Equations (II.17) to (II.19) give the desired solution.

II.C.3 : Solution for simply supported beam, with viscoelastic core

If the core, i.e. layer 2, is viscoelastic, the

solution may be got for sinusoidal excitation conditions by replacing the elastic moduli G_2 and E_2 by complex ones. Denoting loss factor in shear by η_2 and that in direct stress/strain conditions as β_2 for layer 2, the solution for viscoelastic case may be got by replacing G_2 by $G_2(1+\eta_2)$ and E_2 by $E_2(1+i\beta_2)$ in the equations given in II·C·2 , and simplification. The following equation is obtained

$$bw_n[R_{T_n} + i\, I_{T_n}] = f_n \qquad \text{(II.20)}$$

where

$$R_{T_n} = \text{Real Term} = E_3 t_3^3 \left(\frac{n\pi}{L}\right)^4 \left[h_3^r + \frac{(R_1R_2+I_1I_2)-(R_3R_2+I_3I_2)}{R_2^2 + I_2^2}\right]$$

$$I_{T_n} = \text{Imaginary Term} = E_3 t_3^3 \left(\frac{n\pi}{L}\right)^4 \left[h_3^I + \frac{(I_1R_2-I_2R_1)-(I_3R_2-I_2R_3)}{R_2^2 + I_2^2}\right]$$

$$R_2 = f_1^r g_2^r - f_1^I g_2^I - g_1^r g_1^r + g_1^I g_1^I$$

$$I_2 = f_1^I g_2^r + f_1^r g_2^I - g_1^r g_1^I - g_1^r g_1^r$$

$$R_1 = - h_1^r \bar{A} + h_1^I \bar{B}$$

$$I_1 = - h_1^I \bar{A} - h_1^r \bar{B}$$

$$R_3 = h_2^r \bar{C} - h_2^I \bar{D}$$

$$I_3 = h_2^I \bar{C} + h_2^r \bar{D}$$

$$\bar{A} = h_1^r g_2^r - h_1^I g_2^I - h_2^r g_1^r + h_2^I g_1^I$$

$$\overline{B} = h_1^I g_2^r + h_1^r g_2^I - g_1^r h_2^I - g_1^I h_2^r$$

$$\overline{C} = f_1^r h_2^r - f_1^I h_2^I - g_1^r h_1^r + g_1^I h_1^I$$

$$\overline{D} = f_1^I h_2^r + f_1^r h_2^I - g_1^I h_1^r - g_1^r h_1^I$$

In above,

$$f_1^r = \frac{\phi_{2.3} k_2}{\theta_{2.3}} + \alpha_{1.3}\theta_{1.3} + \frac{\alpha_{2.3}\theta_{2.3}}{3} - \theta_{1.3}\varphi_1 \frac{\theta_{2.3}\varphi_2}{3}$$

$$f_1^I = \frac{\phi_{2.3} k_2}{\theta_{2.3}} \eta_2 + \frac{\alpha_{2.3}\theta_{2.3}}{3} \beta_2$$

$$g_1^r = \frac{\phi_{2.3} k_2}{\theta_{2.3}} - \frac{\alpha_{2.3}\theta_{2.3}}{6} + \frac{\theta_{2.3}\varphi_2}{6}$$

$$g_1^I = \frac{\phi_{2.3} k_2}{\theta_{2.3}} \eta_2 - \frac{\alpha_{2.3}\theta_{2.3}}{6} \beta_2$$

$$g_2^r \quad 1 \quad \phi_{2.3} \quad k_2/\theta_{2.3} + \alpha_{2.3}\theta_{2.3}/3 - \varphi_3 - \theta_{2.3}\varphi_2/3$$

$$g_2^I = \eta_2 \, \phi_{2.3} k_2/\theta_{2.3} + \alpha_{2.3}\theta_{2.3}\beta_2/3$$

$$h_1^r = \phi_{2.3} k_2 \left(\frac{1+\theta_{1.3}+2\theta_{2.3}}{2\theta_{2.3}}\right) - \frac{\theta_{2.3}}{12}(1-2\theta_{1.3})\alpha_{2.3} + \theta_{2.3}\varphi_2 \left(1-\frac{2\theta_{1.3}}{12}\right)$$

$$h_1^I = \phi_{2.3} k_2 \left(\frac{1+\theta_{1.3}+2\theta_{2.3}}{2\theta_{2.3}}\right) \eta_2 - \frac{\theta_{2.3}}{12}(1-2\theta_{1.3})\alpha_{2.3}\beta_2$$

$$h_2^r = \phi_{2.3} k_2 \left(\frac{1+\theta_{1.3}+2\theta_{2.3}}{2\theta_{2.3}}\right) + \frac{\theta_{2.3}\theta_{2.3}}{12}(2-\theta_{1.3}) - \theta_{2.3}\varphi_2 \left(\frac{2-\theta_{1.3}}{12}\right)$$

$$h_2^I = \phi_{2.3} k_2 \left(\frac{1+\theta_{1.3}+2\theta_{2.3}}{2\theta_{2.3}}\right)\eta_2 + \frac{\alpha_{2.3}\theta_{2.3}}{12}(2-\theta_{1.3})\beta_2$$

$$h_3^r = \frac{1+\alpha_{1.3}\theta_{1.3}^3}{12} + \frac{\phi_{2.3}k_2}{4\theta_{2.3}}(1+\theta_{1.3}+2\theta_{2.3})^2$$

$$+ \frac{\alpha_{2.3}\theta_{2.3}}{12}(\theta_{1.3}^2 - \theta_{1.3}+1) - (\theta_{1.3}\lambda_1 + \theta_{2.3}\lambda_2 + \lambda_3)$$

$$- \left[\frac{\varphi_1\theta_{1.3}^3 + \varphi_3}{12} + \frac{\theta_{2.3}\varphi_2}{12}(1+\theta_{1.3}^2 - \theta_{1.3})\right]$$

$$h_3^I = \frac{\phi_{2.3}k_2}{4\theta_{2.3}}(1+\theta_{1.3}+2\theta_{2.3})^2\eta_2 + \frac{\alpha_{2.3}\theta_{2.3}}{12}(\theta_{1.3}^2 - \theta_{1.3}+1)\beta_2$$

$$\varphi_i = \frac{\rho_i p^2}{E_3(\frac{n\pi}{L})^2}, \quad (i=1,2,3) \qquad \lambda_i = \frac{\rho_i p^2}{(\frac{n\pi}{L})^4 E_3 t_3^2}$$

$$\phi_{2.3} = \frac{G_2}{E_3 t_3^2 (\frac{n\pi}{L})^2} \qquad \alpha_{1.3} = E_{1/E_3}, \quad \theta_{1.3} = t_{1/t_3},$$

$$\theta_{2.3} = t_{2/t_3}, \qquad \alpha_{2.3} = E_{2/E_3}$$

The coefficient 'f_n' depends on the distribution of loading f(x) along x. For uniformly distributed load of intensity 'f' per unit length, $f_n = \frac{4f}{n\pi}$ (for n=1,3,5...

$= 0$ (for n=2,4,6...

For concentrated load P, applied at a distance L' from one end, $f_n = \frac{2P}{L}\sin\frac{n\pi L'}{L}$ for n = 1,2,3,etc.. [81].

II.C.4 : Simplified C se

Here, the case dealt with in sections II.C.2 and II.C.3 will be simplified, by neglecting some terms as

follows. If we neglect the extensional effect of layer 2 i.e. core, and also all inertia terms except the transverse inertia terms, the equations of motion (II.13) to (II.15) can be simplified to the form:

$$\left.\begin{aligned} AW'''' - C\frac{a}{t_2}\left(w''\frac{a}{t_2} - u_1'\frac{m'}{t_2}\right) + \rho\ddot{w} &= f(x)\sin pt \\ C\frac{m'}{t_2}\left(w'\frac{a}{t_2} - u_1\frac{m'}{t_2}\right) + Du_1'' &= 0 \\ u_1 &= -u_3 m \end{aligned}\right\} \quad \text{(II.21a)}$$

where $A = \frac{b}{12}(E_1 t_1^3 + E_3 t_3^3)$

$C = bt_2 G_2$

$D = b(E_1 t_1 + E_3 t_3 m^2)$

$m = E_1 t_1 / E_3 t_3$

$m' = 1+m$

$a = t_2 + \frac{t_1+t_3}{2}$

$\rho = b(\rho_1 t_1 + \rho_2 t_2 + \rho_3 t_3)$

The boundary conditions as simplified from Appendix I are:

$$\left.\begin{aligned} &\text{For simply supported end:} & w &= 0 \\ & & w'' &= 0 \\ & & u_1' &= 0 \\ &\text{For fixed end:} & w' &= 0 \\ & & u_1 &= 0 \\ & & w &= 0 \end{aligned}\right\} \quad \text{(II.21b)}$$

For free end: $w'' = 0$

$$u_1' = 0$$

$$-2q\, w''' + 2s\left[\left(\frac{w'a}{t_2} - u_1 \frac{m'}{t_2}\right)\frac{a}{t_2}\right] = 0$$

where $q = \frac{b}{24}(E_1 t_1^3 + E_3 t_3^3)$

$$s = \tfrac{1}{2} b t_2 G_2$$

Also equation (II.19) for simply supported beam is simplified to:

$$w_n\left[\left(\frac{n\pi}{L}\right)^4 \left\{A + \frac{a^2/t_2^2}{\left(\frac{m'}{t_2}\right)^2 \frac{1}{D} + \frac{1}{C}\left(\frac{n\pi}{L}\right)^2}\right\} - \rho p^2\right] = f_n \quad \text{(II.22)}$$

For a symmetrical case (i.e. when=layers 1 and 3 are identical), this equation will be compared with that in [51]. In the present notation, eqn. 22 of [51] for a symmetrical 3 layered sandwich beam can be taken as

$$w_n b\left[\frac{E_1 t_1^3}{6}\left(\frac{n\pi}{L}\right)^4 \left\{1 + \frac{3\left(\frac{t_1+t_2}{t_1}\right)^2}{1 + \left(\frac{n\pi}{L}\right)^2 \frac{E_1}{G_2}\frac{t_1 t_2}{2}}\right\} - \rho p^2\right] = f_n$$

(II.23)

Eqn. (II.22) for the case $t_1 = t_3$ and $E_1 = E_3$ reduces to:

$$w_n\left[\left(\frac{n\pi}{L}\right)^4 \left\{\frac{bE_1 t_1^3}{6} + \frac{\left(\frac{t_1+t_2}{t_2}\right)^2}{\left(\frac{2}{t_2}\right)^2 \cdot \frac{1}{2bE_1 t_1} + \frac{\left(\frac{n\pi}{L}\right)^2}{bt_2 G_2}}\right\} - \rho p^2\right] = f_n$$

(II.24

Expressions given in II.23 and II.24 can be shown to be identical.

A comparison can also be made for the expression for natural frequency of simply supported sandwich beam as given in [19]. If $E_1 = E_3 = E$ is substituted in eqn. (II.22), the expression given in brackets determining natural frequency of vibration of beam can be seen to be identical to that given in [19].

Hoff's [16 and 17] resulting differential equations for static analysis of symmetrical sandwich beam, are obtainable from differential equations (II.21), by taking into account the difference in expression for 'γ_2' in both cases, in addition to the substitutions for symmetry $t_1 = t_3$ and $E_1 = E_3$ and also taking away the dynamic terms. In [16 and 17],

$$\gamma_2 = \frac{u_3 - u_1}{t_1 + t_2} + w' \quad \text{(where } u_3 = -u_1 \text{ for symmetrical case)}$$

whereas γ_2 in section II.C.1 is

$$\gamma_2 = \frac{u_1 - u_3}{t_2} - \frac{w'a}{t_2} .$$

Eqn. (II.21a) reduces to that for an ordinary homogeneous beam if the terms for core 2 are eliminated. Replacing G_2 by $G_2(1+\eta_2)$ in eqn. (II.22), the resulting equation for viscoelastic case is obtained as:

$$W \underset{r_{t_n}}{[\text{Real term}} + i \underset{i_{t_n}}{\text{Imaginary term}} - \rho p^2] = f_n \qquad \text{(II.25)}$$

where

$$\text{Real Term} = \left(\frac{n\pi}{L}\right)^4 \left[A + \frac{gC(1+\eta_2^2)\left\{\frac{h}{D}C(1+\eta_2^2)+\left(\frac{n\pi}{L}\right)^2\right\}}{\left\{\frac{h}{D}C(1+\eta_2^2)+\left(\frac{n\pi}{L}\right)^2\right\}^2+\left\{\eta_2\left(\frac{n\pi}{L}\right)^2\right\}^2} \right]$$

$$\text{Imaginary Term} = \frac{g\eta_2\left(\frac{n\pi}{L}\right)^2(1+\eta_2^2)C}{\left\{\frac{h}{D}C(1+\eta_2^2)+\left(\frac{n\pi}{L}\right)^2\right\}^2+\left\{\eta_2\left(\frac{n\pi}{L}\right)^2\right\}^2}$$

$$g = \frac{a^2}{t_2^2}$$

$$h = \left(\frac{m'}{t_2}\right)^2$$

II.C.5 : Beams with Various End Conditions

The solution for beam with simply supported ends has been obtained in previous sections, in series form. For other end conditions, methods of solution to determine dynamic response will be indicated. No detailed solution will be attempted but the use of approximate variational methods will be outlined for the simplified case of section II.C.4.

The differential equations and boundary conditions, taking all layers as elastic are given by equations (II.21a) and (II.21b). For viscoelastic core, shear modulus G_2 has to be replaced by $G_2\left(1+\eta_2\frac{D_t}{p}\right)$

where $D_t = \frac{\partial}{\partial t}$

Since C in eqns. (II.21a) and (II.21b) involves G_2, C will be replaced by $C \quad C' \frac{D_t}{p}$

where $C' = bt_2 G_2 \eta_2$

and $C = bt_2 G_2$

Taking the solution as:

$$\left.\begin{aligned} w &= w_s(x) \sin pt + w_c(x) \cos pt \\ u_1 &= w_{1s}(x) \sin pt + u_{1c}(x) \cos pt \end{aligned}\right\} \qquad (II.26)$$

Substituting in eqn. (II.21a) and equating sine and cos terms identically, the equations of motion are

$$\left.\begin{aligned} Aw''''_s - \frac{Ca}{t_2}\left(w''_s \frac{a}{t_2} - u'_{1s} \frac{m'}{t_2}\right) - \rho p^2 w_s \\ \frac{C'a}{t_2}\left(w''_c \frac{a}{t_2} - u'_{1c} \frac{m'}{t_2}\right) = f(x) \end{aligned}\right\} \qquad (II.27)$$

$$\left.\begin{aligned} Aw''''_c - \frac{Ca}{t_2}\left(w''_c \frac{a}{t_2} - u'_{1c} \frac{m'}{t_2}\right) - \rho p^2 w_c \\ - \frac{C'a}{t_2}\left(w''_s \frac{a}{t_2} - u'_{1s} \frac{m'}{t_2}\right) = 0 \end{aligned}\right\} \qquad (II.28)$$

$$\frac{Cm'}{t_2}\left(w'_s \frac{a}{t_2} - u_{1s} \frac{m'}{t_2}\right) + Du''_{1s} - \frac{C'm'}{t_2}\left(\frac{w'_c a}{t_2} - u_{1c} \frac{m'}{t_2}\right) = 0 \qquad (II.29)$$

$$\frac{Cm'}{t_2}\left(w'_c \frac{a}{t_2} - u_{1c} \frac{m'}{t_2}\right) + Du''_{1c} + \frac{C'm'}{t_2}\left(\frac{w'_s a}{t_2} - u_{1s} \frac{m'}{t_2}\right) = 0 \qquad (II.30)$$

Similarly the boundary conditions (II.21b) can be expressed in terms of w_s, w_c, u_{1s} and u_{1c}. The solution may be obtained by:

1) Finite difference approach: This may be done by replacing the differential equations by difference quotients at a number of points on the beam, obtained by dividing the beam into a number of parts [97]. The resulting equations are a number of simultaneous algebraic equations. This method has been used in [59] for symmetrical layered cantilevers and can be used for above equations as well.

2) By using classical method of solution of simultaneous differential equations, with constant coefficients [98]. Both complementary function and particular solution are to be obtained separately. Obtaining the former involves determination of multiple roots of algebraic polynomial equation and solution of simultaneous algebraic equations.

Both the above mentioned methods involve tedious and time-consuming computation on a digital computer, since the order of differential equations is high. Below, the use of approximate variational methods, which do not involve the direct use of these differential equations, is outlined. These are expected to be simpler and less time-consuming for low frequencies, for which these are intended.

a) Ritz Method: In this method, a solution is assumed in the form of series, involving undetermined coefficients

and substituted in the total energy integral e.g. the assumed solution may be:

$$\left.\begin{aligned} w &= a_1 w_{(1)} + a_2 w_{(2)} + a_3 w_{(3)} + \cdots \\ u_1 &= b_1 u_{1(1)} + b_2 u_{1(2)} + \cdots \end{aligned}\right\} \qquad \text{(II.31)}$$

where each of the terms $w_{(1)}$, $w_{(2)}$, $u_{1(1)}$ etc. is a function of the independent variables, and satisfies geometrical boundary conditions [74, 76-79]. The undetermined coefficients a_1, a_2, a_3, b_1, b_2 etc. are obtained by minimisation of energy integral. In the present case, approximate solution for dynamic response, in elastic case, will be obtained first, from the energy integral for sinusoidal excitations and then shear modulus for core will be made complex, in order to get complex solution for sandwich with viscoelastic core.

e.g. for a cantilever subjected to sinusoidal excitation of intensity f(x) sin pt, boundary conditions for fixed end i.e. at x = 0 are:

$$w = w' = 0, \qquad u_1 = 0$$

For free end i.e. at x = L,

$$\left.\begin{aligned} w'' &= 0, & u_1' &= 0 \\ 2qw''' &+ 2sf\,[u_1 e - w' f] = 0 \end{aligned}\right\} \qquad \text{(II.32)}$$

where $e = \dfrac{1}{t_2} + \dfrac{E_1 t_1}{E_3 t_3 t_2}$

$$f = 1 + \frac{t_1 + t_3}{2t_2}$$

Total energy integral corresponding to the simplified case of section II.C.4 is obtained from section II.C.1

$$\bar{\varphi} = \int_{t_1}^{t_2} \left[\int_0^L \{q(w'')^2 + r(u_1')^2 + s(u_1 e - w'f)^2 - \frac{\rho p^2}{2} w^2 - f(x)\, w \sin pt\} dx \right] dt \qquad \text{(II.33)}$$

where $q = \frac{b}{24}(E_1 t_1^3 + E_3 t_3^3)$

$r = \frac{b}{2}(E_1 t_1 + E_3 t_3 m^2)$

$s = \frac{b}{2} t_2 G_2$

$m = \frac{E_1 t_1}{E_3 t_3}$

Assuming a solution of the form:

$$\left.\begin{aligned} w &= \sum_{j=1,3,5} a_j \left(1 - \cos \frac{j\pi x}{2L}\right) \sin pt \\ u_1 &= \sum_{j=1,3,5} b_j \left(\sin \frac{j\pi x}{2L}\right) \sin pt \end{aligned}\right\} \qquad \text{(II.34)}$$

This satisfies the first 5 boundary conditions, given by eq. (II.32), but the last one is not satisfied. Now, this last boundary condition is a natural boundary condition and is not required to be satisfied in Ritz approximate method [74,77,79]. In this method, the geometrical or displacement boundary conditions have to be satisfied by each term in the series assumed. But natural or forced boundary conditions need not be satisfied, the reason being that minimisation of energy integral gives both Eulers

differential equations and natural boundary conditions. Since an assumed solution minimises the energy integral approximately, both differential equations and natural boundary conditions are satisfied approximately too. The accuracy is expected to enhance as the number of terms in the assumed series are increased.

For illustration, taking one term in the series

$$w = a_1(1 - \cos \frac{\pi x}{2L}) \sin pt$$

$$u_1 = b_1 \sin (\frac{\pi x}{2L}) \sin pt$$

Substituting this in expression for $\bar{\varphi}$ given by eqn. (II.33), integrating with respect to x and substituting expressions for $\frac{\partial \bar{\varphi}}{\partial a_1}$ and $\frac{\partial \bar{\varphi}}{\partial b_1}$ equal to zero, we get

$$\frac{q}{L^3} \frac{\pi^4}{16} a_1 - f\frac{\pi s}{2} (eb_1 - \frac{f\pi}{2L} a_1) - 0.23 \rho p^2 La_1 = f(x) [L - \frac{2I}{}]$$

$$\frac{r}{L} \frac{\pi^2}{4} b_1 + sL\, e(eb_1 - \frac{f\pi}{2L} a_1) - 0$$

Solution of these simultaneous algebraic equations, gives the solution for elastic case. For viscoelastic case, G_2 occurring in above equations is replaced by $G_2(1 i\eta_2)$, making the coefficients of a_1 and b_1 in these equations complex. Simultaneous solution of these equations gives the desired solution. In practice, a few terms might give a reasonably approximate solution, for lower frequencie

b) Lagrangian Multiplier Method

Frequently, it may be difficult to assume a series in Ritz method, which satisfies all the displacement boundary conditions even. In such a case, Lagrangian multiplier method may be employed. It has been used in [75] for static problems. It differs from Ritz method in that the assumed series as a whole is constrained to satisfy those boundary conditions which are not satisfied by each term in the series, e.g. 6th boundary condition in eqn. (II.32), which is a natural boundary condition, was not satisfied by each term of the series assumed in the foregoing Ritz method illustrated. This may be satisfied, however, by using a Lagrangian multiplier. The energy expression is modified in this case as below.

$\bar{\varphi}$ = Energy expression as before - λ(constraining condition)

Taking 2 terms in each series in the solution assumed for a 3 layered cantilever, in the foregoing illustration,

$$\left.\begin{aligned} w &= a_1\left(1 - \cos\frac{\pi x}{2L}\right) \quad a_3\left(1 - \cos\frac{3\pi x}{2L}\right) \\ u_1 &= b_1 \sin\frac{\pi x}{2L} + b_3 \sin\frac{3\pi x}{2L} \end{aligned}\right\} \qquad (II.35)$$

The constraining condition is

$$2qw''' + 2sf\,[u_1 e - w'f] = 0 \text{ at } x = L \qquad (II.36)$$

Substituting solution (II.35) in eqn. (II.36) gives

$$2q[-a_1(\frac{\pi}{2L})^3 + a_3(\frac{3\pi}{2L})^3]$$

$$+ 2sf[e(b_1-b_3)] - 2sf^2[a_1(\frac{\pi}{2L}) - a_3(\frac{3\pi}{2L})] = 0$$

Now, $\bar{\varphi} = \int_{t_1}^{t_2}[\int_o^L \{q(w'')^2 + r(u_1')^2 + s(u_1 e - w'f)^2 - \frac{\rho p^2}{2} w^2$

$$- f(x)\, w \sin pt\}\, dx$$

$$- \lambda\{-2q\, a_1(\frac{\pi}{2L})^3 + 2qa_3(\frac{3\pi}{2L})^3 + 2sef\, b_1$$

$$-2s\, e\, f\, b_3 - 2sf^2 a_1 \frac{\pi}{2L} + 2sf^2 a_3(\frac{3\pi}{2L})\}]\, dt$$

Substituting the assumed solution, integrating with respect to 'x' and equating expressions for

$$\frac{\partial \bar{\varphi}}{\partial a_j} = 0 \qquad (j=1,3)$$

$$\frac{\partial \bar{\varphi}}{\partial b_j} = 0 \qquad (j=1,3)$$

$$\frac{\partial \bar{\varphi}}{\partial \lambda} = 0$$

This gives 5 simultaneous algebraic equations

$$\left.\begin{aligned}
a_1A+a_3B+b_1c+\lambda D &= f(x)[L - \tfrac{2L}{\pi}] \\
a_1F+a_3G+b_3H+\lambda J &= f(x)[L + \tfrac{2L}{3\pi}] \\
a_1K+b_1M+\lambda N &= 0 \\
a_3P+b_3Q+\lambda R &= 0 \\
a_1S+a_3T+b_1U+b_3V &= 0
\end{aligned}\right| \qquad \text{(II.37)}$$

where $A = q(\frac{\pi}{2L})^4 L + Lsf^2(\frac{\pi}{2L})^2 - \rho p^2 L(\frac{3}{2} - \frac{4}{\pi})$

$B = -\rho p^2 L(1 - \frac{4}{3\pi})$

$C = -Lsef(\frac{\pi}{2L})$

$D = 2q(\frac{\pi}{2L})^3 + 2sf^2(\frac{\pi}{2L})$

$F = B$

$G = 9qL(\frac{\pi}{2L})^4 + 9Lsf^2(\frac{\pi}{2L})^2 - \rho p^2 L(\frac{3}{2} + \frac{4}{3\pi})$

$H = -3Lsef\ \frac{\pi}{2L}$

$J = +2sf^2(\frac{3\pi}{2L}) - 2q(\frac{3\pi}{2L})^3$

$K = -Lsef(\frac{\pi}{2L})$

$M = Lr(\frac{\pi}{2L})^2 + Lse^2$

$N = -2sef$

$P = 3K$

$Q = 9Lr(\frac{\pi}{2L})^2 + Lse^2$

$R = -N$

$S = -D$

$T = -J$

$U = R$

$V = N$

For viscoelastic core, G_2(and thereby 's') is made complex, by substituting $G_2(1+i\eta_2)$ for G_2. Solution of simultaneous algebraic eqns. (II.37) involving complex

coefficients gives the desired solution. The approximate solution so obtained has been compared, for a symmetrical cantilever, with the solution obtained in [59], using finite difference technique. The parameters of the sandwich cantilever taken are:

$$t_1 = t_3 = 0.187", \quad t_2 = 0.137", \quad L = 15"$$

$$E_1 = E_3 = 3 \times 10^7 \text{ lb/in}^2,$$

Core material - P.V.C. (sheet A, as referred to in Chapter VI). Properties used, correspond to a temperature of 26.3°C and shear strain amplitude = 0.1×10^{-3}. The root of the cantilever is excited by harmonic displacement $x_o \sin pt$, thus the value of $f(x)$ is $\rho p^2 x_o$. The results obtained for the first resonance are:

	Peak Value of Tip to Root Amplitudes	Frequency corresponding to Peak ratio of Tip to Root Amplitudes
1) From [59], using finite difference solution.	6.495	42.5 c.p.s.
2) Using Eqn. (II.37)	6.466	40.0 c.p.s.

There is a shift of frequency corresponding to peak ratio of tip to root amplitudes, while the peak value of this ratio is almost same in the two cases. Thus, the

above approximate solution, which is simple, gives reasonable results for low frequencies. More terms in the series are required to be included in the assumed solution, for obtaining accurate results, especially at higher frequencies.

II.D: Analysis II

II.D.1 : Equations of motion - derivation

The assumptions made for Analysis II of a 3 layered configuration are discussed in section II.B.2. These assume linear variations of both u and w displacements along thickness. These can be called first order approximations, in the manner of Mindlin [69]. The equations used later in this section will be those in which first order approximation is taken for 'u' displacements but zero order approximation for 'w' displacements.

Mindlin [69] has converted the 3 dimensional equations of elasticity to infinite series of 2 dimensional equations by expanding the displacements in an infinite series of powers of thickness co-ordinate of a plate and by integrating through thickness,

i.e. $u_j = \sum_n z^n (u_j)^n$; z is thickness cordinate, and $(u_j)^n$ implies displacements of order 'n'. The nature of equations for a homogeneous plate with zero and first order approximations have been discussed. Zero order approximations give, for an isotropic plate, reasonable

results for extensional vibrations but not for flexure [69 - Chapter IV]. First order approximations are accurate for flexural vibrations, and in addition accommodate simple thickness modes as well (simple thickness shear and simple thickness stretch modes [69 - Chapter V].

Yi-Yuan Yu [20] has used first order approximations for 'u' displacement and zero order approximation for 'w' displacement, while analysing free vibrations of elastic symmetrical sandwich plates, in plane strain.

First order approximations for layer (i) imply

$$\left.\begin{aligned} u_i^* &= u_i^{(o)} + z u_i^{(1)} \\ w_i^* &= w_i^{(o)} + z w_i^{(1)} \end{aligned}\right| \qquad \text{(II.38)}$$

The notations used in the present derivation are:

For $u_i^{(o)}$; u_i will be used.

For $u_i^{(1)}$; $\bar{u}_i$ will be used.

And, w_i and $\bar{w}_i$ denote $w_i^{(o)}$ and $w_i^{(1)}$ respectively.

So, for a 3 layered laminate, we have 12 parameters, due to

$$u_i,\ \bar{u}_i,\ w_i \text{ and } \bar{w}_i \quad i = 1,2,3 \qquad \text{(Fig.II-3)}$$

However, all these are not independent, from reasons of continuity of displacements at interfaces, Only 8 parameters are independent, since at interfaces,

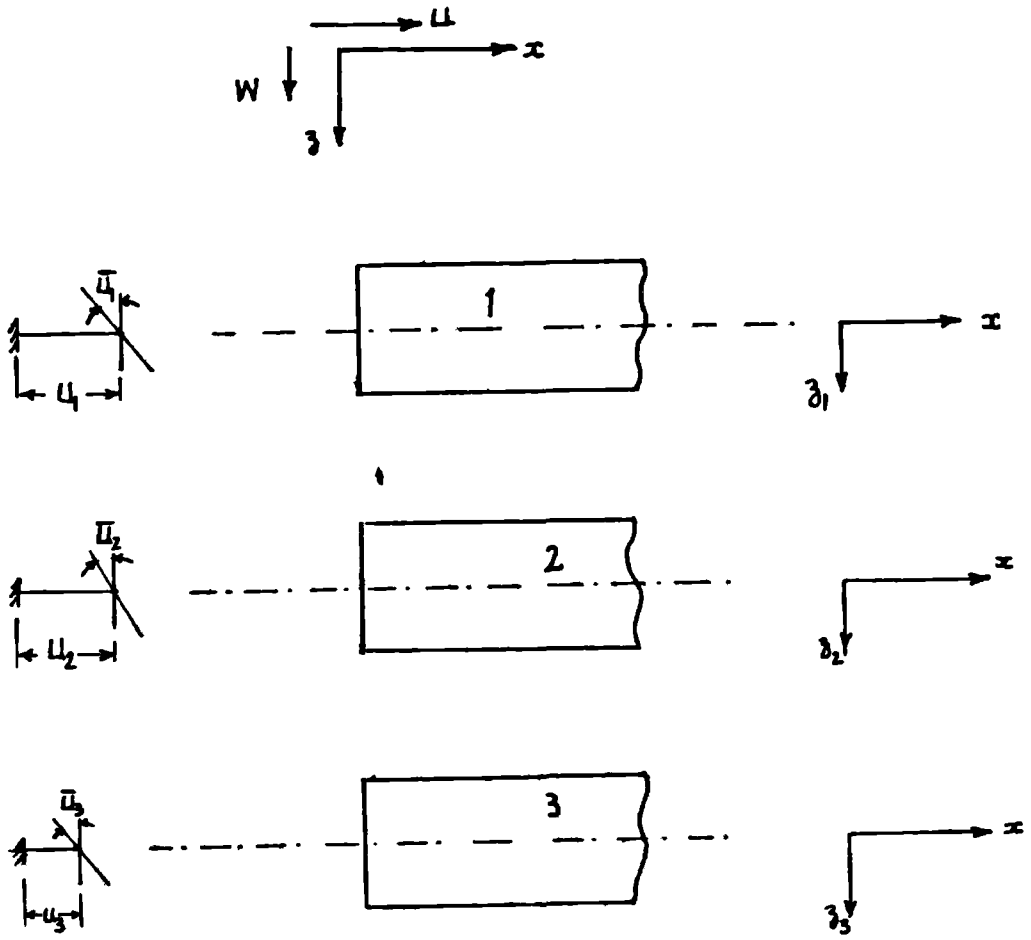

FIG. II-3

$$
\left.
\begin{aligned}
u_1 + \bar{u}_1 \frac{t_1}{2} &= u_2 - \bar{u}_2 \frac{t_2}{2} \\
w_1 \quad \bar{w}_1 \frac{t_1}{2} &= w_2 - \bar{w}_2 \frac{t_2}{2} \\
u_2 \quad \bar{u}_2 \frac{t_2}{2} &= u_3 - \bar{u}_3 \frac{t_3}{2} \\
w_2 + \bar{w}_2 \frac{t_2}{2} &- w_3 - \bar{w}_3 \frac{t_3}{2}
\end{aligned}
\right\} \qquad \text{(II.39)}
$$

The 8 independent parameters used below, will be

$\bar{u}_1$, $\bar{u}_2$, $\bar{u}_3$, u_2 and $\bar{w}_1$, $\bar{w}_2$, $\bar{w}_3$ and w_2.

In [20] and [69], equations of motion have been derived from the variationalequation $\int_v (\tau_{ij,i} - \rho\ddot{u}j)\, \delta u_j dv = 0$. τ is for stress and v is for volume. This equation is derivable from Hamilton's Principle [69 page 3.02 and 1.20]. We shall use Hamilton's Principle as such, as used in Section II.C for Analysis I i.e.

$$\delta \int_{t_1}^{t_2} (T - U + V)\, dt = 0 \qquad \text{(II.40)}$$

For a beam, using plane stress conditions, stress strain relations are: [92]

$$\varepsilon_x = \frac{1}{E} [\sigma_x - \nu\sigma_z]$$

$$\varepsilon_z = \frac{1}{E} [\sigma_z - \nu\sigma_x] ,$$

E is for Young's modulus
ν is for Poisson's ratio
ε is for strain and
σ is for stress

These can be reduced to the form:

$$
\left.
\begin{aligned}
\sigma_x &= E^* e_x + \bar{z}\, e_z \\
\sigma_z &= E^* e_z + \bar{z}\, e_x
\end{aligned}
\right\} \qquad \text{(II.41)}
$$

where $E^* = \frac{E}{1-\nu^2}$

$Z = \frac{\nu E}{1-\nu^2}$

Also $\tau = G\gamma$ (II.42)

where τ is shear stress and γ is shear strain and G is shear modulus.

Now, expression for strain energy

$$U = \Sigma \int_o^v \tfrac{1}{2} [\sigma_x e_x + \sigma_z e_z + \tau\gamma \quad dv$$

Substituting from (II.41) and (II.42)

$$U = \Sigma \int_o^v \tfrac{1}{2} [E^*(e_x^2 \; e_z^2) \quad 2Z \; e_x e_z \quad G\gamma^2] \; dv \quad \text{(II.43)}$$

summed for all layers over the entire volume v. Taking the coordinate system as in Fig.II-3 and dummy coordinate systems xz_1, xz_2 and xz_3 in layers 1, 2 and 3 respectively, and with signs of longitudinal and transverse displacements taken independently, we have for layer (i),

$$\left.\begin{aligned} e_{x_i} - \frac{\partial}{\partial x} u_i^* &= u_i' + \bar{u}_i' \; z_i \\ e_{z_i} - \frac{\partial}{\partial z} w_i^* &= \bar{w}_i \\ \gamma_i = \frac{\partial u_i^*}{\partial z} + \frac{\partial w^*}{\partial x} &= \bar{u}_i \quad w_i' + \bar{w}_i' \; z_i \end{aligned}\right\} \quad \text{(II.44)}$$

Substituting eqn. (II.44) in eqn. (II.43) and simplifying

$$\text{strain energy for layer (i)} = \int_o^L \{\frac{E_i^*}{2}(u_i'^2 t_i + \bar{u}_i'^2 \frac{t_i^3}{12} + \bar{w}_i^2 t_i) + g_i(u_i' \bar{w}_i t_i) + \frac{k_i G_i}{2}(\bar{u}_i^2 t_i + w_i'^2 t_i \; \bar{w}_i'^2 \frac{t_i^3}{12} + 2\bar{u}_i w_i' t_i)\} b \, dx \tag{II.45}$$

where k_i is shear coefficient of layer (i), due to non-uniform distribution of shear stress across thickness.

Total Kinetic Energy 'T' due to layer (i)

$$= \int_o^L \int_{-\frac{t_i}{2}}^{\frac{t_i}{2}} \{\frac{\rho_i}{2}(\dot{w}i + \dot{\bar{w}}_i z_i)^2 b dz_i\} dx + \int_o^L \int_{-\frac{t_i}{2}}^{+\frac{t_i}{2}} \{\frac{\rho_i}{2}(\dot{u}_i \; \dot{\bar{u}}_i z_i)^2 b dz_i\} dx$$

$$= \int_o^L \{\frac{\rho_i}{2}(\dot{w}_i^2 t_i + \dot{\bar{w}}_i^2 \frac{t_i^3}{12})\} b dx + \int_o^L \{\frac{i}{2}(\dot{u}_i^2 t_i + \dot{\bar{u}}_i^2 \frac{t_i^3}{12})\} b dx \tag{II.46}$$

$_i$ is mass density of layer i per unit volume.

Potential energy 'V' due to dynamic loading of intensity f(x)g(t) as in Fig.II.2(c) applied on layer (1)

$$= g(t) \int_o^L f(x) \; (w_1 - \bar{w}_1 \frac{t_1}{2}) \, dx \tag{II.47}$$

Applying Hamilton's Principle as given by eqn. (II.40), expressions for U, T and V being given by eqns. (II.45), (II.46) and (II.47) respectively, summation is done for layers i = 1, 2, 3 for these expressions. Also, u_1, u_3, w_1 and w_3 are eliminated from these expressions by using eqn. (II.39). The details are given in Appendix 2, where 8 simultaneous partial differential equations are deduced by

carrying out the variations of the various energy integrals.

These 8 equations reduce to 5 simultaneous equations (II.48) to (II.52), if variation of w is not taken into account, i.e. $\bar{w}_1$, $\bar{w}_2$ and $\bar{w}_3$ are not taken in the formulation. The remaining unknowns of the system are: u_2, $\bar{u}_1$, $\bar{u}_2$, $\bar{u}_3$ and w_2. w_2 is replaced by w from here onwards.

$$\frac{E_1^*}{2} b\left(\frac{2}{3} t_1^3 \bar{u}_1'' - t_1^2 u_2'' + \frac{t_1^2 t_2}{2} \bar{u}_2''\right) - k_1 G_1 b(t_1 \bar{u}_1 + t_1 w') = \frac{\rho_1}{2} b\left[\ddot{\bar{u}}_1 \frac{t_1^3}{2} + \ddot{u}_2 t_1^2 + \frac{t_1^2 t_2}{2} \ddot{\bar{u}}_2 + \frac{t_1^3}{6} \ddot{\bar{u}}_1\right] \qquad \text{(II.48)}$$

$$\frac{E_1^*}{2} b(2t_1 u_2'' - t_1 t_2 \bar{u}_2'' - t_1^2 \bar{u}_1'') + \frac{E_3^*}{2} b(2t_3 u_2'' + t_2 t_3 \bar{u}_2'' \quad t_3^2 \bar{u}_3'') + b\frac{E_2^*}{2}(2u_2'' t_2) = \frac{\rho_1}{2} b[2t_1 \ddot{u}_2 - t_1 t_2 \ddot{\bar{u}}_2 - t_1^2 \ddot{\bar{u}}_1] + \frac{\rho_3}{2} b[2t_3 \ddot{u}_2 + t_3 t_2 \ddot{\bar{u}}_2 + t_3^2 \ddot{\bar{u}}_3] + \frac{\rho_2}{2} b[2t_2 \ddot{u}_2] \qquad \text{(II.49)}$$

$$\frac{E_1^*}{2} b\left(\frac{t_1 t_2^2}{2} \bar{u}_2'' - t_1 t_2 u_2'' + \frac{t_1^2 t_2}{2} \bar{u}_1''\right) + \frac{E_3^*}{2} b\left(\frac{t_3 t_2^2}{2} \bar{u}_2'' \quad t_2 t_3 u_2'' + \frac{t_3^2 t_2}{2} \bar{u}_2''\right) + \frac{E_2^*}{2} b\left(\frac{t_2^3}{6} \bar{u}_2''\right) - k_2 G_2 t_2 b(w_2' + \bar{u}_2) = \frac{\rho_1}{2} b\left[\frac{t_1 t_2^2}{2} \ddot{\bar{u}}_2 - t_1 t_2 \ddot{u}_2 + \frac{t_1^2 t_2}{2} \ddot{\bar{u}}_1\right] \quad \frac{\rho_3}{2} b\left[\frac{t_3 t_2^2}{2} \ddot{\bar{u}}_2 + t_3 t_2 \ddot{u}_2 + \frac{t_2 t_3^2}{2} \ddot{\bar{u}}_3\right] + \frac{\rho_2}{2} b\left[\ddot{\bar{u}}_2 \frac{t_2^3}{6}\right] \qquad \text{(II.50)}$$

$$b\frac{E_3^*}{2}\left[\frac{2}{3}t_3^3\bar{u}_3''+t_3^2u_2''+\frac{t_2t_3^2}{2}\bar{u}_2''\right]-k_3G_3t_3b(\bar{u}_3+w_2')$$

$$=b\frac{\rho_3}{2}\left[\frac{2}{3}t_3^3\ddot{\bar{u}}_3+t_3^2\ddot{u}_2+\frac{t_2t_3^2}{2}\ddot{\bar{u}}_2\right] \qquad \text{(II.51)}$$

$$bk_1G_1t_1(\bar{u}_1'-w'')\quad bk_3G_3t_3(\bar{u}_3'+w'')+bk_2G_2t_2(\bar{u}_2'-w'')$$

$$=b(\rho_1t_1+\rho_2t_2+\rho_3t_3)\ddot{w}-g(t)f(x) \qquad \text{(II.52)}$$

Boundary conditions for simply supported beam are:

$$\left.\begin{aligned}\bar{u}_1'=\bar{u}_2'=\bar{u}_3'=u_2'=0\\ w=0\end{aligned}\right| \qquad \text{(II.53)}$$

For symmetrical case (i.e. when faces 1 and 3 are identical), $\bar{u}_1=\bar{u}_3$, $u_2=0$

$$E_1=E_3 \text{ and } t_1=t_3.$$

For these conditions, equations (II.48) and (II.51) are identical and eqn. (II.49) disappears. Only 3 equations (II.48), (II.50) and (II.52) exist. These can be shown to be similar to 3 equations of [20]. It is seen that equation (II.52) is similar to III equation of eqn. 30 in [20]. Eqn. (II.50) is similar to II eqn. of eqn. (30) in [20 and L n. (II.48) is identical to the one got by substracting eqn. I and II of eqn. (30) in [20].

There is a discrepancy in eqns. (II.48) to (II.52), which becomes evident when these are compared with eqns. (II.13) to (II.15). E_i^* in eqns. (II.48) to (II.52) involves

Poisson's ratio ν_i, ($E_i^* = \frac{E_i}{1-\nu_i^2}$), but Poisson's ratio does not occur in (II.13) - (II.15). In both cases, transverse displacement is constant at a section, so stresses and strains in transverse direction are not of importance, and hence 'v' is not expected to occur in these beam equations. The reason of occurrence of 'v' in eqns. (II.48) - (II.52) is due to the fact that these equations have been simplified from 8 simultaneous equations in Appendix II, where neglecting effect of σ_z and e_z still leaves stress-strain relation as

$$\sigma_x = E^* e_x \quad \text{(from eqn. II.41)}$$

$$= \frac{E}{1-\nu^2} e_x$$

In eqns. (II.13) to (II.15), $\sigma_x = E e_x$ has been taken. So in eqns. (II.48) - (II.52), the terms E_i^* (i = 1, 2, 3) should be replaced by E_i, for the above-mentioned reasons.

II.D.2 : Solution for simply supported beam - Elastic case

For simply supported beam, assuming a solution in series form, for sinusoidal excitation conditions as:

$$\left.\begin{aligned} u_2 &= \sum_{n=1}^{\infty} u_{2n} \cos \frac{n\pi x}{L} \sin pt \\ \bar{u}_2 &= \sum_{n=1}^{\infty} \bar{u}_{2n} \cos \frac{n\pi x}{L} \sin pt \\ \bar{u}_1 &= \sum_{n=1}^{\infty} \bar{u}_{1n} \cos \frac{n\pi x}{L} \sin pt \end{aligned}\right\} \quad \text{(II.54)}$$

$$\left.\begin{aligned} \bar{u}_3 &= \sum_{n=1}^{\infty} \bar{u}_{3n} \cos \frac{n\pi x}{L} \sin pt \\ w &= \sum_{n=1}^{\infty} w_n \sin \frac{n\pi x}{L} \sin pt \end{aligned}\right\}$$

This solution is for a sandwich with elastic core.

It is seen that the solution above satisfies the boundary conditions and reduces the differential equations (II.48) to (II.52) to algebraic equations, when substituted.

Expanding $f(x) = \sum_{n=1}^{\infty} f_n \sin \frac{n\pi x}{L}$, and substituting eqn. (II.54) in (II.48) - (II.52) gives

$$\left.\begin{aligned} u_{2n}A - \bar{u}_{2n}B - \bar{u}_{1n}C &= w_n D \\ u_{2n}F - \bar{u}_{2n}H - \bar{u}_{1n}J &= w_n K \\ -u_{2n}M - \bar{u}_{2n}N - \bar{u}_{3n}P &= w_n Q \\ -u_{2n}R - \bar{u}_{2n}S + \bar{u}_{3n}T &= -w_n V \\ \bar{u}_{2n}Q_2 + \bar{u}_{1n}Q_1 + \bar{u}_{3n}Q_3 + w_n[I] &= \frac{f_n}{b} \end{aligned}\right\} \qquad \text{(II.55)}$$

where

$$A = \frac{E_1}{2}\left(\frac{n\pi}{L}\right)^2 t_1^2 - \frac{\rho_1 t_1^2}{2} p^2$$

$$B = \frac{E_1}{4}\left(\frac{n\pi}{L}\right)^2 t_1^2 t_2 - \frac{\rho_1 t_1^2 t_2}{4} p^2$$

$$C = \frac{t_1^3}{3} E_1 \left(\frac{n\pi}{L}\right)^2 + k_1 G_1 t_1 - \frac{\rho_1}{3} t_1^3 p^2$$

$$F = E_1 t_1 t_2 \left(\frac{n\pi}{L}\right)^2 + \frac{t_2^2}{2}\left(\frac{n\pi}{L}\right)^2 E_2 - \rho_1 t_1 t_2 p^2 - \frac{\rho_2 t_2^2}{2} p^2$$

$$H = \frac{E_1}{2} t_1 t_2^2 \left(\frac{n\pi}{L}\right)^2 + \frac{E_2}{12} t_2^3 \left(\frac{n\pi}{L}\right)^2 + k_2 G_2 t_2 - \frac{\rho_1 t_1 t_2^2}{2} p^2 - \frac{\rho_2 t_2^3}{12} p^2$$

$$J = \frac{E_1}{2} t_1^2 t_2 \left(\frac{n\pi}{L}\right)^2 - \frac{\rho_1 t_1^2 t_2}{2} p^2$$

$$M = \left(\frac{n\pi}{L}\right)^2 \left[E_3 t_3 t_2 + \frac{E_2}{2} t_2^2\right] - \rho_3 t_2 t_3 p^2 - \frac{\rho_2 t_2^2}{2} p^2$$

$$N = \frac{E_3}{2} t_3 t_2^2 \left(\frac{n\pi}{L}\right)^2 + \frac{E_2 t_2^3}{12}\left(\frac{n\pi}{L}\right)^2 + k_2 G_2 t_2 - \rho_3 \frac{t_2^2 t_3}{2} p^2 - \frac{\rho_2 t_2^3}{12} p^2$$

$$P = \frac{E_3}{2} t_3^2 t_2 \left(\frac{n\pi}{L}\right)^2 - \rho_3 \frac{t_2 t_3^2}{2} p^2$$

$$R = \frac{E_3}{2} t_3^2 \left(\frac{n\pi}{L}\right)^2 - \frac{\rho_3 t_3^2 p^2}{2}$$

$$S = \frac{E_3}{4}\left(\frac{n\pi}{L}\right)^2 t_2 t_3^2 - \frac{\rho_3 t_2 t_3^2 p^2}{4}$$

$$T = -k_3 G_3 t_3 - \left(\frac{n\pi}{L}\right)^2 \frac{t_3^3 E_3}{3} + \frac{\rho_3}{3} t_3^3 p^2$$

$$I = \left(\frac{n\pi}{L}\right)^2 \left[k_1 G_1 t_1 + k_2 G_2 t_2 + k_3 G_3 t_3\right] - \left[\rho_1 t_1 p^2 + \rho_2 t_2 p^2 + \rho_3 t_3 p^2\right]$$

$$D = k_1 G_1 t_1 \left(\frac{n\pi}{L}\right)$$

$$K = k_2 G_2 t_2 \left(\frac{n\pi}{L}\right)$$

$$Q = k_2 G_2 t_2 \left(\frac{n\pi}{L}\right)$$

$$V = -k_3 G_3 t_3 \left(\frac{n\pi}{L}\right)$$

$$Q_j = k_j G_j t_j \left(\frac{n\pi}{L}\right) \quad \text{where } j = 1,2,3$$

II.D.3: Shear Coefficient

Its value for a rectangular beam is well known and is equal to $\frac{2}{3}$, when distribution of shear stresses, in static bending is determined by assuming that warping due

to shear does not effect the bending stresses. In such a case, shear coefficient 'k' is defined as

$$= \frac{\text{average shear stress on a section}}{\text{Shear modulus x angle of shear at neutral axis.}}$$

'k' depends on shape of section and the mode of motion, which affect the distribution of shear at a section.

Mindlin and Deresiewicz [70] have determined the shear coefficient for beams, by equating the lowest thickness-shear frequency obtained from Timoshenko's approximate equation involving 'k' to that obtained from general equations of theory of elasticity. The object is to get accurate results at high frequencies. For a solid beam, this thickness shear frequency is known to occur at very high frequencies.

By using a procedure similar to above, Yu Yi Yuan [21] has found a value of 'k' for a symmetrical sandwich by matching the lowest frequency of thickness shear mode, obtainable from approximate sandwich plate theory and the exact elasticity theory. There is a single value of 'k' for the entire sandwich plate.

For an arbitrary 3 layered beam, in the equations derived in section II.D.1, 3 values of 'k' have been used, value of k being different for each layer. In each layer, the shear strain γ due to assumed displacements ($\gamma = \frac{\partial u}{\partial z} + \frac{\partial w}{\partial x}$) might appear to be constant. But equilibrium

equation $\frac{\partial \sigma_x}{\partial x} + \frac{\partial \tau_{zx}}{\partial z} = 0$ implies that τ_{zx} is varying through the thickness. Hence, in order to get an expression for the transverse shear Q at a section for any layer, Q is taken = kGAγ, A is area and G is shear modulus. For Section II.C, k_2 is required to be found, if extension effect of core 2 is taken into account. If this effect is not taken into account, it may be seen from equilibrium considerations that shear strain is constant across the thickness of core and hence $k_2 = 1$.

Below, the values of k for each layer will be determined, by making the assumption that warping due to shear does not affect the longitudinal stresses due to bending. Now, the additional effect taken in section II.D, compared to those in II.C are the shear effects in faces. Since we assume that the introduction of shear effects does not affect the longitudinal stresses due to bending, the distribution of shear stresses in various layers due to bending will be found from section II.C.

Considering the various layers as shown in Fig.II-4, y_i and z_i are dummy coordinates in layer (i) where i = 1,2,3. Taking τ_1 as the shear stress in layer 1 at a distance z_1 from interface and u_{y1} as the longitudinal displacement at distance y_1 from the interface between layers 1 and 2.

$$u_{yL} = u_1 - w' \frac{t_1}{2} + y_1 w' \quad \text{(From section III.C.1 - Fig.II-2)} \qquad \text{(II.56)}$$

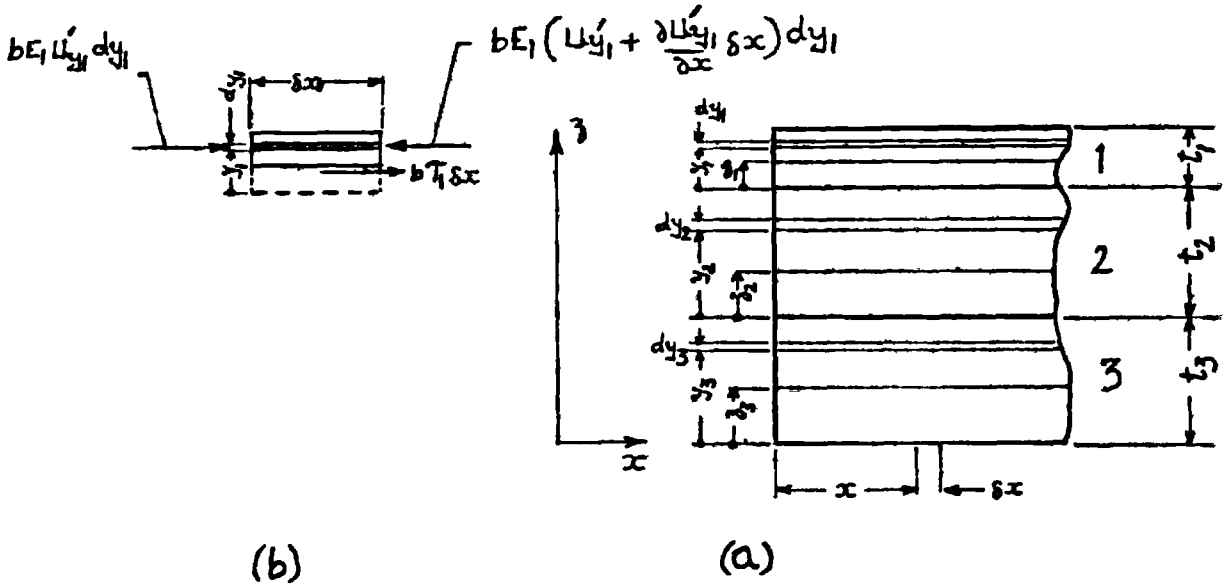
$bE_1 u'_{y1} dy_1$
$bE_1 \left(u'_{y1} + \frac{\partial u'_{y1}}{\partial x} \delta x\right) dy_1$
$b\tau_1 \delta x$
3
x
1
2
3
t_1
t_2
t_3
x
δx
(b)
(a)

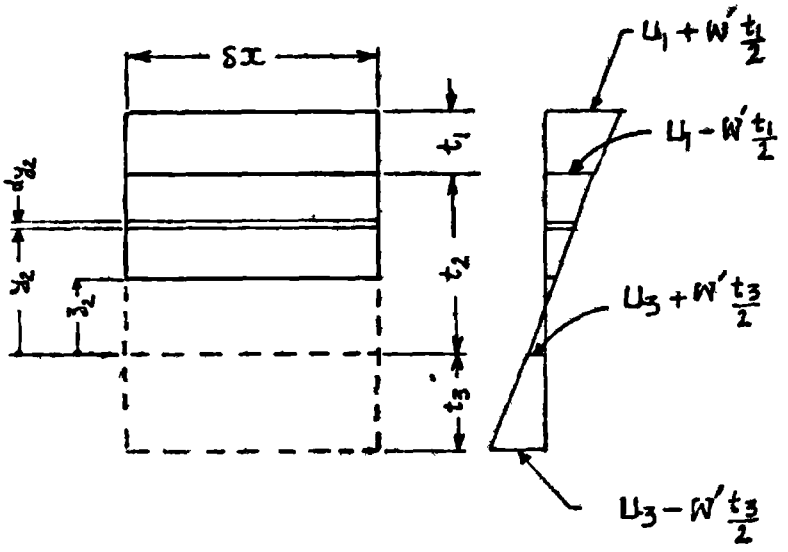
δx
t_1
t_2
t_3
$u_1 + w' \frac{t_1}{2}$
$u_1 - w' \frac{t_1}{2}$
$u_3 + w' \frac{t_3}{2}$
$u_3 - w' \frac{t_3}{2}$
(c)
(d)

FIG II-4

Equilibrium of forces in 'x' direction, acting on the element as shown in Fig.II-4(b) gives:

$$\tau_1 \, b \, \delta x = b \, E_1 \, \delta x \int_{z_1}^{t_1} (u''_{y1}) \, dy_1 .$$

Substituting for u_{y1} and simplifying, τ_1

$$- E_1[(u_1'' - w''' \frac{t_1}{2})(t_1 - z_1) \quad \frac{w'''}{2} (t_1^2 - z_1^2]$$

(II.57)

τ_1 is zero at $z_1 = t_1$, i.e. at free surface.

Shear force Q_1 in layer (1) $= b \int_{t_1}^{o} \tau_1 dz_1$

Substituting for τ_1 and integrating,

$$Q_1 = -bE_1[u_1'' \frac{t_1^2}{2} + w''' \frac{t_1^3}{12}] \qquad \text{(II.58)}$$

Similarly, for layer 3, using y_3 and z_3 as dummy coordinates, u_{y3} as longitudinal displacement at distance y_3 and τ_3 as shear stress at distance z_3 from free surface, and employing the same procedure as for layer 1,

$$\tau_3 = E_3[u_3'' - w''' \frac{t_3}{2})z_3 + \frac{w''}{2} z_3^2] \qquad \text{(II.59)}$$

τ_3 is zero at free surface, i.e. where $z_3 = 0$

Shear force $Q_3 = b \int_{o}^{t_3} \tau_3 dz_3$

$$bE_3[u_3'' \frac{t_3^2}{2} \quad \frac{w'''}{12} t_3^3] \qquad \text{(II.60)}$$

Taking τ_2 as shear stress in layer 2 at distance z_2 from

interface of layers 2 and 3 and u_{y_2} as the longitudinal displacement at distance y_2 from the same interface, (Figs. II-4 c and d)

$$u_{y_2} = Py_2 + Q$$

$$\text{where} \quad P = \frac{(u_1 - w' \frac{t_1}{2}) - (u_3 + w' \frac{t_3}{2})}{t_2}$$

$$Q = u_3 + w' \frac{t_3}{2}$$

Equilibrium of forces in x direction, as shown in Fig. II-4(c) gives

$$\tau_2 b\delta x = bE_1\delta x \int_o^{t_1} \{u_1'' + w'''(y_1 - \frac{t_1}{2})\} dy_1 + bE_2\delta x \int_{z_2}^{t_2} (P''y_2 + Q'')\, dy_2$$

$$\text{or} \quad \tau_2 = E_1 u_1'' t_1 + E_2 \left[\frac{P''}{2}(t_2^2 - z_2^2) + Q''(t_2 - z_2)\right] \qquad \text{(II.61)}$$

$$Q_2 = b \int_o^{t_2} \tau_2 dz_2$$

$$= b\left[E_1 u_1'' t_1 t_2 + \frac{E_2 P''}{3} t_2^3 + \frac{E_2 Q''}{2} t_2^2\right] \qquad \text{(II.62)}$$

For each layer, k will be taken as

$$= \frac{\text{Average shear stress in the layer}}{\text{Shear modulus x Angle of shear at middle of layer}}$$

$$= \frac{\text{Average shear stres in layer}}{\text{Shear stress at middle of layer}} \qquad \text{(II.63)}$$

Value of k for each layer can be written down, knowing expressions for τ and Q for each layer, as given by equations

(II.57) to (II.62).

Substituting the solution for simply supported beams,

viz. $$w = \sum_{n=1}^{\infty} w_n \sin \frac{n\pi x}{L}$$

$$u_1 = \sum_{n=1}^{\infty} u_{1n} \cos \frac{n\pi x}{L}$$

and simplifying

$$k_1 = \frac{\sum_{n=1}^{\infty}[\frac{u_{1n}t_1}{2} + \frac{w_n t_1^2}{12}(\frac{n\pi}{L})]}{\sum_{n=1}^{\infty}[\frac{u_{1n}t_1}{2} + \frac{w_n t_1^2}{8}(\frac{n\pi}{L})]} \qquad \text{(II.64)}$$

$$k_3 = \frac{\sum_{n=1}^{\infty}[\frac{-u_{3n}t_3}{2} + \frac{w_n t_3^2}{12}(\frac{n\pi}{L})]}{\sum_{n=1}^{\infty}[\frac{-u_{3n}t_3}{2} + \frac{w_n t_3^2}{8}(\frac{n\pi}{L})]} \qquad \text{(II.65)}$$

$$k_2 = \frac{\sum_{n=1}^{\infty}[E_1 t_1 u_{1n} + E_2 t_2(\frac{u_{1n}}{3} + \frac{u_{3n}}{6}) + E_2 t_2(\frac{n\pi}{L})w_n(\frac{t_3}{12} - \frac{t_1}{6})]}{\sum_{n=1}^{\infty}[E_1 t_1 u_{1n} + E_2 t_2(\frac{3}{8}u_{1n} + \frac{u_{3n}}{8}) + E_2 t_2(\frac{n\pi}{L})w_n(-\frac{3}{16}t_1 + \frac{t_3}{16})]} \qquad \text{(II.66)}$$

As discussed earlier, if $E_2 = 0$, i.e. extension effect of layer 2 is not taken into account, $k_2 = 1$.

For any given situation, the values of k_1, k_2 and k_3 can be calculated if w_n and u_{1n} are known. These should be got from analysis I given in Section II.C. Since k_2

required in II.C is not known, initially it may be taken equal to 1 and w_n and u_{1n} may be computed. A new value of k_2 is got from eqn. (II.66). This value may be used again and the process repeated till two consecutive values obtained are almost similar.

Thus, thevalues of k_1, k_2 and k_3 required in section II.D and k_2 in section II.C may be got from equations derived above. These values are meant for the elastic case, i.e. when all layers are elastic. For a 3 layered configuration, with viscoelastic core, strictly speaking, k_i as defined by eqn. (II.63) is a complex quantity. So in response analysis of a sandwich involving viscoelastic laminates, k_i should be regarded as complex in the equations of motion, but it makes the equations more complicated. However in calculating modal loss factor, 'k_i' might be taken as real, since at a normal mode, the phase difference between average shear stress and shear stress at middle of any layer is expected to be small, especially if the material loss factor is low. In the present work, k_i has been taken as a real quantity, for simplicity, since the evaluation of damping is done at a normal mode and the response analysis is carried out at low frequencies involving core viscoelastic materials which are not rigid.

Values of k_i have been listed for a given sandwich

in section III.B. The values are nearly equal to 1, but k_2 tends to have different value for a sandwich having a rigid core.

II.D.4 : Solution for Simply Supported Beam with Viscoelastic Core

The solution for a 3 layered sandwich with elastic core, and simply supported ends has been already obtained in section II.D.2. For viscoelastic core, when the sandwich is subjected to sinusoidal excitation conditions, the moduli for the core can be replaced by their complex values. Replacing G_2 by $G_2(1+ i\eta_2)$ and E_2 by $E_2(1+i\beta_2)$ in eqns. (II.55) gives the solution required. In above, η_2 is the loss factor in shear and β_2 is that under direct stress/strain conditions.

The solution for transverse displacement is given by

$$W = \sum_{n=1}^{\infty} w_n \sin \frac{n\pi x}{L} \sin pt$$

where w_n is given by

$$bw_n[R_{T_n} + iI_{T_n}] = f_n \qquad \text{(II.67)}$$

$$R_{T_n} = \text{Real Term} = (I^r - Q_1 \frac{D}{C} - Q_3 \frac{V}{T}) + \frac{\left[(R_1R_2+I_1I_2)(Q_1\frac{A}{C}+Q_3\frac{R}{T} - Q_2{}^i(I_3R_2-I_2R_3) + (R_3R_2+I_3I_2)(Q_2{}^r-Q_1\frac{B}{C} + Q_3 \frac{S}{T})\right]}{R_2^2 + I_2^2}$$

I_{T_n} = Imaginary Term =

$$I^i + \frac{\left[\begin{array}{l}(I_1R_2-I_2R_1)(Q_1\frac{A}{C}+Q_3\frac{R}{T}) \\ +Q_2{}^i(R_3R_2+I_3I_2)+(I_3R_2-I_2R_3)(Q_2{}^r-\frac{Q_1B}{C}+Q_3\frac{S}{T})\end{array}\right]}{R_2{}^2+I_2{}^2}$$

where $R_1 = (VP-TQ)(BJ-CH)-TCQ^IH^I+(TN+SP)(DJ-CK)+TCN^IK^I$

$I_1 = TN^I(DJ-CK)-CK^I(TN+SP)-TQ^I(BJ-CH)-CH^I(VP-TQ)$

$R_2 = (RP+TM)(BJ-CH)+TCM^IH^I+(SP\ TN)(AJ-CF)+TCN^IF^I$

$I_2 = TM^I(BJ-CH)-CH^I(RP+TM)+TN^I(AJ-CF)-CF^I(SP+TN)$

$R_3 = (VP-TQ)(AJ-CF)-TCQ^IF^I-(DJ-CK)(RP+TM)-CTK^IM^I$

$I_3 = -TQ^I(AJ-CF)-CF^I(VP-TQ)+CK^I(RP\ TM)-TM^I(DJ-CK)$

$F^I = (\frac{n\pi}{L})^2\ [t_2{}^2\ \frac{E_2}{2}\beta_2]$

$H^I = \frac{E_2}{12}\ (\frac{n\pi}{L})^2t_2{}^3\beta_2+k_2G_2t_2\eta_2$

$K^I = k_2G_2t_2\eta_2(\frac{n\pi}{L})$

$M^I = (\frac{n\pi}{L})^2\ [\frac{E_2}{2}\ t_2{}^2\beta_2]$

$N^I = (\frac{n\pi}{L})^2\ [\frac{E_2t_2{}^3}{12}\ \beta_2]+k_2G_2t_2\eta_2$

$Q^I = \frac{n\pi}{L},\ k_2G_2t_2\eta_2$

$Q_2{}^I = k_2G_2t_2\eta_2(\frac{n\pi}{L})$

$I^I = (\frac{n\pi}{L})^2\ [k_2G_2t_2\eta_2]$

Expressions for the remaining terms A, C, D etc. are given with equation (II.55).

Further

$$u_{2n} = w_n\left[\frac{X}{Y}\right] \tag{II.68}$$

$$\bar{u}_{2n} = w_n\left[\frac{Z}{Y}\right] \tag{II.69}$$

$$\bar{u}_{1n} = w_n\left[\frac{A}{C}\frac{X}{Y} - \frac{B}{C}\frac{Z}{Y} - \frac{D}{C}\right] \tag{II.70}$$

$$\bar{u}_{3n} = w_n\left[\frac{R}{T}\frac{X}{Y} + \frac{S}{T}\frac{Z}{Y} + \frac{V}{T}\right] \tag{II.71}$$

where

$$\frac{X}{Y} = \frac{R_1R_2+I_1I_2}{R_2^2\ I_2^2} + i\,\frac{I_1R_2-I_2R_1}{R_2^2+I_2^2}$$

$$\frac{Z}{Y} = \frac{R_3R_2\ I_3I_2}{R_2^2+I_2^2} + i\,\frac{I_3R_2-I_2R_3}{R_2^2+I_2^2}$$

Substituting for u_{2n}, $\bar{u}_{2n}$ and $\bar{u}_{1n}$ and $\bar{u}_{3n}$ in eqn. (II.54) gives complete solution.

CHAPTER III : SOME STUDIES ON 3-LAYERED CONFIGURATIONS

III.A Damping effectiveness

III.A.1 : Expressions defining damping effectiveness

The resonant response of a distributed system is damping controlled in the same way as that of a lumped parameter spring mass system [50, 61]. On this stipulation, criteria for damping effectiveness are derived in [49]. The displacement response to sinusoidal excitation at a normal mode is obtained from the equation

$$-mp^2q + K(1+ i\eta_s)q = f_o \sin pt \qquad \text{(III.1)}$$

where q is the generalized displacement coordinate for any mode, f_o is the amplitude of harmonic loading, m is the generalized mass, K is generalized stiffness, and η_s is the damping loss factor of the system. The relations of η_s to other definitions of damping like critical damping ratio, log. decrement, ratio of energy dissipated per cycle to maximum strain energy etc. are given in [2 and 61].

Resonant response for damped structure = $\frac{f_o}{K\eta_s}$

Before the addition of damping, resonant response of untreated structure = $f_o/K_R\eta_R$, $\eta_R \ll \eta_s$

K_R and η_R being the generalized stiffness and damping of the untreated system.

(ii) Criterion for displacement response effectiveness

$$(DRE) = k\eta_s \qquad (III.2)$$

where $k = K/K_R$.

On the same basis, other criteria are derived in [49] for reducing stress, velocity, acceleration etc. Such criteria are applicable for studying damping effectiveness of the system at one mode only. However, there may be more than one mode present, due to geometry of the structure or space distribution of excitation. The influence of the latter is discussed in section III.E.

The solutions of Chapter II can be expressed in a form similar to eqn. III.1 e.g. equation II.25 of the simplified case of analysis I, which is the equation for the nth term in the series solution assumed, corresponds to equation III.1. Both these equations are for a single mode of vibration. For eqn. II.25, the expressions for various criteria can be written as follows.

$$k\eta_s \text{ or DRE for nth mode} = \frac{\text{Imaginary term in eqn. II.25}}{K_R}$$

K_R being dynamic rigidity of the reference system. If the effectiveness of a 3 layered unsymmetrical sandwich is compared with that of a solid beam of thickness t_s and Young's modulus E_s,

$$K_R = \left(\frac{n\pi}{L}\right)^4 \frac{bE_s t_s^3}{12}$$

Also, η_s or loss factor of sandwich, corresponding to nth mode $= \dfrac{\text{Imaginary term in eqn. II.25}}{\text{Real term in eqn. II.25}}$

Taking $E_s = E_3$

$t_s = t_3$ and using notations

$\theta_{i.3} = \dfrac{t_i}{t_3}$; $i = 1,2$

$\alpha_{1.3} = \dfrac{E_1}{E_3}$

$\phi_{2.3} = G_2 \,/\, E_3 t_3^2 (\dfrac{n\pi}{L})^2$

and after algebraic simplification,

$$\eta_s = \frac{H\eta_2}{(1+\alpha_{1.3}\theta_{1.3}^3)(M^2+\eta_2^2) + HM} \qquad \text{(III.3)}$$

where $H = \dfrac{3\phi_{2.3}}{\theta_{2.3}} (2\theta_{2.3}+\theta_{1.3}+1)^2(1+\eta_2^2)$

$M = \dfrac{\phi_{2.3}}{\theta_{2.3}} (\dfrac{1}{\alpha_{1.3}\theta_{1.3}}+1)(1+\eta_2^2) +1$

$$k\eta_s = \frac{H\eta_2}{M^2 \eta_2^2} \qquad \text{(III.4)}$$

(or D.R.E.)

For a generalised mode 'n', longitudinal stress at extreme fibres of layer 3

$$= E_3[u_3' \pm w'' \frac{t_3}{2}] \qquad \text{(III.5)}$$

where +ve sign is for the fibre at the interface of layers 2 and 3 and -ve sign for the outside fibre.

Substituting the assumed solution given in section II.C, eqn. III.5 becomes

$$= E_3 \left[-u_{3n}\left(\frac{n\pi}{L}\right) \mp \left(\frac{n\pi}{L}\right)^2 w_n \frac{t_3}{2}\right] \sin \frac{n\pi x}{L} \qquad \text{(III.6)}$$

Expression for u_{3n} is obtained in terms of w_n from eqn. II.21a after the substitution of the assumed solution. Using this to eliminate u_{3n} in eqn. (III.6), the longitudinal stress at the centre of the beam, at extreme fibres of layer '3' for mode 'n' is

$$- E_3\left(\frac{n\pi}{L}\right)^2 \left[\frac{mm' \frac{ac}{t_2^2}}{D\left(\frac{n\pi}{L}\right)^2 + C\left(\frac{m'}{t_2}\right)^2} - \frac{t_3}{2}\right] w_n \qquad \text{(III.7)}$$

where -ve sign gives the stress at the interface of layers 2 and 3, while ve sign gives that at the outside of layer 3. G_2 involved in 'C' has to be taken as $G_2(1+\imath\eta_2)$ for the viscoelastic core.

In a solid beam with parameters t_s and E_s, having the same generalized transverse motion 'w_n' at mode 'n',

Stress induced at the outer fibres

$$= \pm \frac{E_s t_s}{2} \left(\frac{n\pi}{L}\right)^2 w_n \qquad \text{(III.8)}$$

Stress response effectiveness (denoted by S R.E.) for the sandwich $= (k\eta_s)\, \varepsilon^{-1}$ (III.9)

where ε is the ratio of absolute value of stresses given by equations III.7 and III.8 and $(k\eta_s)$ is the transverse displacement response effectiveness.

Taking E_s and t_s as E_3 and t_3 respectively,

ε is given by

$$\varepsilon = 2\sqrt{R^2 + I^2} \qquad \text{(III.10)}$$

where

$$R = \frac{\frac{\alpha_{1.3}\theta_{1.3}}{2}(1+\theta_{1.3}+2\theta_{2.3})\left[\frac{\theta_{2.3}\alpha_{1.3}\theta_{1.3}}{\phi_{2.3}}(1+\alpha_{1.3}\theta_{1.3})(1+\eta_2^2)\right]}{\left[\frac{\theta_{2.3}\alpha_{1.3}\theta_{1.3}}{\phi_{2.3}}+(1+\alpha_{1.3}\theta_{1.3})\right]^2+\left[\eta_2(1+\alpha_{1.3}\theta_{1.3})\right]^2}$$

and

$$I = \frac{\frac{\theta_{2.3}}{2\phi_{2.3}}(\alpha_{1.3}\theta_{1.3})^2\eta_2(1+\theta_{1.3}+2\theta_{2.3})}{\left[\frac{\theta_{2.3}\alpha_{1.3}\theta_{1.3}}{\phi_{2.3}}+(1+\alpha_{1.3}\theta_{1.3})\right]^2+\left[\eta_2(1+\alpha_{1.3}\theta_{1.3})\right]^2}$$

$k\eta_s$ is given by eqn. (III.4).

In above, the damping effectiveness criteria have been derived for the simplified case of analysis I viz. from eqn. II.25. Below, the derivation of these criteria from eqn. II.20 (Analysis I - general case) and eqn. II.67 (Analysis II) will be pointed out.

In each case, the equation is of the form:

$$bw_n[R_{T_n} + iI_{T_n}] = f_n \qquad \text{(III.11)}$$

where expressions for real term 'R_{T_n}' and imaginary term 'I_{T_n}' are given in eqns. II.20 and II.67. Both R_{T_n} and

I_{T_n} involve frequency terms since all the inertia terms have been included in the derivation. However, in the simplified case, for which criteria have been derived in eqn. III.3, III.4 and III.9, it was possible to separate frequency terms from both real and imaginary terms, since only translatory inertia terms are included. The definitions of η_s, $k\eta_s$ etc. are applicable at a mode 'n' and the frequency of excitation corresponding to that mode is given by:

$$p^2 = \frac{K_R k \eta_s}{} \qquad \text{(III.12)}$$

However, for the general case of equation (III.11), frequency 'p' corresponding to the 'nth' mode is determined from $R_{T_n} = 0$. At this frequency, terms in 'I_{T_n}' involving 'p' may be determined. Then,

$$k\eta_s = \frac{bI_{T_n}}{\frac{bE_s t_s^3}{12}\left(\frac{n\pi}{L}\right)^4} \quad , \qquad \text{(III.13)}$$

where E_s and t_s are for the chosen reference system.

Because of inclusion of terms involving p' in both R_{T_n} and I_{T_n}, equations (III.1) and (III.11) are no longer similar and so there are no straightforward expressions for 'K' generalized and 'm' generalized and hence for an expression for 'η_s' in this case.

If only transverse inertia terms are taken in the

analysis, the equations II.20 and II.67 can be reduced to the form:

$$w_n \text{ [Real term '} r_{t_n} \text{'} + i \text{ Imag. term '} i_{t_n} \text{'} - \rho p^2] = f_n \qquad \text{(III.14)}$$

where 'r_{t_n}' and 'i_{t_n}' are obtained from the terms given in eqns. II.20 and II.67 for analysis I and II respectively, by eliminating all terms involving 'p'. Equations III.1, III.14 and also II.25 are of the same form and hence for nth mode,

$$\left.\begin{aligned} \eta_s &= \frac{i_{t_n}}{r_{t_n}} \\ k\eta_s &= \frac{i_{t_n}}{K_R} \end{aligned}\right\} , \qquad \text{(III.15)}$$

K_R being the generalized rigidity of the reference system.

III.A.2: Discussion on the effect of system parameters on damping effectiveness

(i): Expressions for η_s, DRE and SRE given by eqns. III.3, III.4 and III.9 respectively, are seen to be functions of the following parameters:- $\phi_{2.3}$, η_2, $\theta_{2.3}$, $\theta_{1.3}$ and $\alpha_{1.3}$. $\phi_{2.3}$ is called the shear parameter and has been chosen in such a way that it involves the in-phase shear modulus of layer 2, Young's modulus and thickness of layer 3, beam length and the modal number. All the ratios are taken with respect to one of the faces, being layer 3 in

this section. Layer 1 has been referred to as the 'cover' and layer 2 as the 'core'. Effect of each of the system parameters will be discussed.

Eqn. (III.3), when differentiated with respect to $\phi_{2.3}$ gives a stationary value of η_s. The value of $\phi_{2.3}$ corresponding to this is given by

$$(\phi_{2.3}{}^2)_{OPT.} = \frac{(1+\alpha_{1.3}\theta_{1.3}{}^3)(1+\eta_2{}^2)}{h^2(1+\alpha_{1.3}\theta_{1.3}{}^3)+ah} \qquad \text{(III.16a)}$$

where

$$a = \frac{3}{\theta_{2.3}}(1+\theta_{1.3}+2\theta_{2.3})^2(1+\eta_2{}^2)$$

$$h = \frac{1}{\theta_{2.3}}\left(\frac{1}{\alpha_{1.3}\theta_{1.3}}+1\right)(1+\eta_2{}^2)$$

This stationary value subsequently is seen to be a maximum value. Eqn. (III.16a) for shear parameter $\phi_{2.3}$ thus gives an optimum value of loss factor 'η_s'. Similarly, eqn. (III.4) for $k\eta_s$ becomes maximum at a value of $\phi_{2.3}$ given by

$$(\phi_{2.3})_{OPT.} = \frac{\sqrt{1+\eta_2{}^2}}{h} \qquad \text{(III.16b)}$$

where 'h' is same as in eqn. (III.16a). Fig.III-1 shows plots of $(\phi_{2.3})_{optimum}$ for η_s and $k\eta_s$, given by eqns. (III.16a) and (III.16b) respectively, for certain chosen parameters. The values of $(\phi_{2.3})_{opt.}$ are seen to increase with increase of core thickness ratio $\theta_{2.3}$ and

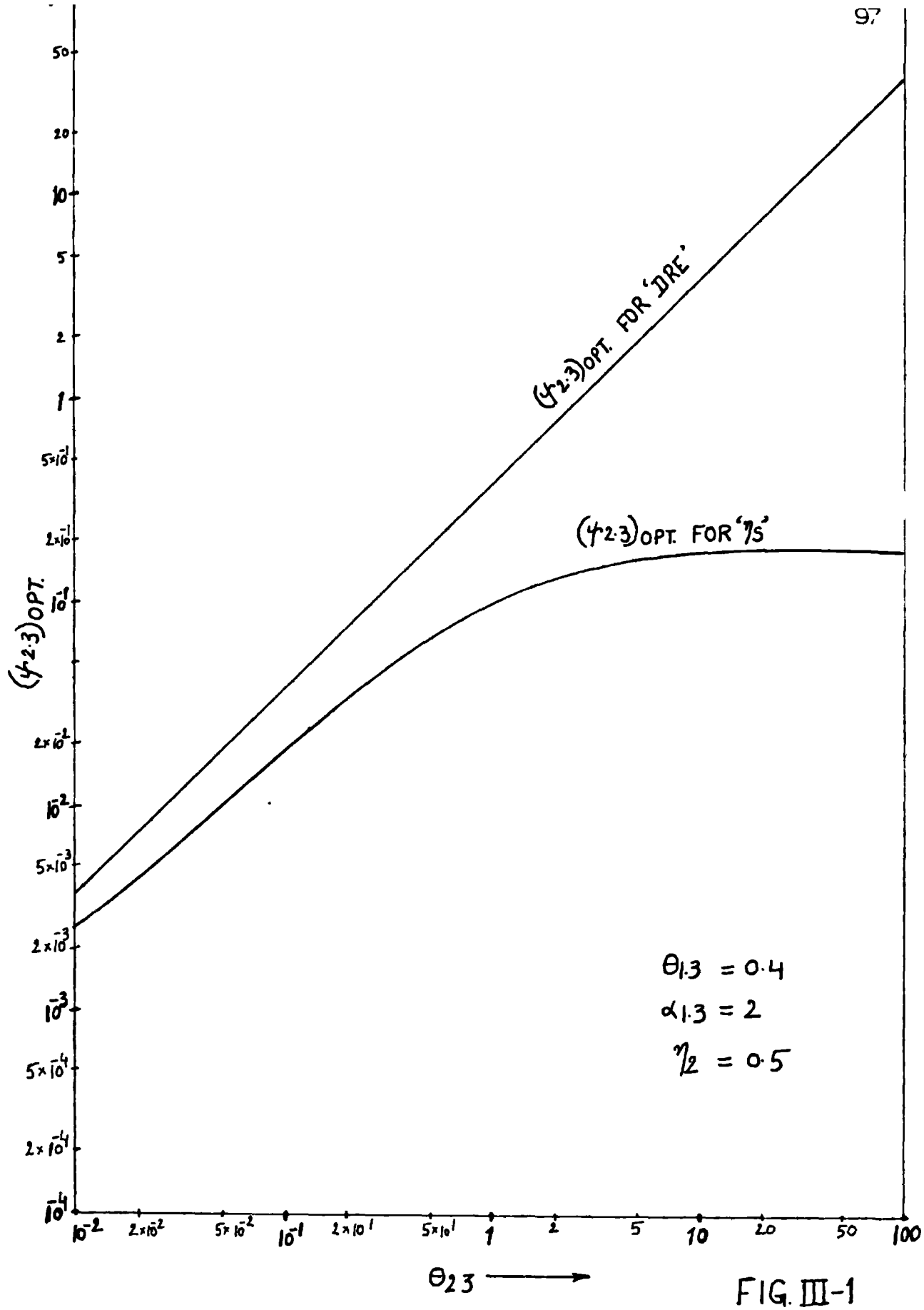
$(\psi_{2.3})_{OPT.}$ FOR 'IRE'
$(\psi_{2.3})_{OPT.}$ FOR 'ηs'
$(\psi_{2.3})_{OPT.}$
$\theta_{1.3} = 0.4$
$\alpha_{1.3} = 2$
$\eta_2 = 0.5$
θ_{23} ⟶
50
20
10
5
2
1
5×10^{-1}
2×10^{-1}
10^{-1}
2×10^{-2}
10^{-2}
5×10^{-3}
2×10^{-3}
10^{-3}
5×10^{-4}
2×10^{-4}
10^{-4}
10^{-2}
2×10^{-2}
5×10^{-2}
10^{-1}
2×10^{1}
5×10^{1}
1
2
5
10
20
50
100

FIG. III-1

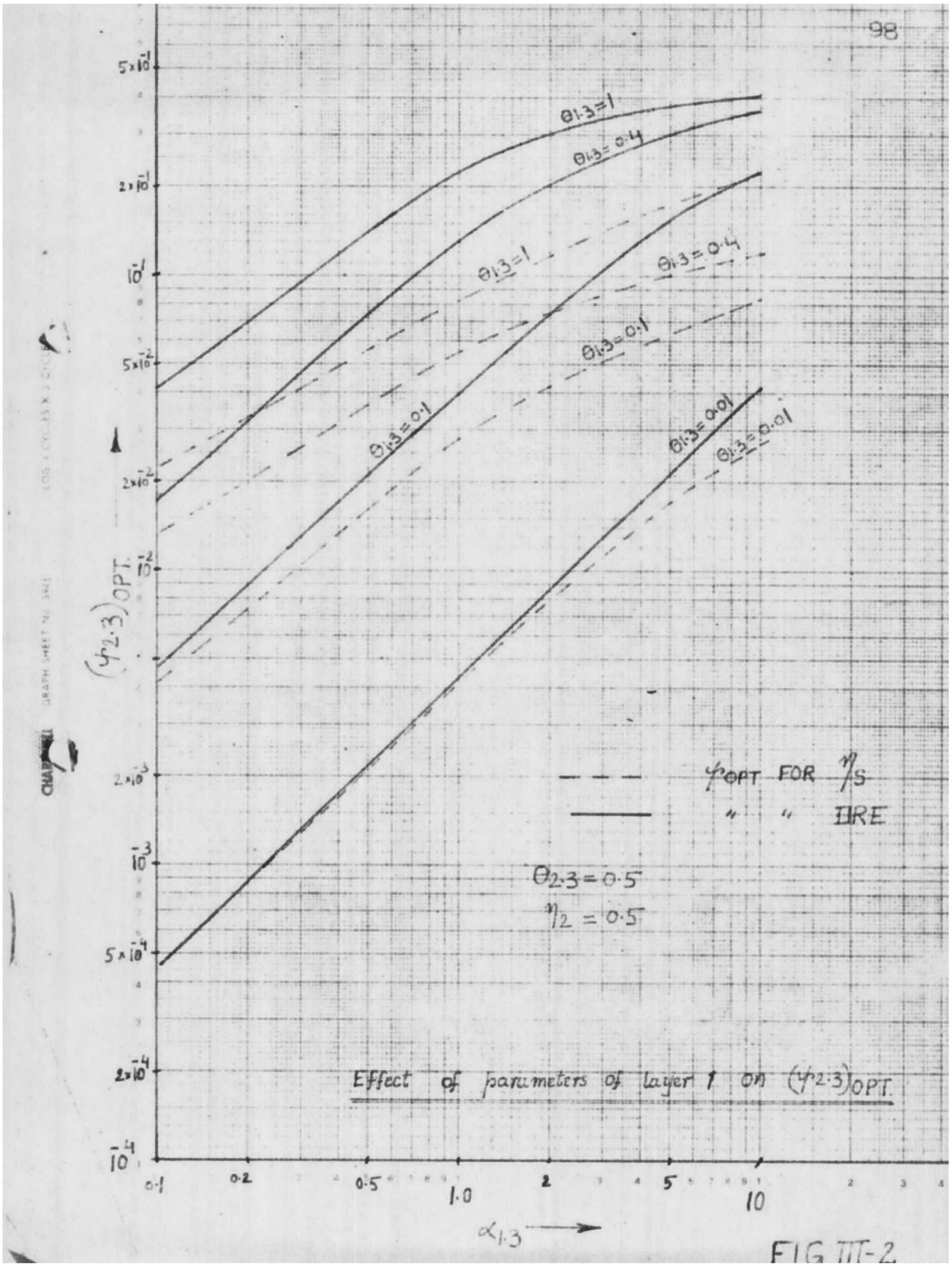

Effect of parameters of layer 1 on $(\psi_{2\cdot3})_{OPT.}$

FIG III-2

values of $(\phi_{2.3})_{opt.}$ for 'η_s' and '$k\eta_s$' are different. Fig. III-2 indicates how the optimum value of shear parameter may be varied by changing the parameters of the cover, viz. $\alpha_{1.3}$ and $\theta_{1.3}$. It is seen that the stiffer the cover used, the higher is the value of $(\phi_{2.3})_{opt.}$.

Fig. III-3 shows the influence of core material loss factor η_2 on optimum damping obtainable and the corresponding value of shear parameter, for a chosen sandwich beam, whose parameters are given on the Fig. Increase of η_2 is seen to increase $(\eta_s)_{opt.}$ almost linearly, while corresponding $(\phi_{2.3})_{opt.}$ is reduced as η_2 increases.

Fig.III-4 is a plot of η_s vs. $\phi_{2.3}$ for varying values of core thickness ratio $\theta_{2.3}$. The curves show a maximum value of η_s for optimum value of $\phi_{2.3}$. Since $\phi_{2.3}$ involves 'n', the modal number of vibrations, the sandwich will have different η_s at various modes. Also, for a given mode, only an optimum value of core shear modulus G_2 will give the maximum damping. The curves are seen to be flatter for higher values of ratios $\theta_{2.3}$. The optimum value of η_s is seen to increase with increase in $\theta_{2.3}$.

Fig. III-5 is drawn for DRE and SRE (for maximum stress at the outer fibre of layer 3) and behaviour is

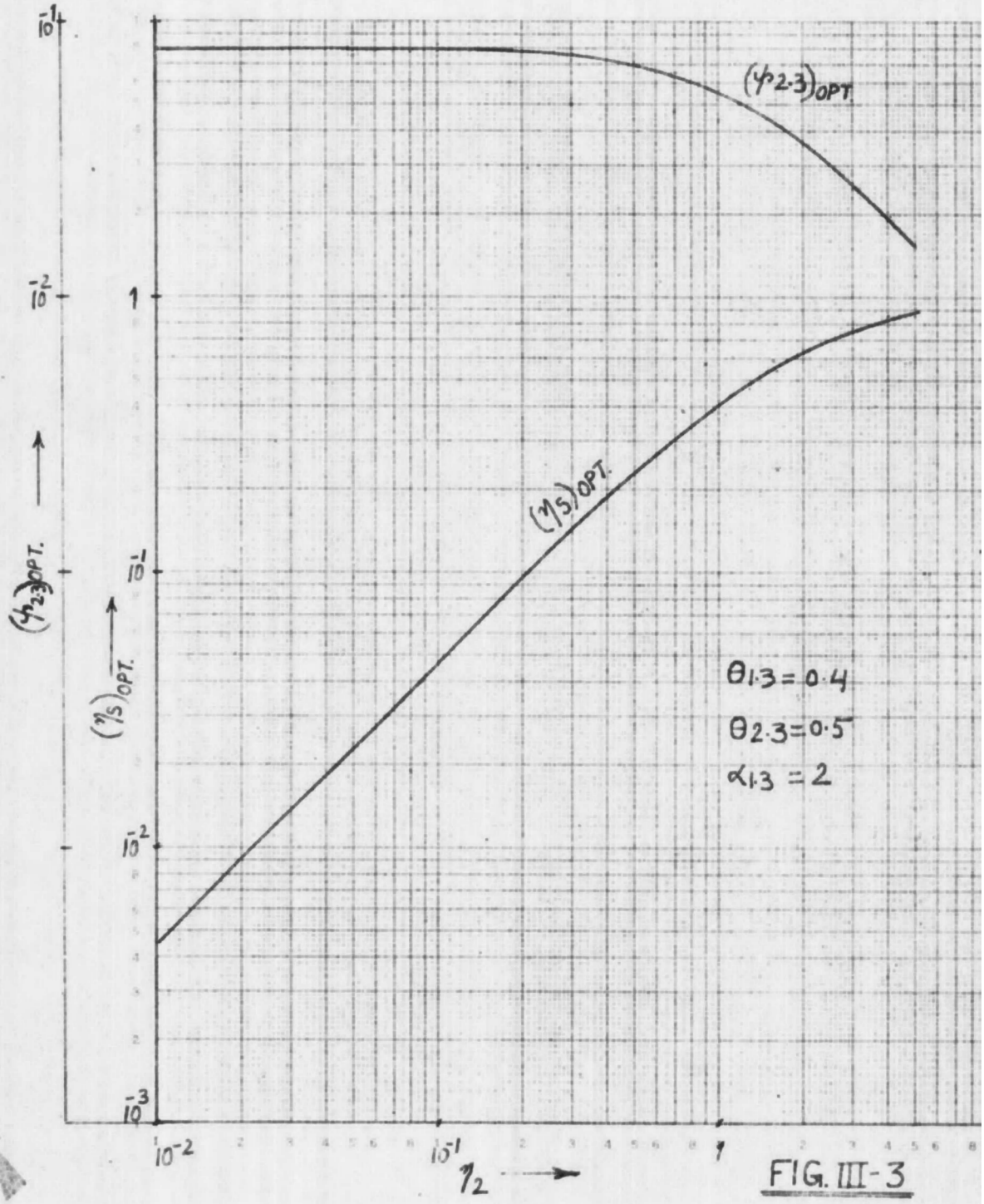
$(\eta_{2\cdot3})_{OPT}$
$(\eta_S)_{OPT}$
$\theta_{1\cdot3} = 0.4$
$\theta_{2\cdot3} = 0.5$
$\alpha_{1\cdot3} = 2$
η_2
10^{-1}
1
10^{-2}
10^{-3}

FIG. III-3

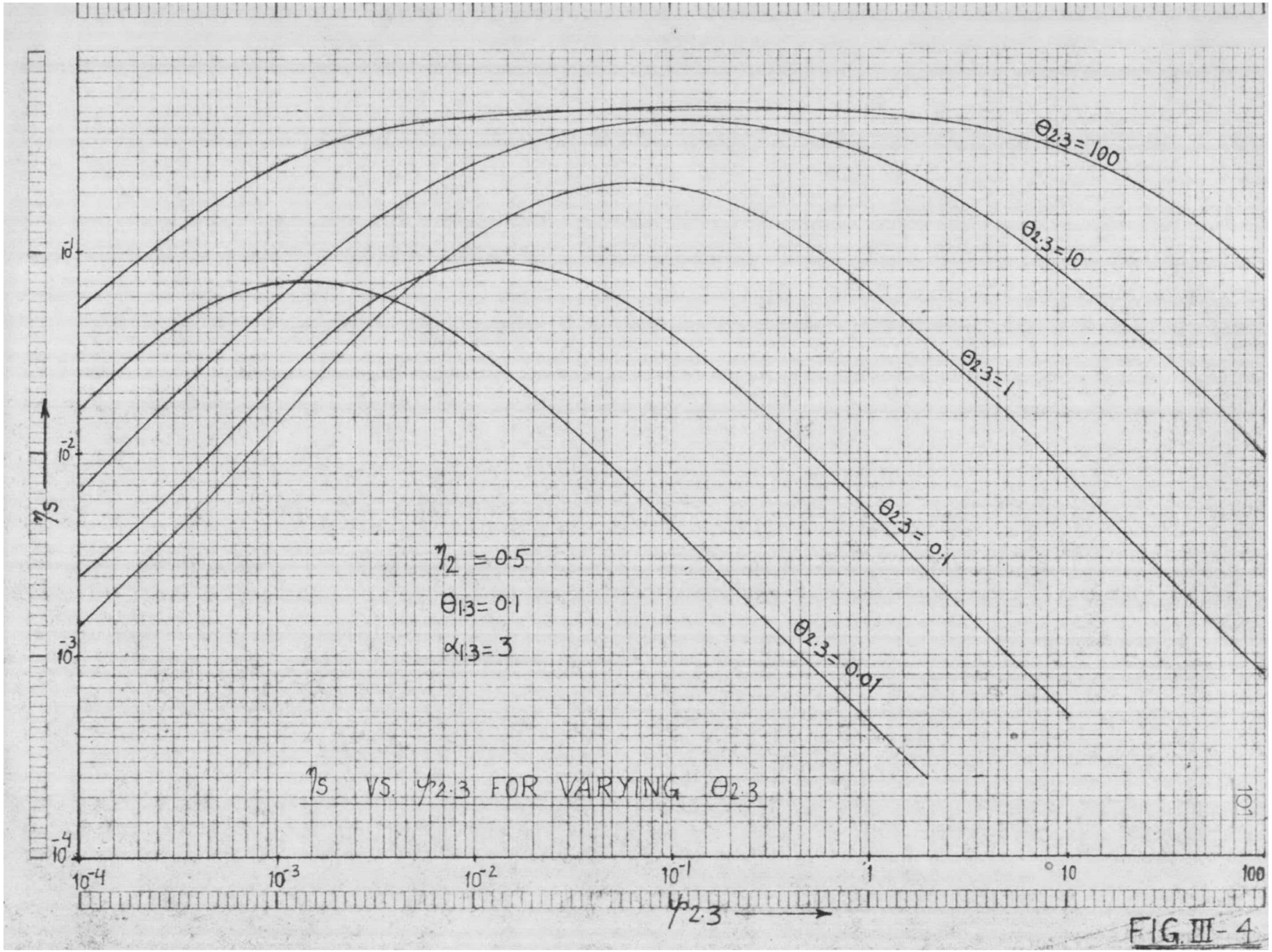
$\theta_{2\cdot3}=100$
$\theta_{2\cdot3}=10$
$\theta_{2\cdot3}=1$
$\theta_{2\cdot3}=0.1$
$\theta_{2\cdot3}=0.01$
$\eta_2 = 0.5$
$\theta_{1\cdot3}=0.1$
$\alpha_{1\cdot3}=3$
η_S VS. $\psi_{2\cdot3}$ FOR VARYING $\theta_{2\cdot3}$
η_S
$\psi_{2\cdot3}$
10^{-1}
10^{-2}
10^{-3}
10^{-4}
10^{-4}
10^{-3}
10^{-2}
10^{-1}
1
10
100

FIG. III-4

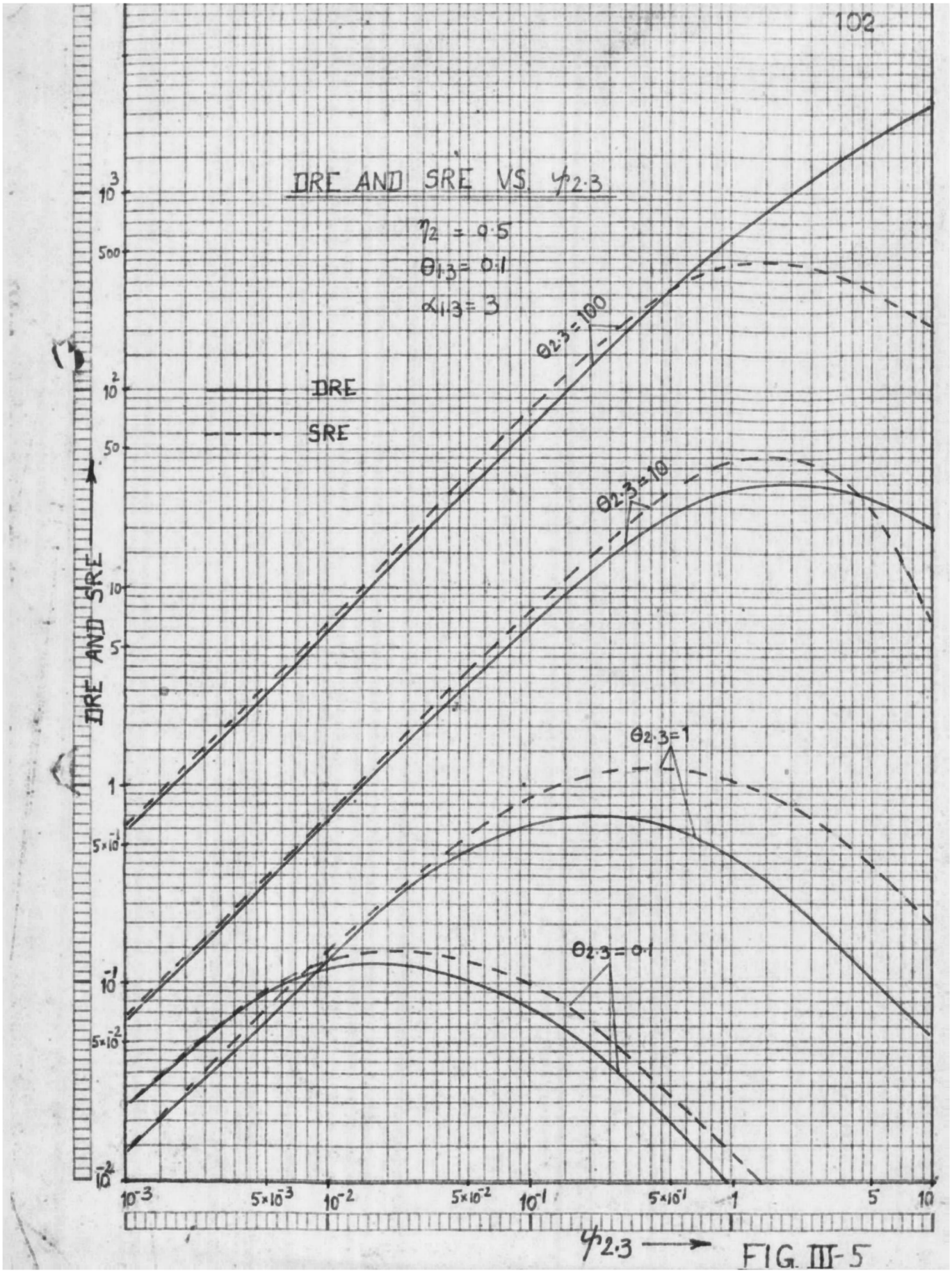
DRE AND SRE VS. $\psi_{2\cdot3}$
$\eta_2 = 0.5$
$\theta_{1\cdot3} = 0.1$
$\alpha_{1\cdot3} = 3$
DRE
SRE
$\theta_{2\cdot3}=100$
$\theta_{2\cdot3}=10$
$\theta_{2\cdot3}=1$
$\theta_{2\cdot3}=0.1$
DRE AND SRE
10^3
500
10^2
50
10
5
1
5×10^{-1}
10^{-1}
5×10^{-2}
10^{-2}
10^{-3}
5×10^{-3}
10^{-2}
5×10^{-2}
10^{-1}
5×10^{-1}
1
5
10
$\psi_{2\cdot3}$

FIG. III-5

similar to that of Fig.III-4 for η_s except that the values of $(\phi_{2.3})_{opt.}$ are different from those of η_s, for the same parameters of the system.The influence of $\theta_{2.3}$ for varying values of $\phi_{2.3}$may also be seen from Figs. III-4 and III-5. It is expected that increase of $\theta_{2.3}$ would increase η_s and $k\eta_s$. This is seen to be true for high values of $\phi_{2.3}$, but for low values of $\phi_{2.3}$, increase of $\theta_{2.3}$ decreases η_s and DRE at first till a minimum value is reached after which further increase of$\theta_{2.3}$ increases both η_s and DRE. For a given sandwich, it may be determined from expressions for η_s and $k\eta_s$, by differentiation with respect to $\theta_{2.3}$, whether such a minimum value is likely to occur, e.g. for $k\eta_s$, a necessary but not sufficient condition for a stationary value with respect to $\theta_{2.3}$ is found to be:

$$1 + \theta_{1.3} > 2\theta_{2.3}.$$

The shear damping in the core is due to the constraining effect of the cover. Fig. III-6 is drawn for indicating effect of cover parameters on η_s and DRE. For a given thickness ratio $\theta_{1.3}$, increase of $\alpha_{1.3}$ increases DRE due to increase of dynamic rigidity. However, an optimum value of η_s is seen to occur at a certain value of $\alpha_{1.3}$, as shown in the figure.

It is seen from the foregoing discussion that all

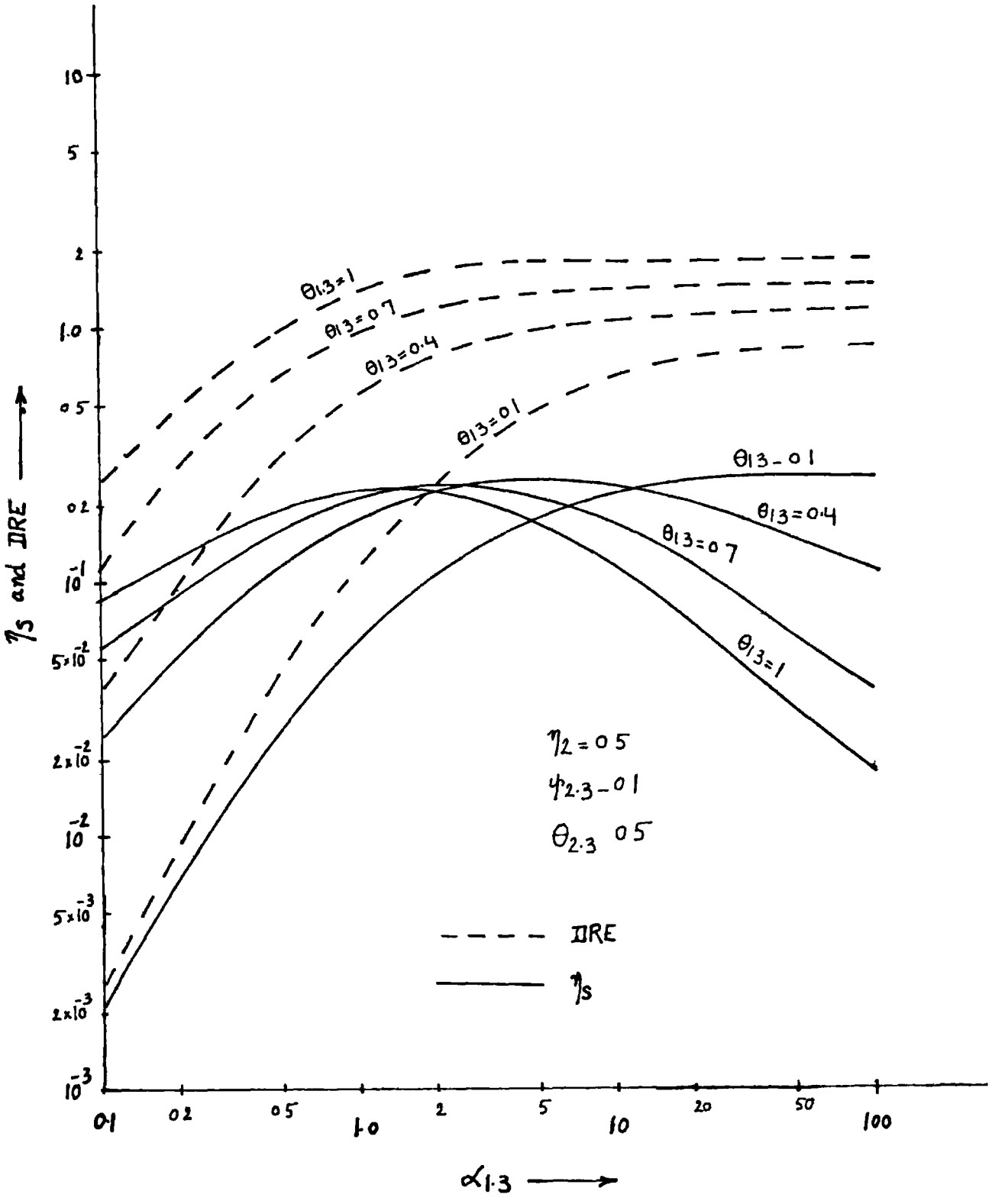
10
5
2
1.0
0.5
0.2
10^{-1}
5×10^{-2}
2×10^{-2}
10^{-2}
5×10^{-3}
2×10^{-3}
10^{-3}
0.1
0.2
0.5
1.0
2
5
10
20
50
100
η_s and IRE
$\alpha_{1.3}$
$\theta_{1.3}=1$
$\theta_{13}=0.7$
$\theta_{13}=0.4$
$\theta_{13}=0.1$
$\theta_{13}=0.1$
$\theta_{13}=0.4$
$\theta_{13}=0.7$
$\theta_{13}=1$
$\eta_2=0.5$
$\psi_{2.3}=0.1$
$\theta_{2.3}$ 0.5
IRE
η_s

FIG III-6

the geometrical and physical parameters of the system influence the damping obtainable from the system, since these determine the strains and stresses associated with the system.

(ii) Previously, the reference system for the comparison of the ratio of rigidity of the sandwich and solid reference beam, was taken as $E_s = E_3$ and $t_s = t_3$. Below the reference system will be taken as:

$E_S = E_3$ and $t_s = t_1+t_3$ = Total thickness of the faces. It will be possible to study the effect of using various face combinations, keeping the total thickness of the sandwich same. In this case, expressions for $k\eta_s$ and k, for simplified case of Analysis I, of section II.C.4, are:

$$k\eta_s = \frac{X\eta_2}{Y^2+\eta_2^2} \qquad \text{(III.17)}$$

$$k = \lambda^3 + \alpha_{1.3}(1-\lambda)^3 + \frac{XY}{Y^2+\eta_2^2} \qquad \text{(III.18)}$$

where $X = \frac{3\varphi}{\delta}(1+2\delta)^2(1+\eta_2^2)$

$$Y = \frac{\varphi}{\delta}\left[\frac{1}{\alpha_{1.3}(1-\lambda)} + \frac{1}{\lambda}\right](1+\eta_2^2) + 1$$

φ being $= \dfrac{G_2}{E_3 t_s^2 \left(\frac{n\pi}{L}\right)^2}$

$$\alpha_{1.3} = E_{1/E_3}$$

$$\lambda = t_3/t_s$$

$$\text{and} \quad \delta = t_2/t_s.$$

Expression for 'η_s' can be written from eqns. III.17 and III.18.

'k' in eqn. (III.18) is the ratio of dynamic rigidity of sandwich to that of solid reference beam.

$k_{static} = \lambda^3 + \alpha_{1.3}(1-\lambda)^3$, k_{static} being the ratio of static rigidity of sandwich (taking account of both faces only) to that of the solid reference beam.

Figs. III-7 to III-10 are plotted for k, $k\eta_s$, η_s and k_{static} vs λ for varying values of $\alpha_{1.3}$. Each Fig. is for a particular value of φ, the shear parameter. λ=0.5 corresponds to a symmetrical sandwich and other values of 'λ' give various unsymmetrical cases, keeping the total thickness of faces same. k_{static} is minimum for a symmetrical sandwich (being =0.25) and so an unsymmetrical sandwich is to be preferred for increased static stiffness. For $\alpha_{1.3} = 1$, η_s and $k\eta_s$ decrease for unsymmetrical cases (i.e. for λ>0.5). The decrease is not very significant for Figs. III-7 and III-8, which are for low values of 'φ'. However, a proper choice of $\alpha_{1.3}$ in an unsymmetrical case can improve the damping performance, as shown in Figs. III-7 to III-10. Thus, a suitable design of an unsymmetrical 3 layered sandwich might be preferred for better performance under static conditions and reasonable damping

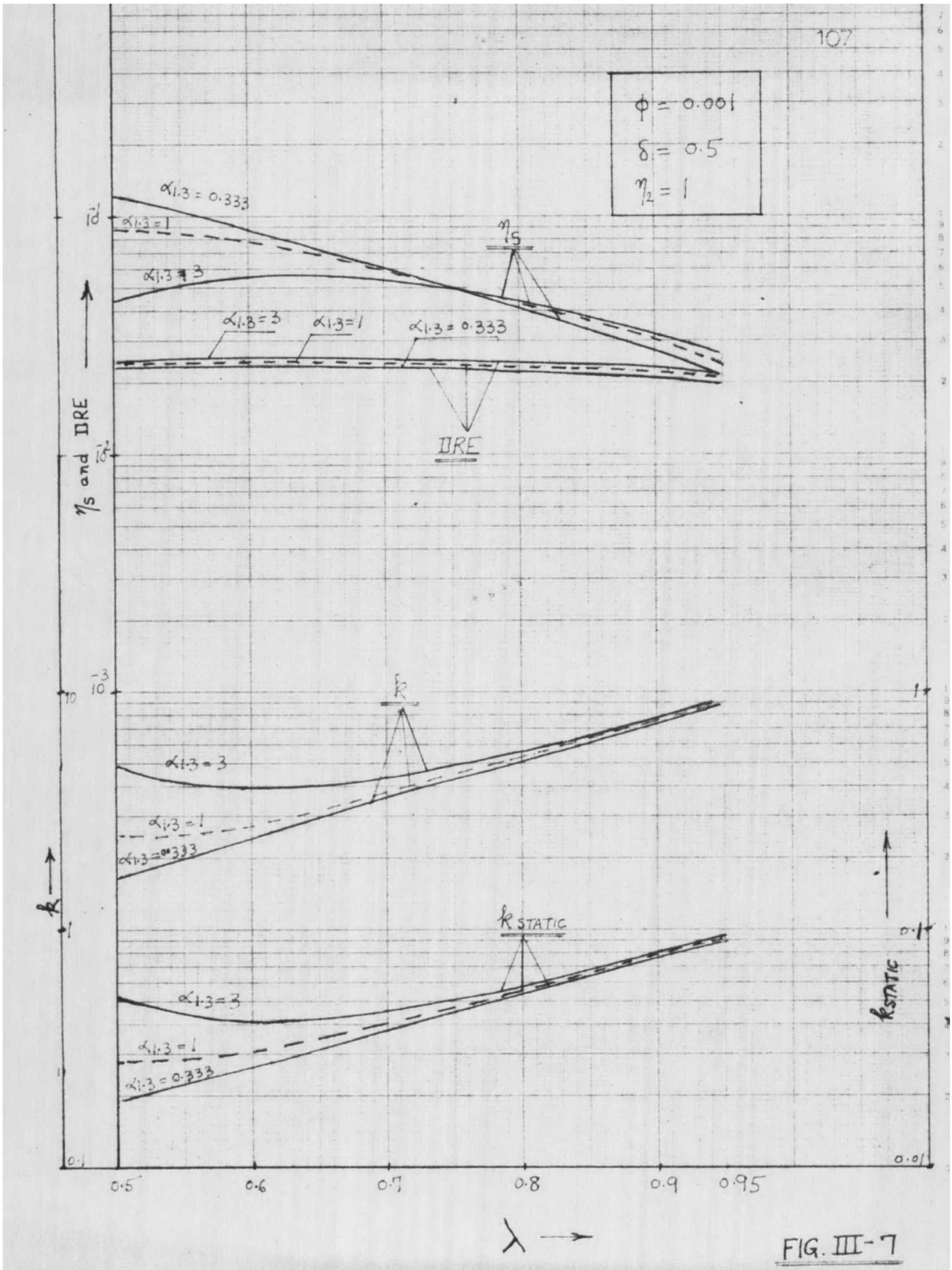
$\phi = 0.001$
$\delta = 0.5$
$\eta_{12} = 1$
$\alpha_{1.3} = 0.333$
$\alpha_{1.3} = 1$
$\alpha_{1.3} = 3$
η_s
$\alpha_{1.3} = 3$
$\alpha_{1.3} = 1$
$\alpha_{1.3} = 0.333$
IIRE
η_s and IIRE
10^{-2}
10^{-3}
10
k
k
$\alpha_{1.3} = 3$
$\alpha_{1.3} = 1$
$\alpha_{1.3} = 0.333$
k STATIC
$\alpha_{1.3} = 3$
$\alpha_{1.3} = 1$
$\alpha_{1.3} = 0.333$
1
0.1
0.01
k STATIC
0.5
0.6
0.7
0.8
0.9
0.95
λ

FIG. III-7

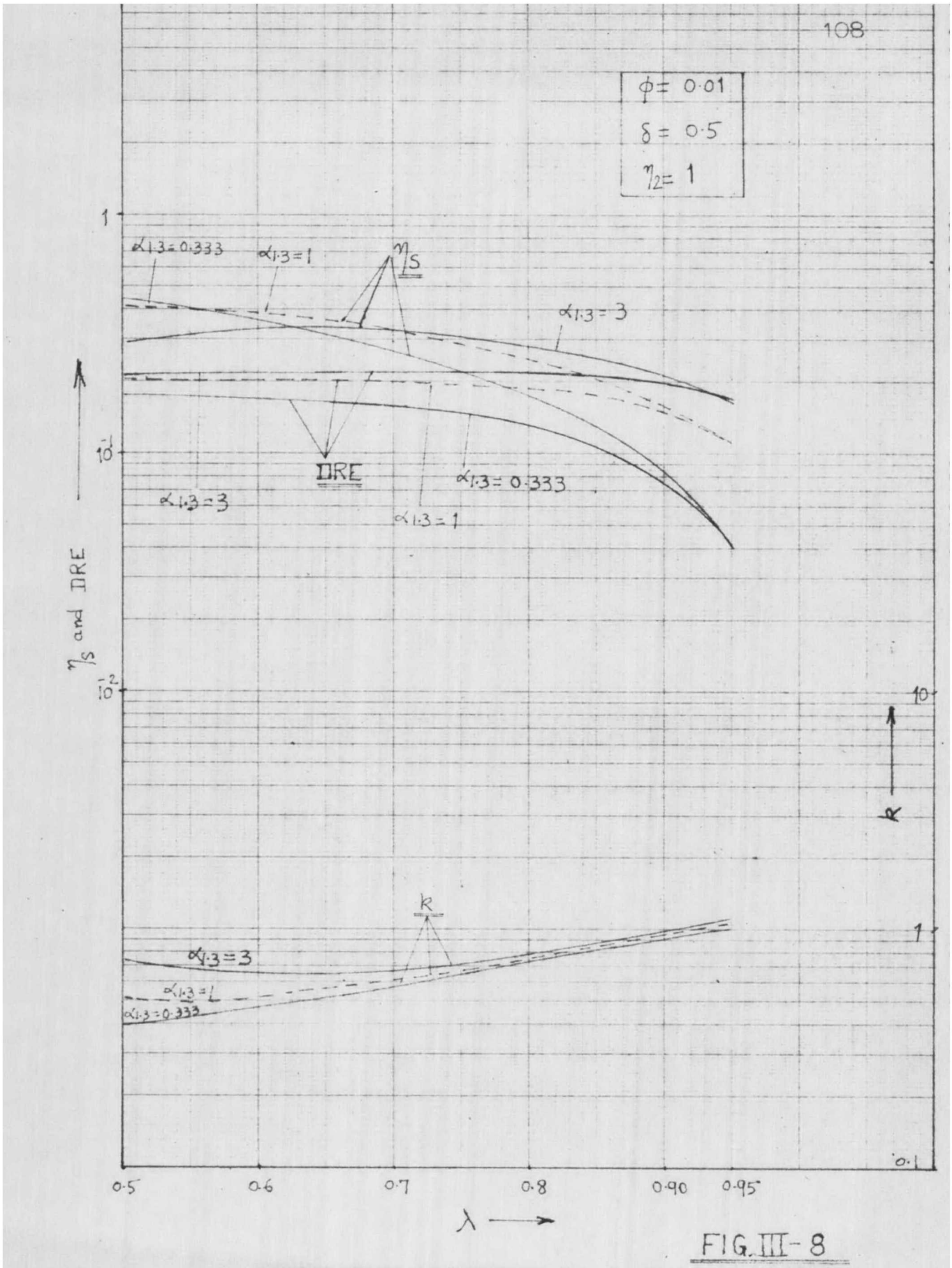
$\phi = 0.01$
$\delta = 0.5$
$\eta_2 = 1$
1
10^{-1}
10^{-2}
η_s and IRE
$\alpha_{1.3} = 0.333$
$\alpha_{1.3} = 1$
η_s
$\alpha_{1.3} = 3$
IRE
$\alpha_{1.3} = 0.333$
$\alpha_{1.3} = 3$
$\alpha_{1.3} = 1$
10
α
K
1
$\alpha_{1.3} = 3$
$\alpha_{1.3} = 1$
$\alpha_{1.3} = 0.333$
0.1
0.5
0.6
0.7
0.8
0.90
0.95
λ ⟶

FIG. III-8

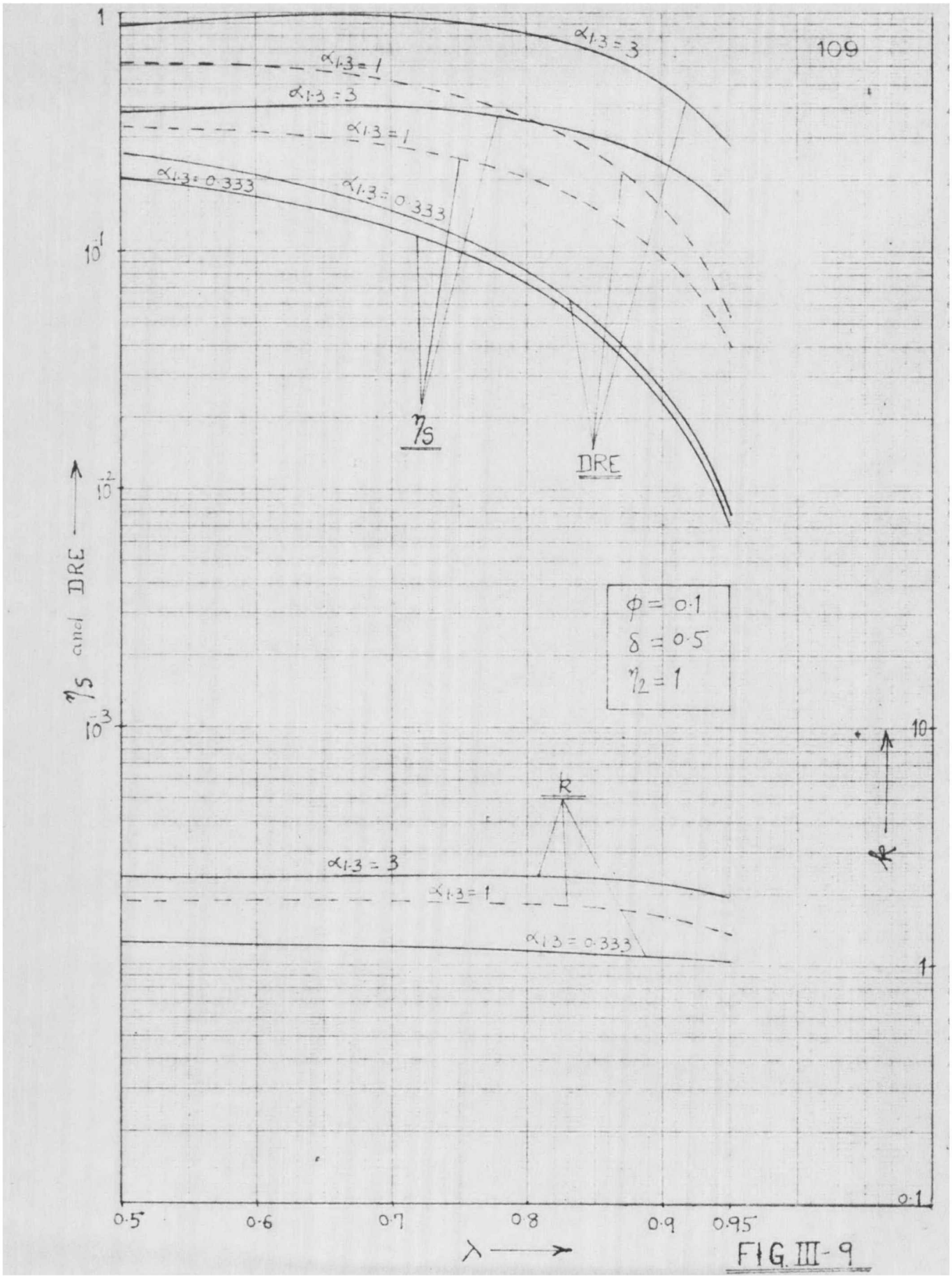
1
10^{-1}
10^{-2}
10^{-3}
η_S and DRE
$\alpha_{1\cdot3} = 3$
$\alpha_{1\cdot3} = 1$
$\alpha_{1\cdot3} = 0.333$
η_S
DRE
$\phi = 0.1$
$\delta = 0.5$
$\eta_2 = 1$
R
10
1
0.1
0.5
0.6
0.7
0.8
0.9
0.95
λ

FIG. III-9

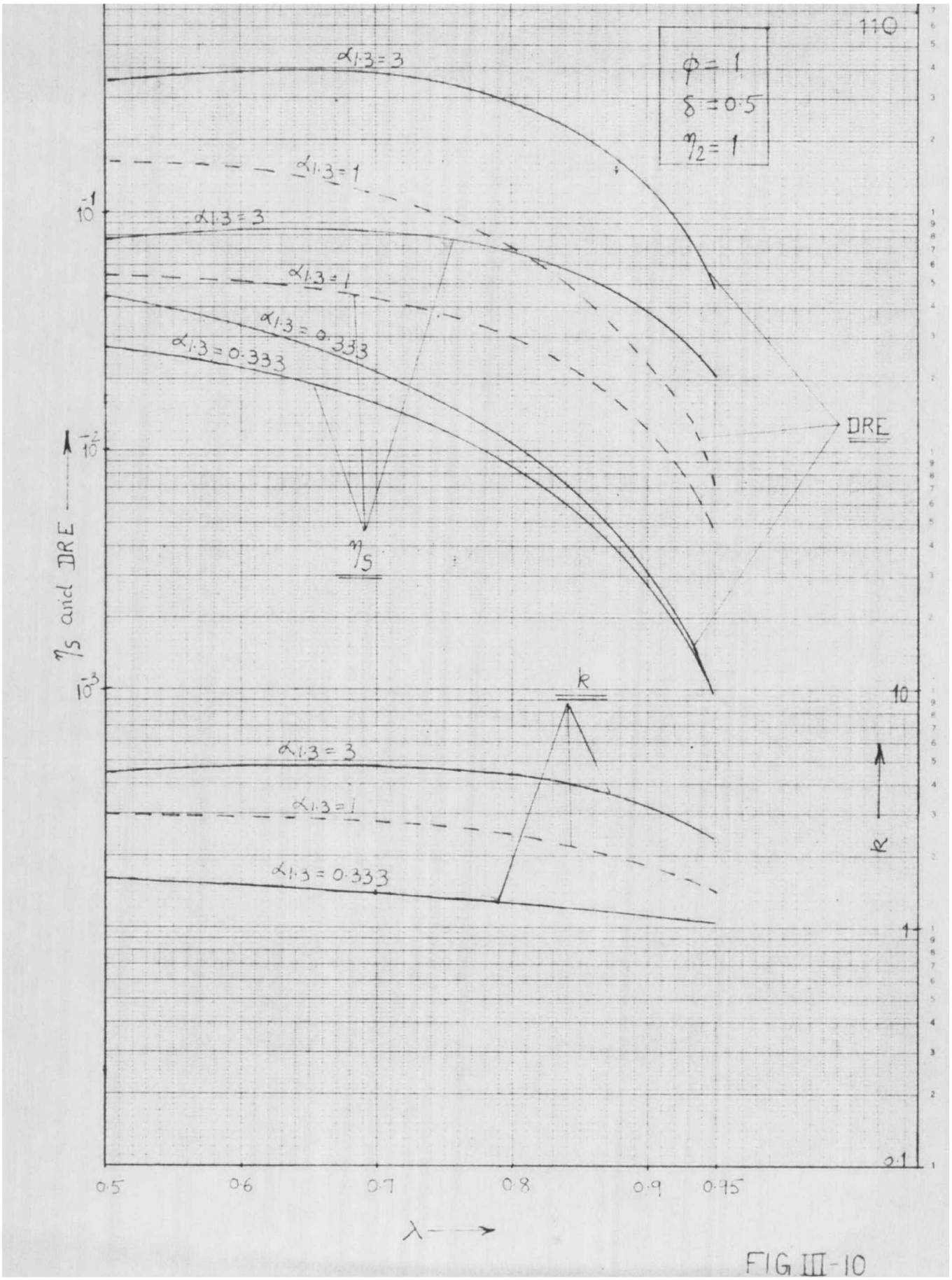
$\phi = 1$
$\delta = 0.5$
$\eta_2 = 1$
$\alpha_{1.3} = 3$
$\alpha_{1.3} = 1$
$\alpha_{1.3} = 3$
$\alpha_{1.3} = 1$
$\alpha_{1.3} = 0.333$
$\alpha_{1.3} = 0.333$
DRE
η_s
k
$\alpha_{1.3} = 3$
$\alpha_{1.3} = 1$
$\alpha_{1.3} = 0.333$
η_s and DRE ——→
10^{-1}
10^{-2}
10^{-3}
10
1
0.1
k
0.5
0.6
0.7
0.8
0.9
0.95
λ ——→

FIG III-10

under dynamic conditions, compared to a symmetrical sandwich of the same total thickness.

Figs. III-11 and III-12 are plotted for η_s, $k\eta_s$ and k vs. φ for varying values of λ, $\alpha_{1.3}$ and δ. The graphs for $k\eta_s$ and η_s show an optimum value at certain values of shear parameter φ. Comparisons of these graphs indicate that the graphs for 'η_s' are flatter for larger values of 'δ' (viz. for thick core) than those with smaller values of 'δ'. In practice, a variation of φ may occur due to change in G_2 because of change in frequency and also in modal number 'n'. Thick cored sandwich gives higher damping 'η_s' for a larger range of φ'. However, the situation is not similar for $k\eta_s$ or DRE as shown in Fig. III-12.

It may also be seen that the maximum value of 'η_s' for δ = 10 in Fig. III-12 is not very much different for various values of λ i.e. in these cases, the face thickness ratio has no appreciable effect on maximum damping.

When $\alpha_{1.3}$ = 1, symmetrical case (i.e. λ = 0.5) always gives higher damping than any unsymmetrical case. However, for $\alpha_{1.3}$ = 3, the value of λ for maximum damping, is different.

Graphs similar to those given in Figs. III-11 and III-12 are useful not only in indicating effect of sytem parameters but also in determining the performance

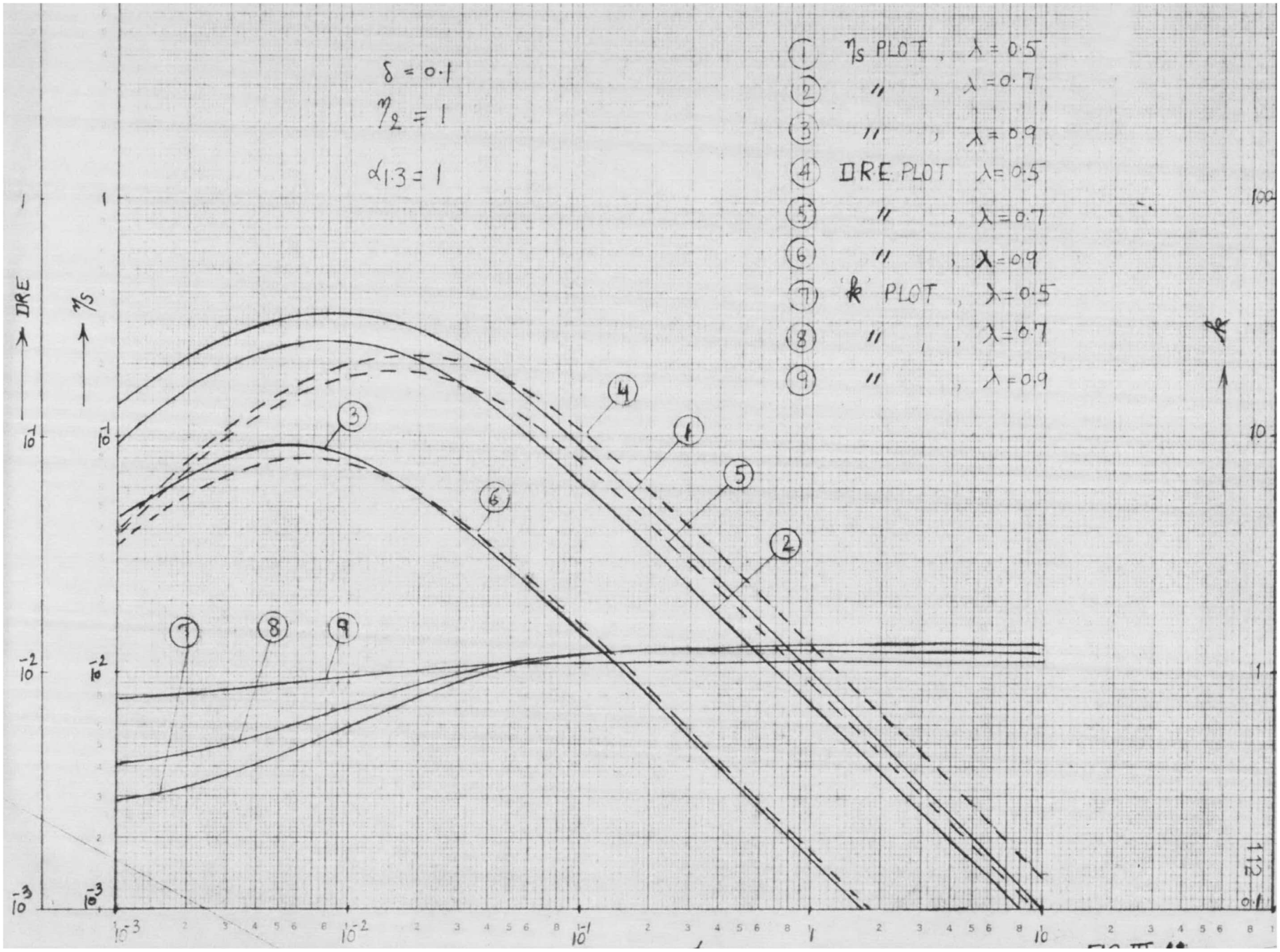
δ = 0·1
η2 = 1
α1·3 = 1
① ηs PLOT , λ = 0·5
② " , λ = 0·7
③ " , λ = 0·9
④ DRE PLOT λ = 0·5
⑤ " , λ = 0·7
⑥ " , λ = 0·9
⑦ k PLOT , λ = 0·5
⑧ " , λ = 0·7
⑨ " , λ = 0·9
DRE
ηs
k
112

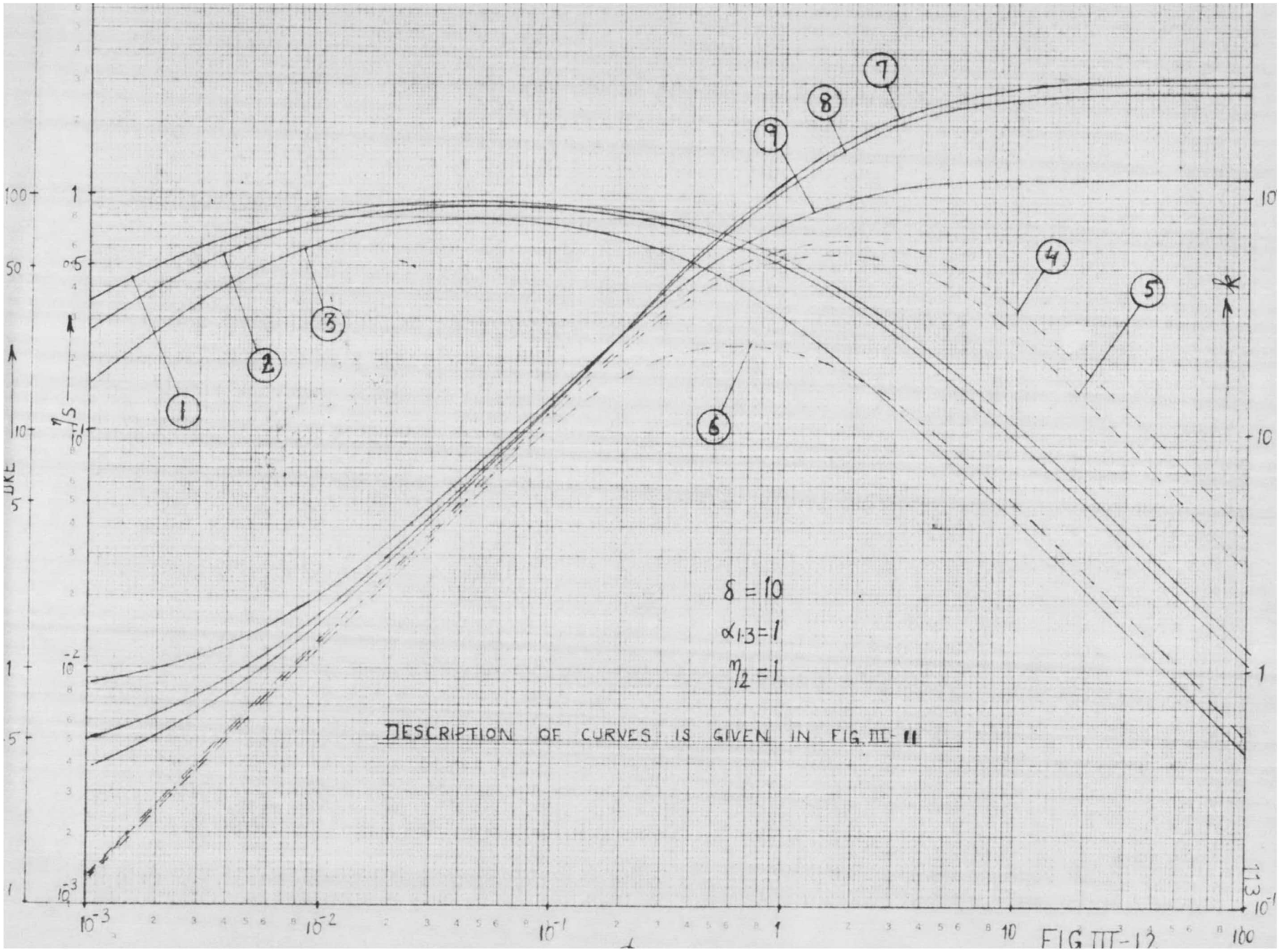
δ = 10
α1-3 = 1
η2 = 1
DESCRIPTION OF CURVES IS GIVEN IN FIG III-11
FIG III-12

characteristics of any 3 layered sandwich. For any modal number 'n' and shear modulus G_2 for the core, φ is calculated and on the appropriate graph gives the position of the operating point. In addition to giving η_s, $k\eta_s$ and nearness to optimum conditions, the dynamic displacement response can be got from

$$w = \sum_{n=1} \frac{f_n}{K_R(k+ik\eta_s)-\rho p^2} \qquad \text{(III.19)}$$

Detailed application of these graphs for design study is discussed in section III.E.

III.B: Extensional effect of the core

In a 3 layered sandwich, with the core made of a viscoelastic material, shear effect is usually predominant in the core and most of the damping in the system is due to that effect. In an unsymmetrical case, however, if the viscoelastic core is thick and rigid and one of the faces is less rigid compared to the other face, one might expect damping due to direct strains in the core as well in addition to that due to shear, the former type is known as extensional damping [60]. Since the equations of Chapter II contain both these effects, it is possible to study the extensional effect of the core as below.

Most viscoelastic materials are taken as incompressible [72, 92] and so $E_2 = 3G_2$. Also extensional damping

loss factor β_2 is taken equal to that in shear η_2[60, 73].

Fig.III-13 shows Graphs of total damping and also damping due to shear effect in the core only. It is seen that as the constraining effect of layer '1' is reduced by decreasing $\alpha_{1.3}$, extensional damping effect increases. In Fig.III-14, a plot of η_s vs $\phi_{2.3}$ for varying values of $\alpha_{1.3}$, is drawn. It is seen that the curve for loss factor η_s is flat, for lower values of $\alpha_{1.3}$, as $\phi_{2.3}$ varies. The variation in $\phi_{2.3}$ may be regarded as that in modal number 'n' and hence high damping may be expected in such a case, over a large frequency range. This is due to the extensional damping, which is predominant when $\alpha_{1.3}$ is small and which is not sensitive to variation with model number 'n', as is known in a 2 layered configuration [30]. In table T-1, the extensional damping is seen to be of significance at either very low or high values of $\phi_{2.3}$, when shear effect is not of importance. In Table T-2, results are given for a symmetrical sandwich. Before calculating 'η_s' by analysis II, shear coefficients 'k_i' required therein are calculated from section II.D.3. Extensional damping effect becomes apparent for values of core shear modulus G_2 greater than 10^4 lb/in^2, in the case illustrated, even when there is enough constraining of the viscoelastic core, by the outer faces.

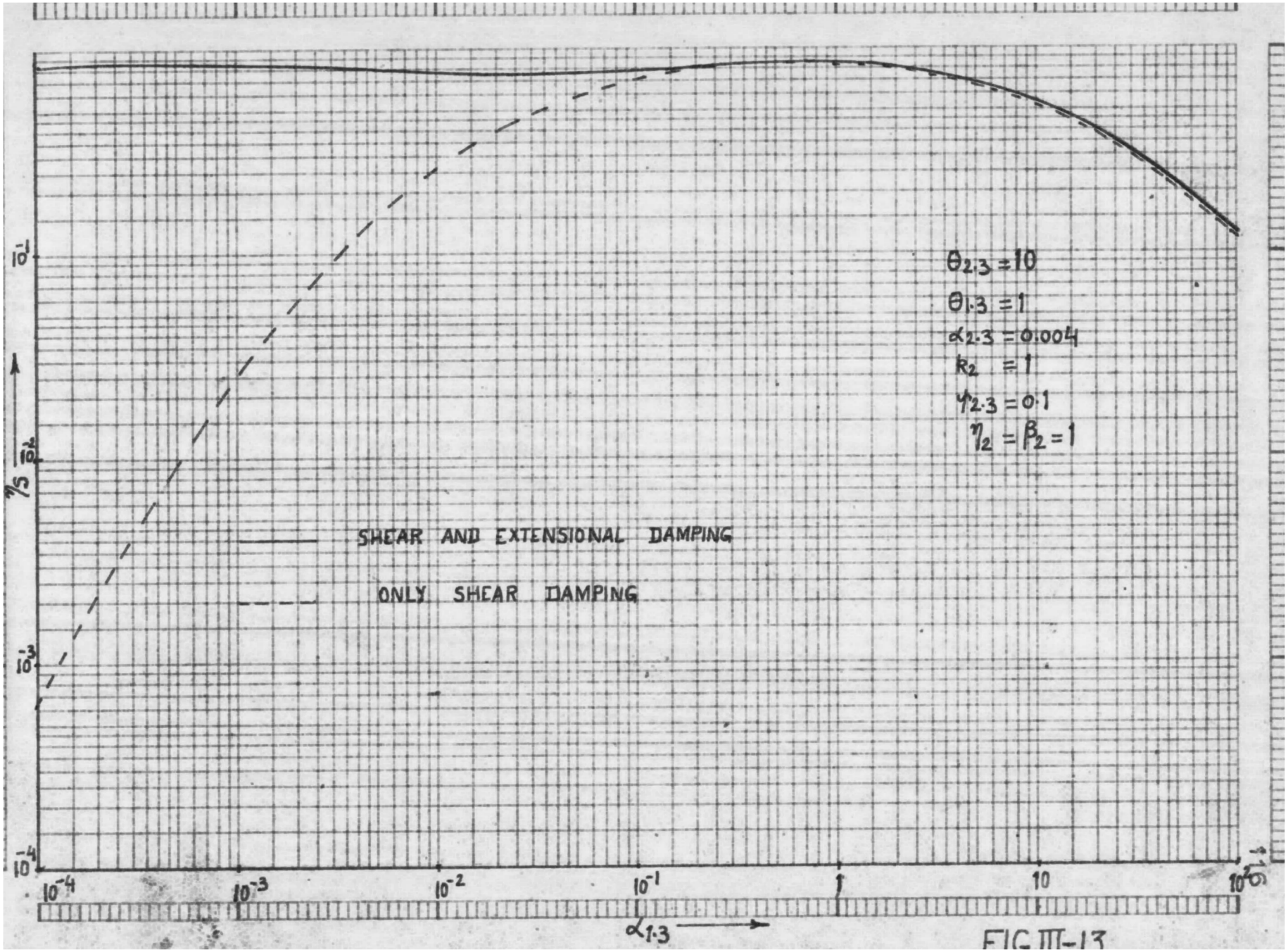
$\theta_{2\cdot3} = 10$
$\theta_{1\cdot3} = 1$
$\alpha_{2\cdot3} = 0.004$
$R_2 = 1$
$\psi_{2\cdot3} = 0.1$
$\eta_2 = \beta_2 = 1$
SHEAR AND EXTENSIONAL DAMPING
ONLY SHEAR DAMPING
η_S
10^{-1}
10^{-2}
10^{-3}
10^{-4}
10^{-4}
10^{-3}
10^{-2}
10^{-1}
1
10
10^2
$\alpha_{1\cdot3}$

FIG III-13

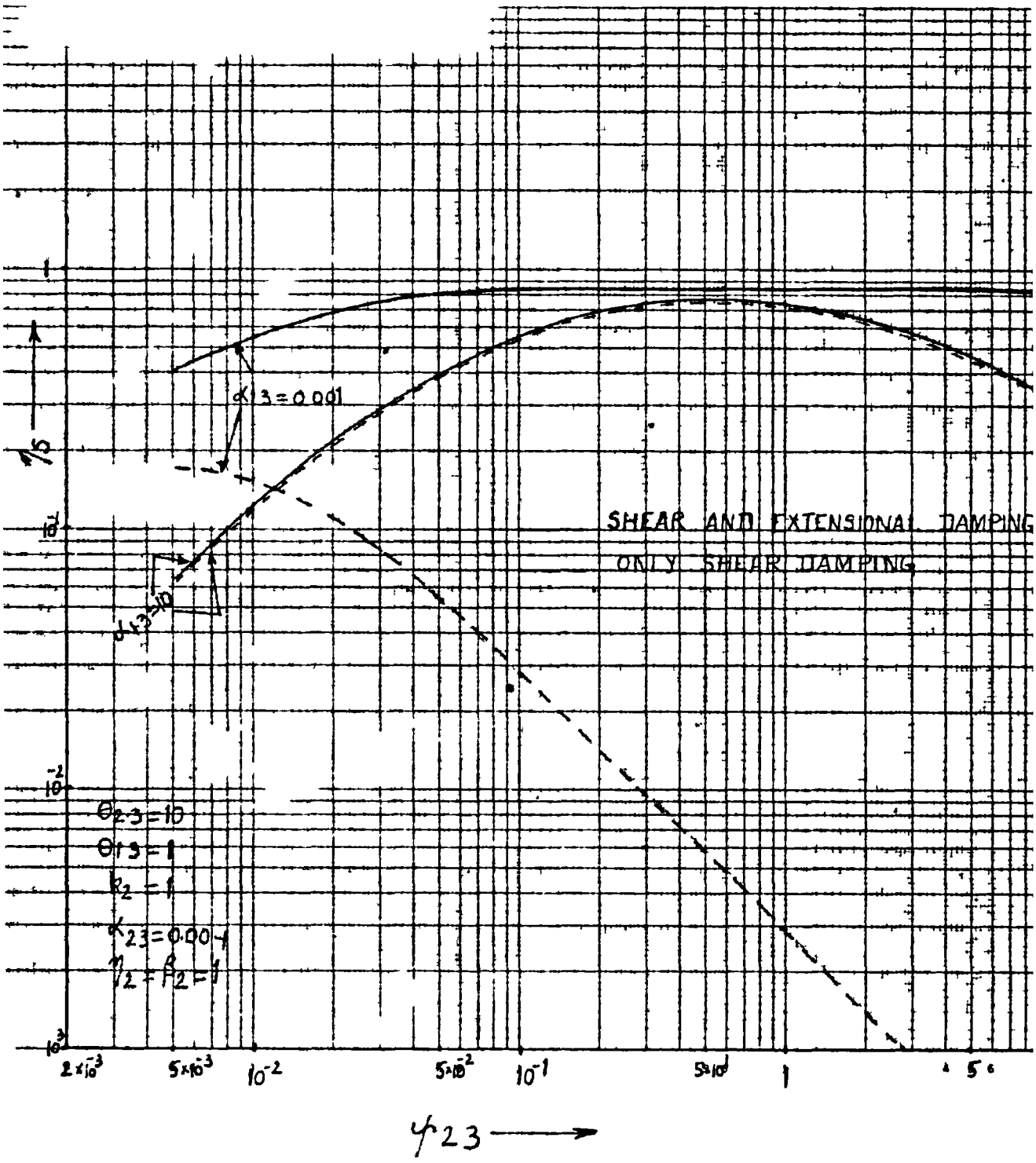
1
$\alpha_{13}=0.001$
SHEAR AND EXTENSIONAL DAMPING
ONLY SHEAR DAMPING
$\theta_{23}=10$
$\theta_{13}=1$
$k_2=1$
$\alpha_{23}=0.004$
$\eta_2=\beta_2=1$
2×10^{-3}
5×10^{-3}
10^{-2}
5×10^{-2}
10^{-1}
5×10^{-1}
1
5
ψ_{23}

FIG III-14

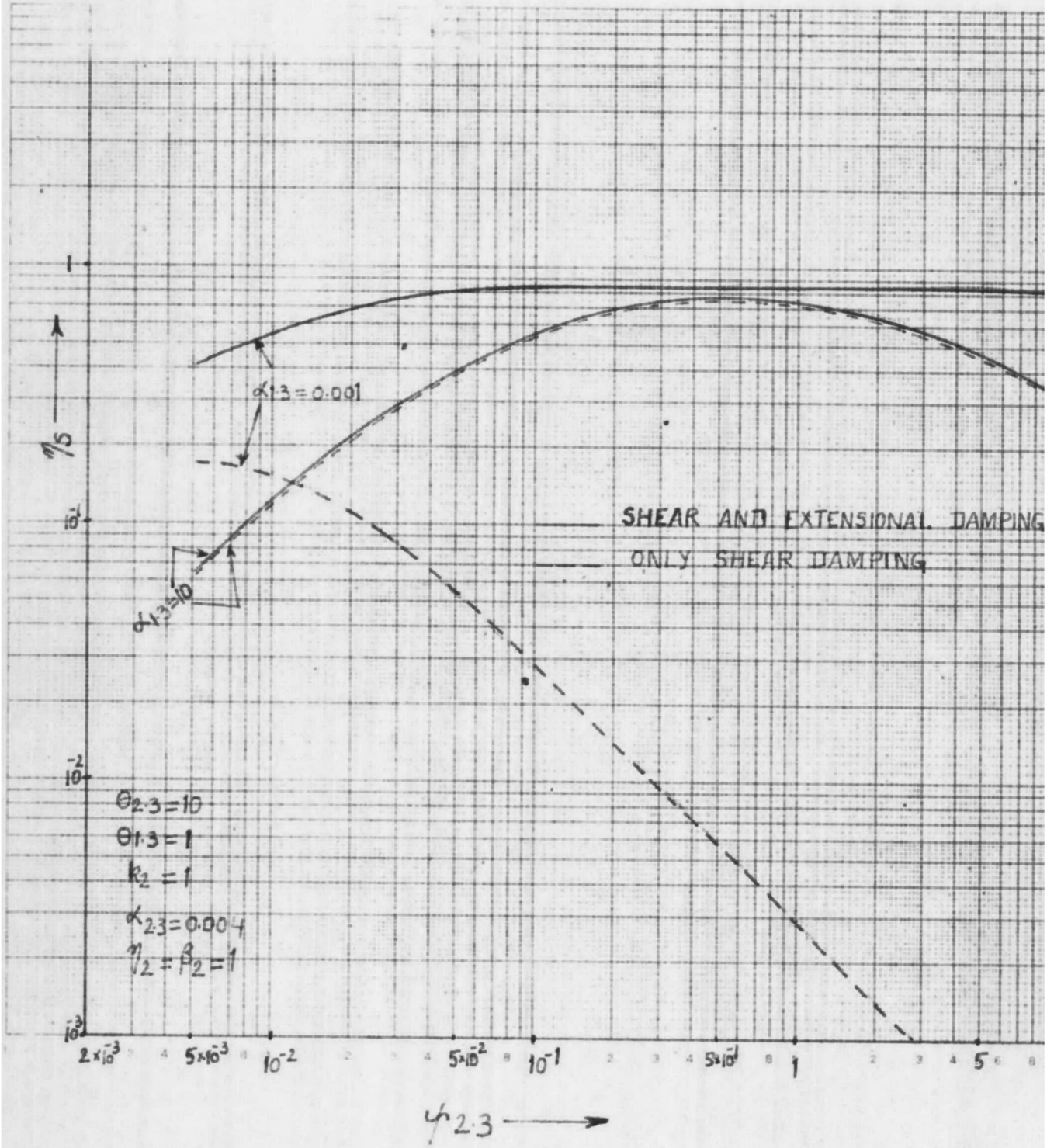
1
η_S
10^{-1}
10^{-2}
10^{-3}
$\alpha_{1.3}=0.001$
$\alpha_{1.3}=10$
SHEAR AND EXTENSIONAL DAMPING
ONLY SHEAR DAMPING
$\theta_{2.3}=10$
$\theta_{1.3}=1$
$k_2=1$
$\alpha_{2.3}=0.004$
$\eta_2=\beta_2=1$
2×10^{-3}
5×10^{-3}
10^{-2}
5×10^{-2}
10^{-1}
5×10^{-1}
1
5
$\psi_{2.3}$

FIG. III-14

TABLE T-1

	$\psi_{2.3}$ =0.0001	$\psi_{2.3}$ =0.001	$\psi_{2.3}$ = 0.01	$\psi_{2.3}$ = 0.1	$\psi_{2.3}$ = 1	$\psi_{2.3}$ = 10
η_s Shear and Extensional Damping in the Core	0.01393	0.074453	0.41055	0.61765	0.19874	0.042492
η_s Shear Damping in Core	0.0073287	0.068474	0.40669	0.60677	0.17844	0.021565

In above table,

$$\theta_{2.3} = 5, \quad \theta_{1.3} = 0.1, \quad k_2 = 1$$

$$\alpha_{2.3} = 0.0015, \quad \eta_2 = \beta_2 = 1, \quad \alpha_{1.3} = 1$$

TABLE T-2

G_2 lb/in^2	Values of 'k_i'		η_s		
	k_1 or k_3	k_2	Including both Shear and Extensional Damping	Including Shear Damping Only	
100	0.9719	0.9998	0.7981	0.79807	Analysis
10^3	0.9847	0.9977	0.309799	0.30899	II has
10^4	0.9854	0.9977	0.046673	0.042938	been used
10^5	0.9855	0.9787	0.039904	0.0044675	for calcu-
5×10^5	0.9855	0.9153	0.155803	8.9672×10^{-4}	lating η_s here.

In above table, $E_1 = E_3 = 1.125 \times 10^7$ lb/in^2

$t_1 = t_3 = 0.1"$, $t_2 = 1"$

$G_1 = G_3 = 4.25 \times 10^6$ lb/in^2, $\eta_2 = \beta_2 = 1$

$\frac{n\pi}{L} = 0.04$

III.C: Comparisons

The results obtained from analysis I and analysis II will be compared with each other and also with those obtained from [60]. For this purpose, a number of cases are analysed and results are tabulated in tables T-3 to T-5. η_s and $k\eta_s$ are calculated from results of Chapter II and the form of relations used, correspond to equation III.15. The values of shear coefficients required in each case have been calculated, using procedure given in section II.D.3. Loss factor η_s is also calculated from [60 page 61 eqn. 20]. Expression for $k\eta_s$ is not directly available from [60] and hence has not been calculated.

II.C.1: Comparison of results from analysis I and II

Analysis II is expected to be more accurate for modes involving short wavelengths i.e. at high frequencies, since it includes shear effect in faces as well. Tables T-3 and T-4 illustrate this point. When the core thickness is small and thickness of each face is large as for Table T-3, the percentage difference between results of analysis I and II is more pronounced when the modal number is high or for modes of short wavelengths. The percentage differences were calculated over the values of analysis II. When the core thickness is more as in table T-4, shear effect occurs mostly in the core even at higher modes and

so the corresponding percentage difference is not high in table T-4. In both these tables, results of η_s obtained from analysis I were generally found to be higher than those from analysis II and hence will not be on safe side if used in practice. It may be seen that these tables are drawn for high values of 'n', which in practice will be involved only if the excitation frequencies encountered are very high. This has been done for the sake of illustration.

III.C.1 : Comparisons with previous work

Results of η_s obtained from [60] and the present work were compared. The percentage differences calculated over the results of analysis II of Chapter II, are given in table T-5. There is significant difference for long beams and low order modes. The difference is seen to increase as G_2 increases. The values of 'η_s' obtained from analysis I and II for the cases quoted were nearly same. The discrepancy in results obtained from [60] may be attributed to certain assumptions made therein, which are not included in the present work. In [60 eqn.19 page 58], a stress strain law for the core is assumed which is not strictly correct when the extensional effect of the core is taken into account. Other approximations involved in [60 eqns. 15 page 60] are:

TABLE T-3

G_2 lb/in^2	100		1000		10^4		10^5	
$\frac{n\pi}{L}$ /in	0.5714	2.2857	0.5714	2.2857	0.5714	2.2857	0.5714	2.2357
% Difference in η_s between analysis I and II	0.1203	7.359	0.257	7.433	1.0768	8.24	1.8506	15.854
% Difference in '$k\eta_s$' between Analysis I and II	1.287	20.945	1.4095	21.078	2.437	22.418	4.054	35.37

For the table, the following values were used:

$E_1 = E_3 = 1.125 \times 10^7$ lb/in^2 $\quad t_1 = t_3 = 0.25"$ $\quad t_2 = 0.05"$

$G_1 = G_3 = 3.749 \times 10^6$ lb/in^2 $\quad \eta_2 = \beta_2 = 1$

TABLE T-4

G_2 lb/in^2	100		1000		10^4		10^5	
$\frac{n\pi}{L}$ /in	0.5714	2.2857	0.5714	2.2857	0.5714	2.2857	0.5714	2.2857
% Difference in 'η_s' between analysis I and II	-0.3085	0.7122	-0.2391	0.7504	0.2359	1.123	1.263	4.515
% Difference in '$k\eta_s$' between analysis II and III	0.8505	13.437	0.8803	13.485	1.185	13.816	2.806	17.189

For the table, t_2 = 0.2".

The remaining values are same as in Table T-3.

TABLE T-5

G_2 lb/in^2	1000		5,000		10,000		50,000	
$\frac{n\pi}{L}$ /in	0.025	0.1	0.025	0.1	0.025	0.1	0.025	0.1
% Difference in η_s from [60] and Analysis II	-1.83	9.4×10^{-3}	-33.47	-2.485	-70.62	-10.04	-109.8	-79.2

For the table, the following values were used:

$E_1 = E_3 = 1.125 \times 10^7$ lb/in^2, $G_1 = G_3 = 3.749 \times 10^6$ lb/in^2

$t_1 = 0.03125"$, $t_2 = 0.3125"$, $t_3 = 0.0625"$

$\eta_2 = \beta_2 = 1$

$$E_2 t_2 \ll E_3 t_3$$

$$(E_1 t_1)^2 \ll (E_3 t_3)^2.$$

Thus, results for thick rigid cored unsymmetrical sandwich may be in error if results of [60] are employed.

Another assumption made in [60] involves the calculation of resonance frequencies of layered beam, treating it as a single solid one, when frequencies vs η_s plots are drawn. This has been justified for a taped structure in which the tape is very thin compared to the base plate, and the resonance frequencies of the taped structure may be taken equal to those of the base plate. This effect has been determined in table T-6 for a chosen 3 layered unsymmetrical case. 'k' is the rigidity ratio of sandwich, with respect to the reference system, which is $E_s = E_3$

and $t_s = t_1 + t_3$ in this case.

TABLE T-6

$\eta_2 = 1$ $\alpha_{1.3} = 1$

$\delta = 0.1305$ $\lambda = 0.87$

φ	10^{-4}	10^{-3}	10^{-2}	10^{-1}	1
k	0.6644	0.697	0.9237	1.161	1.1963

Value of 'k', if only solid base plate (layer 3) is considered as in [60] is $=\lambda^3 - 0.658$. Fromt table T-6, $k = 1.1963$ when $\varphi - 1$. Since frequencies are proportional to $\sqrt{k}$, in such a situation, the ratio of corresponding resonant frequencies will be approximately 1.35 (neglecting the mass of the thin viscoelastic layer) giving an error of 35% if frequencies of solid base plate are employed as in [60].

III.D : Resonance curves due to sinusoidal motion of end supports

The solution for a simply supported sandwich beam subjected to harmonic loading of intensity f(x) sin pt, is given by eqn. II.18 (for analysis I), wherein the various coefficients f_1, g_1, f_3 etc., are complex, because the moduli for viscoelastic layer 2 are taken as complex.

If the beam is subjected to sinusoidal transverse motion of amplitude x_o sin pt at each end (motion at each end being in phase), it is shown in [81 and 99] that the relative transverse motion of any point on the beam, with respect to the ends, is obtained by taking a loading of uniform intensity $f(x) = \rho p^2 x_o$, where ρ is the mass density of beam per unit length and f(x) is the amplitude of loading intensity which varies sinusoidally. This is explained in [99] from the theory of relative

motion that the equations of motion relative to a moving coordinate system may be obtained by employing additional forces equal to mass x acceleration of system of reference.

In Section II.C.2, f(x) has been taken as

$$f(x) = \sum_{n-1}^{\infty} f_n \sin \frac{n\pi x}{L}$$

Multiplying both sides by $\sin \frac{m\pi x}{L}$ and integrating from 0 to L, it is seen that

$$f_n = \frac{2}{L} \int_0^L f(x) \sin \frac{n\pi x}{L} \, dx \qquad \text{(III.20a)}$$

Taking f(x) = F, a uniform intensity of loading, it is seen that

$$f_n = -\frac{4F}{n\pi} \text{ when } n = 1, 3, 5 \text{ etc.}$$

$$= 0 \text{ when } n = 2, 4, 6 \text{ etc.}$$

W^R, i.e. the motion of a point on the beam, with respect to ends may be obtained from

$$W^R = \sum_{n-1}^{\infty} w_n \sin \frac{n\pi x}{L}$$, where w_n is obtained from eqn. (II.20) viz.

$$bw_n [R_{T_n} + i I_{T_n}] = f_n$$

w_n in phase with excitation $= \dfrac{f_n R_{T_n}}{b(R_{T_n}^2 + I_{T_n}^2)}$

and out of phase component of w_n being

$$= \frac{-f_n \, I_{T_n}}{b(R_{T_n}^2 + I_{T_n}^2)}$$

For drawing the resonance curves for W^R, the values of W^R are calculated at a number of frequencies, the number of terms in the series taken being large enough till the w_n terms corresponding to high values of 'n' are negligible. For high frequencies, more terms in the series would be required.

The series employed is convergent. This may be verified easily in any particular problem when the terms are calculated on a digital computer, where it may be seen that the increase of terms beyond a certain number in the series may hardly affect the answer. However, for the simplified case of Section II.C.4, this may be seen as below.

$$W^R = \sum_{n-1,3}^{\infty} w_n \sin \frac{n\pi x}{L}$$

$$= \sum_{n=1,3}^{\infty} \frac{4F \sin \frac{n\pi x}{L}}{n\pi(r_{t_n} + i\, i_{t_n} - \rho p^2)} \quad ; \text{ for}$$

end-displacement excitation.

Using expressions for 'k' and '$k\eta_s$' as defined in Section III.A.1,

$$W^R = \sum_{n-1,3}^{\infty} \frac{4F \sin \frac{n\pi x}{L}}{n\pi\left[\left(\frac{n\pi}{L}\right)^4 \frac{bE_s t_s^3}{12}\{k+ik\eta_s\} - \rho p^2\right]} \qquad \text{(III.20b)}$$

From [100], it is seen that a series of the type

$f(n) = \frac{1}{n^P}$ is convergent if $P > 1$. From Figs. III-11 and III-12, it is seen that with the increase of the shear parameter, 'k' increases or remains constant. Also from figs. III-5, III-11 and III-12, it may be observed that a change of shear parameter causes a linear variation in '$k\eta_s$', in regions away from optimum values, where the curves are flatter. Since the shear parameter involves only 'n^2', the power of 'n' in the denominator of eqn. (III.20b) is always expected to be greater than unity, making the series convergent. It is desirable, however, that at any frequency of excitation 'p', the number of terms in the series should be sufficiently large so that in the nth term of the series, 'r_{t_n}' is much greater than ρp^2.

Since eqns. II.20 and II.67 are similar, the above procedure for obtaining resonance curves from analysis I, also holds for analysis II.

For illustration, resonance curves have been drawn for a chosen case in Fig. III-15. In the Fig., the absolute value of transverse displacement amplitude at the middle of the beam is plotted, the absolute transverse motion

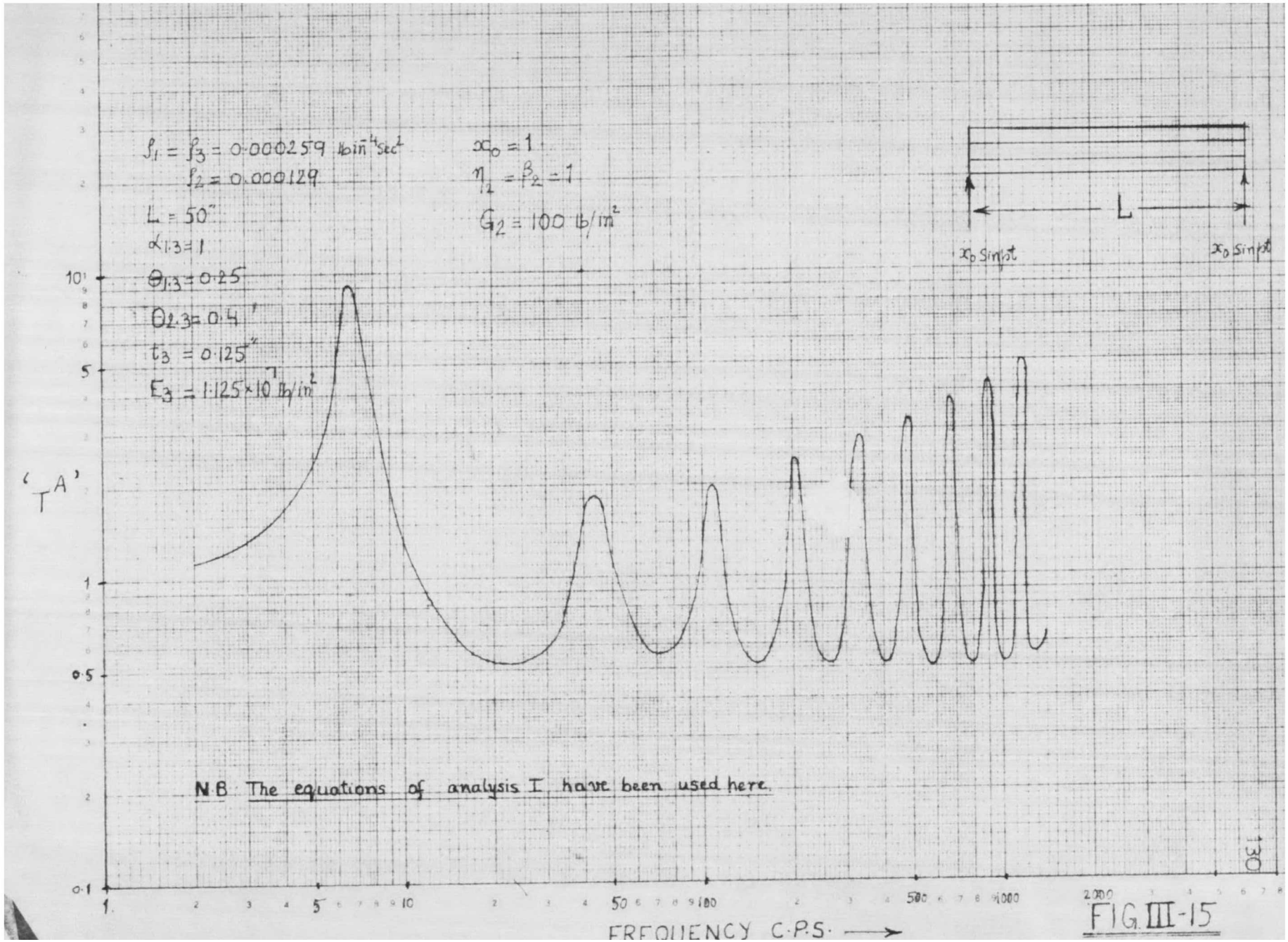
$\rho_1 = \rho_3 = 0.000259$ lb in^{-4} sec^2
$\rho_2 = 0.000129$
L = 50"
$\alpha_{1:3} = 1$
$\theta_{1:3} = 0.25$
$\theta_{2:3} = 0.4$
$t_3 = 0.125$"
$E_3 = 1.125 \times 10^7$ lb/in^2
$x_0 = 1$
$\eta_{12} = \beta_2 = 1$
$G_2 = 100$ lb/in^2
L
$x_0 \sin pt$
$x_0 \sin pt$
'TA'
10
5
1
0.5
0.1
1
5
10
50
100
500
1000
2000
FREQUENCY C.P.S. →
N.B The equations of analysis I have been used here.
130

FIG. III-15

being $W^A - W^R + x_o$ (vectorial addition)

W^A is absolute motion

and W^R is motion with respect to the ends.

In the Fig., the amplitude at the lowest mode is seen to be highest and at first decreases for higher modes but gradually increases later, because of low damping at higher modes, for the configuration chosen.

In practice, values of G_2, η_2 and β_2 vary with frequency and for each frequency, the corresponding properties should be used. In above illustration, however, constant values are employed since it is not drawn for any specific core material.

III.E : Correlating Damping Effectiveness and Resonant Response Analysis and Application of These Studies

The validity of damping effectiveness studies of previous sections will be discussed. It will be determined whether these have any relation with the displacement resonant response due to any harmonic excitation, and in particular to the end displacement type of excitation, employed in Section III.D. Results for peak displacement amplitude and corresponding frequencies will be given in dimensionless form for the above mentioned displacement type of excitation and finally application and use of these studies will be discussed.

III.E.1 : Correlating damping effectiveness and resonant response analysis

In Chapter II, it has been shown that the expression for transverse displacement response can be written as

$$W = \sum_{n=1}^{\infty} \frac{f_n}{R_{T_n} \quad i \; I_{T_n}} \sin \frac{n\pi x}{L} \sin pt \qquad \text{(III.21)}$$

Expressions for R_{T_n} and I_{T_n} are given in Section II.C.3 for analysis I and II.D.4 for analysis II. Definitions of η_s and $k\eta_s$ (or DRE) for each mode, corresponding to each single term in the series, are given in Section III.A.

If it is assumed that by a suitable application of dynamic loading (generalized loading), the response 'w' is due to only one term in the series say nth, then at frequency given by $R_{T_n} = 0$, all points on the beam will be in phase, such a frequency may be called the nth mode frequency i.e. F_n

At nth mode frequency, transverse displacement response is inversely proportional to I_{T_n}, since $R_{T_n} - 0$. I_{T_n} is proportional to $k\eta_s$ representing the displacement response effectiveness for the corresponding mode. In practice, with any general type of dynamic loading, at a frequency corresponding to nth mode, there may be contribution to total dynamic response from other terms in the series. Under these conditions, $k\eta_s$ may not adequately

represent the displacement response effectiveness.

When the excitation is of the type given in Section III.D i.e. both ends of the simply supported beam are subjected to sinusoidal displacement excitation of same magnitude and phase,

f_n is given in Section III.D as $= \frac{4f}{n\pi}$, n=1,3,5, ...

$= 0$, n=2,4,6, ...

where $f = \rho p^2 x_o$, x_o being amplitude of vibration of beam ends.

Taking $x_o = 1$ and the displacement amplitude at centre of beam relative to the ends as T^R,

$$T^R = \sum_{n=1,3}^{\infty} \frac{\frac{4}{n\pi} p^2}{r_{t_n} + i\, i_{t_n} - \rho p^2} \sin \frac{n\pi}{2} \qquad \text{(III.22)}$$

For simplified case of analysis I, r_{t_n} and i_{t_n} are given in eqn. (II.25) and do not involve any frequency terms. If only transverse inertia terms are included, eqns. (II.20) and (II.67) can be reduced to a form similar to eqn. (III.22); η_s according to Section III.A for nth mode $= \frac{i_{t_n}}{r_{t_n}}$.

It may be seen from eqn. (III.22) that at nth mode frequency,

Contribution of nth term in series to T^R

$$= \frac{\frac{4}{n\pi} \rho p^2}{i\, i_{t_n}} = \frac{\frac{4}{n\pi}}{i\eta_s} \qquad \text{(III.23)}$$

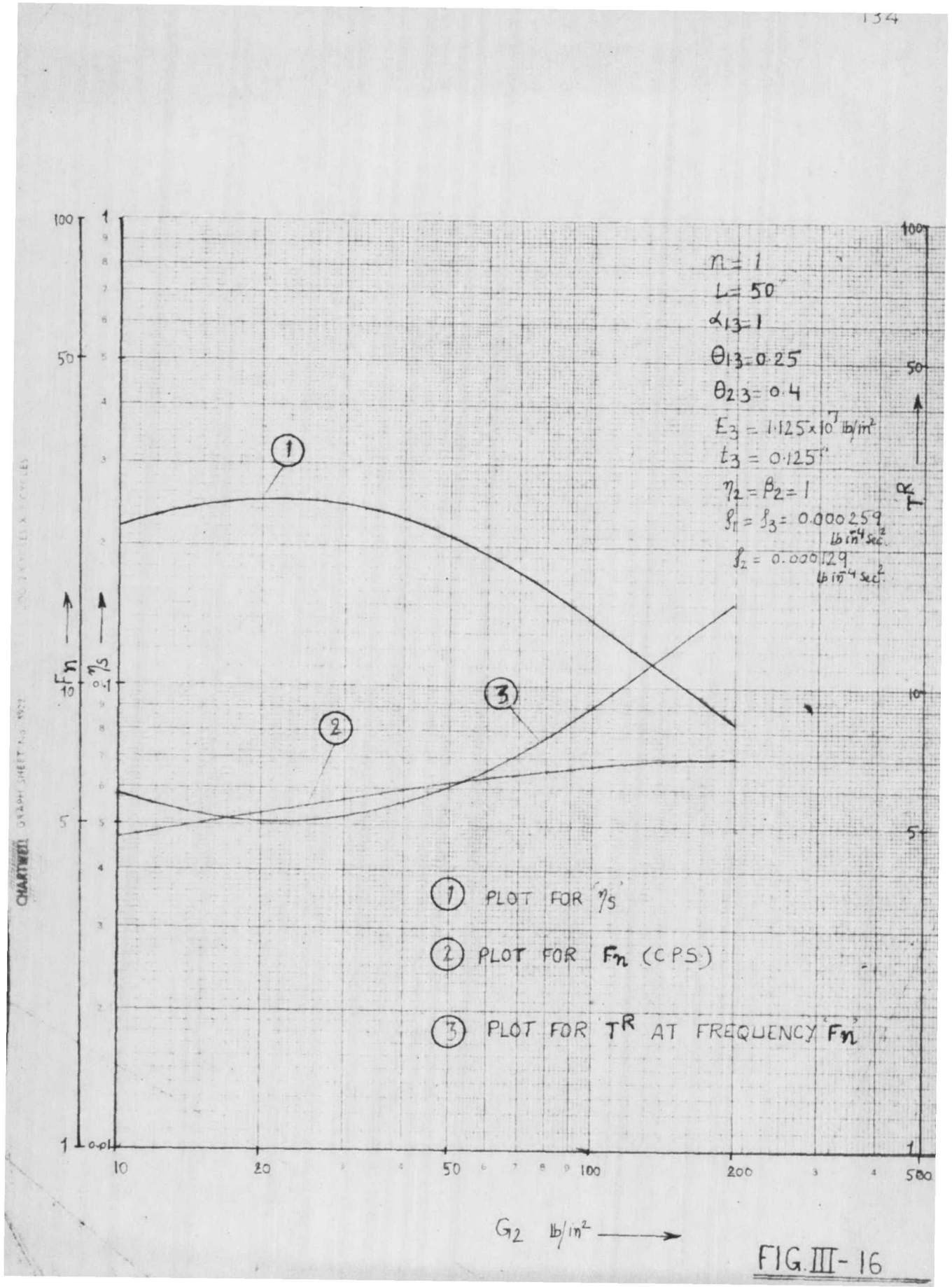
n = 1
L = 50
α13 = 1
θ13 = 0.25
θ23 = 0.4
E3 = 1.125 x 10^7 lb/in^2
t3 = 0.125"
η2 = β2 = 1
ρ1 = ρ3 = 0.000259 lb in^-4 sec^2
ρ2 = 0.000129 lb in^-4 sec^2
1 PLOT FOR ηs
2 PLOT FOR Fn (CPS)
3 PLOT FOR T^R AT FREQUENCY Fn
Fn
ηs
αL
G2 lb/in^2 ⟶

FIG. III-16

$n = 3$

Remaining parameters and description of plots are given in Fig. III 16

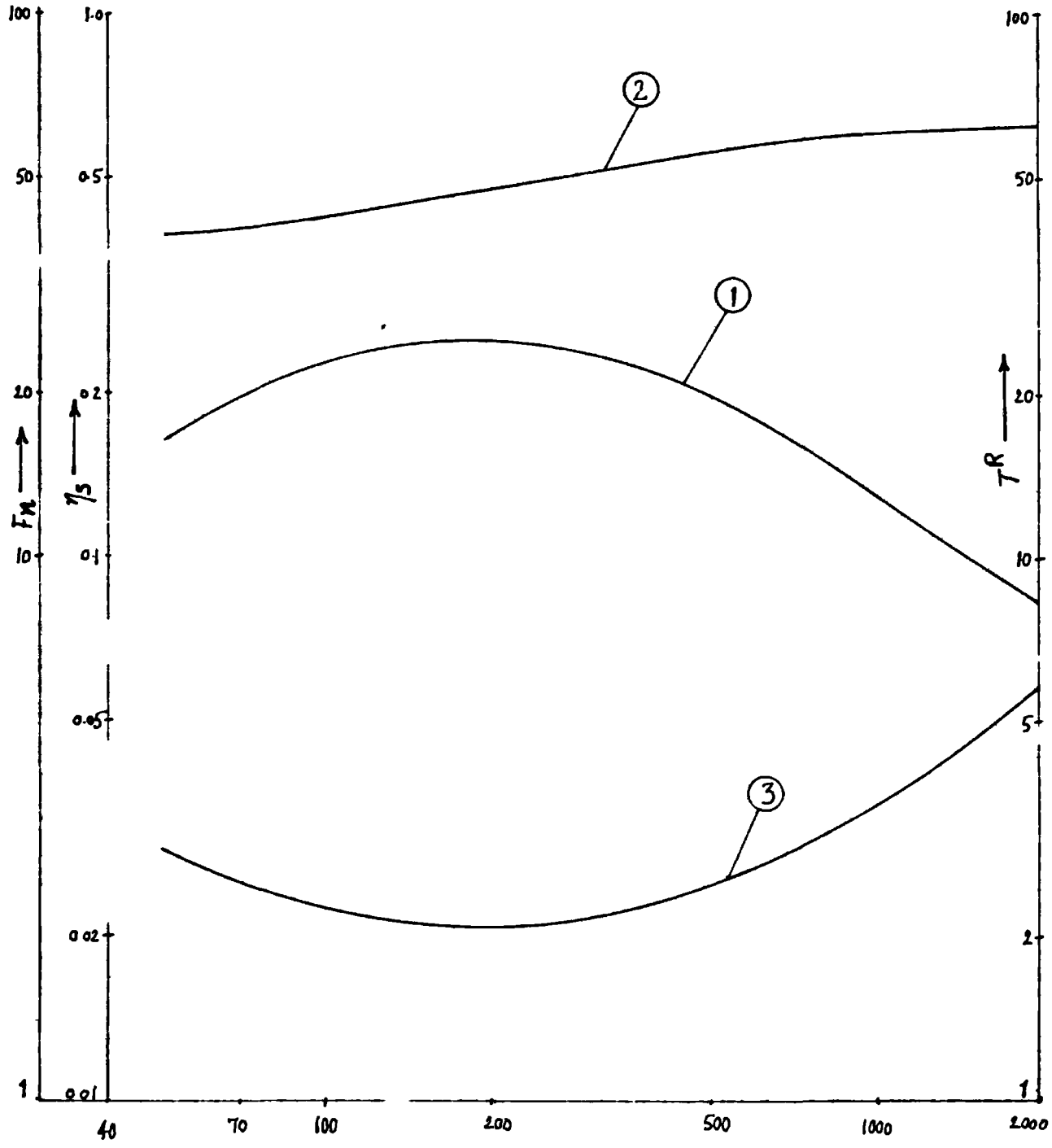

FIG III-17

1a, 1b, 1c : Plots of η_s for $n = 5, 7, 9$ respectively.

2a, 2b, 2c . Plots of F_n for $n = 5, 7, 9$ respectively

3a, 3b, 3c Plots of T^R for $n = 5, 7, 9$ respectively

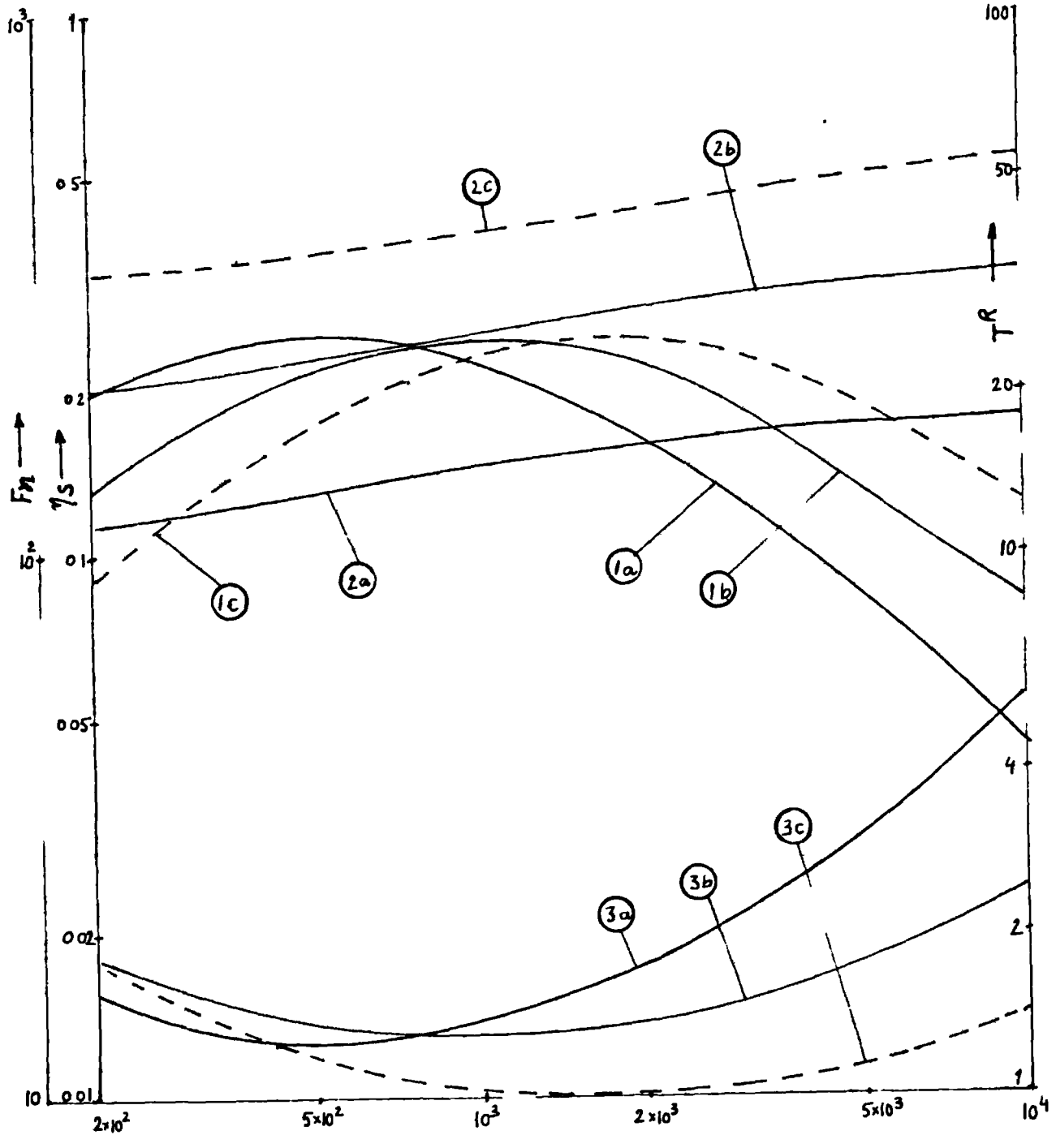

FIG III-19

(Since at nth mode frequency, $r_{t_n} = \rho p^2$).

At nth mode frequency, nth term in the series given by eqn. III.23 is expected to be predominant in T^R and so η_s, in this case would be an adequate measure for displacement response effectiveness. To verify this, figs. III.16 to III.18 are drawn for first 5 resonances encountered in the end displacement type of excitation chosen. The values plotted are: modal frequency, corresponding modal loss factor and T^R at the model frequency. These are plotted against core shear modulus G_2. Each of the Figs. shows that T^R becomes minimum at almost the same value of G_2 as the one at which η_s becomes maximum. For low order modes, T^R is inversely proportional to η_s, while this is only approximately true for high order modes e.g. when n 7 or 9.

III.E.2 : The peak displacement response

For any general type of excitation, the modal frequencies as defined in Section III.E .1 may be different from the frequencies corresponding to peak displacement amplitudes (called peak frequencies hereafter). Also, peak T^R, T^A and stresses will occur at different frequencies, T^A is the ratio of amplitude of absolute motion of middle of the beam to end amplitude, for the end displacement type of excitation, T^R being as defined in Section III.E.1. For

a chosen case, with parameters, are listed in Fig.III-16, peak frequencies for T^A, T^R corresponding to the first five peaks are listed in Tables T-7 to T-11, together with the corresponding modal frequencies for various modes. Each table refers to a single peak and a mode and the value of core shear modulus is varied. It may be seen that in all these tables, peak frequencies for T^A and modal frequencies are nearly same, while peak frequency for T^R is different from these, for higher modes. In practice, it is tedious to determine peak frequencies, while modal frequencies may be calculated easily. So, it is particularly useful to find that peak frequencies for T^A and modal frequencies are nearly same.

In order to plot peak T^A and corresponding frequencies for various values of shear parameter, a new shear factor 'S' will be defined, which unlike $\phi_{2.3}$ in Chapter II, does not include the modal number 'n .

Taking shear factor $$S = \frac{G_2}{E_3 t_3^2 (\frac{\pi}{L})^2} \qquad \text{(III.24)}$$

and dimensionless frequency factor

$$Y = \sqrt{\frac{p^2}{(\frac{\pi}{4})^4 E_3 t_3^3}} \qquad \text{(III.25)}$$

From eqn. (III.22), displacement of any point on the beam with respect to the ends, when each end is excited with a

TABLE T-7

Frequency c.p.s.	G_2 lb/in^2					
	10	25	40	50	75	100
Modal frequency corresponding to n=1	4.725	5.4831	5.9401	6.1485	6.4864	6.6846
I Peak frequency for T^R	4.8	5.7	6.1	6.3	6.6	6.8
I Peak frequency for T^A	4.7	5.5	6.0	6.2	6.5	6.7

TABLE T-8

Frequency c.p.s.	G_2 lb/in^2				
	100	300	500	1000	2000
Modal frequency corresponding to n = 3	43.164	51.87	56.179	60.734	63.0
II Peak frequency for T^R	41.5	49.6	54.5	59.7	63.0
II Peak frequency for T^A	43.6	52.5	56.5	61.0	63.6

TABLE T-9

Frequency c.p.s.	G_2 lb/in^2				
	100	300	1000	2000	10000
Modal frequency corresponding to n=5	107.3	121.27	148.51	163.36	180.05
III peak frequency for T^R	111	132.5	161	172	181
III peak frequency for T^A	107	122.2	150	163.4	180

TABLE T-10

Frequency c.p.s.	G_2 lb/in^2				
	100	300	1000	2000	10000
Modal frequency corresponding to n=7	202.46	218.3	259.31	292.02	344.4
IV peak frequency for T^R	199.5	206	232	268	339
IV peak frequency for T^A	202	220	261	294	345

TABLE T-11

Frequency c.p.s.	G_2 lb/in^2				
	100	300	1000	2000	10000
Modal frequency corresponding to n= 9	329.12	345.74	394.61	443.18	551.5
V peak frequency for T^R	331.5	363	497	521.2	575
V peak frequency for T^A	329.5	345	397	444	552

displacement x_o sin pt (x_o - 1 here is

$$= \sum_{n=1,3}^{\infty} \frac{\frac{4}{n\pi} Y^2 \sin \frac{n\pi x}{l}}{(n^4 r_{t_n} - Y^2) + I(i_{t_n}) n^4} \sin pt \qquad \text{(III.26)}$$

The expressions for r_{t_n} and i_{t_n} are given below, from the analysis I of Chapter II, when longitudinal and rotational inertia terms are not included.

$$r_{t_n} - h_3^r \quad \frac{(R_1R_2+I_1I_2)-(R_3R_2+I_3I_2)}{R_2^2 + I_2^2} \qquad \text{(III.27)}$$

$$i_{t_n} = h_3^I \quad \frac{(I_1R_2-I_2R_1)-(I_3R_2-I_2R_3)}{R_2^2 + I_2^2} \qquad \text{(III.28}$$

Expressions for R_2, I_2, R_1, I_1, R_3, I_3, $\overline{A}$, $\overline{B}$, $\overline{C}$, $\overline{D}$ are as given in eqn. II.20. However,

$$f_1^r = \frac{Sk_2}{\theta_{2.3}} + \alpha_{1.3}\theta_{1.3} + \frac{\alpha_{2.3}\theta_{2.3}}{3}$$

$$f_1^I = \frac{Sk_2}{2.3}\eta_2 + \frac{\alpha_{2.3}\theta_{2.3}}{3}\beta_2$$

$$g_1^r = \frac{Sk_2}{\theta_{2.3}} - \frac{\alpha_{2.3}\theta_{2.3}}{6}$$

$$g_1^I = \frac{Sk_2}{\theta_{2.3}}\eta_2 - \frac{\alpha_{2.3}\theta_{2.3}}{6}\beta_2$$

$$g_2^r = 1 + \frac{Sk_2}{\theta_{2.3}} + \frac{\alpha_{2.3}\theta_{2.3}}{3}$$

$$g_2^I = \eta_2 \frac{Sk_2}{\theta_{2.3}} \quad \frac{\alpha_{2.3}\theta_{2.3}}{3} \beta_2$$

$$h_1^r = Sk_2 \left(\frac{1+\theta_{1.3}\ 2\theta_{2.3}}{2\theta_{2.3}}\right) - \frac{\theta_{2.3}}{12}(1-2\theta_{1.3})\alpha_{2.3}$$

$$h_1^I = Sk_2 \left(\frac{1+\theta_{1.3}+2\theta_{2.3}}{2\theta_{2.3}}\right)\eta_2 \frac{\theta_{2.3}}{12} (1-2\theta_{1.3})\alpha_{2.3}\beta_2$$

$$h_2^r \quad Sk_2\left(\frac{1+\theta_{1.3}\ 2\theta_{2.3}}{2\theta_{2.3}}\right) + \frac{\alpha_{2.3}\theta_{2.3}}{12}(2 - \theta_{1.3}$$

$$h_2^I = Sk_2\left(\frac{1+\theta_{1.3}+2\theta_{2.3}}{2\theta_{2.3}}\right)\eta_2 + \frac{\alpha_{2.3}\theta_{2.3}}{12}(2-\theta_{1.3})\beta_2$$

$$h_3^r = \frac{1+\alpha_{1.3}\theta^3_{1.3}}{12} \quad \frac{Sk_2}{4\theta_{23}} (1+\theta_{1.3}+2\theta_{2.3})^2$$

$$\frac{\alpha_{2.3}\theta_{2.3}}{12} (\theta_{1.3}^2 - \theta_{1.3} \quad 1)$$

$$h_3^I = \frac{Sk_2}{4\theta_{2.3}} (1+\theta_{1.3}+2\theta_{2.3})^2\eta_2 + \frac{\alpha_{2.3}\ 2.3}{12}(\theta_{1.3}^2-\theta_{1.3}+1)\beta_2$$

For a chosen case with parameters as given in Fig. III-19, Graphs of peak value of T^A and corresponding frequency factor 'Y' are drawn using the above equations, for various values of shear factor 'S'. For each value of S, frequency factor Y is varied in eqn. (III.26) and the value giving a peak value to T^A is noted. Graphs corresponding to the first two peaks are given in Fig.III-19 and Fig.III-21. Also, Graphs for η_s corresponding to n=1 and n-3 are drawn in Fig . III-20 and Fig.III-22 respectively. It is

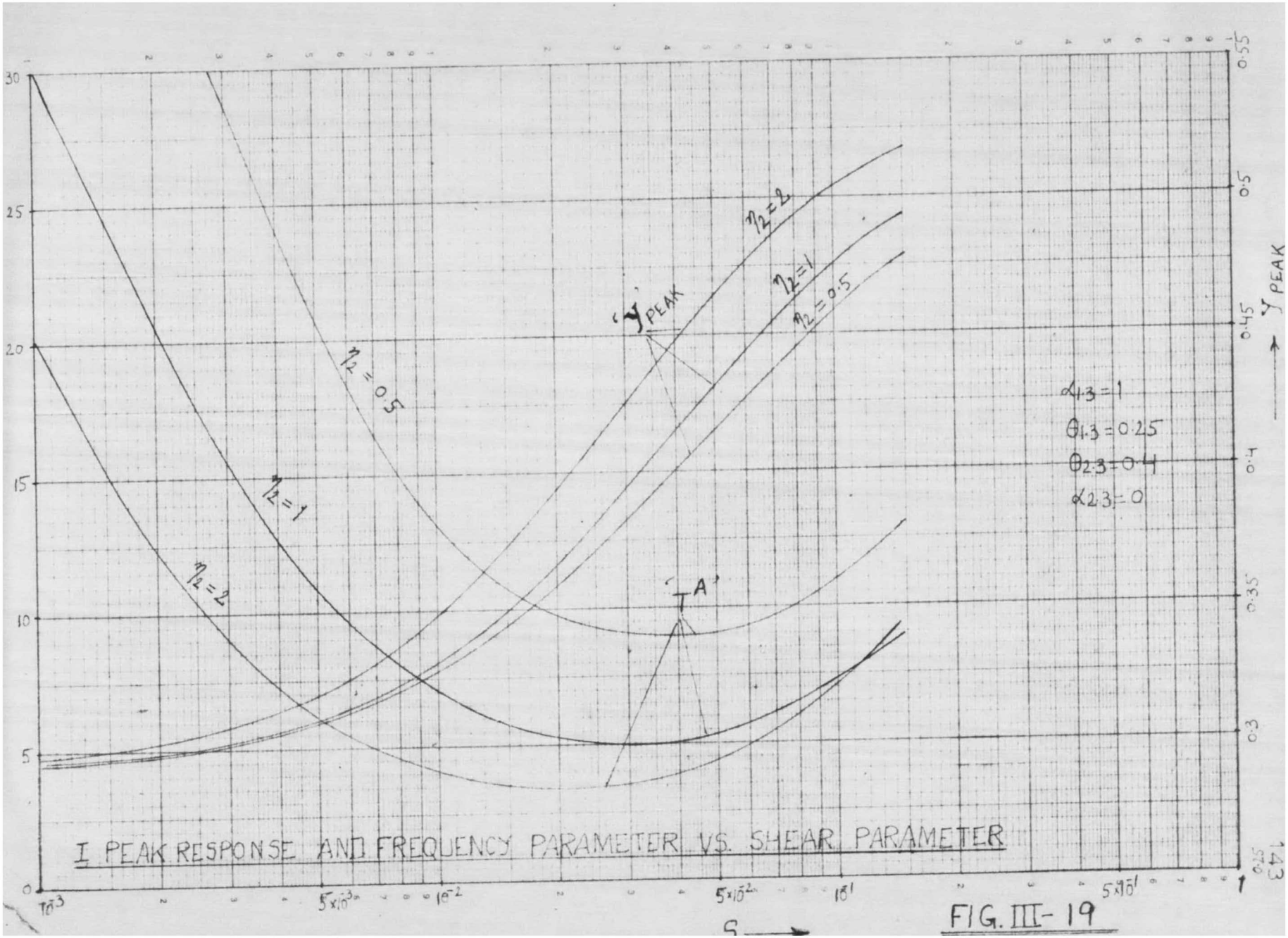

I PEAK RESPONSE AND FREQUENCY PARAMETER VS. SHEAR PARAMETER

FIG. III-19

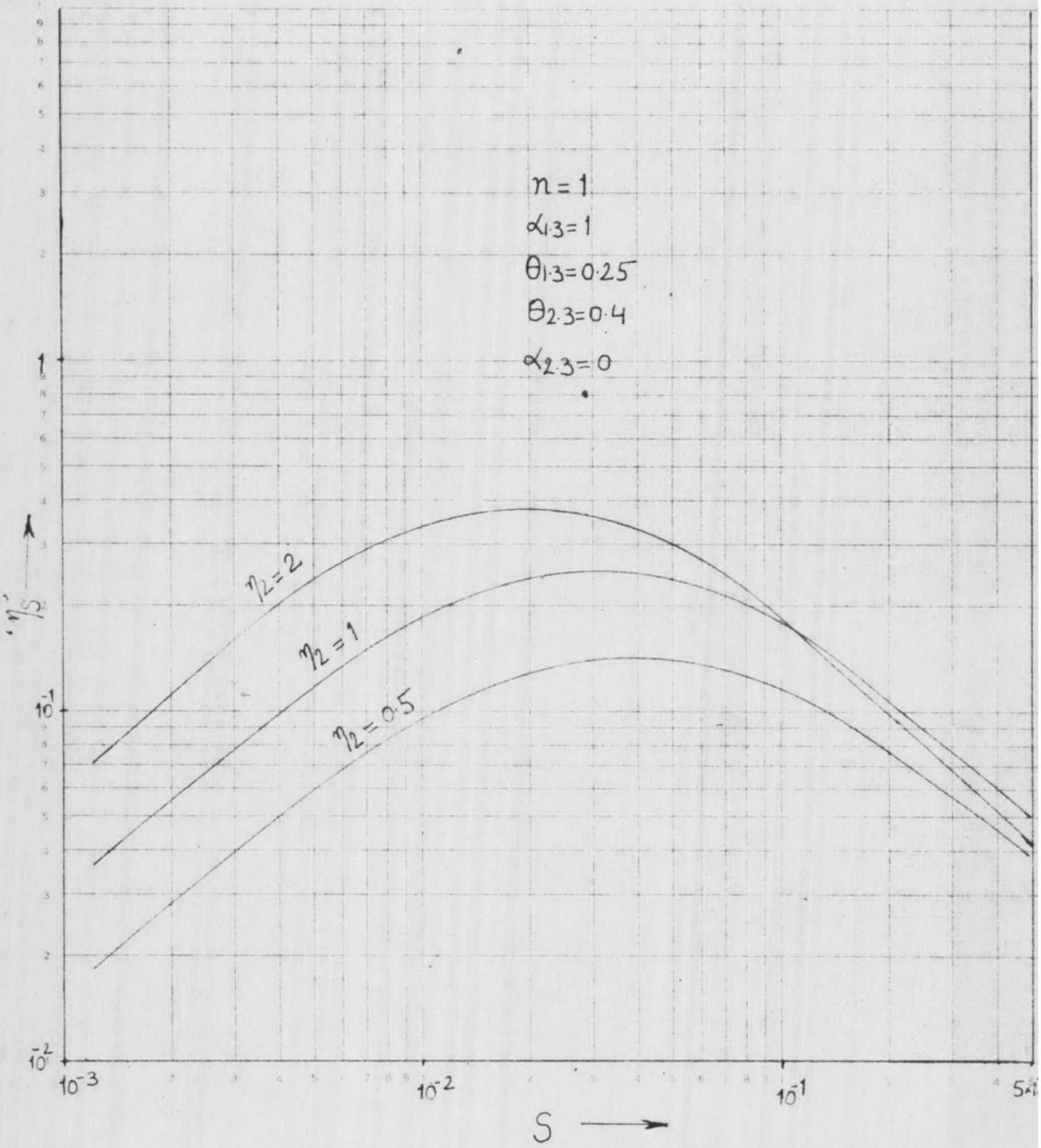
n = 1
α1·3 = 1
θ1·3 = 0·25
θ2·3 = 0·4
α2·3 = 0
η2 = 2
η2 = 1
η2 = 0·5
η'/S
1
10⁻¹
10⁻²
10⁻³
10⁻²
10⁻¹
S

FIG III-20

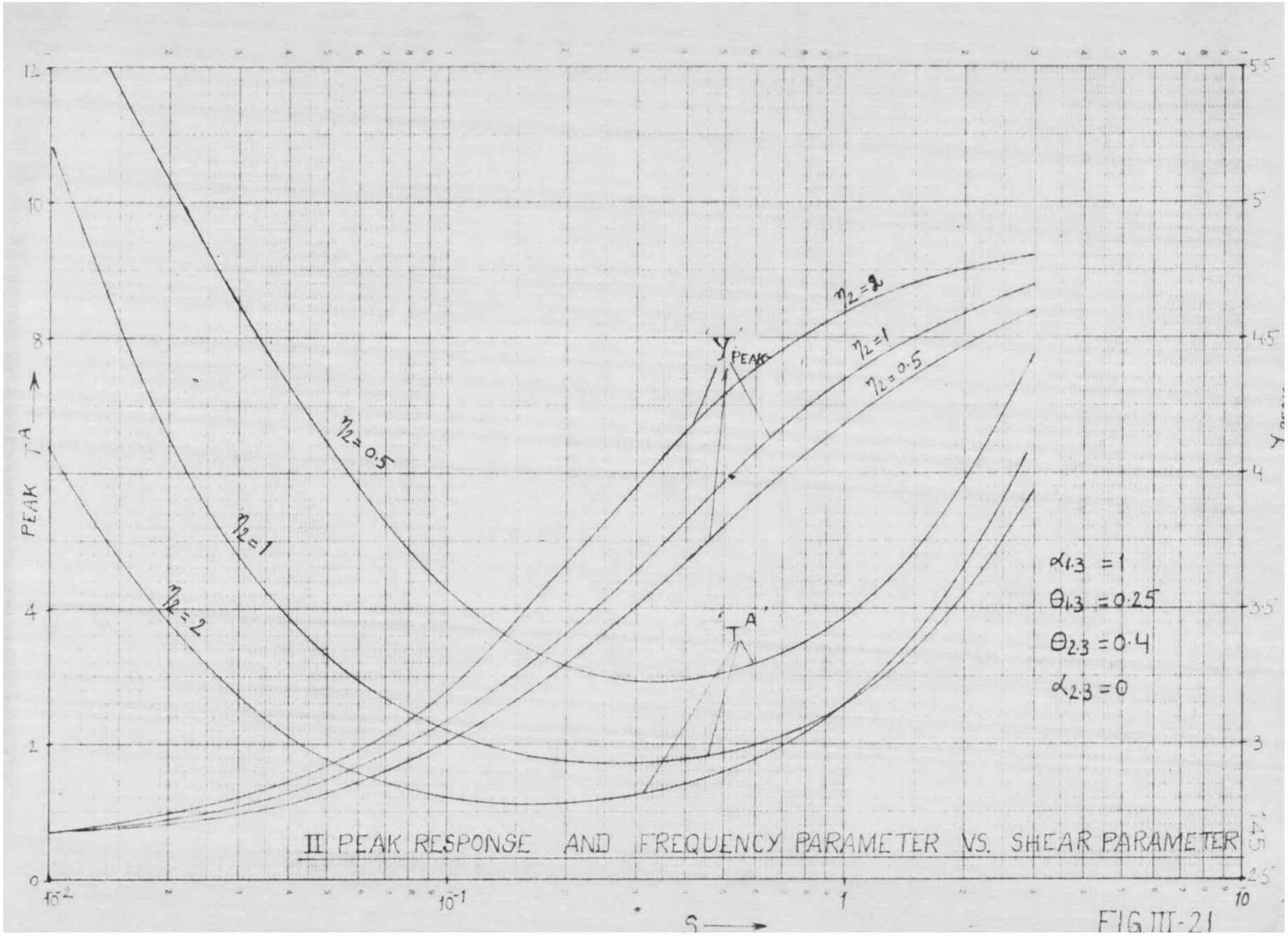

II PEAK RESPONSE AND FREQUENCY PARAMETER VS. SHEAR PARAMETER

FIG III-21

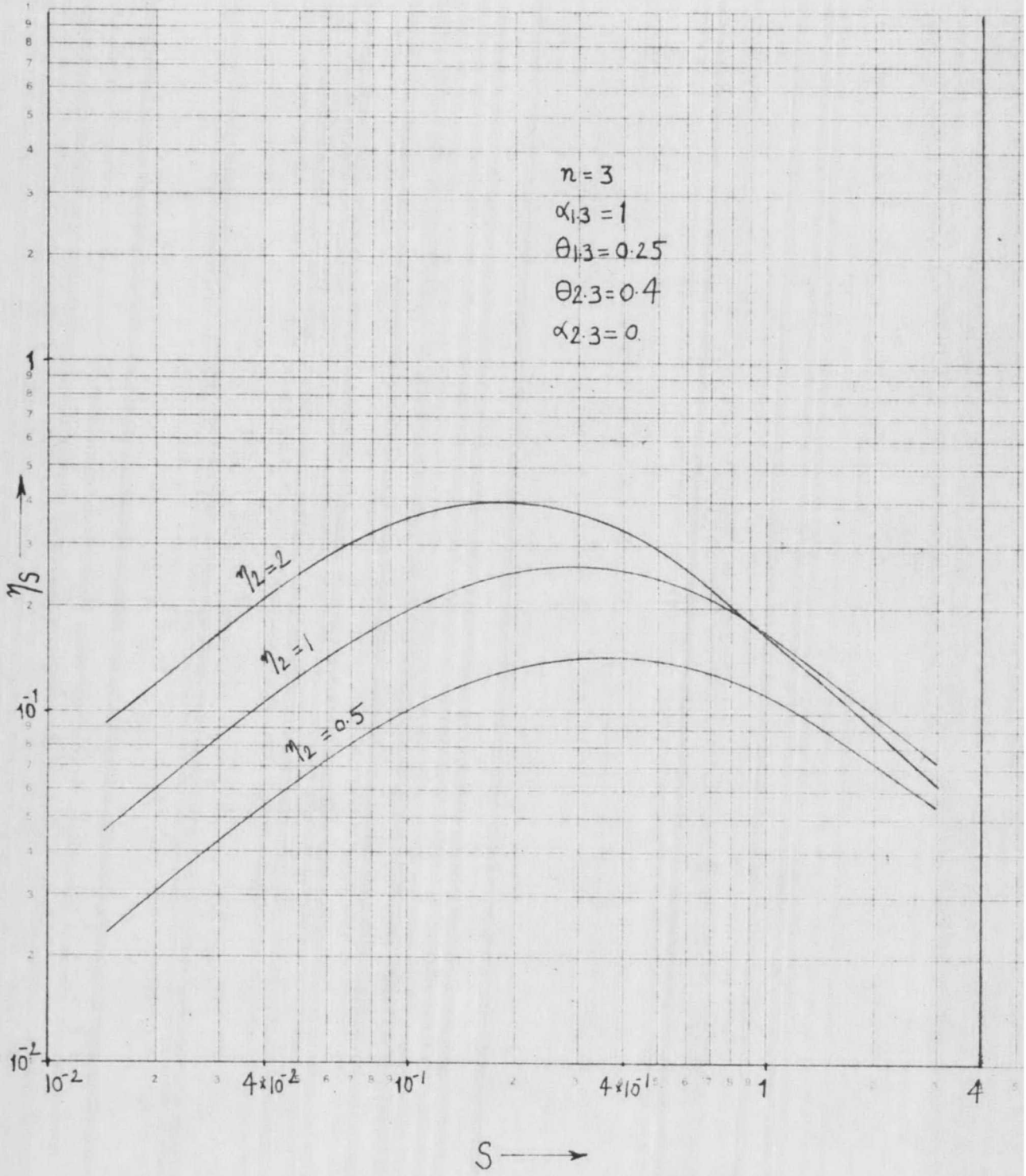
n = 3
α1.3 = 1
θ1.3 = 0.25
θ2.3 = 0.4
α2.3 = 0
η2 = 2
η2 = 1
η2 = 0.5
ηS
S
10⁻¹
10⁻²
4×10⁻²
4×10⁻¹
1
4

FIG III-22

seen from the above figs. that values of T^A for first peak are almost inversely proportional to η_S for n=1, as S is varied. Similarly, values of T^A for second peak are inversely proportional to η_S for n=3. Because of the symmetrical type of excitation used here, resonances occur only for the odd numbered modes. Application of these Figs. is discussed in the next Section.

III.E.3 : Application of optimum damping studies

As discussed in Section III.A, the damping in a 3 layered sandwich with viscoelastic core is optimum at a certain value of shear parameter only. This can be seen from Figs. III-4, III-5, III-11 and III-12. The peak displacement response also becomes minimum at a certain value of shear factor, as shown in Figs. III-19 and III-21. If the excitation of the system is such that a generalized mode is excited or the contribution of other modes at resonance is negligible, Figs. similar to Figs. III-4, III-5 or III-11 and III-12 are useful at design stage. However, if the excitation is such that it is likely to involve contribution of many modes at any resonance, graphs for peak response e.g. Figs. III-19 and Fig.III-21,are desirable.

The Figs. mentioned above have not been drawn for any particular viscoelastic material. An actual viscoelastic material has frequency dependent properties, i.e.

values of both G_2 and η_2 are dependent on the frequency of oscillation. In order to use these curves for an actual material, a number of trials have to be made e.g. to determine the resonant frequency for any mode for a given sandwich beam, using Figs. similar to Figs. III-11 and III-12, shear parameter may be calculated from suitably assumed viscoelastic material properties and corresponding value of 'k' determined from the appropriate curves. Modal frequency can be calculated from 'k'. Then, it may be checked from the material properties whether the properties assumed initially, correspond to this frequency. If not, new starting values of material properties, which correspond to this frequency, may be assumed and the procedure repeated till it is found that the values of material properties used correspond to the modal frequency determined. Knowing this, loss factor 'η_s' can also be got from these Figs, and it may be seen whether the damping obtainable at that mode is the optimum one. If not, the properties of the ideal material required for optimum conditions may be determined from these curves. This may be done for all possible modes of the sandwich beam, likely to be encountered in a given frequency range and the viscoelastic material properties desired at each model frequency for optimum conditions, may be specified. Thus, one can specify the type of frequency dependence of the material

properties required in order to attain optimum damping conditions, throughout a given frequency range.

A simple example of obtaining the type of frequency dependence of material properties is given as follows. If it is assumed that loss factor η_2 is constant at all frequencies and it is desired that optimum damping should occur at all modes, shear parameter φ or $\Phi_{2.3}$ must correspond to the optimum conditions and should remain constant at that value. This will be constant if G_2 is $\propto n^2$ (III.29) (all other parameters of the system reamining unchanged).

Using notations of Section III.A.1,

$$W = \sum_{n=1}^{\infty} \frac{f_n}{K_R(k+i\,k\eta_S)-\rho p^2} \sin\frac{n\pi x}{L} \sin pt \quad \text{(III.30)}$$

Keeping in view the definition of modal frequency as given in Section III.E.1, it is seen from equation (III.30) that the various modal frequencies are proportional to n^2, since K_R is $\propto n^4$. Using eqn. (III.29), it is found then that G_2 should vary linearly with frequency.

If the space distribution of excitation is known, Figs. corresponding to III-19 to III-22 may be drawn, giving peak response and corresponding frequencies. Here, the desired conditions are the minimum values of peak response and these plots can be used in a manner similar to the optimum damping plots explained above.

III.F: High Frequency Effects

If only transverse inertia terms are included in the equations of motion, the solution for elastic case (i.e. when all layers are elastic) involves only square of the frequency terms e.g. equations (II.22) in analysis I, which is the solution for simply supported sandwich beam, involves only p^2 terms. In this case, corresponding to each modal number, a frequency can be calculated, this being the natural frequency of flexural vibration. If translational and rotational inertia terms are also included then the solution involves higher powers of frequency terms and for each modal number, a family of modes exists, e.g. eqns. (II.19) for analysis I and eqns. (II.55) for analysis II. In eqn. (II-19), corresponding to any value of n, 3 values for natural frequencies can be obtained by putting right hand side equal to zero. The mode corresponding to the lowest frequency will be predominantly flexural, while those occurring at higher frequencies will be of thickness shear type. In [20-22, 28], the various families of modes thus obtained are discussed.

At a thickness shear frequency, for an infinite beam, there is no transverse displacement and longitudinal displacements are independent of x' [21, 69]. Above this frequency, the modes get coupled [70]. Such a frequency known as cut-off frequency occurs at a very high frequency

for a homogeneous beam. For a sandwich structure, however, it may occur at quite low frequencies [26], making it desirable to study the effect, which may be of importance, in practice. The behaviour of sandwich beams at these high frequencies does not appear to have been studied.

It may be seen that thickness-shear frequency (i.e. cut-off frequency) of an infinite sandwich beam with

$\rho_1 = \rho_3 = 0.000259$ lb $in^{-4} sec^2$

$\rho_2 = 0.0001295$ lb $in^{-4} sec^2$

$\alpha_{1.3} = \theta_{1.3} = 1$

$\theta_{2.3} = 4$

$E_3 = 10^7$ lb/in^2, $t_3 = 0.25"$ and $G_2 = 100$ lb/in^2

is as low as 300 c.p.s.

If L = 50",for a simply supported case, corresponding to n=1, the frequency of the mode belonging to the second family, which is predominantly of the thickness-shear type, is around 1400 c.p.s. These values are calculated from the frequency equations of symmetrical sandwich cases given in [22]. Hence if the excitations are likely to occur at frequencies around this value, the exclusion of translational and rotational inertia terms is likely to involve error in results.

Resonance curves have been drawn for a particular case, parameters chosen being given on Fig.III-23, with the ends of simply supported laminated beam, subjected to sinusoidal displacement of amplitude x_o sin pt. The

core is made of plasticized P.V.C. and the dynamic properties of the material used in this section for each frequency are taken from [71]. Curves of longitudinal stress amplitude at the middle of the beam, occurring on the outer fibre of layer 3 and its phase with respect to the ends, shear strain amplitude in the core at ends of the beam and its phase relative to end-displacement, and plots of T^R, the amplitude of displacement at middle of beam relative to ends for $x_o = 1$ are given in Figs. III-23 to III-26. These are drawn for analysis I in Section II-C, when all inertia terms are included in the equations and also when only transverse inertia terms are included, in order to indicate the importance of longitudinal and rotational inertia terms.

Longitudinal stress at the outer fibre of layer 3 is given as

$$- E_3 \left(u'_3 - w'' \frac{t_3}{2}\right)$$

$$= \sum_{n=1,3}^{\infty} E_3 \left[-\left(\frac{n\tau}{L}\right) u_{3n} + \left(\frac{n\tau}{L}\right)^2 w_n \frac{t_3}{2}\right] \sin \frac{n\pi x}{L} \sin pt \qquad \text{(III.31)}$$

Simultaneous solution of eqns. (II.18 , taking the coefficients involving moduli of layer 2 as complex, determine u_{3n} and w_n and hence the stress in eqn. III.31).

Expression for shear strain 'γ_2' is given by eqn. (II.2) and the solution to be substituted by eqn. (II.17 .

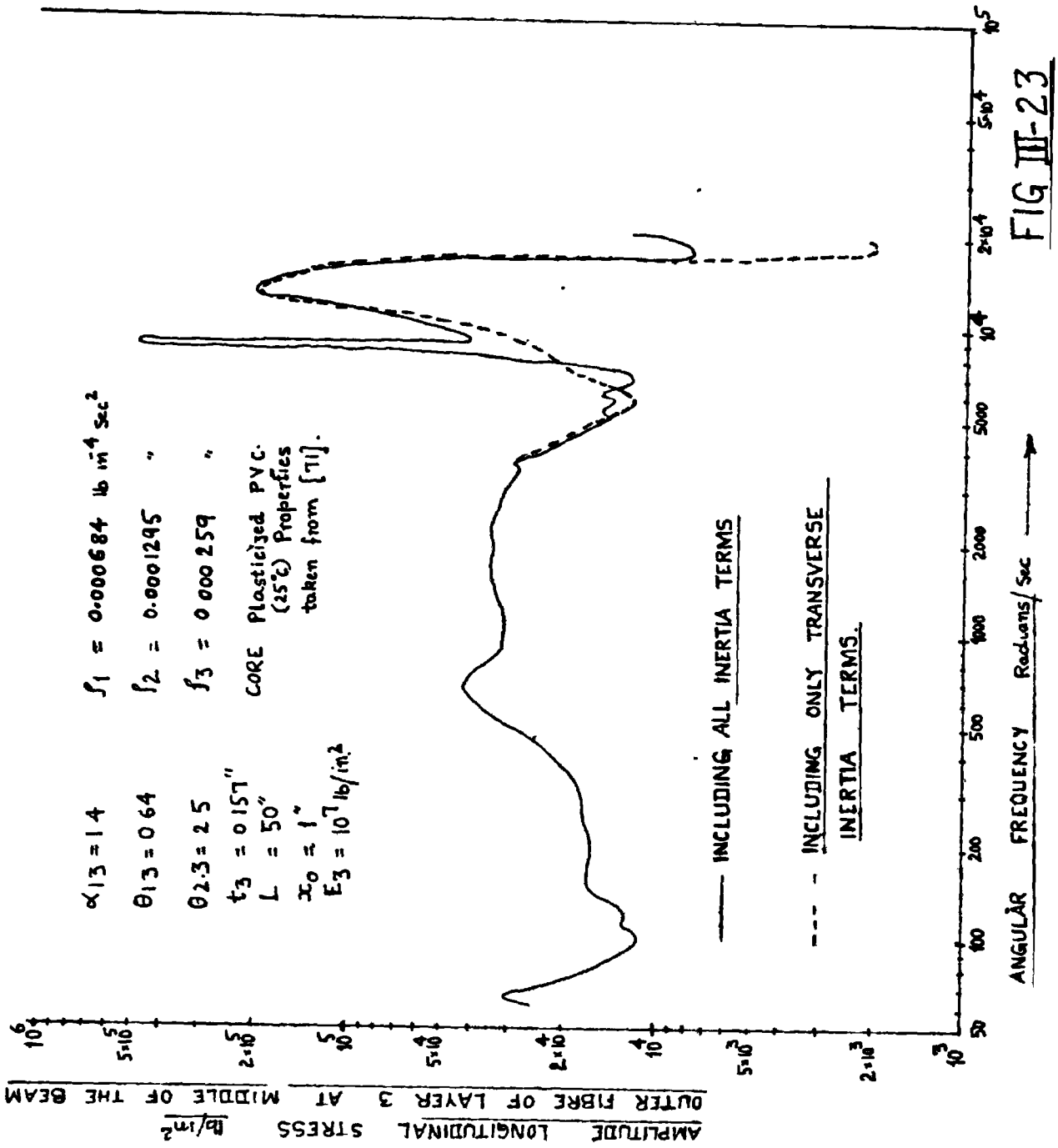
AMPLITUDE LONGITUDINAL STRESS lb/in²
OUTER FIBRE OF LAYER 3 AT MIDDLE OF THE BEAM
ANGULAR FREQUENCY Radians/Sec
INCLUDING ALL INERTIA TERMS
INCLUDING ONLY TRANSVERSE INERTIA TERMS.
α13 = 1.4
θ13 = 0.64
θ2.3 = 2.5
t3 = 0.157"
L = 50"
x0 = 1"
E3 = 10^7 lb/in²
f1 = 0.000684 lb in^-4 sec²
f2 = 0.0001295 "
f3 = 0.000259 "
CORE Plasticized PVC. (25°C) Properties taken from [71].

FIG III-23

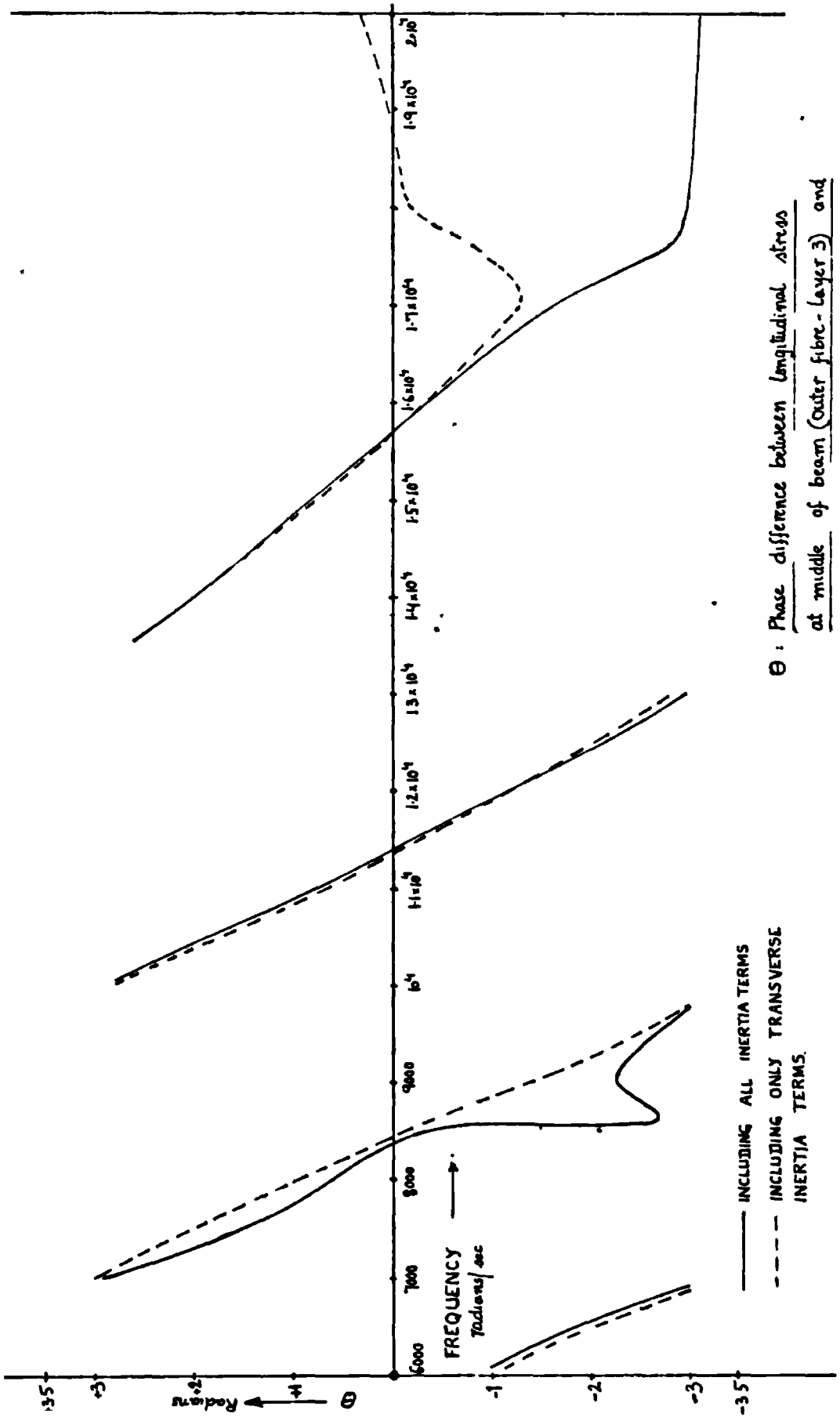

θ : Phase difference between longitudinal stress at middle of beam (outer fibre - layer 3) and end motion.

Parameters used are given in Fig. III-13

FIG III-24

Similar expressions are derivable from Section II.D for analysis II. However, for plotting the Figs. III-23 to III-26, analysis I was employed.

It is seen from Figs. III-23, that at higher frequencies, the longitudinal and rotational inertia terms change the value of longitudinal stress amplitude considerably. A peak around 8500 R.P.S. which occurs in thecurve, for which all inertia terms are included, appears to be due to the mode of thickness-shear type. The phase angle in Fig. III-24 is also considerably affected due to the neglect of longitudinal and rotational inertia terms. Similar situation holds for shear strain amplitude in Fig. III-25. However, the transverse displacements were not seen to be affected to any degree of significance by the inclusion of longitudinal and rotational inertia terms and hence only one curve is drawn in Fig.III-26. Only the longitudinal displacements appear to be affected and hence stresses and strains in Figs. III-23 to III-25 are changed at high frequencies.

It may be noted from the above mentioned graphs that the corresponding peaks for stress and displacement amplitudes occur at different frequencies. Also, some bumps are seen to occur in thecurves (e.g. around 100 R.P.S. in Figs. III-26), which are not due to the nearness of a resonant mode, but are due to abrupt change in material properties with frequency, which occur in the properties

γ_A = Amplitude of shear strain at beam ends.

θ = Phase difference between shear strain at end and end motion.

Parameters used are given in Fig. III-23.

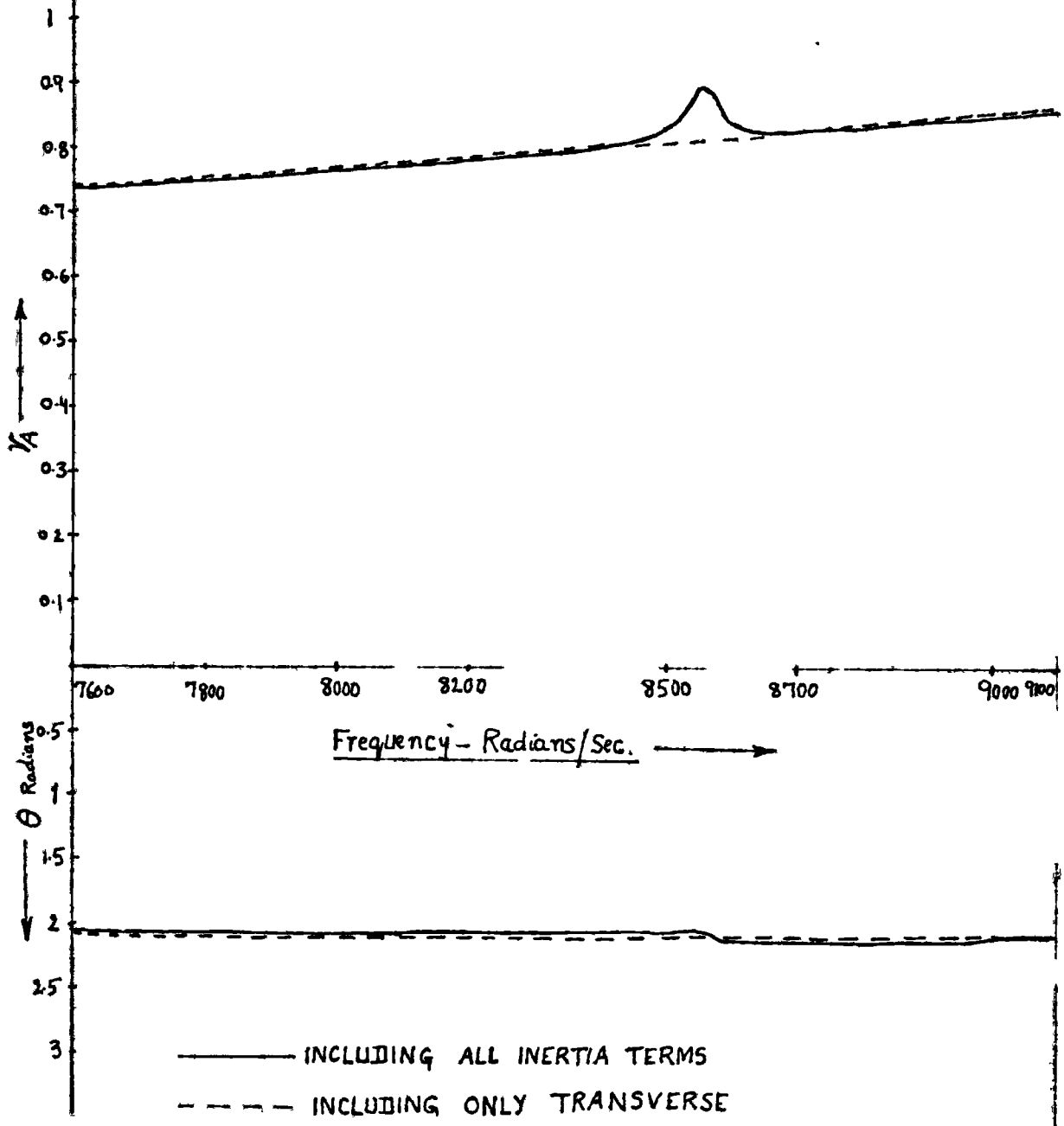

FIG. III-25

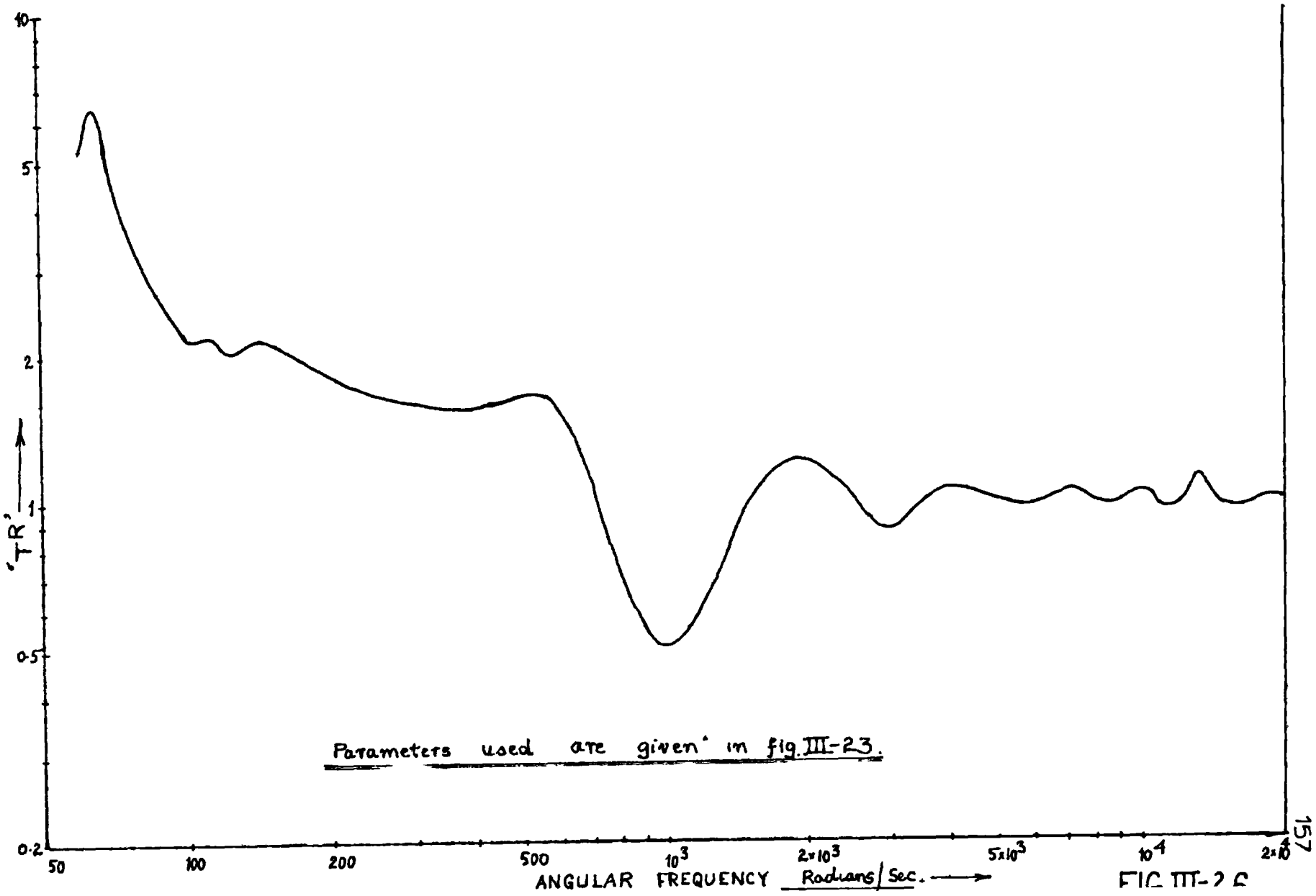

Parameters used are given in fig. III-23.

FIG III-2 C

given in [71].

III.G Inclusion of Effect of Non-Linearity Due to Amplitude Dependence of Viscoelastic Material Properties

The dynamic properties of viscoelastic materials viz. the in-phase shear modulus and the loss factor have been taken to be independent of strain amplitude in Chapter II and in other sections of the present Chapter. In practice, some viscoelastic materials have their properties dependent on the strain amplitude, to a significant extent. The flexural vibrations of a sandwich beam result in shear strain in the core. If a viscoelastic material having strain dependent properties forms the core of a 3 layered sandwich beam, the effective dynamic properties of the core will vary along the beam length. This effect will be taken account of, in the present section.

III.G.1 : Approximate solution for dynami response, with assumed non-linearity

Here, the amplitude dependence of dynamic properties of the core material in shear, will be taken into account for an assumed stress strain law. The stress strain law taken is.

$$\sigma = (A_1 + A_2 \frac{\partial}{\partial t}) \gamma + (C_1 + C_2 \frac{\partial}{\partial t}) \gamma^3 \qquad \text{(III.32)}$$

σ = shear stress

γ = shear strain.

An approximate solution is attempted from the variational integral using Ritz method.

The stationary value of functional $\bar{\varphi}$, according to Hamilton's principle, is equivalent to the equilibrium problem [80, p.221], where

$$\bar{\varphi} = \int_{t_1}^{t_2} (T-U+V)\, dt \qquad \text{(III.33)},$$

'T' is kinetic energy, 'U' is strain energy and 'V' is potential energy of time dependent forces.

The last mentioned forces make the system non-conservative. The admissible motion must be compatible with constraints and must coincide with actual motion at $t = t_1$ and t_2.

$\delta\bar{\varphi} = 0$ gives

$$\int_{t_1}^{t_2} (\delta T-\delta U-\delta V)dt = 0 \qquad \text{(III.34)}$$

The stress strain law used for the core material is given in Eqn. (III.32), where the terms C_1 and C_2 are due to non-linearity of the system.

The strain energy expression U is got from Section II.C.1 for the simplified case of Section II.C.4,

$$U = q\int_o^L (w'')^2 dx + r\int_o^L (u_1')^2\,dx + bt_2\int_o^L \frac{A_1\gamma^2}{2}\,dx + bt_2\int_o^L \frac{C_1\gamma^4}{4}\,dx \qquad \text{(III.35)}$$

where $q = \frac{b}{24}E_1t_1^3 + \frac{b}{24}E_3t_3^3$

$$r = \frac{bE_1t_1}{2} + \frac{bE_1^2t_1^2}{2E_3t_3}$$

$$\gamma = u_1e - w'f$$

$$e = \frac{1}{t_2} + \frac{E_1t_1}{E_3t_3t_2}$$

$$f = 1 + \frac{t_1 + t_3}{2t_2}$$

Subscript 1 in u_1 will be dropped from now on, for convenience. δU is got by the procedure as before, by giving increments u and δw to the terms u and w respectively, eliminating all higher powers of these increments and converting all the derivatives of δw and u, by integrating by parts.

δU is got as $-\int_o^L \int [2qw'''' \delta w - 2ru'' u$

$$+bt_2A_1e(ue-w f)\delta u+bt_2A_1f(u'e-w''f)\,\delta w$$

$$+bt_2c_1e(ue-w'f)^3\,\delta u$$

$$+3bt_2c_f u'e-w''f)(ue-w f)^2\,\delta w]\,dx \qquad \text{(III.36)}$$

δT is same as in Chapter II, being

$$= - \int_0^L \rho \ddot{w} \quad w \, dx \qquad \text{(III.37)}$$

where $\rho \quad b.\rho_1 t_1 + \rho_2 t_2 + \rho_3 t_3)$

$$\delta V = \int_0^L \int [F \sin pt \; \delta w - bt_2(A_2 \dot{\gamma}) \delta\gamma - bt_2(3C_2 \gamma^2 \dot{\gamma}) \delta\gamma] \, dx \qquad \text{(III.38)}$$

where F is the intensity of external dynamic loading per unit length, and is equal to $\rho p^2 x_o$, if the ends of the beam are subjected to a displacement excitation of $x_o \sin pt$.

In eqn. (III.38), -ve sign is used for virtual work of damping forces [79 p.277].

Substituting for γ in eqn. (III.38) and reducing $\delta w'$ to δw by integration by parts,

$$\delta V = \int_0^L \int [(F \sin pt)\delta w - bt_2 A_2 (\dot{u}e - \dot{w}'f) \, e\delta u$$

$$- bt_2 A_2 (\dot{u}'e - \dot{w}''f) \, f\delta w - 3bc_2 t_2 (ue - w'f)^2 (\dot{u}e - \dot{w}'f) \, e\delta u$$

$$- 3bc_2 t_2 f \{(ue - w'f)^2 (\dot{u}'e - \dot{w}''f)$$

$$+ 2(ue - w'f)(u'e - w''f)(\dot{u}e - \dot{w}'f)\} \, \delta w] \, dx \qquad \text{(III.39)}$$

The equations of motion can be written down, by using $\delta \bar{\varphi} = 0$ and grouping the terms separately for arbitrary displacements δw and δu. But, below an approximate solution will be found for the problem, using Ritz's variational method. In this method, a solution, which is consistent

with the external geometric constraints, is assumed and the variational integral is minimized with respect to the unknown parameters involved in solution. No direct use of equations of motion is made.

Only a periodic solution of the same frequency as excitation is considered. The solution assumed is:

$$\left.\begin{aligned} w &= w_{1s} \sin pt + w_{1c} \cos pt \\ u &= u_{1s} \sin pt + u_{1c} \cos pt \end{aligned}\right| \qquad \text{(III.40)}$$

where w_{1s}, w_{1c}, u_{1s} and u_{1c} are functions of x. These are assumed so that the required geometrical boundary conditions are satisfied

$$\left.\begin{aligned} w_{1s} &= \sum_{1}^{n} w_{sn} \sin \frac{n\pi x}{L} \\ w_{1c} &= \sum_{1}^{n} w_{cn} \sin \frac{n\pi x}{L} \\ u_{1s} &= \sum_{1}^{n} u_{sn} \cos \frac{n\pi x}{L} \\ u_{1c} &= \sum_{1}^{n} u_{cn} \cos \frac{n\pi x}{L} \end{aligned}\right| \qquad \text{(III.41)}$$

This corresponds to the linear solution of Chapter II. It is taken that the non-linearity of the system changes only the values of the parameters w_{sn}, w_{cn}, u_{sn}, u_{cn}, without changing the form of the solution given by eqn. (III.41). This might not hold for highly non-linear

systems, but for those in which the contribution of non-linear terms in stress strain law is small (as is true for common materials), this assumption should be satisfactory. A similar form of solution has been assumed by Sethna [83], while analysing the free vibrations of homogeneous beams with a non-linear viscoelastic law. However in [83], after substituting the assumed solution in the differential equations of motion, the resulting equations are treated by the method of averaging due to Kryloff and Bogoliuboff. The use of approximate variational methods for non-linear vibration problems is discussed in [79-82, 84-86, 93].

Equations (III.40) are substituted in eqns. for δU, δT and δV and integration is performed over the time period of motion viz. t_1 and t_2 are taken as 0 and $\frac{2\pi}{p}$ respectively. After performing the integration w.r.t. t, and combining terms of δU, δT and δV according to equation (III.34), we get

$$\int_0^L \Big[\Big\{2q\,\frac{\pi}{p}\,w_{1s}'''' + bt_2A_1f\,\frac{\pi}{p}\,m_1 + 3bt_2c_1f\Big(\frac{\pi}{4p}\Big)$$

$$3m_1^2m_1' + m_2^2\,m_1' + 2m_1m_2m'_2) - \rho p^2\,\frac{\pi}{p}\,w_{1s}$$

$$- \Big[\frac{\cdot}{p} - (bt_2A_2fpm_2'\,\frac{\pi}{p}) + (3fbt_2c_2p)\Big(\frac{\pi}{4p}\Big)(2m_1m_1'\,m_2$$

$$- m_2^2m_2' - 3m_1^2m'_2)\;6fbt_2c_2p\Big(\frac{\pi}{4p}\Big)(m_1^2m_2 - m_2^2m_2' - 2m_1m_1\,m_2\Big\}\delta w_{1s}$$

$$+\Big\{2q\,\frac{\pi}{p}\,w_{1c}'''' + bt_2A_1f\,\frac{\pi}{p}\,m_2' + 3bt_2c_1f\Big(\frac{\pi}{4p}\Big)(2m_1m_2m_1' + m_1^2m_2' + 3m_2^2m_2')$$

$$-\rho p^2 \frac{\pi}{p} w_{1c} + bt_2 A_2 f p m_1' \frac{\pi}{p} \; 3fbt_2 c_2 p \left(\frac{\pi}{4p}\right)(m_1^2 m_1' - 2m_1 m_2 m_2' + 3m_2^2 m_1')$$

$$+ (6fbt_2 c_2 p)\left(\frac{\pi}{4p}\right)(m_1^2 m_1' - m_2^2 m_1 + 2m_1 m_2 m_2')\} \delta w_{1c}$$

$$+ \{-2r \frac{\pi}{p} u_{1s}'' + bt_2 A_1 e \frac{\pi}{p} m_1 + bt_2 c_1 e \left(\frac{3\pi}{4p}\right)(m_1^3 + m_1 m_2^2)$$

$$- pbt_2 A_2 e m_2 \left(\frac{\pi}{p}\right) - 3bt_2 c_2 e p \left(\frac{\pi}{4p}\right)(m_1^2 m_2 + m_2^3)\} u_{1s}$$

$$+ \{-2r \frac{\pi}{p} u_{1c}'' \; bt_2 A_1 e \frac{\pi}{p} m_2 + bt_2 c_1 e \left(\frac{3\pi}{4p}\right)(m_2^3 + m_1^2 m_2)$$

$$pbt_2 A_2 e (m_1 \frac{\pi}{p}) \; (3ebt_2 c_2 p)\left(\frac{\pi}{4p}\right)(m_1^3 + m_2^2 m_1)\} \delta u_{1c}] \, dx = 0$$

(III.42)

where $m_1 = eu_{1s} - fw_{1s}'$, $m_2 = eu_{1c} - fw_{1c}'$

$m_1' = eu_{1s}' - fw_{1s}''$, $m_2' = eu_{1c}' - fw_{1c}''$

Taking only 3 terms in the series assumed in eqn. (III.41), substituting these in eqn. (III.42), performing integration with respect to x, we get 12 non-linear simultaneous algebraic equations, for arbitrary values of δw_{s1}, δw_{s2} etc. These equations were solved on the Atlas digital computer, in which use is made of the Newton-Raphson iterative procedure.

It is possible to show from the simultaneous algebraic equationsobtained that if the terms involving c_1 and c_2 are eliminated, the equations obtained resemble those derived in simplified analysis I of Section II.C.4

if the assumed solution is substituted in the latter.

An alternative approach for solution is to solve directly by finite differences, the 4 simultaneous non-linear ordinary differential equations, which can be obtained from parenthesis { } in eqn. III.42, for arbitrary values of δw_{1s}, δw_{1c}, δu_{1s} and u_{1c}.

In the Newton-Raphson iterative method [87,88] for solution of simultaneous non-linear algebraic equations, the iteration process is started with an assumed solution. If x_1, x_2 ... x_n is the assumed solution and if the required solution is at $(x_1+\varepsilon_1, x_2+\varepsilon_2 \ldots x_n+\varepsilon_n)$, for 'n' simultaneous equations, then the 'n' variable form of Taylor's theorem [87] gives:

$$f_i(x_1+\varepsilon_1, x_2+\varepsilon_2 \ldots\ldots, x_n+\varepsilon_n)$$

$$= f_i(x_1, x_2 \ldots x_n) + \sum_{r=1}^{n} \varepsilon_r \frac{\partial f_i}{\partial x_r} + O(\varepsilon^2) \qquad \text{(III.43)}$$

$$(i = 1 \ldots n)$$

whence for a second order process, we take $(\varepsilon_1 \ldots \varepsilon_n)$ to be the solution of a set of linear simultaneous equations,

$$\varepsilon_1 \frac{\partial f_i}{\partial x_1} \quad \varepsilon_2 \frac{\partial f_i}{\partial x_2} + \ldots\ldots \quad \varepsilon_n \frac{\partial f_i}{\partial x_n} = -f_i \qquad \text{(III.44)}$$

$$(i = 1 \ldots n).$$

The process is repeated with the new solution, till the solution to the desired degree of accuracy is obtained.

This method is used in Mercury library programme No.557 (Institute of Computer Science, University of London), which has been used in the present work. The solution for the corresponding linear problem (i.e. neglecting non-linear terms) is used as the starting solution and the non-linear solution is obtained after a number of iterations when residues are reduced to a negligible value. With this approach in the illustration given below, the final solution converged in each calculation, to a value which gave negligible residues.

III.G.2 : Illustration

For a beam, the ends of which are subjected to a displacement excitation x_o sin pt, with the parameters given in Fig.III-27, a resonance curve is drawn for the first resonance. It may be seen that only 3 terms are used in the assumed series solution (Eqn. III.41) and so the solution is expected to be accurate only near the first resonance. For higher frequencies, more terms are required in eqn. (III.41), the rest of the procedure being the same as explained.

The stress strain law used is

$$\sigma = (A_1 + A_2 \frac{\partial}{\partial t})\gamma \quad (C_1 + C_2 \frac{\partial}{\partial t})\gamma^3,$$

where γ is shear strain and σ is shear stress.

If $\gamma = \gamma_o \sin pt$,

then,

$$\sigma - (\eta_1 + \frac{3}{4} c_1 \gamma_o^2 \gamma_o \sin pt \ (A_2 + \frac{3}{4} c_2 \gamma_o^2) p\gamma_o \cos pt$$

$$+ \text{terms involving } \sin 3pt \text{ and } \cos 3pt \qquad \text{(III.45)}$$

It has been seen that in most viscoelastic materials [89], the non-linearity exhibited is to such an extent that at all the shear strain amplitudes, the σ-γ plot remains an ellipse or the $\sin 3pt$ and $\cos 3pt$ in eqn. III.45 can be taken to be negligible. The solution given in Section III.G.1 also has been restricted only to the period which is the same as that of the excitation frequency.

$$\text{So,} \quad G_1 = \frac{\sigma \text{ in phase with } \gamma}{\gamma_o} = A_1 + \frac{3}{4} c_1 \gamma_o^2$$

$$G_2 = \frac{\sigma \text{ in quadrature with } \gamma}{\gamma_o} = \bar{A}_2 \ \frac{3}{4} \bar{c}_2 \gamma_o^2 \qquad \text{(III.46)}$$

$$\text{where } \bar{A}_2 = pA_2 \text{ and } \bar{c}_2 = pc_2$$

The various material constants are frequency dependent and their values should be taken accordingly when the dynamic response at each frequency is computed.

At any frequency 'p' radians/second and $\gamma_o = 0$, $G_1 = \eta_1$ and $G_2 = \bar{A}_2$. For the sake of illustration, the material properties of the core will be taken as follows,

for all values of 'p'.

$$A_1 = 1000 \text{ lb/in}^2, \quad \bar{A}_2 = 666.67 \text{ lb/in}^2$$

$$c_1 = -5000 \text{ lb/in}^2, \quad \bar{c}_2 = -2466.7 \text{ lb/in}^2$$

In practice, G_1 and G_2 can be experimentally obtained at any value of p' and 'γ_o' and then it can be found if the assumed stress strain law is obeyed at each frequency. If so, A_1, A_2, c_1 and c_2 can be determined at each frequency, using eqn. (III.46).

Figs. III-27 to III-29 give graphs of amplitude and phase of transverse and longitudinal displacements for non-linear stress strain law (Curve No.1) and also for linear stress strain law (in Curve No.2), with values corresponding to $\gamma_o = 0$. It is seen that the non-linearity changes the peak response and corresponding frequency. It was found from the computations for Curve No.2 that the maximum shear strain at beam ends is around 0.3, in the linear case considered and is zero at the middle of the beam. So, Curve No.3 is drawn in Figs. III-27 and III-28, using equations for linear stress strain law, with material properties corresponding to γ_o 0.3. The curve for the non-linear case is seen to be in between the two curves corresponding to the two curves for linear cases, as might be expected.

In practice, the stress strain law used in this

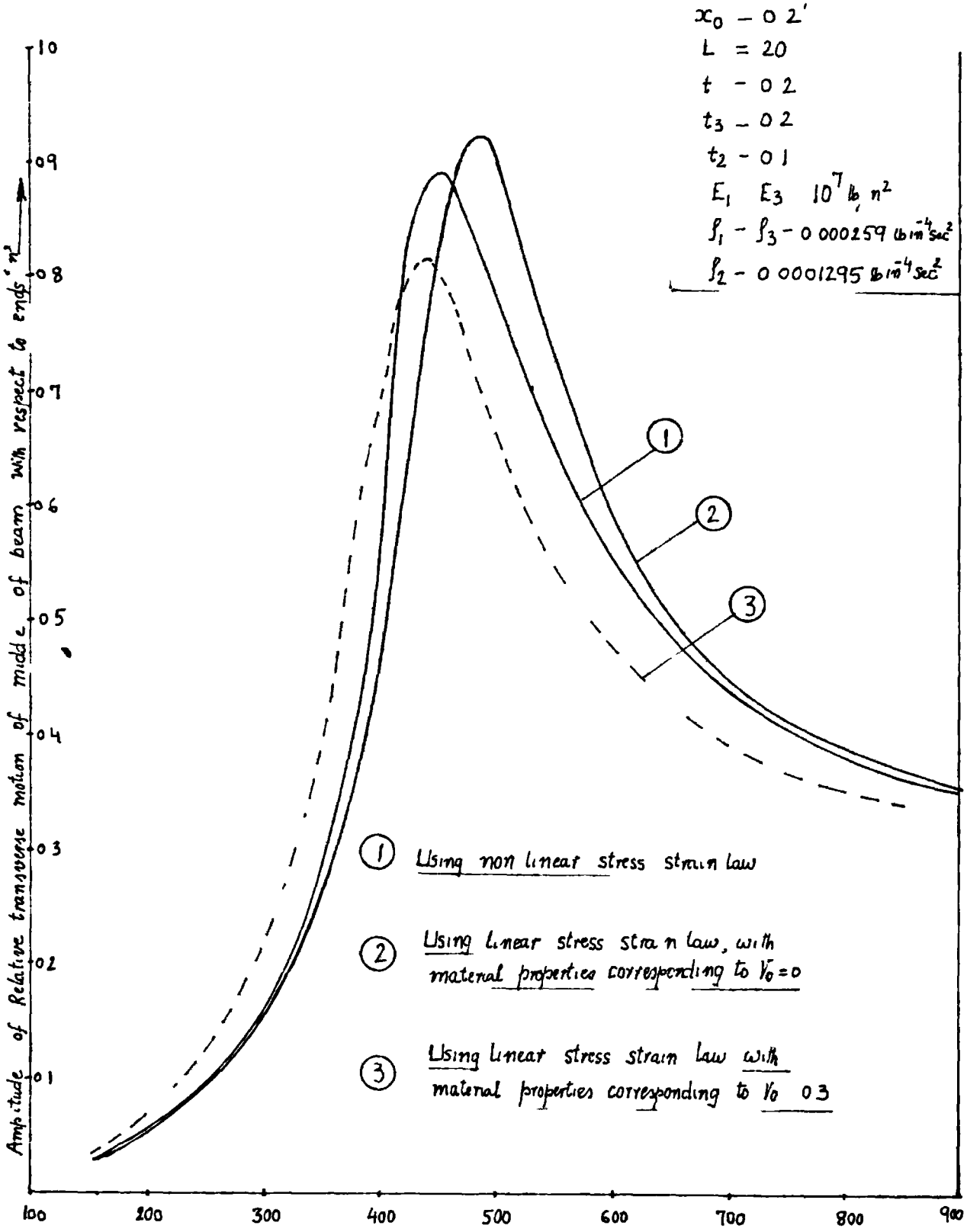
$x_0 - 0.2'$
$L = 20$
$t - 0.2$
$t_3 - 0.2$
$t_2 - 0.1$
$E_1 \quad E_3 \quad 10^7$ lb, in^2
$\rho_1 - \rho_3 - 0.000259$ lb in^{-4} sec^2
$\rho_2 - 0.0001295$ lb in^{-4} sec^2
Amplitude of Relative transverse motion of middle of beam with respect to ends, in
0.1
0.2
0.3
0.4
0.5
0.6
0.7
0.8
0.9
1.0
100
200
300
400
500
600
700
800
900
1
2
3
(1) Using non linear stress strain law
(2) Using linear stress strain law, with material properties corresponding to $\nu_0 = 0$
(3) Using linear stress strain law with material properties corresponding to ν_0 0.3

FIG III-2.7

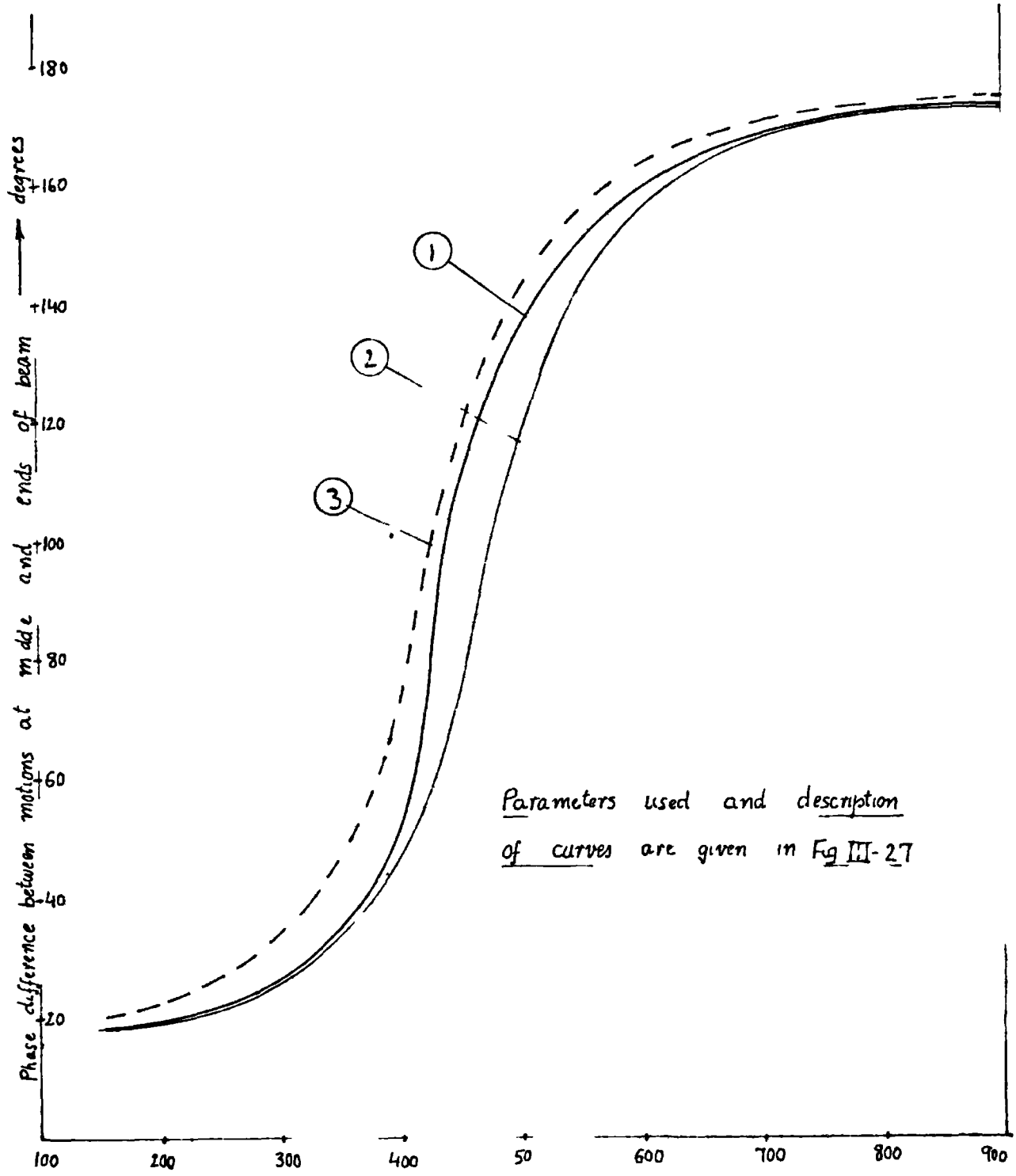
180
+160
+140
+120
+100
80
60
40
20
degrees
Phase difference between motions at middle and ends of beam
1
2
3
Parameters used and description of curves are given in Fig III-27
100
200
300
400
50
600
700
800
900
Frequency Radians/sec

FIG. III-28

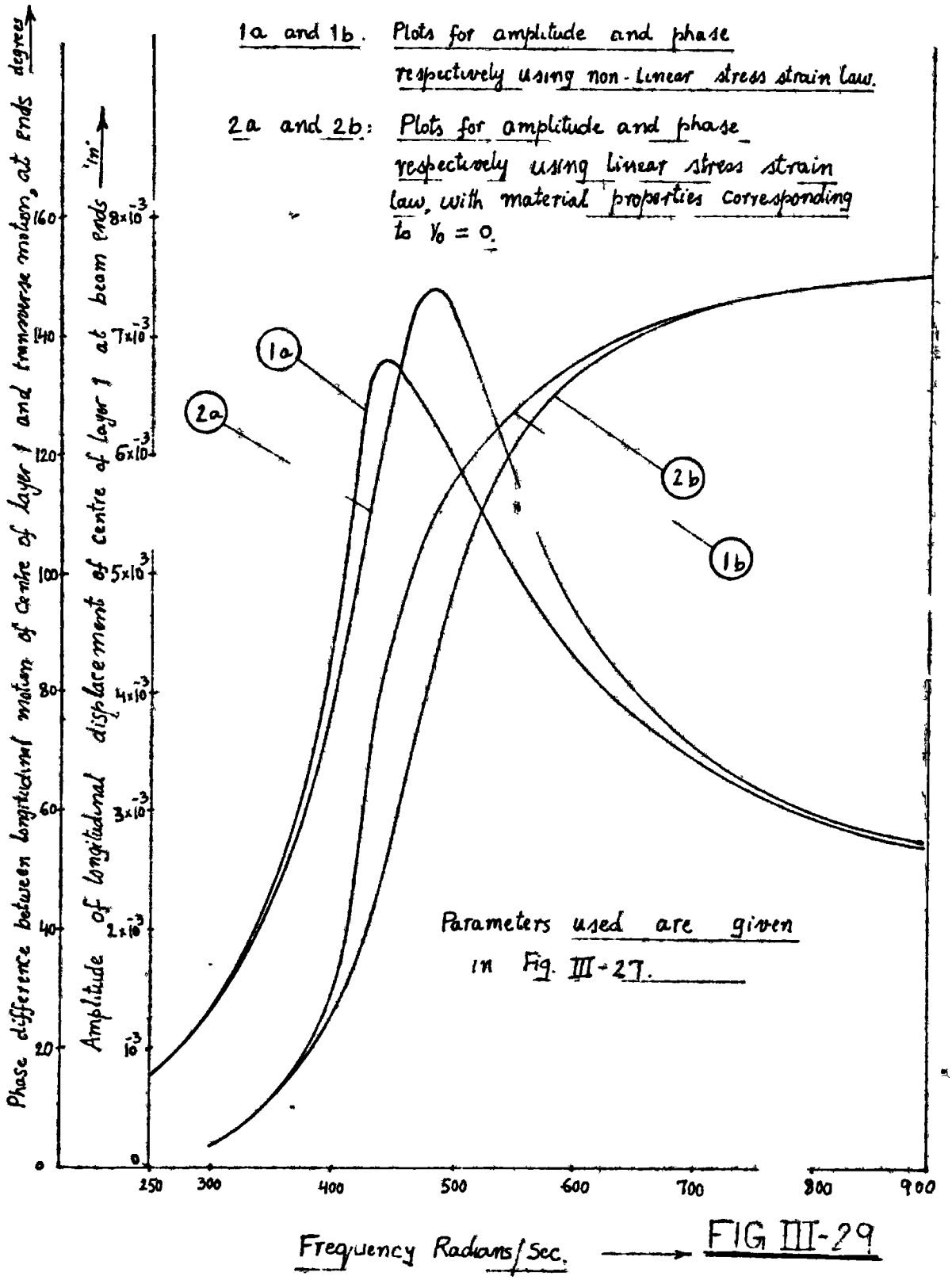
1a and 1b. Plots for amplitude and phase respectively using non-linear stress strain law.
2a and 2b: Plots for amplitude and phase respectively using linear stress strain law, with material properties corresponding to ν0 = 0.
Phase difference between longitudinal motion of centre of layer 1 and transverse motion, at ends degrees
Amplitude of longitudinal displacement of centre of layer 1 at beam ends 'in'
1a
2a
2b
1b
Parameters used are given in Fig. III-27.
Frequency Radians/Sec.

FIG III-29

section may not hold accurately for a given viscoelastic material at all frequencies. In that case, one has to include more terms of different order in the eqn. (III.32) and obtain the material constants by curve fitting. Also, for higher frequencies, more terms in the assumed series solution (eqn. III.41) have to be included.

CHAPTER IV: FURTHER MULTILAYERED CONFIGURATIONS HAVING ALTERNATE ELASTIC AND VISCOELASTIC LAYERS

Further cases of laminated beams will be analysed in this Chapter. The laminates or layers are arranged in such a way that the viscoelastic and elastic layers occur alternately. The properties of each layer are different from those of any other layer in the sandwich, i.e. all cases are of unsymmetrical type. Complete analysis of the 5 and 7 layered unsymmetrical cases will be done in this Chapter, though by the application of similar procedure, a sandwich with any number of layers can be analysed. For each case, firstly the equations of flexural vibrations of sandwich beams will be derived, their solution given for simply supported beams and then the effect of important physical parameters, occurring in the equations, on the damping of sandwich and the applicability of each case will be discussed.

IV.A.1: 5 layered Case - Equations of Motion

Fig. IV-1(a) shows the configuration, together with the notations used in the derivation. Layers 2 and 4 are viscoelastic. The following assumptions have been made.

1) Layers 1, 3 and 5 are assumed to bend according to Bernoulli-Euler's theory, and shear effect in these

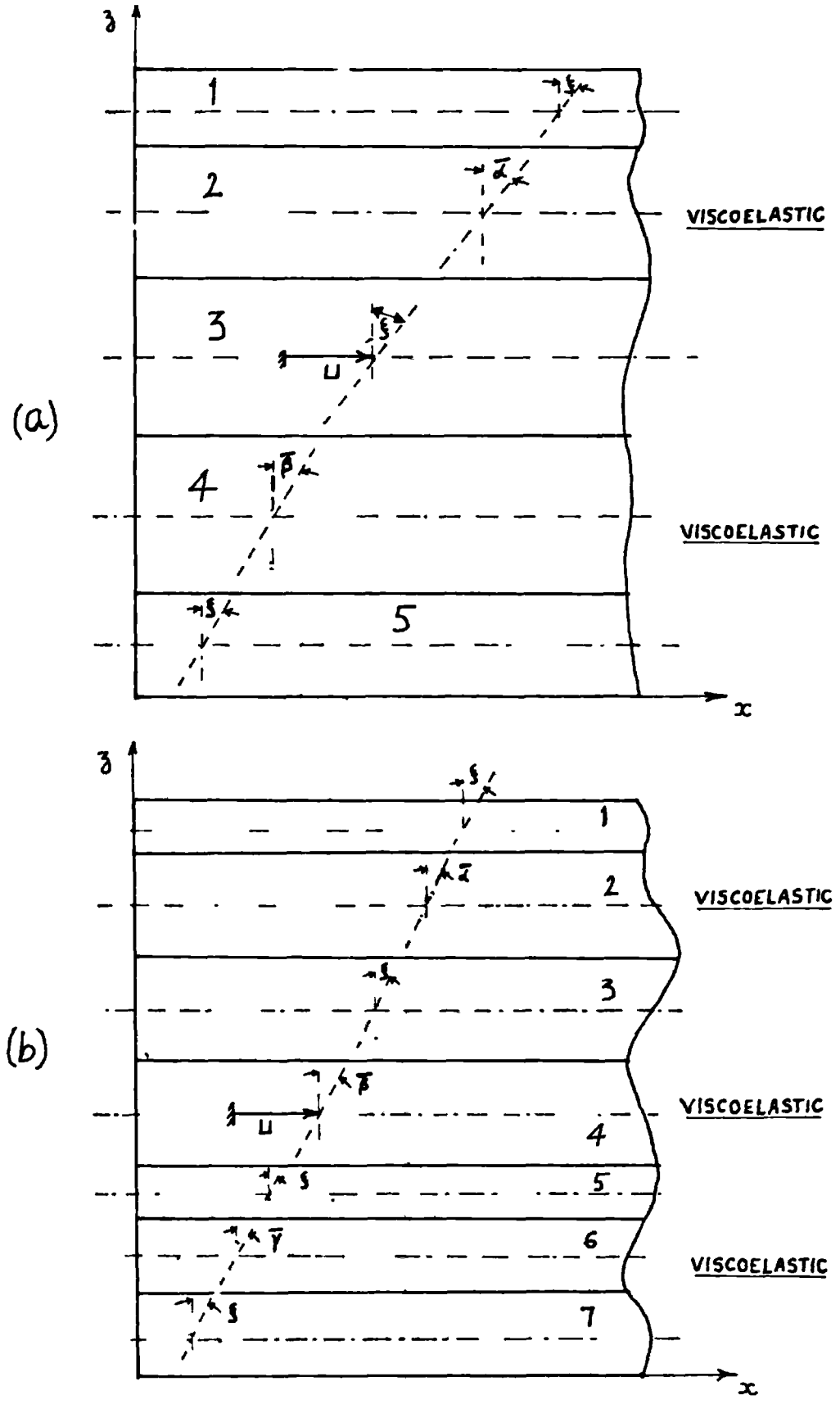
(a)
z
x
1
2
3
4
5
VISCOELASTIC
VISCOELASTIC
u
(b)
z
x
1
2
3
4
5
6
7
VISCOELASTIC
VISCOELASTIC
VISCOELASTIC
u

FIG. IV-1

is not of importance.

2) In layers 2 and 4, the shear effect is of importance and in these layers, the normals to the longitudinal fibres rotate through angles $\bar{\alpha}$ and $\bar{\beta}$ respectively. Layer 2 takes up only shear and effect of direct stresses is not of importance in that layer, whilst both effects of shear and direct stresses are included in layer 4, which may be a stiff viscoelastic layer.

3 All displacements are assumed small, as in linear elasticity theory.

4 At a section, the transverse displacement w remains constant throughout the thickness of the laminated beam.

5 There is perfect continuity at all interfaces and no slip occurs there while the sandwich is bending.

6) The longitudinal displacements vary linearly in each layer, though with different slopes as shown in Fig.IV-1(a). The longitudinal displacement of middle of one of the layers (taken layer 3 in this case) is taken as 'u'.

7) The strain dependence of viscoelastic material properties is not taken into account in these derivations.

8) Only transverse inertia terms are included.

The assumptions made above are almost similar to those

for analysis I of the 3 layered laminate analysed in Section II.C,except assumption 8. The studies made on the 3 layered sandwich in Chapter II act as a guide for showing the effect of any of the assumptions, e.g. effect of shear in non-viscoelastic layers (metals in practice), effect of inertia terms other than transverse ones and non-linearity due to strain dependence of viscoelastic materials. These studies justify the neglect of the above mentioned effects for subsequent derivations, unless applied to situations in which

(i) very thick metal faces are employed

(ii) very high frequencies are involved and one is concerned with stress-resonances in the system

(iii) large strain variations are likely to occur in the system.

If required, however, the effect of any of these may be included by the same procedure as used for 3 layered beams in previous Chapters.

Using notations as in Fig.IV-1(a) and sign convention, similar to that in Fig. II-2(a), shear strain of layer 2 - $\overline{\alpha}$ - w'

where w is the transverse displacement.

Shear strain of layer 4 $\overline{\beta}$ - w'.

The normal to the longitudinal fibres in layers 3, 2, 1, 4,5 rotates through angles of ξ, (= flexural angle =w',

in the absence of shear effect), $\bar{\alpha}$, ξ, $\bar{\beta}$, ξ respectively.

The longitudinal displacements of middle of these layers, are:

For layer 3 : u

For layer 1 : $u \quad \xi \frac{t_3}{2} + \bar{\alpha} t_2 \; \xi \frac{t_1}{2}$

For layer 4 : $u - \xi \frac{t_3}{2} - \frac{\bar{\beta} t_4}{2}$

For layer 5 : $u - \bar{\beta} t_4 - \xi(\frac{t_3}{2} \quad \frac{t_5}{2})$

As shown in Section II.D.1, strain energy due to direct strain in a layer i, having the longitudinal displacement of the middle fibre as u_i and rotation of its normal as $\bar{u}_1$, is given by

$$\int_o^L b \int_{-\frac{t_1}{2}}^{\frac{t_i}{2}} \tfrac{1}{2} E_1 \{(u_i' + \bar{u}_i' z_i)^2\} \, dz_i \, dx$$

$$\frac{bE_i}{2} \int_o^L (u_i'^2 t_1 \; \bar{u}_i'^2 \frac{t_i^3}{12}) \, dx$$

Total Strain Energy U' of sytem is given by

$$U - q_2 \int_o^L (\bar{\alpha} - w')^2 \, dx + q_4 \int_o^I (\bar{\beta} - w')^2 \, dx$$

$$r_1 \left[\int_o^L \{(u' \; \bar{\alpha}' t_2 + w'' \frac{t_1 + t_3}{2})^2 + (w''^2 \frac{t_1^2}{12}) \right.$$

$$r_3 \left[\int_o^L \{u'^2 + w''^2 \frac{t_3^2}{12}\} \, dx \right]$$

$$+ r_4 \left[\int_o^L \{(u'-\bar{\beta}' \frac{t_4}{2} - w'' \frac{t_3}{2})^2 + \bar{\beta}'^2 \frac{t_4^2}{12} \} dx \right]$$

$$+ r_5 \left[\int_o^L \{(u'-\bar{\beta}' t_4 - w'' \frac{t_3+t_5}{2})^2 + w''^2 \frac{t_5^2}{12} \} dx \right]$$

where $q_2 = \frac{1}{2} bG_2 t_2$

$q_4 = \frac{1}{2} bk_4 G_4 t_4$, k_4 being shear coefficient

$r_i = \frac{1}{2} bE_i t_i \quad (i = 1,3,4,5)$

Kinetic Energy 'T' due to transverse displacement

$$= \frac{1}{2} \rho \int_o^L (w')^2 dx$$, where ρ is the mass density of sandwich per unit length.

Potential Energy 'V' due to external forces

$$= g(t) \int_o^L f(x) W dx,$$

$f(x)$ $g(t)$ is intensity of loading as in Fig.II-2(c).

Application of Hamilton s Principle gives the following equations of motion and boundary conditions, the details of derivation are given in Appendix 3.

$$2q_2(\bar{\alpha} - w') - 2r_1 t_2 (u'' + \bar{\alpha}'' t_2 + w''' \frac{t_1+t_3}{2}) = 0 \qquad \text{(IV.1)}$$

$$2q_4(\bar{\beta} - w') + u''(r_4 t_4 + 2r_5 t_4) - \bar{\beta}''(\frac{2}{3} r_4 t_4^2 + 2r_5 t_4^2)$$

$$- w''' [\frac{r_4 t_4 t_3}{2} + r_5(t_4 t_3 + t_4 t_5)] = 0 \qquad \text{(IV.2)}$$

$$2(r_1+r_3+r_4+r_5)u'' + 2r_1 t_2 \bar{\alpha}'' - \bar{\beta}''(r_4 t_4 + 2r_5 t_4)$$

$$+ w''' [r_1(t_1+t_3) - r_4 t_3 - r_5(t_3+t_5)] - 0 \qquad \text{(IV.3)}$$

$$2q_2(\bar{\alpha}' - w'') + 2q_4(\bar{\beta}' - w'') + 2r_1\left[\left(u''' + \bar{\alpha}'''\right)t_2 + w''''\,\frac{t_1+t_3}{2}\right)\frac{t_1+t_3}{2} + w''''\frac{t_1^2}{12}\right] + 2r_3\left[w''''\,\frac{t_3^2}{12}\right] - r_4 t_3\left[\left(u''' - \bar{\beta}'''\,\frac{t_4}{2} - w''''\,\frac{t_3}{2}\right)\right]$$

$$+ 2r_5\left[w''''\,\frac{t_5^2}{12} - \left(u''' - \bar{\beta}'''\right)t_4 - w''''\,\frac{t_3+t_5}{2}\right)\left(\frac{t_3}{2}\,\frac{t_5}{2}\right)\right]$$

$$= -\rho\ddot{w}^{\circ} + g(t)\, f(x) \qquad \text{(IV.4)}$$

Boundary conditions for simply supported ends are :

At $x = 0$, $x = L$,

$$\left.\begin{aligned} w = w'' &= 0 \\ u' = \bar{\alpha}' = \bar{\beta}' &= 0 \end{aligned}\right| \qquad \text{(IV.5)}$$

IV.A.2 : Solution

For sinusoidal excitations and simply supported ends, assuming the solution in the form of series

$$\left.\begin{aligned} w &= \sum_{n=1}^{\infty} w_n \sin\frac{n\pi x}{L} \sin pt \\ u &= \sum_{n=1}^{\infty} u_n \cos\frac{n\pi x}{L} \sin pt \\ \bar{\alpha} &= \sum_{n=1}^{\infty} \bar{\alpha}_n \cos\frac{n\pi x}{L} \sin pt \\ \bar{\beta} &= \sum_{n=1}^{\infty} \bar{\beta}_n \cos\frac{n\pi x}{L} \sin pt \end{aligned}\right| \qquad \text{(IV.6)}$$

Also, expanding the loading $f(x) \sin pt = \sum_{n-1}^{\infty} f_n \sin\frac{n\pi x}{L} \sin pt$

It is seen from eqns. (IV.6) , that boundary conditions IV.5 are satisfied and on substitution, equa-

tions IV.1 - IV.4 are reduced to algebraic equations as given below

$$\left.\begin{aligned} \bar{\alpha}_n A + U_n B + W_n C &= 0 \\ \bar{\beta}_n D - U_n F + W_n H &= 0 \\ -\bar{\ }_n J + \bar{\beta}_n K - U_n L - W_n M &= 0 \\ \bar{\alpha}_n N \quad \bar{\beta}_n P + U_n Q + W_n [I-\rho p^2] &= f_n \end{aligned}\right| \qquad \text{(IV.7)}$$

where $A = (\frac{n\pi}{L})^2 E_5 t_5^3 \{\phi_{2.5}\theta_{2.5}+\alpha_{1.5}\theta_{1.5}\theta^2_{2.5}\}$

$B = J = (\frac{n\pi}{L})^2 E_5 t_5^2 \{\alpha_{1.5}\theta_{1.5}\theta_{2.5}\}$

$C = N = (\frac{n\pi}{L})^3 E_5 t_5^3 \{-\phi_{2.5\ 2.5}+\frac{1}{2}\alpha_{1.5}\theta_{1.5}\theta_{2.5}(\theta_{1.5}+\theta_{3.5})\}$

$D = (\frac{n\pi}{L})^2 E_5 t_5^3 \{\phi_{4.5}\theta_{4.5}k_4 + \frac{1}{3}\alpha_{4.5}\theta^3_{4.5}\ \theta^2_{4.5}\}$

$F = K = (\frac{n\pi}{L})^2 E_5 t_5^2 \{\frac{1}{2}\alpha_{4.5}\theta_{4.5}{}^2+\theta_{4.5}\}$

$H = P = (\frac{n\pi}{L})^3 E_5 t_5^3 \{-\phi_{4.5}\theta_{4.5}k_4+ \frac{1}{4}\alpha_{4.5}\theta_{4.5}{}^2\theta_{3.5}$

$+ \frac{1}{2}(\theta_{4.5}\theta_{3.5}+\theta_{4.5})\}$

$L = (\frac{n\pi}{L})^2 E_5 t_5 \{\alpha_{1.5}\theta_{1.5}+\alpha_{3.5}\theta_{3.5}+\alpha_{4.5}\theta_{4.5}+1\}$

$M = Q = (\frac{n\pi}{L})^3 E_5 t_5^2 \{\frac{1}{2}\alpha_{1.5}\theta_{1.5}(\theta_{1.5}+\theta_{3.5})-\frac{1}{2}\alpha_{4.5}\theta_{4.5}\theta_{3.5}$

$- \frac{1}{2}(1\ \theta_{3.5})$

$I = (\frac{n\pi}{L})^4 E_5 t_5^3 \{\phi_{2.5}\theta_{2.5}+\phi_{4.5}\theta_{4.5}k_4+ \frac{\alpha_{1.5}\theta_{1.5}}{4}(\theta_{1.5}+\theta_{3.}$

$\frac{1}{12}\alpha_{1.5}\theta^3_{1.5}\quad \frac{1}{12}\alpha_{3.5}\theta_{3.5}{}^3$

$\frac{1}{4}\alpha_{4.5}\theta_{4.5}\theta^2_{3.5}\quad \frac{1}{12}+\frac{1}{4}(1\ {}_{3.5})^2\}$

$$\alpha_{i.5} = \frac{E_i}{E_5} \quad ; \quad i = 1,3,4$$

$$\theta_{j.5} = \frac{t_j}{t_5} \quad ; \quad j = 1,2,3,4$$

$$\phi_{p.5} = \frac{G_p}{E_5 t_5^2 (\frac{n\pi}{L})^2} \quad ; \quad p = 2,4$$

In order to get the solution when layers 2 and 4 are viscoelastic, the moduli of these layers have to be replaced by their complex values viz.

shear modulus G_2 by $G_2(1+ i\eta_2)$,

G_4 by $G_4(1 \quad i\eta_4)$

and E_4 by $E_4(1 \quad i\beta_4)$

η_2 and η_4 are loss factors in shear for layers 2 and 4 respectively and β_4 is that in direct stress conditions for layer 4.

By the above mentioned substitution, the various constants A, B, C etc. in eqn. (IV.7) become complex. The solution to the problem is obtained by solving 4 simultaneous complex algebraic equations as given by eqn. (IV.7). These equations may be coverted to 8 simultaneous algebraic equations, with real coefficients by substituting

$w_n = w_n^r + i\, w_n^i$

$u_n = u_n^r + i\, u_n^i$, with similar expressions for $\overline{\alpha}_n$ and $\overline{\beta}_n$.

The 4 equations in eqn. (IV.7) may be reduced to a single equation in w_n. This equation, after replacing the various elastic moduli by complex moduli, takes the form

$$bw_n(\frac{n\pi}{L})^4 E_5 t_5^3 [z_{rn} + iz_{in}] - \rho p^2 w_n = f_n \qquad \text{(IV.8)}$$

The expressions for z_{rn} and z_{in} are easily obtainable by the algebraic process as explained above and are not given here. In the present work, the algebraic computations involved were done on the Atlas digital computer.

The sandwich loss factor for nth mode is defined according to Section III.A.1, whereby

$$\eta_s = \frac{z_{rn}}{z_{in}} \qquad \text{(IV.9)}$$

Similarly, $k\eta_s = \dfrac{b(\frac{n\pi}{L})^4 E_5 t_5^3 (z_{in}}{(\frac{n\pi}{L})^4 b \frac{E_s t_s^3}{12}}$

$$= \frac{E_5 t_5^3 (z_{in})}{\frac{E_s t_s^3}{12}} \qquad \text{(IV.10)}$$

E_s and t_s, as in Section III.A.1 are the parameters of the reference solid beam chosen for comparison of dynamic rigidity with that of the sandwich. This gives $k\eta_s$ or the displacement response effectiveness as a dimensionless quantity. In subsequent studies, only the numerator in eqn. (IV.10) is taken as representing the Displacement Response Effectiveness (denoted by DRE), without referring

to any reference system. This is only for reasons of convenience; $k\eta_s$ with respect to any reference system may be got from these values of DRE, using eqn. (IV.10).

If both ends of sandwich beam are excited by sinusoidal transverse displacement $x_o \sin pt$, both ends being in phase, then the displacements everywhere in the beam may be determined as in Section III.D.

Loading intensity f(x) in this case is = $\rho p^2 x_o$ and f_n is given by eqn. (III.20).

Writing eqn. (IV.8) as

$$w_n[z'_{rn} + iz'_{in} - \rho p^2] = f_n \qquad \text{(IV.11)}$$

where $z'_{rn} - (\frac{n\pi}{L})^4 E_5 t_5^3 \quad (z_{rn})$

$$z'_{in} = (\frac{n\pi}{L})^4 E_5 t_5^3 \quad (z_{in})$$

As in Section III.D,

$$\left.\begin{aligned} (w_n) \text{ in phase with excitation} &= \frac{f_n z'_{rn}}{(z'^2_{rn} + z'^2_{in})} \\ (w_n) \text{ out of phase (or in quadrature with excitation)} &= \frac{f_n z'_{in}}{(z'^2_{rn} + z'^2_{in})} \end{aligned}\right| \qquad \text{(IV.12)}$$

The transverse displacement of any point on the beam (relative to the ends) can be got from eqn. (IV.6) viz

$$w = \sum_{n=1}^{\infty} w_n \sin \frac{n\pi x}{L} \sin pt \qquad \text{(IV.13)}$$

IV.A.3 : Effect of various system parameters on damping effectiveness and comparisons with other arrangements

Values of modal loss factor 'η_s' and displacement response effectiveness, D R E) according to the definitions given in previous section, will be plotted for sandwich beams, varying certain important parameters. The performance of 5 layered beams will be compared with that of a 3 layered one, over a wide frequency range of excitation. The value of shear coefficient 'k_4 for layer 4 has been taken equal to unity which is reasonable as determined from the analysis of 3 layered case, unless the layer is very thick and rigid.

(i In Figs. IV-2 to IV-5, performance of 3 layered unsymmetrical beams will be compared with two possible 5 layered arrangements. In Fig. IV-2, taking layer 'c' as the solid beam to be damped, layers 'b' and 'a' are added for damping in the 3 layered beam, whilst in the 5 layered one, two cases are possible. In case I, layers d' and 'e are added on the side opposite to the one on which 'b' and 'a' are arranged, but in case II, layers 'd' and 'e' are added on the same side.

In Figs. IV-2 and IV-3, layers 'd' and 'e' are similar to 'b' and 'a' respectively. Values of sandwich loss factor 'η_s' are plotted against Q_b where $Q_b = G_b/(\frac{n\pi}{L})^2$,

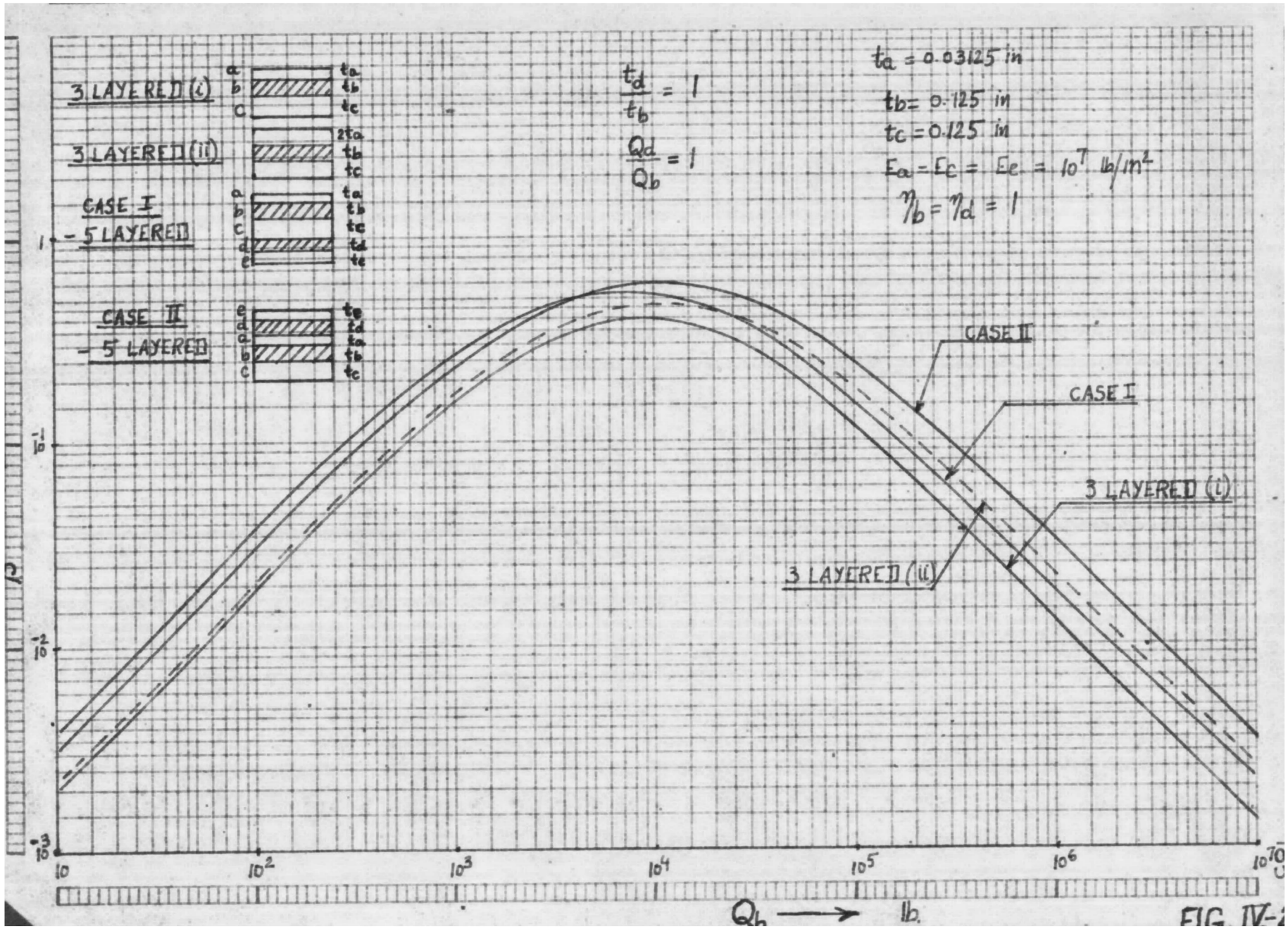
3 LAYERED (i)
3 LAYERED (ii)
CASE I
5 LAYERED
CASE II
5 LAYERED
$\frac{t_d}{t_b} = 1$
$\frac{Q_d}{Q_b} = 1$
$t_a = 0.03125$ in
$t_b = 0.125$ in
$t_c = 0.125$ in
$E_a = E_c = E_e = 10^7$ lb/in^2
$\eta_b = \eta_d = 1$
CASE II
CASE I
3 LAYERED (i)
3 LAYERED (ii)
$Q_b \longrightarrow$ lb.

FIG. IV-

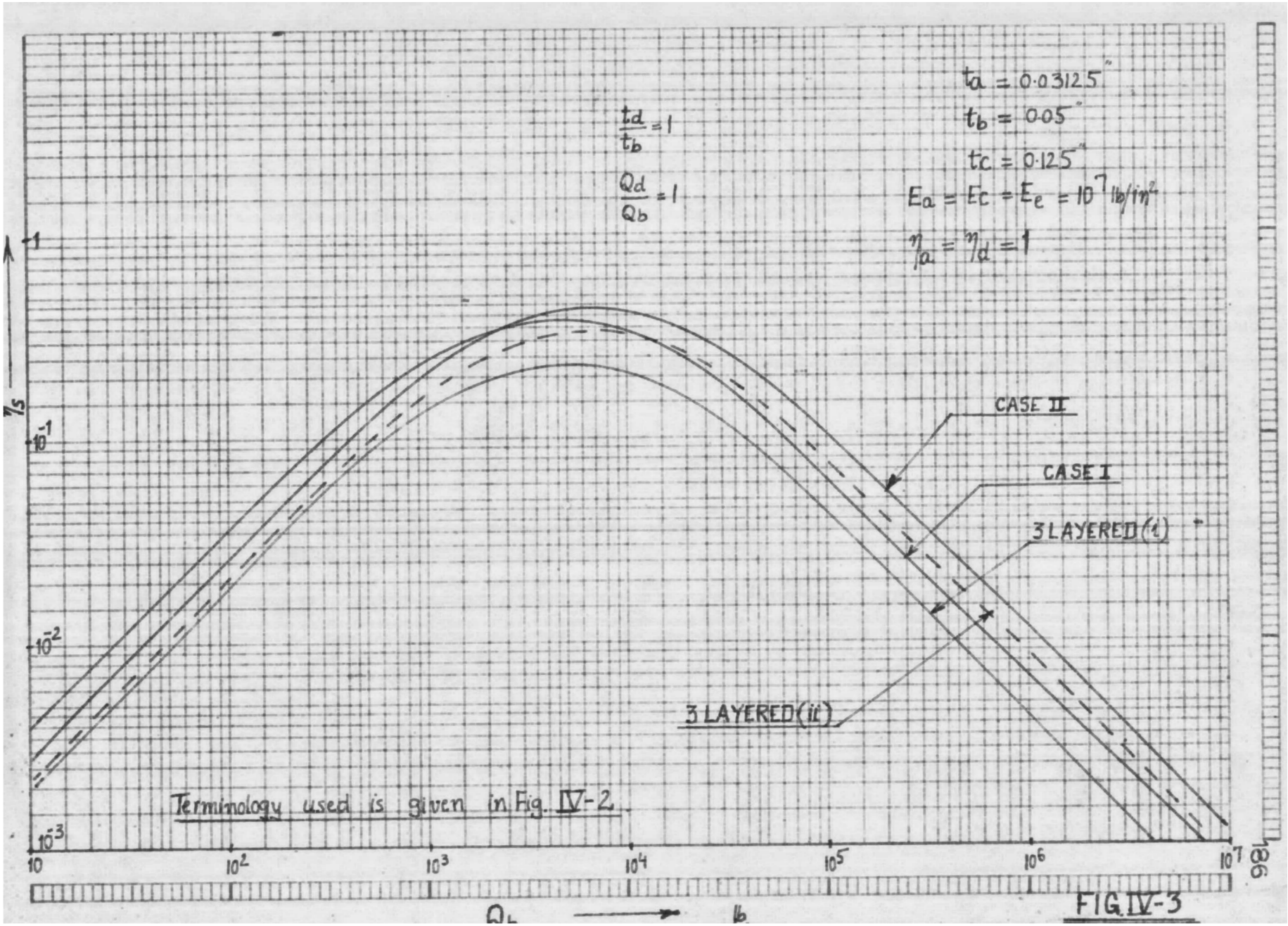
$t_a = 0.03125"$
$t_b = 0.05"$
$t_c = 0.125"$
$E_a = E_c = E_e = 10^7$ lb/in²
$\eta_a = \eta_d = 1$
$\frac{t_d}{t_b} = 1$
$\frac{Q_d}{Q_b} = 1$
CASE II
CASE I
3 LAYERED (i)
3 LAYERED (ii)
η_s
1
10^{-1}
10^{-2}
10^{-3}
10
10^2
10^3
10^4
10^5
10^6
10^7
Q_b → lb
Terminology used is given in Fig. IV-2.
136

FIG IV-3

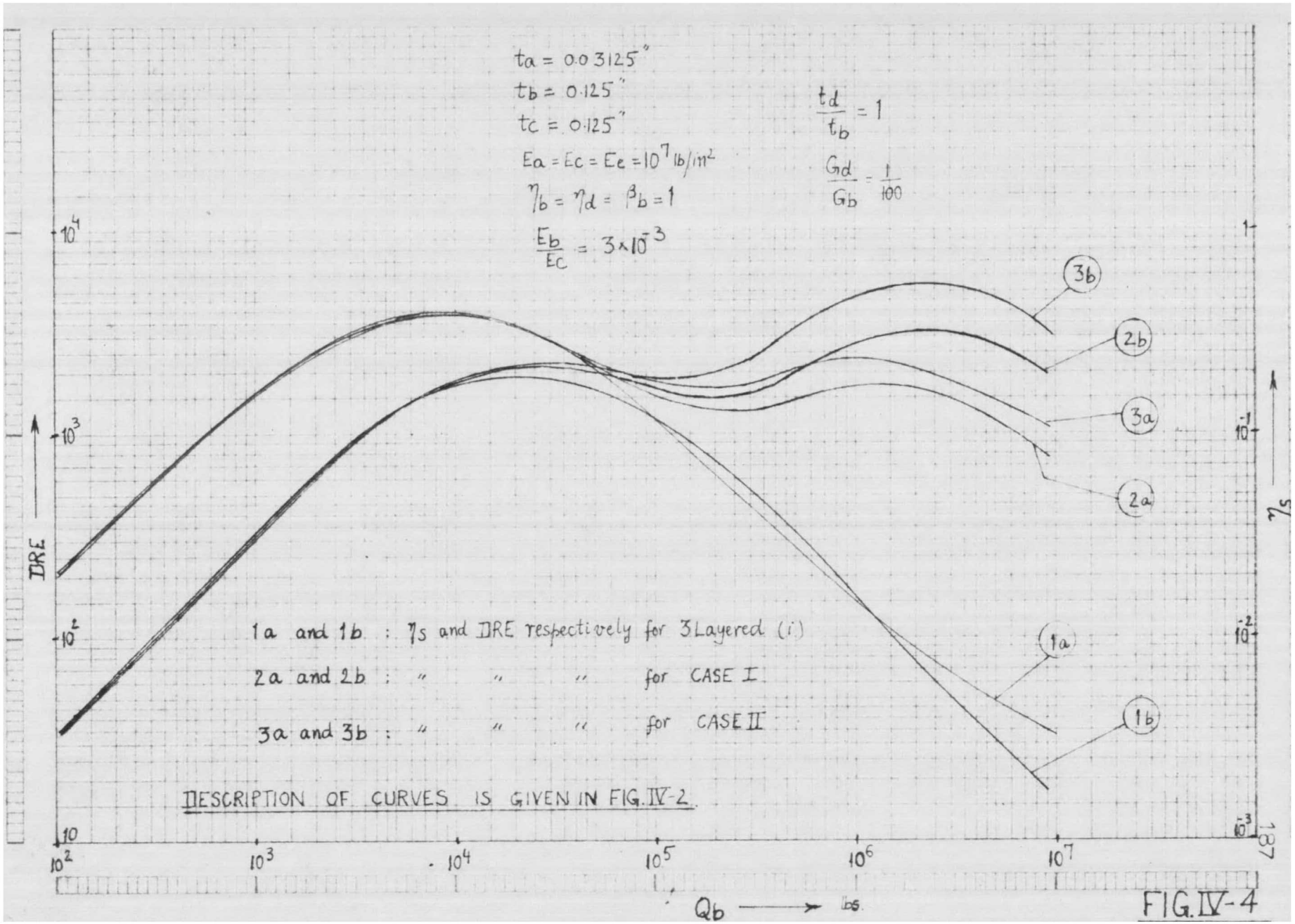
$t_a = 0.03125"$
$t_b = 0.125"$
$t_c = 0.125"$
$E_a = E_c = E_e = 10^7$ lb/in²
$\eta_b = \eta_d = \beta_b = 1$
$\frac{E_b}{E_c} = 3 \times 10^{-3}$
$\frac{t_d}{t_b} = 1$
$\frac{G_d}{G_b} = \frac{1}{100}$
DRE
η_s
Q_b ⟶ lbs.
3b
2b
3a
2a
1a
1b
1a and 1b : η_s and DRE respectively for 3 Layered (i)
2a and 2b : " " " for CASE I
3a and 3b : " " " for CASE II
DESCRIPTION OF CURVES IS GIVEN IN FIG. IV-2

FIG. IV-4

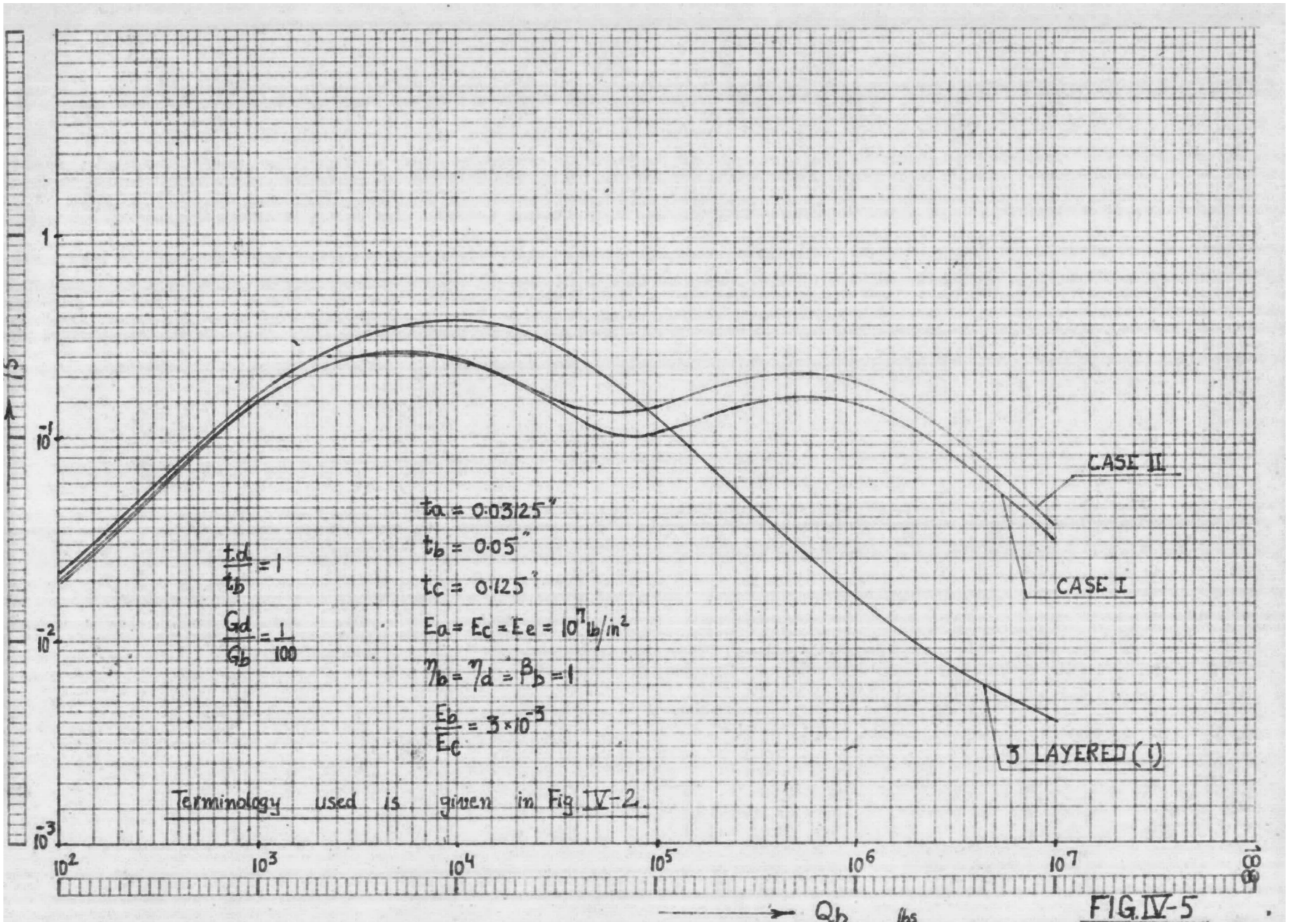
1
10^{-1}
10^{-2}
10^{-3}
10^{2}
10^{3}
10^{4}
10^{5}
10^{6}
10^{7}
10^{8}
$\frac{t_d}{t_b} = 1$
$\frac{G_d}{G_b} = \frac{1}{100}$
$t_a = 0.03125"$
$t_b = 0.05"$
$t_c = 0.125"$
$E_a = E_c = E_e = 10^7 lb/in^2$
$\eta_b = \eta_d = \beta_b = 1$
$\frac{E_b}{E_c} = 3 \times 10^{-3}$
CASE II
CASE I
3 LAYERED (I)
Terminology used is given in Fig. IV-2.
Q_b lbs

FIG. IV-5

G_b being shear modulus of layer 'b'. Only shear damping in various layers is included. The difference between Fig. IV-2 and IV-3 is in the value of 't_b' taken. It is seen from these that in both cases I and II, 5 layered beam gives considerably higher damping than the 3 layered one, at all frequencies, the peak value of damping obtainable in case II is higher than that from case I. Some of the conclusions given in [60] for multi taped beams are not seen to hold . In [60], it is stated that a constraining tape used on each side of a solid plate doubles the damping, which would be obtainable from a single tape, at all frequencies (corresponding to case I of the 5 layered arrangement) and that if multi-tapes are used on one side (corresponding to case II), there is increase in damping at low frequencies but not appreciably at high frequencies. Also, if in a 3 layered case 't_a' is doubled, keeping t_b' and 't_c' constant, the damping obtained is the same as that given by case II of the 5 layered arrangement. From Figs. IV-2 and IV-3, none of the above mentioned conclusions are seen to hold strictly.

In Figs. IV-4 to IV-5, the layer 'd' added to the 3 layered case is taken to have its shear modulus different from that of layer 'b . The value of G_d/G_b is taken = $\frac{1}{100}$ in these Figs. In layer 'd', only shear damping is

taken into account while in layer b , both shear and extensional damping effects are included since it is 100 times as stiff as layer 'd'. Value of E_b is taken = $3G_b$, as for an incompressible material. It is known from a 3 layered case that the decrease of core shear modulus will shift the optimum damping peak to a lower value of 'n' i.e. higher Q_b and lower frequency. So, it may be imagined that the addition of a less rigid layer d' to the 3 layered sandwich, might give an additional peak at a higher value of Q_b. This is seen to be true in Figs. IV-4 to IV-5. In Fig. IV-4, at low values of Q_b, η_s obtained in 3 layered and both the 5 layered cases are nearly same, but in the latter configurations, damping is more, at higher values of Q_b (i.e. lower frequencies). Case II is seen to give higher damping than case I. Same situation is seen to hold for D R E in Fig. IV-4. Thus, the frequency response of 5 layered configurations, having layers of different viscoelastic materials tends to be flatter than that for the 3 layered one i.e. high damping is possible at a number of modes or in a large frequency range. It was observed that the double peaks in the damping graphs occur only for high ratios of G_b/G_d. For the case analysed in Fig.IV-4, it was seen that this ratio must be higher than 40 for the double peaks to occur.

(ii) In Figs. IV-6 and IV-7, effect of $\frac{Q_4}{Q_2}$ and $\frac{t_4}{t_2}$ on η_s and DRE is studied for a chosen 5 layered configuation.

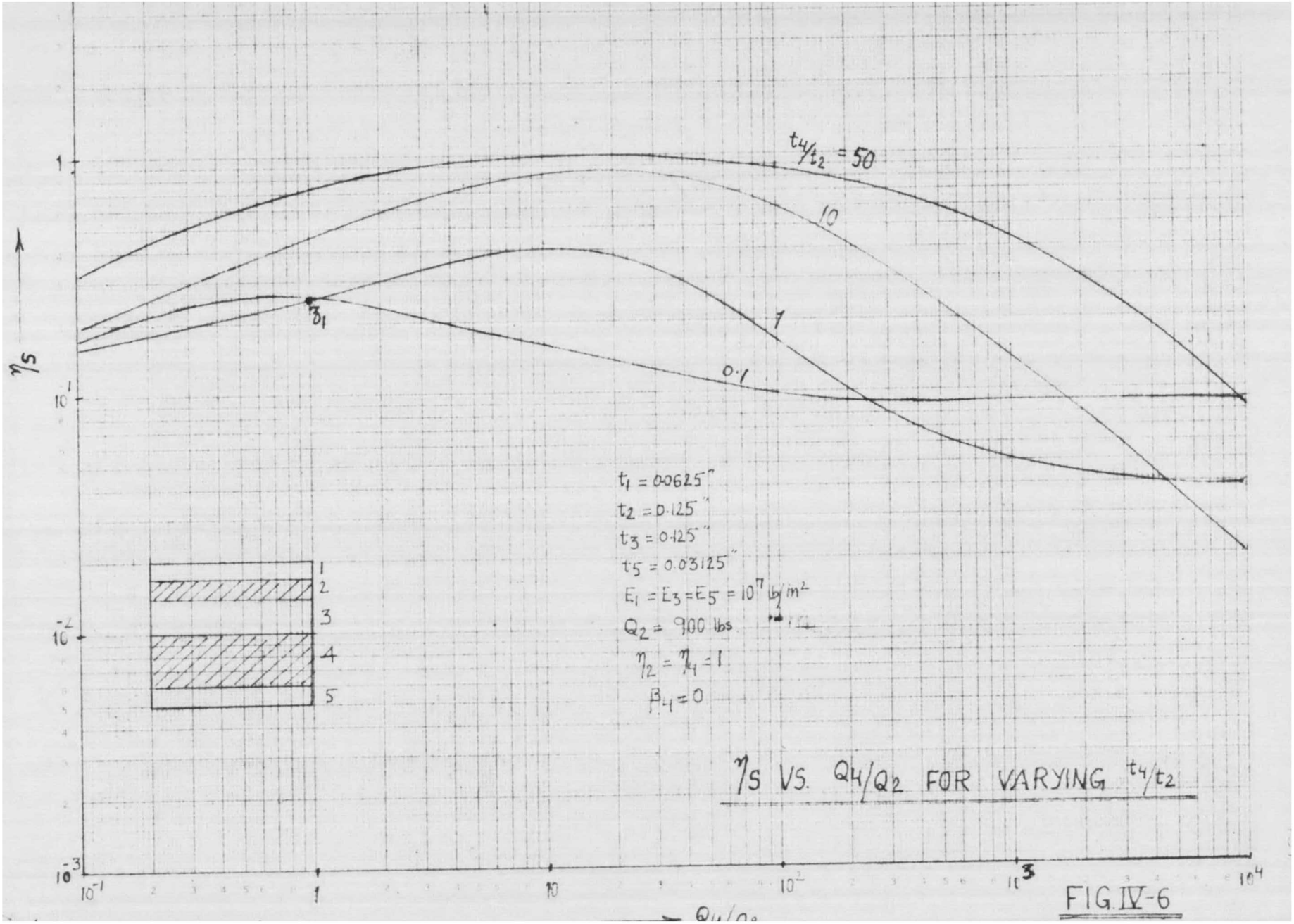

η_S VS. Q_4/Q_2 FOR VARYING t_4/t_2

FIG. IV-6

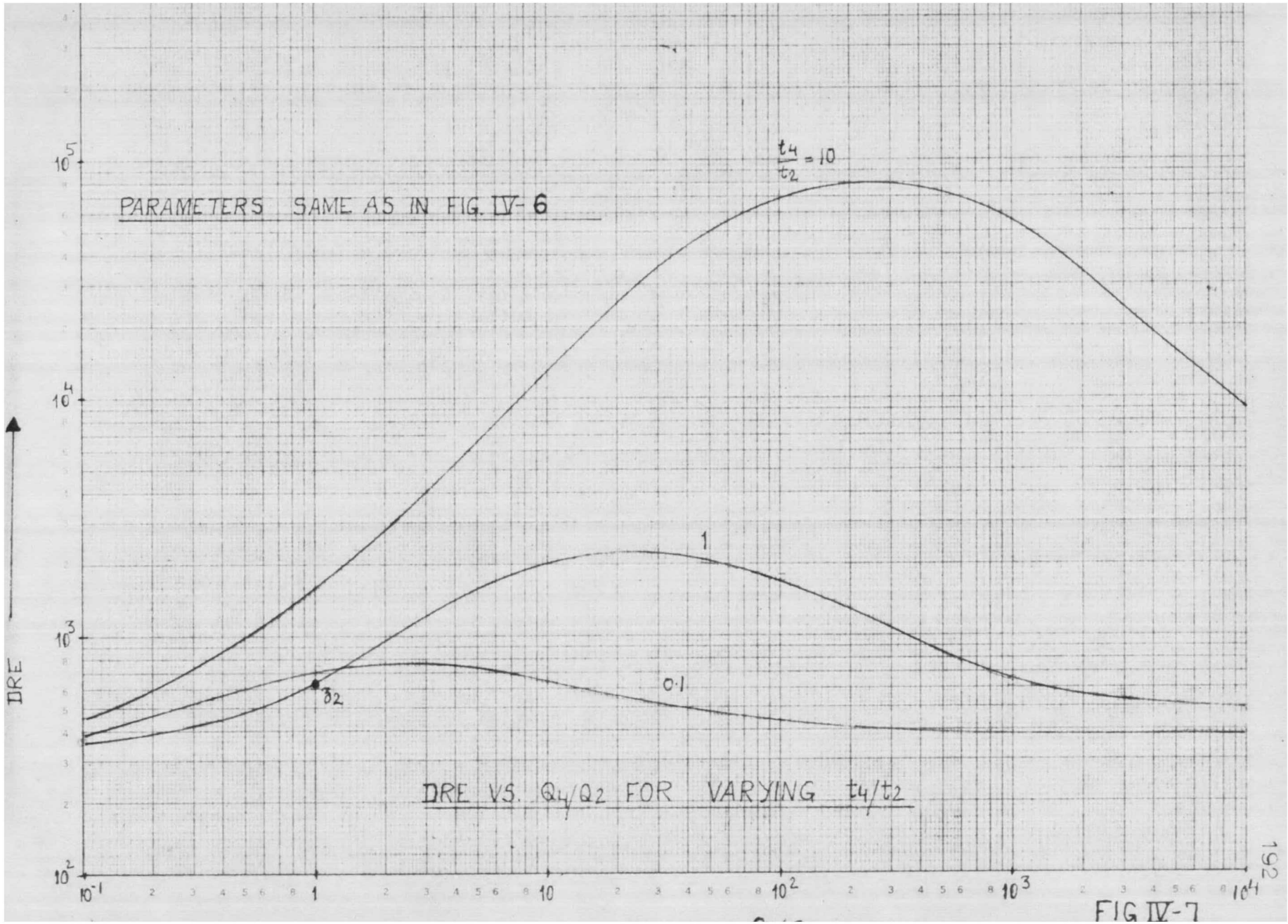
PARAMETERS SAME AS IN FIG. IV-6
$\frac{t_4}{t_2} = 10$
1
0.1
δ_2
DRE
10^5
10^4
10^3
10^2
10^{-1}
1
10
10^2
10^3
10^4
DRE VS. Q_4/Q_2 FOR VARYING t_4/t_2

FIG IV-7

Only shear damping is included in layers 2 and 4. For the system chosen, optimum value of η_s is seen to occur for a certain ratio Q_4/Q_2. This ratio increases for higher values of t_4/t_2

The same is true for DRE. Too high a value of Q_4/Q_2 might make the system very stiff, reducing the deformation of the viscoelastic layer and the energy dissipated and hence the system damping might be reduced. Again, points z_1 and z_2 in Figs. IV-6 and IV-7 respectively correspond to the case when $\frac{Q_4}{Q_2} = 1$ and $\frac{t_4}{t_2} = 1$, i.e. when both viscoelastic layers are of the same material and thickness. It may be seen that for a given situation, a considerable increase in damping is possible, by making the two viscoelastic layers different and by a careful choice of their thickness and shear moduli ratio. Usually, an increase of $\frac{t_4}{t_2}$ would increase the η_s and DRE, except for very high or low values of $\frac{Q_4}{Q_2}$.

(iii) In Fig. IV-8, the values of η_s and DRE are plotted for a chosen set of parameters of a 5 layered sandwich beam. Shear damping due to layers 2 and 4 is included and Figs. are drawn with and without the extensional damping of layer 4. It is seen that the influence of extensional damping is considerable, at higher values of $\frac{Q_4}{Q_2}$ and $\frac{t_4}{t_2}$. In these figs, $E_5/E_3 = 1$. One might expect a higher contribution of extensional damping to the total

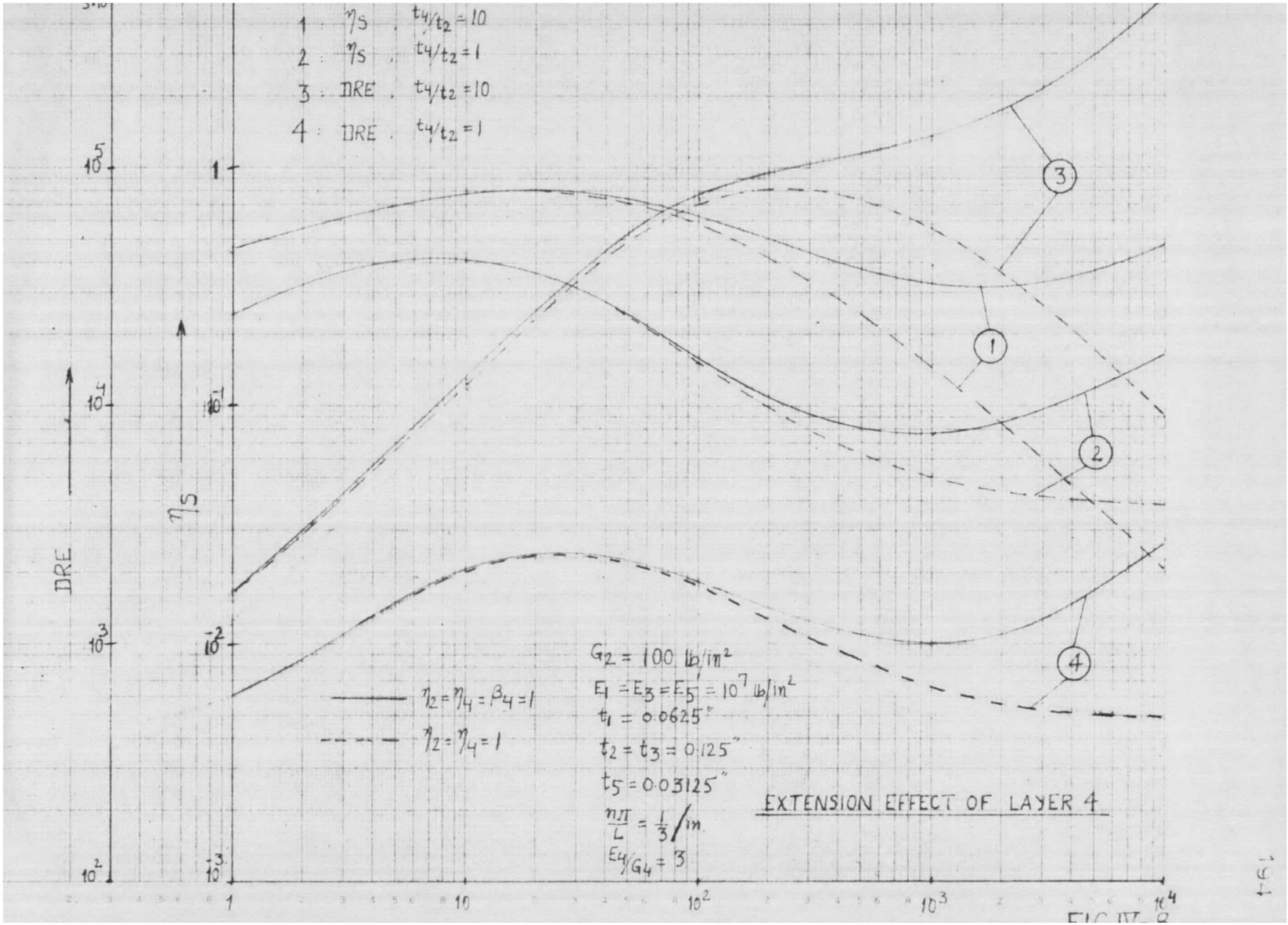
1 : η_S , $t_4/t_2 = 10$
2 : η_S , $t_4/t_2 = 1$
3 : DRE , $t_4/t_2 = 10$
4 : DRE , $t_4/t_2 = 1$
DRE
η_S
10^5
10^4
10^3
10^2
1
10^{-1}
10^{-2}
10^{-3}
1
10
10^2
10^3
10^4
$\eta_2 = \eta_4 = \beta_4 = 1$
$\eta_2 = \eta_4 = 1$
$G_2 = 100$ lb/in^2
$E_1 = E_3 = E_5 = 10^7$ lb/in^2
$t_1 = 0.0625$"
$t_2 = t_3 = 0.125$"
$t_5 = 0.03125$"
$\frac{n\pi}{L} = \frac{1}{3}$/in
$E_4/G_4 = 3$
EXTENSION EFFECT OF LAYER 4

FIG IV-8

one, if E_5/E_3 is low.

(iv) In Figs. IV-9 to IV-11, η_s and DRE are plotted for varying ratios of E_5/E_3 and G_4/G_2 against $(\frac{L}{n\pi})^2$. For higher values of G_4/G_2 as in Figs. IV-9 and IV-11, layer 4 is rigid and extensional damping in that layer contributes to the total damping significantly. For lower values of E_5/E_3, the curve for 'η_s' is flatter, i.e. η_s is high at a number of modes which may be excited. $E_5/E_3 = 0$ means that the layer 5 is eliminated and layer 4 contributes mostly the extensional and not the shear damping. Low values of E_5/E_3 result in decreased dynamic rigidity and so improvement in η_s is offset by decrease in 'k', thereby giving poor displacement response effectiveness.

For low values of G_4/G_2 e.g. in Fig. IV-10, where this ratio is 1, there is one peak occurring in the curve for η_s and the contribution due to extensional damping in layer 4 is small, and so the frequency response (or the damping expected at a number of modes is poor, when compared to that in Fig.IV-9.

It may be seen that in Fig.IV-9 when $G_4/G_2 = 1000$, $E_5/E_3 = 1$ and $t_4/t_2 = 1$, 2 peaks occur in the curves for η_s and DRE. Now in Fig. IV-11, for the same values of parameters except t_4/t_2, which is 10 here, only one of the peaks is significant. This is as a result of thicker

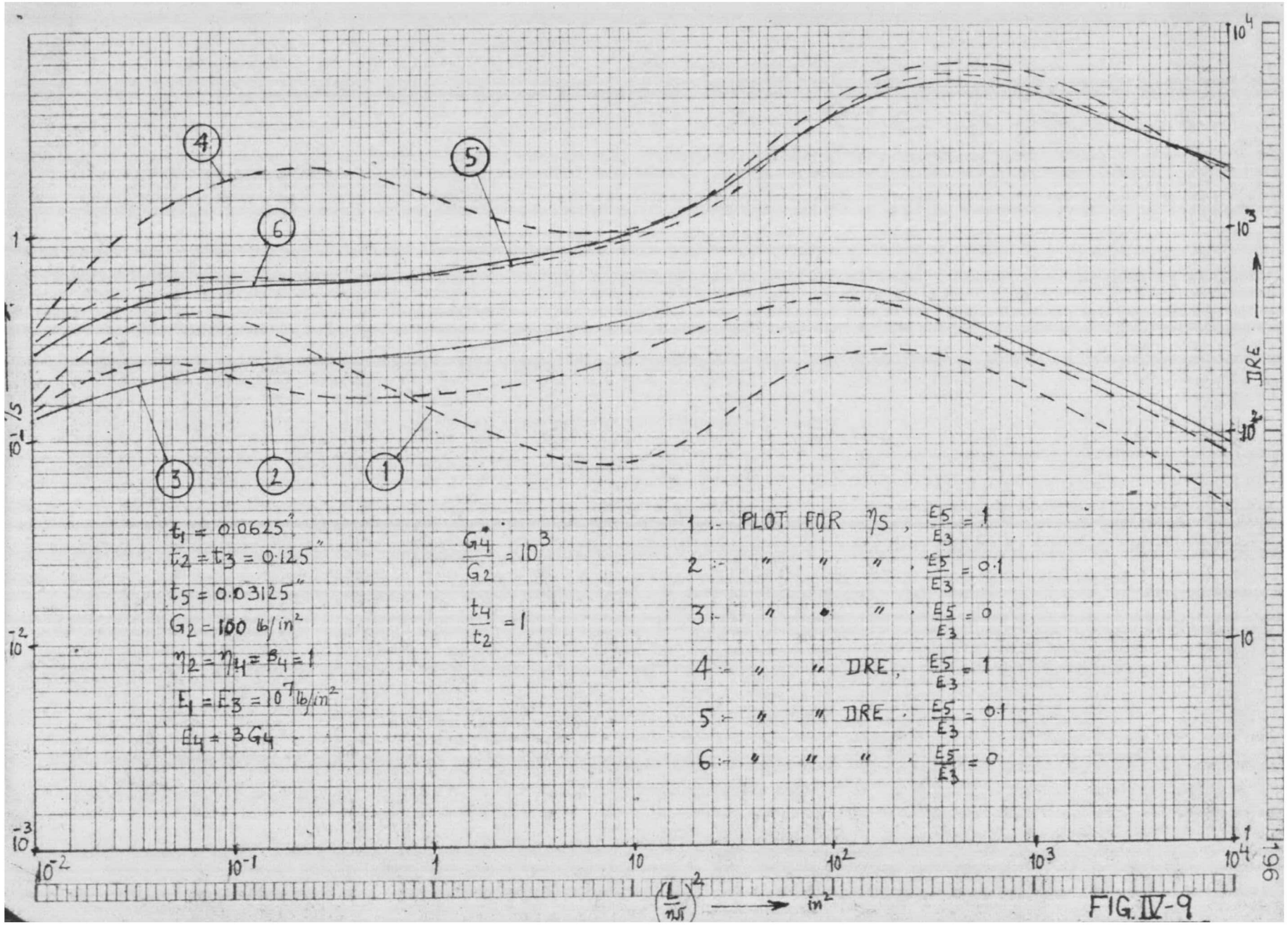
4
5
6
3
2
1
$t_1 = 0.0625''$
$t_2 = t_3 = 0.125''$
$t_5 = 0.03125''$
$G_2 = 100\ lb/in^2$
$\eta_2 = \eta_4 = \beta_4 = 1$
$E_1 = E_3 = 10^7\ lb/in^2$
$E_4 = 3G_4$
$\frac{G_4}{G_2} = 10^3$
$\frac{t_4}{t_2} = 1$
1 :- PLOT FOR η/s , $\frac{E_5}{E_3} = 1$
2 :- " " " , $\frac{E_5}{E_3} = 0.1$
3 :- " " " , $\frac{E_5}{E_3} = 0$
4 :- " " DRE , $\frac{E_5}{E_3} = 1$
5 :- " " DRE , $\frac{E_5}{E_3} = 0.1$
6 :- " " " , $\frac{E_5}{E_3} = 0$
η/s
DRE
10^{-3}
10^{-2}
1
10
10^2
10^3
10^4
10^{-2}
10^{-1}
1
10
10^2
10^3
10^4
$\left(\frac{L}{\pi\sqrt{}}\right)^2$
in^2

FIG. IV-9

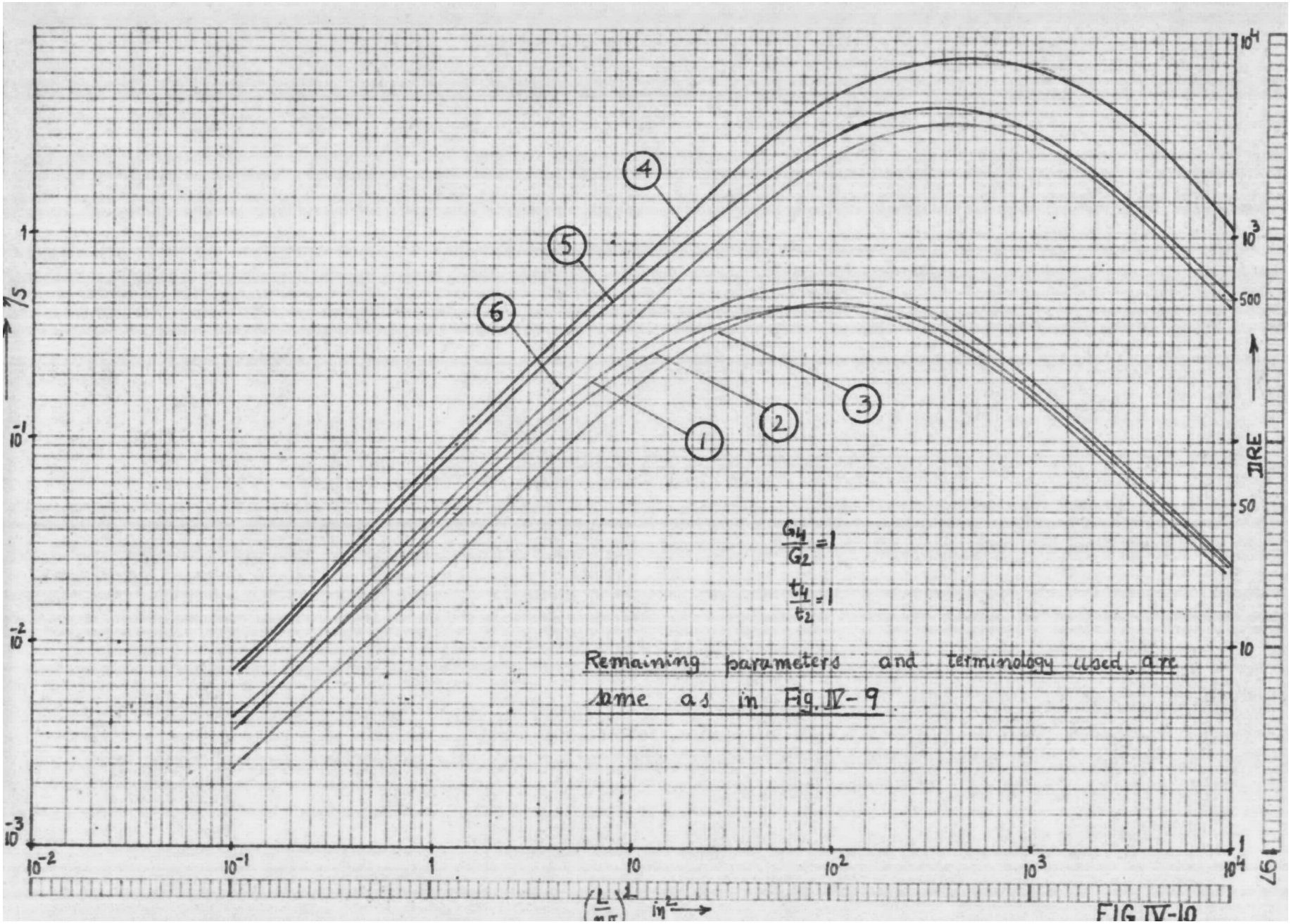
1
10^{-1}
10^{-2}
10^{-3}
10^{-2}
10^{-1}
1
10
10^{2}
10^{3}
10^{4}
10^{4}
10^{3}
500
50
10
1
IIRE
$\frac{G_4}{G_2}=1$
$\frac{t_4}{t_2}=1$
Remaining parameters and terminology used are same as in Fig. IV-9
1
2
3
4
5
6
$\left(\frac{L}{\pi r}\right)^2$ in^2 →
197

FIG IV-10

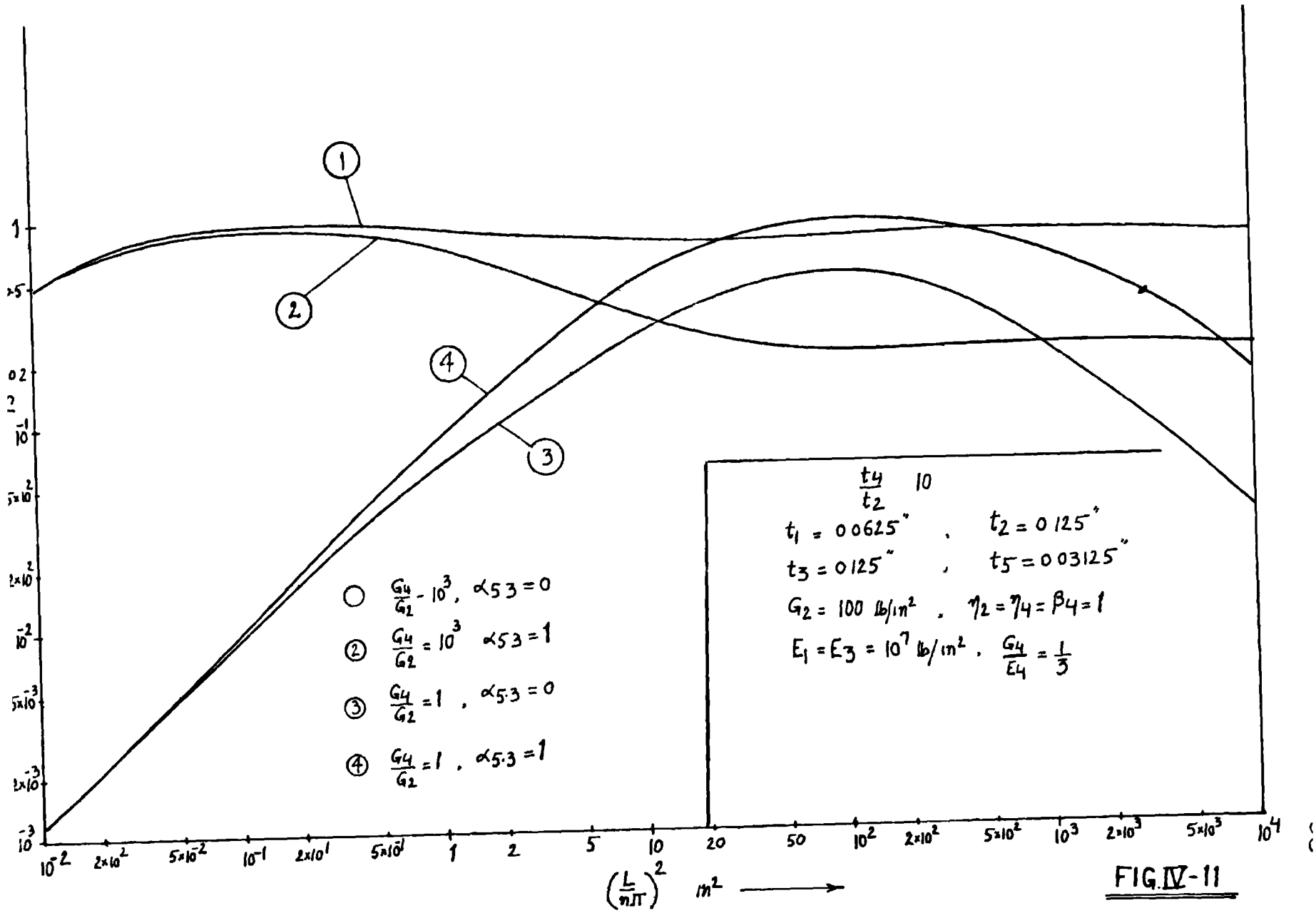
1
×5
0 2
2
10^-1
5×10^-2
2×10^-2
10^-2
5×10^-3
2×10^-3
10^-3
10^-2
2×10^-2
5×10^-2
10^-1
2×10^-1
5×10^-1
1
2
5
10
20
50
10^2
2×10^2
5×10^2
10^3
2×10^3
5×10^3
10^4
(L/nπr)^2 in^2
1
2
3
4
○ G4/G2 - 10^3, α53 = 0
② G4/G2 = 10^3 α53 = 1
③ G4/G2 = 1 , α53 = 0
④ G4/G2 = 1 , α53 = 1
t4/t2 10
t1 = 00625"
t2 = 0125"
t3 = 0125"
t5 = 00 3125"
G2 = 100 lb/in^2 . η2 = η4 = β4 = 1
E1 = E3 = 10^7 lb/in^2 . G4/E4 = 1/3

FIG. IV-11

viscoelastic layer 4 which appears to have suppressed the peak that might have resulted as a result of layer 2.

IV.B.1 : 7 Layered Configuration - Equations of Motion

Fig. IV-2 shows the configuration, in which all the seven layers are different from one another. Layers 2, 4 and 6 are made of viscoelastic materials. Also, the configuration may be considered as a conventional sandwich (with honeycomb core for instance), damped by additional constrained viscoelastic layers on each side.

The assumptions made for derivations are almost similar to those for 5 layered case, discussed in Section IV.A.1 and will not be repeated here. The only difference is that here all viscoelastic layers take up only shear (and no direct stresses). The longitudinal displacement of middle fibre of layer 4 is denoted by u, and these displacements vary with slopes of $\bar{\alpha}$, $\bar{\beta}$, $\bar{\gamma}$ in viscoelastic layers 2, 4 and 6 respectively.

Using notations as in Fig. IV-1 (b) and sign convention as in Fig.II-2(a),

Shear strain of layer 2 = $\bar{\alpha} - w'$

where w is the transverse displacement,

Shear strain of layer 4 = $\bar{\beta} - w'$

Shear strain of layer 6 = $\bar{\gamma} - w'$

The normals to the longitudinal fibres in layers 1, 3, 5 and 7 rotate through ξ ($\xi = w'$, in the absence of shear

effect), whilst the angles in layers 2,4 and 6 are $\bar{\alpha}$, $\bar{\beta}$ and $\bar{\gamma}$ respectively.

Following the procedure of Section IV.\.1, the expression for total strain energy 'U' of sandwich is:

$$U = q_2 \int_o^L (\bar{\alpha}-w)^2 dx \quad q_4 \int_o^L (\bar{\beta}-w)^2 dx \quad q_6 \int_o^L \bar{\gamma}-w')^2 dx$$

$$+r_3 \left[\int_o^L (u + \bar{\beta}' \frac{t_4}{2} + w'' \frac{t_3}{2})^2 dx \quad \int_o^L w''^2 \frac{t_3^2}{12} dx\right]$$

$$r_1 \left[\int_o^L (u' \quad \bar{\beta}' \frac{t_4}{2} + \bar{\alpha}\, t_2 + w''\, t_{31})^2 dx + \int_o^L w''^2 \frac{t_1^2}{12} dx\right]$$

$$r_5 \left[\int_o^L (u' - \bar{\beta}' \frac{t_4}{2} - w'' \frac{t_5}{2})^2 dx \quad \int_o^L w''^2 \frac{t_5^2}{12} dx\right]$$

$$r_7 \left[\int_o^L (u' - \bar{\beta} \quad \frac{t_4}{2} - \bar{\gamma}'\, t_6 - w''t_{57})^2 dx + \int_o^L w''^2 \frac{t_7^2}{12} dx\right]$$

where t_k is thickness of laminate (k), k = 1, 2 ... 7

$$t_3 - t_3 + \frac{t_1}{2}$$

$$t_{57} = t_5 + \frac{t_7}{2}$$

$$q_j = \frac{b}{2} t_j G_j \; ; \qquad j = 2,4,6$$

$$r_i = \frac{b}{2} t_i E_i \; ; \qquad i = 1,3,5,7$$

E_i for layer 'ı' and G_j for layer 'j' are Young's modulus and shear modulus respectively, b is width of the beam.

Kinetic Energy T due to transverse displacements

$$= \tfrac{1}{2} \rho \int_o^L (\dot{w}^2 \, dx,$$

ρ is mass density per unit length of sandwich.

Potential Energy V due to external dynamic loading of intensity f(x) g(t) is

$$= g(t) \int_0^L f(x)\, w\, dx .$$

By the application of Hamilton's Principle, as before, the following equations of motion and boundary conditions (Details given in Appendix 4) are got. Equations of motion are:

$$2q_2(\bar{\alpha}-w') - 2r_1 t_2 (u'' + \bar{\beta}'' \frac{t_4}{2} + \bar{\alpha}'' t_2 + w''' t_{31}) = 0 \qquad \text{(IV.14}$$

$$2q_4(\bar{\beta}-w) - r_3 t_4 (u'' \bar{\beta}'' \frac{t_4}{2} + w''' \frac{t_3}{2}) \; r_5 t_4 (u'' - \bar{\beta}'' \frac{t_4}{2} - w''' \frac{t_5}{2})$$

$$- r_1 t_4 (u'' + \bar{\beta}'' \frac{t_4}{2} + \bar{\alpha}'' t_2 + w''' t_{31}) \; r_7 t_4 (u'' - \bar{\beta}'' \frac{t_4}{2} - \bar{\gamma}'' t_6 - w'' t_{57}$$

$$0 \qquad \text{(IV.15)}$$

$$2q_6(\bar{\gamma}-w') \; 2 \cdot_7 t_6 (u'' - \bar{\beta}'' \frac{t_4}{2} - \bar{\gamma}'' t_6 - w''' t_{57}) \; - \; 0 \qquad \text{(IV.16)}$$

$$- 2r_3 (u'' - \bar{\beta}'' \frac{t_4}{2} \; w'' \; \frac{t_3}{2}) - 2r_1 (u'' + \bar{\beta}'' \frac{t_4}{2} \; \bar{\alpha}'' t_2 \; w'' \; t_{31})$$

$$- 2r_7 (u'' - \bar{\beta}'' \frac{t_4}{2} - \bar{\gamma}'' t_6 - w''' t_{57}) - 2r_5 (u'' - \bar{\beta}'' \frac{t_4}{2} - w''' \frac{t_5}{2}) = 0$$

(IV.17

$$2q_2(\bar{\alpha} - w'') + 2q_4(\bar{\beta}' - w'') + 2q_6(\bar{\gamma}' - w'') + r_3 t_3 (u''' + \bar{\beta}' \; ' \; \frac{t_4}{2} + w'''' \frac{t_3}{2})$$

$$\frac{r_3 t_3^{\,2} + r_1 t_1^{\,2} + r_5 t_5^{\,2} + r_7 t_7^{\,2}}{6} w'''' - r_5 t_5 (u \; '' - \bar{\beta} \quad \frac{t_4}{2} - w'''' \frac{t_5}{2})$$

$$2r_1 t_{31} (u''' + \bar{\beta}''' \frac{t_4}{2} + \bar{\alpha}''' t_2 + w'''' t_{31})$$

$$- 2r_7 t_{57} (u \quad - \bar{\beta} \quad \frac{t_4}{2} - \bar{\gamma} \; '' t_6 - w'''' t_{57}) \; - \; - \; \ddot{w} + g(t \; f(x)$$

(IV.18

Boundary conditions for simply supported ends are.

$$w = w'' - 0$$
$$u = \bar{\alpha}' - \bar{\beta} = \bar{\gamma} - 0 \qquad \text{(IV.19)}$$

IV.B.2 . Solution

For sinusoidal excitations, and both ends of the sandwich beam simply supported, the solution can be assumed as:

$$\left.\begin{aligned} w &= \sum_{n=1}^{\infty} w_n \sin \frac{n\pi x}{L} \sin pt \\ u &= \sum_{n=1}^{\infty} u_n \cos \frac{n\pi x}{L} \sin pt \\ \bar{\alpha} &= \sum_{n=1}^{\infty} \bar{\alpha}_n \cos \frac{n\pi x}{L} \sin pt \\ \bar{\beta} &= \sum_{n=1}^{\infty} \bar{\beta}_n \cos \frac{n\pi x}{L} \sin pt \\ \bar{\gamma} &= \sum_{n=1}^{\infty} \bar{\gamma}_n \cos \frac{n\pi x}{L} \sin pt \end{aligned}\right\} \qquad \text{(IV.20)}$$

This assumed solution satisfies the boundary conditions of eqn. (IV.19) and after substitution in eqns. IV.14 - IV.18, the latter equations are reduced to algebraic equations. Making G_2, G_4 and G_6 complex, i.e. Replacing G_2 by $G_2(1+i\eta_2)$, G_4 by $G_4(1+i\eta_4)$ and G_6 by $G_6(1+i\eta_6)$ gives the solution when these layers are viscoelastic.

Below the solution will be given for the simplified case when layers 1 and 7 are similar, and layers 3 and 5 are similar, i.e. it is a 7 layered symmetrical case. Here $\bar{\ } = \bar{\gamma}$ and $u = 0$. Eqns. (IV.14) and (IV.16 are

similar and equation (IV.17) will not be present if the variable u is not included in the derivation. Substitution of eqn. (IV.20) gives:

$$\left.\begin{aligned} \bar{\alpha}_n A \quad \bar{\beta}_n B + w_n C &= 0 \\ \bar{\alpha}_n B + \bar{\beta}_n D + w_n F &= 0 \\ \bar{\alpha}_n C \quad \bar{\beta}_n F \quad w_n[I-\rho p^2] &= f_n \end{aligned}\right| \qquad \text{(IV.21)}$$

where $f(x) = \sum_{n-1}^{\infty} f_n \sin \frac{n\pi x}{L}$ as before

$$\lambda = (\tfrac{n\pi}{L})^2 E_1 t_1^3 \{2\phi_{2.1}\theta_{2.1} + 2\theta^2_{2.1}\}$$

$$B = (\tfrac{n\pi}{L})^2 E_1 t_1^3 \{\theta_{2.1}\theta_{4.1}\}$$

$$C = \tfrac{n\pi}{L}^3 E_1 t_1^3 \{-2\phi_{2.1}\theta_{2.1} + 2\theta_{2.1}(\theta_{3.1}+\tfrac{1}{2})\}$$

$$D = (\tfrac{n\pi}{L})^2 E_1 t_1^3 \{\phi_{4.1}\theta_{4.1} + \tfrac{1}{2}\alpha_{3.1}\theta_{3.1}\theta^2_{4.1} \quad \tfrac{1}{2}\theta^2_{4.1}\}$$

$$F = (\tfrac{n\pi}{L})^3 E_1 t_1^3 \{-\phi_{4.1}\theta_{4.1} + \tfrac{1}{2}\alpha_{3.1} \quad \theta^2_{3.1}\theta_{4.1} \quad \theta_{4.1}(\theta_{3.1}+\tfrac{1}{2}$$

$$I = (\tfrac{n\pi}{L})^4 E_1 t_1^3 \{2\phi_{2.1}\theta_{2.1} \quad \phi_{4.1}\theta_{4.1} + \tfrac{1}{2}\alpha_{3.1}\theta^3_{3.1}$$

$$+ \tfrac{1}{6}(1 \quad \alpha_{3.1}\theta^3_{3.1}) + 2(\tfrac{1}{2} \quad \theta_{3.1})^2\}$$

$$\theta_{m.1} = t_{m/t_1} \; ; \quad m = 2,3,4$$

$$\phi_{k.1} = \frac{G_k}{E_1 t_1^2 (\frac{n\pi}{L})^2} \; , \quad k - 2,4$$

and $$\alpha_{j.1} = \frac{E_j}{E_1} \; , \quad j - 1,3$$

Substituting G_2 by $G_2(1+i\eta_2)$ and G_4 by $G_4(1+i\eta_4)$ in eqn. (IV.21), elimination and algebraic simplification, gives a single equation in w_n as

$$b\left(\frac{n\pi}{L}\right)^4 E_1 t_1^3 \, w_n \, [z_{rn}+i\, z_{in}] - \rho p^2 w_n = f_n \qquad \text{(IV.22)}$$

ρ being $= bt_1(2\rho_1+2\rho_2\theta_{2.1}+2\rho_3\theta_{3.1}+\rho_4\theta_{4.1})$,

ρ_1, ρ_2, ρ_3 and ρ_4 are the mass densities per unit volume of layers 1, 2, 3 and 4 respectively. The expressions for z_{rn} and z_{in} are not given here but are easily obtainable as explained above.

Rewriting eqn. (IV.22) as

$$w_n[z_{rn}+i\, z'_{in} - \rho p^2] = f_n \qquad \text{(IV.23)}$$

where

$$z'_{rn} = b\left(\frac{n\pi}{L}\right)^4 E_1 t_1^3 \, (Z_{rn})$$

$$z'_{in} = b\left(\frac{n\pi}{L}\right)^4 E_1 t_1^3 \, (Z_{in})$$

The expressions for η_s and DRE for this configuration are similar to those for the 5 layered case given in Section IV.A.2,

$$\eta_s \text{ for nth mode} = \frac{z'_{in}}{z'_{rn}} \qquad \text{(IV.24)}$$

$$k\eta_s \text{ being} = \frac{z'_{in}}{b\left(\frac{n\pi}{L}\right)^4 \frac{E_s t_s^3}{12}}$$

$$= \frac{E_1 t_1^3 \, (z_{in})}{\frac{E_s t_s^3}{12}} \qquad \text{(IV.25)}$$

As in Section IV.A.2, no reference system has been chosen for comparison of dynamic rigidity with that of the sandwich and the numerator in eqn. (IV.25) is designated as DRE and evaluated in Section IV.B.3 for studying effect of various parameters.

If both ends of the sandwich beam are excited by sinusoidal transverse displacement x_o sin pt, both ends being in phase, then the displacements elsewhere in the beam may be determined using eqns. (IV.12) and (IV.13) since eqns (IV.11) and (IV.23) are similar.

IV.B.3 : Effect of various system parameters on damping effectiveness and comparisons with other arrangements

In this section, the effect of parameters of a symmetrical 7 layered sandwich is studied. The numbering of various layers is given in Figs. IV-12.

(i) Fig. IV -12 gives graphs of η_s and DRE, as affected by the thickness of layer 4. Material loss factor of layer '4' is taken as zero. The arrangement is equivalent to a conventional sandwich, damped by using constrained viscoelastic layers on each side. It is generally known that increase of t_4 would increase the damping of such a sandwich construction [94], since the distance of viscoelastic layers from the flexural axis of sandwich is increased as t_4 increases.

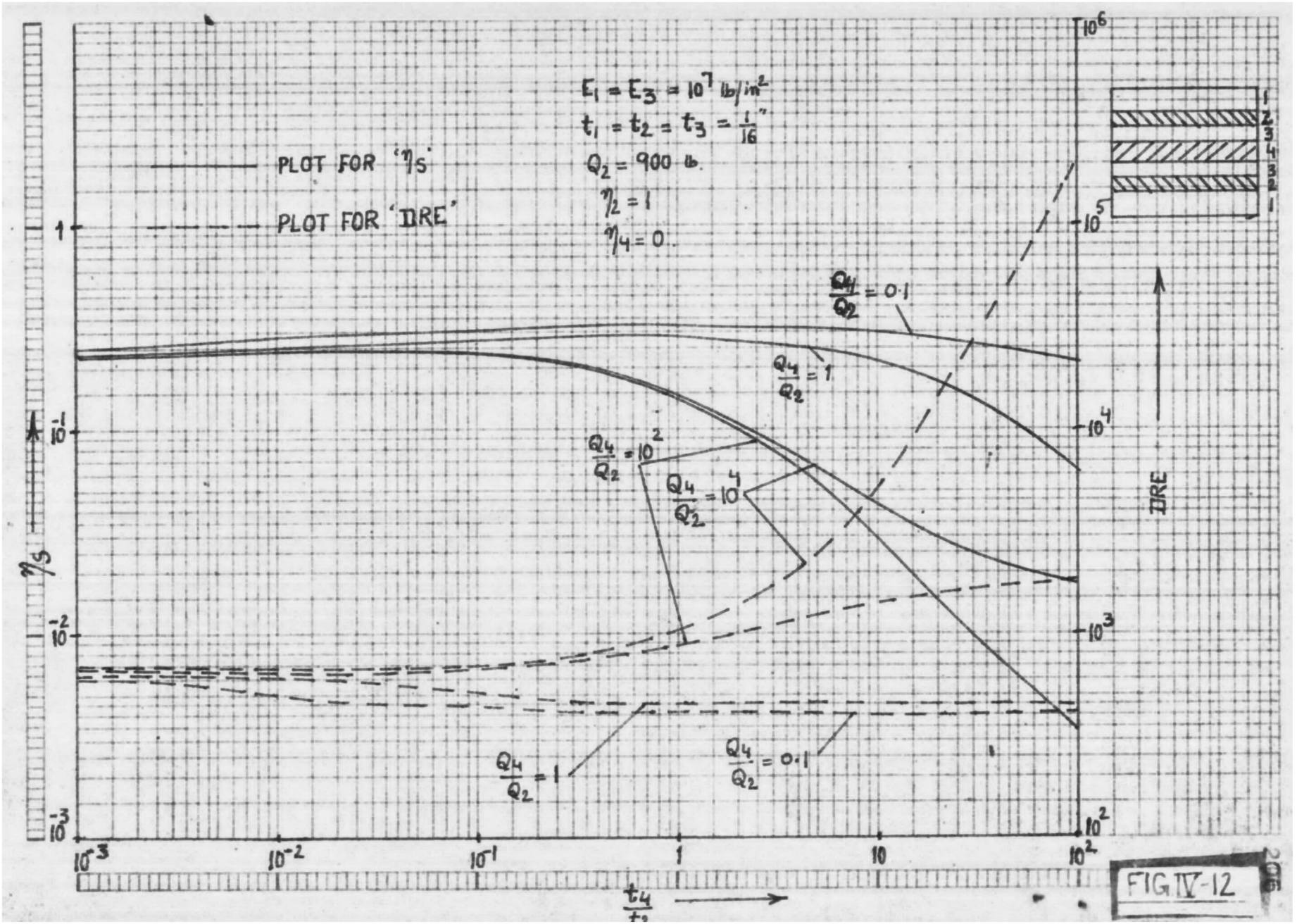
$E_1 = E_3 = 10^7$ lb/in^2
$t_1 = t_2 = t_3 = \frac{1}{16}$"
$Q_2 = 900$ lb.
$\eta_2 = 1$
$\eta_4 = 0$.
PLOT FOR 'η_s'
PLOT FOR 'IRE'
$\frac{Q_4}{Q_2} = 0.1$
$\frac{Q_4}{Q_2} = 1$
$\frac{Q_4}{Q_2} = 10^2$
$\frac{Q_4}{Q_2} = 10^4$
$\frac{Q_4}{Q_2} = 1$
$\frac{Q_4}{Q_2} = 0.1$
η_s
IRE
$\frac{t_4}{t_2}$
1
10^{-1}
10^{-2}
10^{-3}
10^6
10^5
10^4
10^3
10^2
10^{-3}
10^{-2}
10^{-1}
1
10
10^2
1
2
3
4
3
2
1

FIG IV-12

However, in Fig. IV-12, this is not seen to hold, since an optimum 'η_s' occurs at a certain value of t_4, as shown in the Fig. This may be explained by the fact that an increase in thickness t_4 would increase the total strain energy of the system and may not correspondingly increase the energy dissipation, which is merely due to he constraining action of met.l layers 1 and 3. However, in Fig.IV-12, a graph of DRE shows that for higher values of $\frac{t_4}{t_2}$ and $\frac{Q_4}{Q_2}$, the displacement response effectiveness increases. This is due to the fact that, at these high values of $\frac{t_4}{t_2}$ and $\frac{Q_4}{Q_2}$, the increase in 'k' compensates for the decrease in η_s, thus increasing $k\eta_s$ or DRE of the system.

(ii) In Figs. IV-13 and IV-14, a comparison is made between a 7 layered sandwich and a 3 layered one. In the 7 layered case, viscoelastic layers 2 and 4 are taken to be of the same material while the core thickness in the 3 layered case is taken as equal to $2t_2 + t_4$, i.e. same total thickness of viscoelastic material is used in the two configurations. Alternatively, it may be said that the elimination of metal layers 3 in the 7 layered case would give the corresponding 3 layered configuration.

Fig. IV-13 shows that when t_4/t_2 0.1, the 7 layered ' se is better than the corresponding 3 layered one, from r nt of view of damping at low values of Q_2 i.e. when 'n' i high or frequency is high. The behaviour for higher

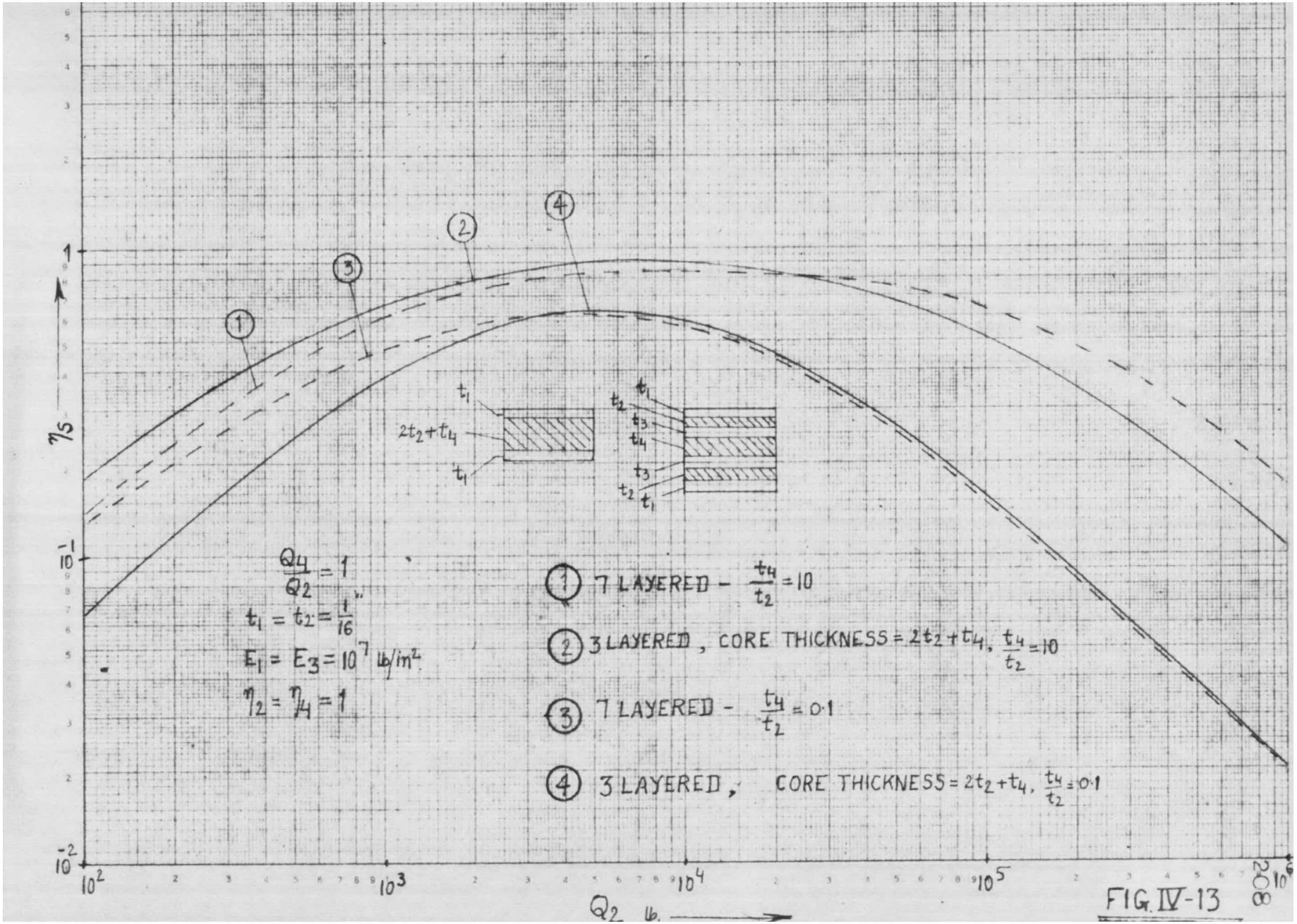
1
2
3
4
η_S
10^{-1}
10^{-2}
10^2
10^3
10^4
10^5
Q_2 lb.
t_1
$2t_2+t_4$
t_1
t_1
t_2
t_3
t_4
t_3
t_2
t_1
$\frac{Q_4}{Q_2} = 1$
$t_1 = t_2 = \frac{1}{16}$"
$E_1 = E_3 = 10^7$ lb/in^2
$\eta_2 = \eta_4 = 1$
1 7 LAYERED – $\frac{t_4}{t_2} = 10$
2 3 LAYERED, CORE THICKNESS $= 2t_2 + t_4$, $\frac{t_4}{t_2} = 10$
3 7 LAYERED – $\frac{t_4}{t_2} = 0.1$
4 3 LAYERED, CORE THICKNESS $= 2t_2 + t_4$, $\frac{t_4}{t_2} = 0.1$

FIG. IV-13

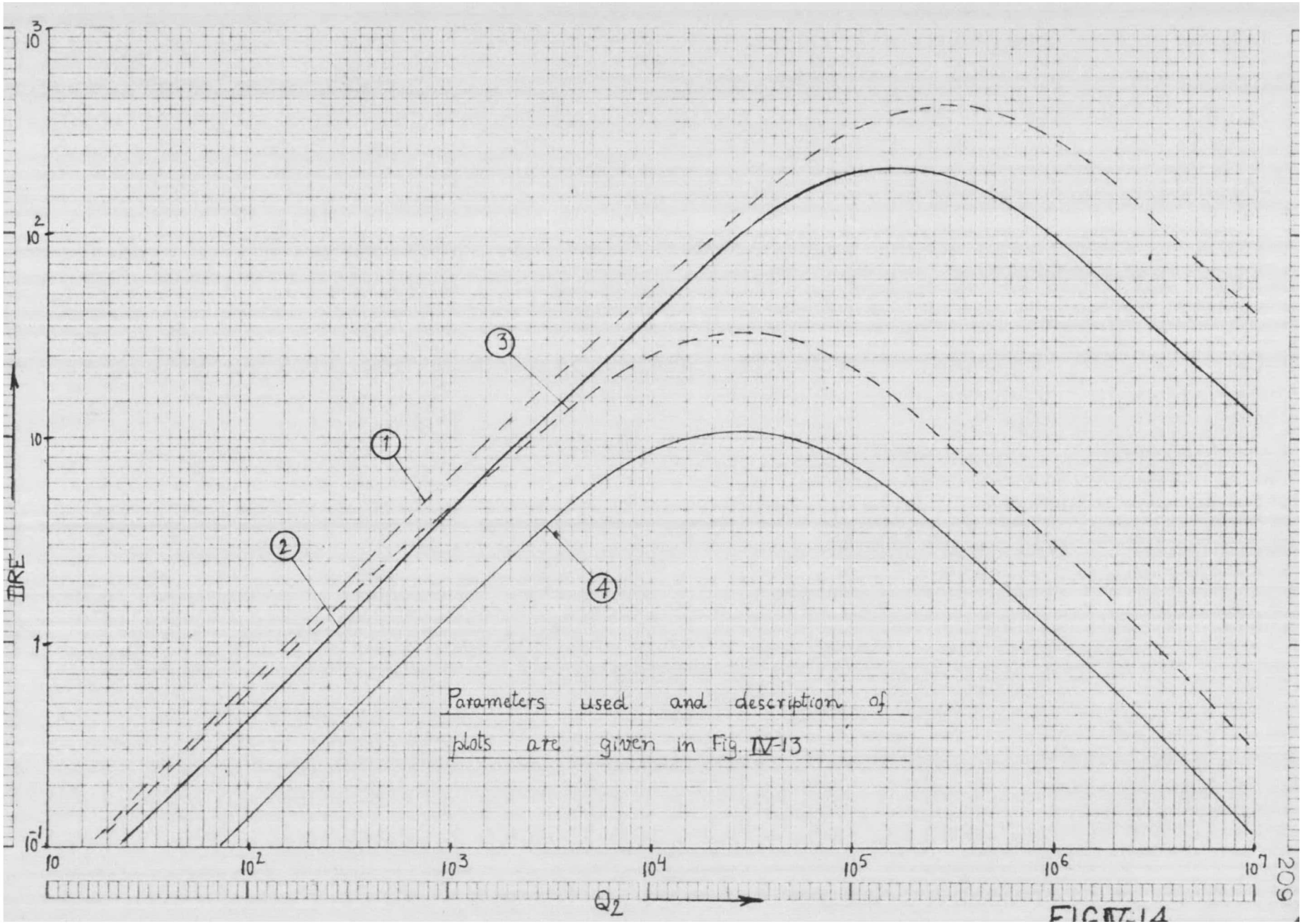
10^3
10^2
10
1
10^{-1}
DRE
1
2
3
4
Parameters used and description of plots are given in Fig. IV-13.
10
10^2
10^3
10^4
10^5
10^6
10^7
Q_2

FIG IV-14

values of Q_2 is nearly the same in both cases. For $\frac{t_4}{t_2}$ =10, the curves for the two cases are similar except for a shift between the two curves. Fig. IV-14 for DRE vs. Q_2 shows the values for 7 layered case are always higher than those of corresponding 3 layered configuration. This might be explained by the fact that in the cases analysed, 7 layered case is dynamically more stiff, because of additional layers 3, hence k and $k\eta_s$ are more.

(iii) Fig. IV-15 illustrates the effect of using visco-elastic layers 2 and 4 in the seven layered case with shear moduli values different from each other, i.e. for varying values of ratio $\frac{Q_4}{Q_2}$. Both layers 2 and 4 are assumed to have the same material loss factor. Two peaks are seen to occur for the loss factor η_s, when plotted against the dimensionless shear parameter $\phi_{2.1}$, for values of $\frac{Q_4}{Q_2}$ = 100 and 0.01, while a single peak occurs for $\frac{Q_4}{Q_2}$ = 1. It may also be seen that curves drawn for $\frac{Q_4}{Q_2}$ - 100 and 0.01 indicate high damping for a much larger range of $\phi_{2.1}$, the shear parameter, than the curve for $\frac{Q_4}{Q_2}$=1 However, the peak values of η_s when Q_4 and Q_2 are unequal, are less than the corresponding peak value when Q_4 and Q_2 are equal. But, unequal values of Q_4 and Q_2 should be preferred in practice,if reasonable amount of damping is required over awide range of $\phi_{2.1}$. In practice, $\phi_{2.1}$ may vary, due to variation of 'n' i.e. at different

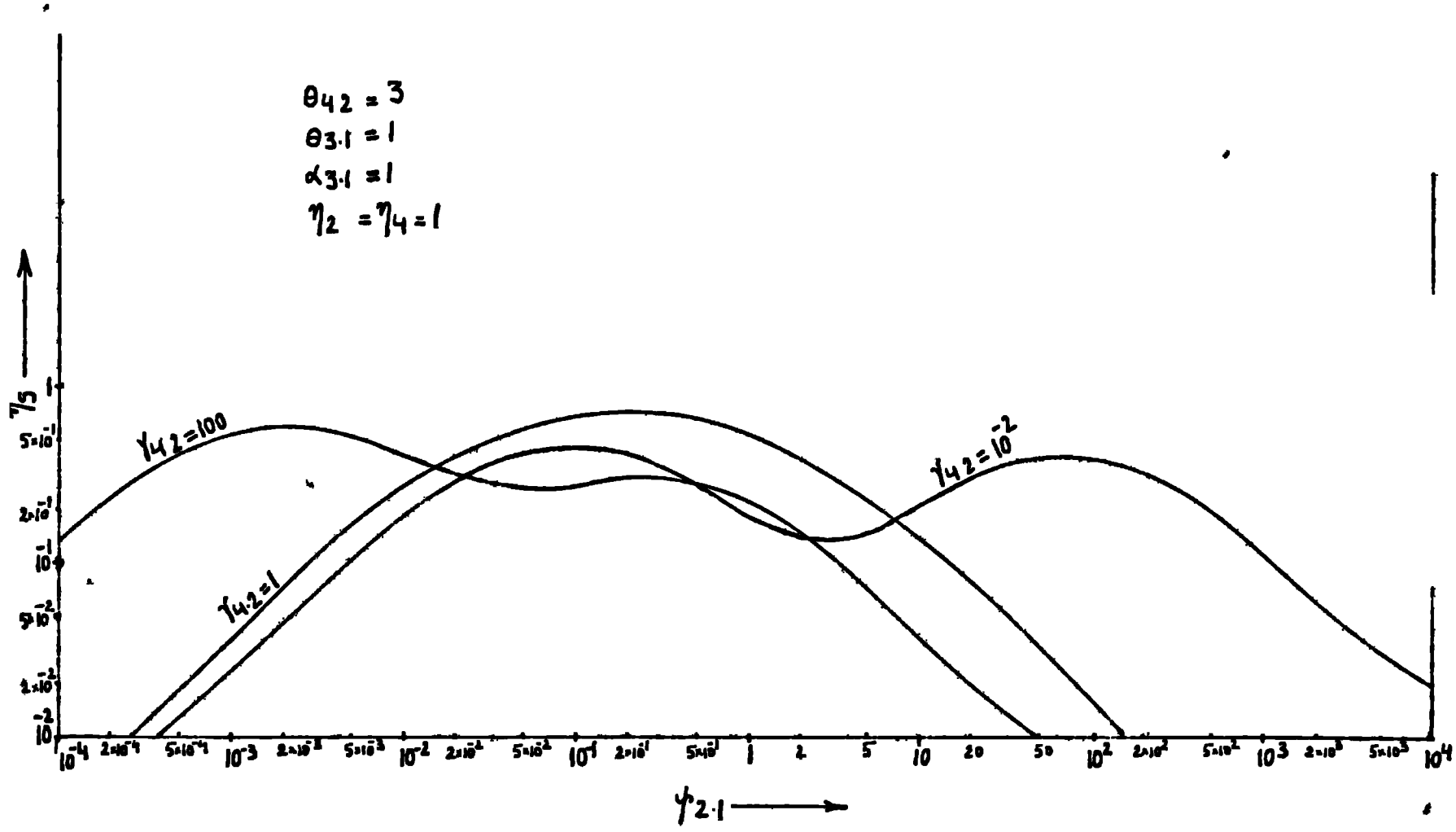
$\theta_{42} = 3$
$\theta_{3.1} = 1$
$\alpha_{3.1} = 1$
$\eta_2 = \eta_4 = 1$
$\gamma_{4.2}=100$
$\gamma_{4.2}=1$
$\gamma_{4.2}=10^{-2}$
η_5
$\psi_{2.1}$

FIG. IV-15

modes in a large frequency range, and also G_2 might vary due to temperature or frequency dependence of viscoelastic material properties.

IV.C : Any Number of Layers

In Section IV.A, analysis has been shown for a 5 layered sandwich, while in IV.B., this has been done for a 7 layered configuration. In each case, the elastic (metals generally) and viscoelastic layers are arranged alternately, with the elastic layers on the outside. If the number of layers is more, a similar procedure should give the equations of motion. If there are 'N' viscoelastic layers and 'N+1' elastic layers arranged alternately, the number of equations of motion obtained by a purely elastic analysis will be: N+2, according to the assumptions of previous sections, viz. same transverse displacement at each section and the longitudinal displacements varying with different slopes throughout thickness in each layer. In order to define longitudinal displacement of each fibre at a section, the entire section is assumed to move with a displacement 'U' and then variation assumed in each layer through its thickness, slopes being $\bar{\alpha}_1$ .... $\bar{\alpha}_n$ in the viscoelastic layers and ξ i.e. flexural angle ($-w'$) in the metal layers.

With the conversion of the above elastic analysis to viscoelastic one under sinusoidal excitation, the number of equa-

tions is doubled, since each 'displacement or slope parameter' defining the system (e.g. u, w, $\bar{\alpha}$, etc.) has inphase and out of phase components.

However, if the shear effect in all the layers is included, the number of equations obtained for purely elastic analysis will be. 2N+3. (Parameters defining the system being u, w and slopes in '2N+1' layers.)

CHAPTER V : MULTICORED CONFIGURATIONS

The laminated beams analysed in this Chapter, are those in which two different types of viscoelastic layers may occur adjacently, instead of occurring alternately as in Chapter IV. Such configurations have been called as the multicored ones', in the present work. This designation appears appropriate when these are compared with a 3 layered configuration, which involves a single core.

Two such configurations are analysed. These are shown in Figs. V-1(a) and V-1(b), the former is a 4 layered unsymmetrical case and the latter is a 5 layered symmetrical one.

V.A.1 : 4 Layered Unsymmetrical Case - Equations of Motion

Fig. V-1(a) shows the configuration, together with the notation used in the analysis. Layers 2 and 3 are viscoelastic. The following assumptions are made for the analysis.

1) Layers 1 and 4 are assumed to bend according to Bernoulli-Euler's theory and shear effect in these layers is not of importance.

2) In layers 2 and 3, shear effect is of importance and in these layers, the normals to the longitudinal fibres rotate through angles $\overline{\alpha}$ and $\overline{\beta}$ respectively. Layer 2 takes up shear and effect of direct stresses is not of importance

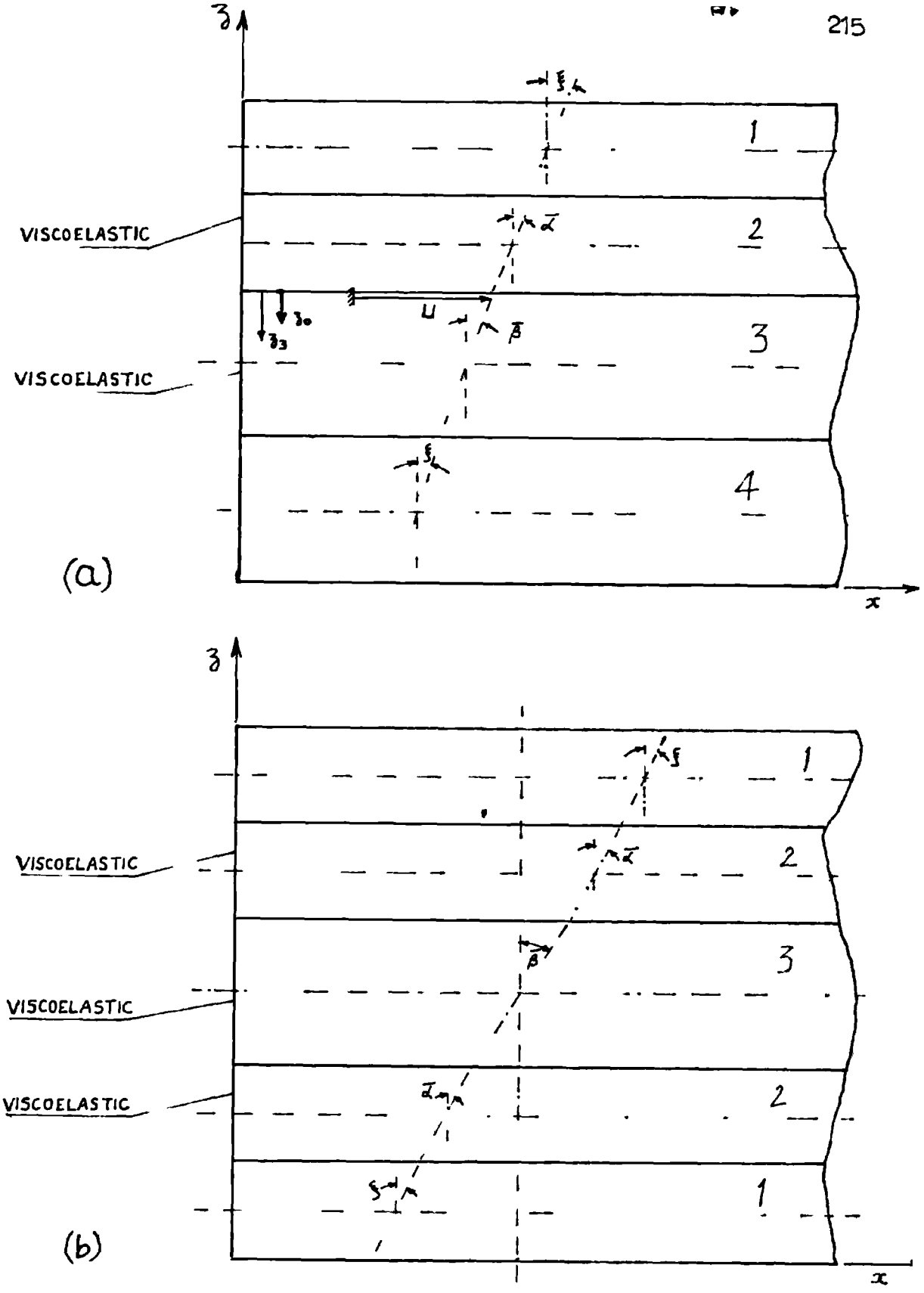
z
1
2
VISCOELASTIC
3
VISCOELASTIC
4
(a)
x
z
1
2
VISCOELASTIC
3
VISCOELASTIC
2
VISCOELASTIC
1
(b)
x

FIG V 1

in that layer, while both these effects are included in layer 3. It is necessary to include the effect of direct stresses in addition to shear in layer 3 if it is rigid and thick.

3) The longitudinal displacements vary linearly through each layer, though with different slopes, as shown in Fig.V-1(a), being ξ, the flexural angle in the outer layers 1 and 4 and $\bar{\alpha}$ and $\bar{\beta}$ in layers 2 and 3 respectively. The longitudinal displacement at the interface of layers 2 and 3 is taken as 'u'.

The remaining assumptions are same as assumption 3, 4, 5, 7 and 8 as discussed in Section IV.A.1 and the discussion about the limitations applies to this case as well.

Taking 'w' as the transverse displacement at a section, and using sign convention according to Fig.II-2 (a), we have,

Shear strain of layer 2 $\quad \bar{\alpha} - w'$

and that of layer 3 $- \quad \bar{\beta} - w'$.

The normal to the longitudinal fibres in layers 1 and 4 rotates through ξ ($\xi - w'$ in the absence of shear effect in these layers, as assumed) and such angles in layers 2 and 3 are $\bar{\alpha}$ and $\bar{\beta}$ respectively.

The longitudinal displacements of mid-fibres of these layers are.

For layer 1 : $u + \bar{\alpha}\, t_2 + \xi \frac{t_1}{2}$

For layer 3 : $u - \bar{\beta} \frac{t_3}{2}$

For layer 4 : $u - \bar{\beta}\, t_3 - \xi \frac{t_4}{2}$

Expression for total strain Energy 'U' =

$$q_2 \int_o^L (\bar{\alpha}-w')^2\, dx + q_3 \int_o^L (\bar{\beta}-w')^2\, dx$$

$$+ r_1 \int_o^L [(u'+\bar{\alpha}' t_2 + w'' \frac{t_1}{2})^2 + w''^2 \frac{t_1^2}{12}]\, dx$$

$$+ r_4 \int_o^L [(u'-\bar{\beta}' t_3 - w'' \frac{t_4}{2})^2 + w''^2 \frac{t_4^2}{12}]\, dx$$

$$+ r_3 \int_o^L [(u'-\bar{\beta}' \frac{t_3}{2})^2 + \bar{\beta}'^2 \frac{t_3^2}{12}]\, dx$$

where $q_3 = \frac{1}{2} b k_3 t_3 G_3$

$q_2 = \frac{1}{2} b t_2 G_2$

$r_j = \frac{1}{2} b t_j E_j \qquad (j = 1,3,4)$

k_3 is shear coefficient, an expression for this is derived in Appendix 6.

Kinetic Energy 'T' = $\frac{1}{2} \rho \int_o^L (\dot{w})^2\, dx$

ρ = mass density/unit length of the sandwich.

Potential Energy 'V due to external loading of intensity f(x)g(t)

$$= g(t) \int_o^L f(x)\, w\, dx$$

Application of Hamilton s principle gives the equations of

motion and boundary conditions. Details are given in Appendix 5.

Equations of motion are:

$$2q_2(\bar{\alpha}-w')-2r_1t_2\left(u''+\bar{\alpha}''t_2+w'''\,\frac{t_1}{2}\right) = 0 \qquad (V.1)$$

$$2q_3(\bar{\beta}-w')+2r_4t_3\left(u''-\bar{\beta}''t_3-w'''\,\frac{t_4}{2}\right) -2r_3\left(\bar{\beta}''\,\frac{t_3^2}{3}-\frac{t_3}{2}\,u''\right) = 0 \qquad (V.2)$$

$$2r_1\left(u''+\bar{\alpha}''t_2+w'''\,\frac{t_1}{2}\right)+2r_4\left(u''-\bar{\beta}''t_3-w'''\,\frac{t_4}{2}\right) +2r_3\left(u''-\bar{\beta}''\,\frac{t_3}{2}\right) = 0 \qquad (V.3)$$

$$2q_2(\bar{\alpha}'-w'')+2q_3(\bar{\beta}'-w'')+r_1t_1\left(u'''+\bar{\alpha}'''t_2+w''''\,\frac{t_1}{2}\right) + \frac{r_1t_1^2}{6}\,w''''-r_4t_4\left(u'''-\bar{\beta}'''t_3-w''''\,\frac{t_4}{2}\right)+\frac{r_4t_4^2}{6}\,w'''' = -\rho\ddot{w}+g(t)f(x) \qquad (V.4)$$

Boundary conditions for simply supported ends are

$$\text{At } x = 0,\ L\ ; \qquad w = w'' = 0 \qquad u' = \bar{\alpha}' = \bar{\beta}' = 0 \qquad (V.5)$$

V.A.2 : Solution

For sinusoidal excitation, assuming the solution in the form of series.

$$w = \sum_{n=1}^{\infty} w_n \sin\frac{n\pi x}{L}\ \sin pt$$

$$u = \sum_{n=1}^{\infty} u_n \cos\frac{n\pi x}{L}\ \sin pt \qquad (V.6)$$

$$\bar{\alpha} = \sum_{n=1}^{\infty} \bar{\alpha}_n \cos \frac{n\pi x}{L} \sin pt$$

$$\bar{\beta} = \sum_{n=1}^{\infty} \bar{\beta}_n \cos \frac{n\pi x}{L} \sin pt$$

Also expanding $f(x) \sin pt = \sum_{n=1}^{\infty} f_n \sin \frac{n\pi x}{L} \sin pt$.

Substitution of the above solution in eqns. (V.1) to (V.4) shows that boundary conditions are satisfied and the equations of motion are reduced to algebraic equations, namely

$$\begin{aligned}
&\bar{\alpha}_n A + u_n B + w_n C = 0 \\
&\bar{\beta}_n D - u_n F + w_n H = 0 \\
&\bar{\alpha}_n B - \bar{\beta}_n F + u_n J + w_n K = 0 \\
&\bar{\alpha}_n C + \bar{\beta}_n H + u_n K + w_n [I - \rho p^2] = f_n
\end{aligned} \qquad (V.7)$$

where

$$A = \left(\frac{n\pi}{L}\right)^2 E_4 t_4^3 \{\phi_{2.4}\theta_{2.4} + \alpha_{1.4}\theta_{1.4}\theta^2_{2.4}\}$$

$$B = \left(\frac{n\pi}{L}\right)^2 E_4 t_4^2 \{\alpha_{1.4}\theta_{1.4}\theta_{2.4}\}$$

$$C = \left(\frac{n\pi}{L}\right)^3 E_4 t_4^3 \{-\phi_{2.4}\theta_{2.4} + \tfrac{1}{2}\alpha_{1.4}\theta^2_{1.4}\theta_{2.4}\}$$

$$D = \left(\frac{n\pi}{L}\right)^2 E_4 t_4^3 \{\phi_{3.4}\theta_{3.4} + \theta^2_{3.4} + \tfrac{1}{3}\alpha_{3.4}\theta^3_{3.4}\}$$

$$F = \left(\frac{n\pi}{L}\right)^2 E_4 t_4^2 \{\theta_{3.4} + \tfrac{1}{2}\alpha_{3.4}\theta^2_{3.4}\}$$

$$H = \left(\frac{n\pi}{L}\right)^3 E_4 t_4^3 \{-\phi_{3.4}\theta_{3.4} + \tfrac{1}{2}\theta_{3.4}\}$$

$$J = \left(\frac{n\pi}{L}\right)^2 E_4 t_4 \left\{\alpha_{1.4}\theta_{1.4}+1+\alpha_{3.4}\theta_{3.4}\right\}$$

$$K = \left(\frac{n\pi}{L}\right)^3 E_4 t_4^2 \left\{\tfrac{1}{2}\alpha_{1.4}\theta^2_{1.4}-\tfrac{1}{2}\right\}$$

$$I = \left(\frac{n\pi}{L}\right)^4 E_4 t_4^3 \left\{\phi_{2.4}\theta_{2.4}+\phi_{3.4}\theta_{3.4}+\frac{1}{3}\alpha_{1.4}\theta^3_{1.4}+\frac{1}{3}\right\}$$

$$\alpha_{i.4} = \frac{E_i}{E_4} \; ; \quad i = 1,3$$

$$\theta_{j.4} = \frac{t_j}{t_4} \; ; \quad j = 1,2,3$$

$$\phi_{k.4} = \frac{G_k}{E_4 t_4^2 \left(\frac{n\pi}{L}\right)^2} \; ; \quad k = 2,3$$

To get the solution when layers 2 and 3 are viscoelastic, the elastic moduli of these layers have to be replaced by their complex values, i.e. G_2 by $G_2(1+i\eta_2)$, G_3 by $G_3(1+i\eta_3)$ and E_3 by $E_3(1+i\beta_3)$, where η_2 and η_3 are the loss factors of layers 2 and 3 respectively in shear while β_3 is the loss factor of layer 3 in direct stress case. Substituting the complex moduli into equations (V.7) makes the various coefficients A, B, C etc. complex, and the solution to the problem is obtained by solving the 4 simultaneous complex algebriac equations. These may be reduced to 8 simultaneous algebraic equations with real coefficients as explained in Section IV.A.2.

After elimination and simplification, it is possible to get a single equation in w_n, from eqn. (V.7), after substitution of complex moduli. It takes the form

$$w_n b \left(\frac{n\pi}{L}\right)^4 E_4 t_4^3 [Z_{rn} + iZ_{in}] - \rho p^2 w_n = f_n \qquad (V.8)$$

The expressions for Z_{rn} and Z_{in} are not given here, but may be obtained as explained above. The computations, in the present work, were done on the Atlas digital computer.

Eqn. (V.8) may be written in the form,

$$w_n [Z'_{rn} + iZ'_{in} - \rho p^2] = f_n \qquad (V.9)$$

where $Z'_{rn} = b\left(\frac{n\pi}{L}\right)^4 E_4 t_4^3 \quad (Z_{rn})$

$$Z'_{in} = b\left(\frac{n\pi}{L}\right)^4 E_4 t_4^3 \quad (Z_{in})$$

As in Section IV.B.2,

$$'\eta_s' \text{ for nth mode} = \frac{Z'_{in}}{Z'_{rn}} \qquad (V.10)$$

$$k\eta_s = \frac{Z'_{in}}{b\left(\frac{n\pi}{L}\right)^4 \frac{E_s t_s^3}{12}}$$

$$= \frac{Z_{in}(E_4 t_4^3)}{\frac{E_s t_s^3}{12}} \qquad (V.11)$$

E_s and t_s being the parameters of a solid beam which might be chosen for comparison with the dynamic rigidity of the sandwich. In the next section, the numerator in eqn. (V.11) is designated as DRE (Displacement response effectiveness) and evaluated for studying influence of various parameters.

For the case of the sandwich beam being excited at each end by transverse displacements of amplitude $x_o \sin pt$, transverse displacement at other locations may be determined using eqns. (IV.12) and (IV.13). This is due to the fact that eqns. (IV.11) and (V.9) are similar.

V.A.3 : Effect of various system parameters on damping effectiveness and comparisons with other arrangements

(i): Figs. V-2 to V-4 are meant to illustrate the effect of properties of layer '3' on the overall damping of the system. Only layer '2' is taken to be the damping layer and material loss factors η_3 and β_3 for layer 3 are taken to be zero. The parameters varied are: $\frac{t_3}{t_2}$ and $\frac{Q_3}{Q_2}$. In fact, layer 3 can be regarded as a 'spacer' in this case. It is seen from the above mentioned Figs. that optimum damping occurs at certain values of $\frac{t_3}{t_2}$ and $\frac{Q_3}{Q_2}$. The spacer should not be as stiff as possible as might appear from [60] but for optimum damping, the corresponding value has to be determined for the given set of parameters, the reason being that a very stiff layer 3 will no doubt increase the shear motion of layer 2 but the overall system damping might decrease due to increased contribution of strain energy due to layer 3.

In [60], it is recommended that for high damping, $\frac{G_3}{t_3}$

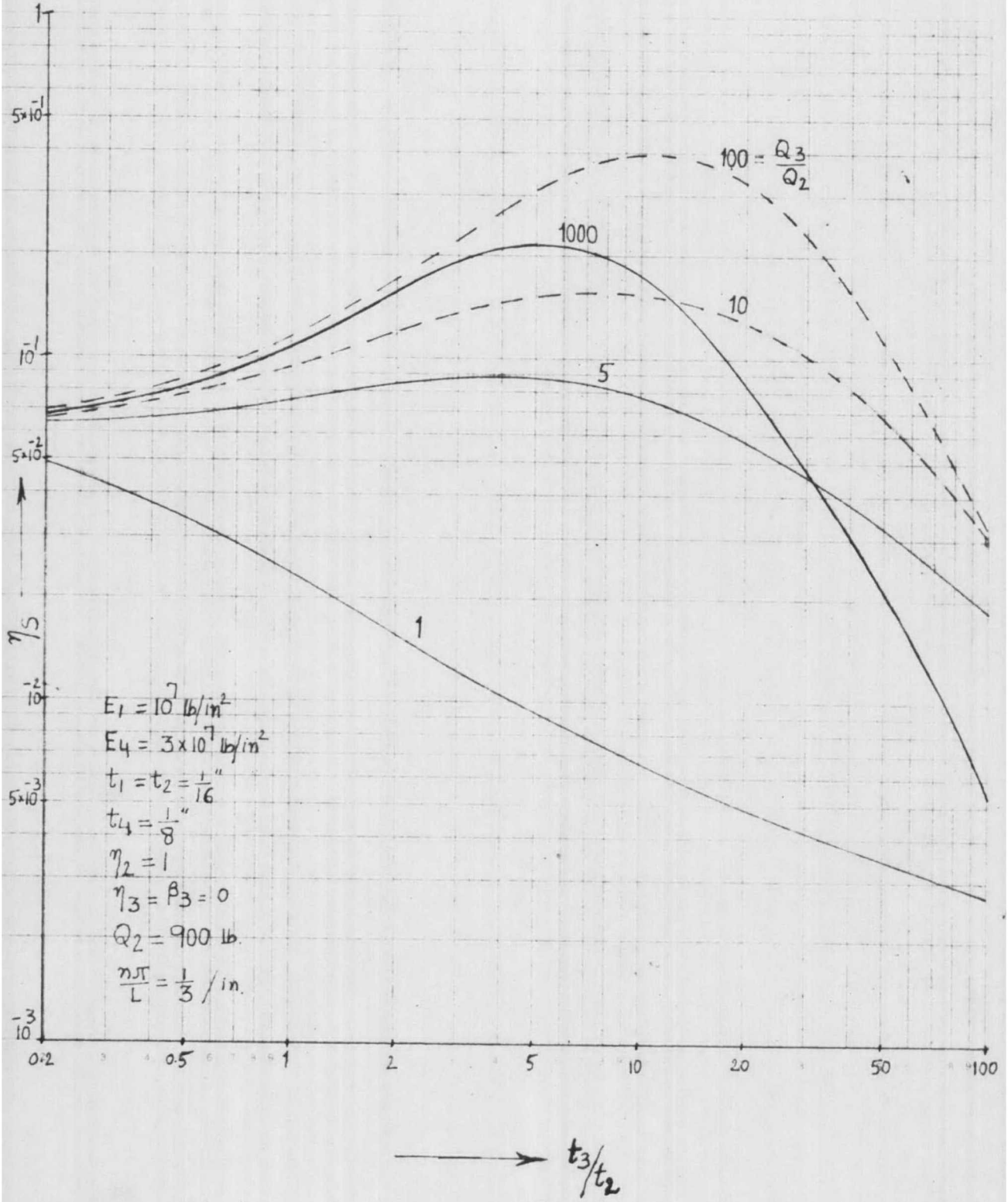

η_S VS. t_3/t_2 FOR VARYING Q_3/Q_2

FIG. V-2

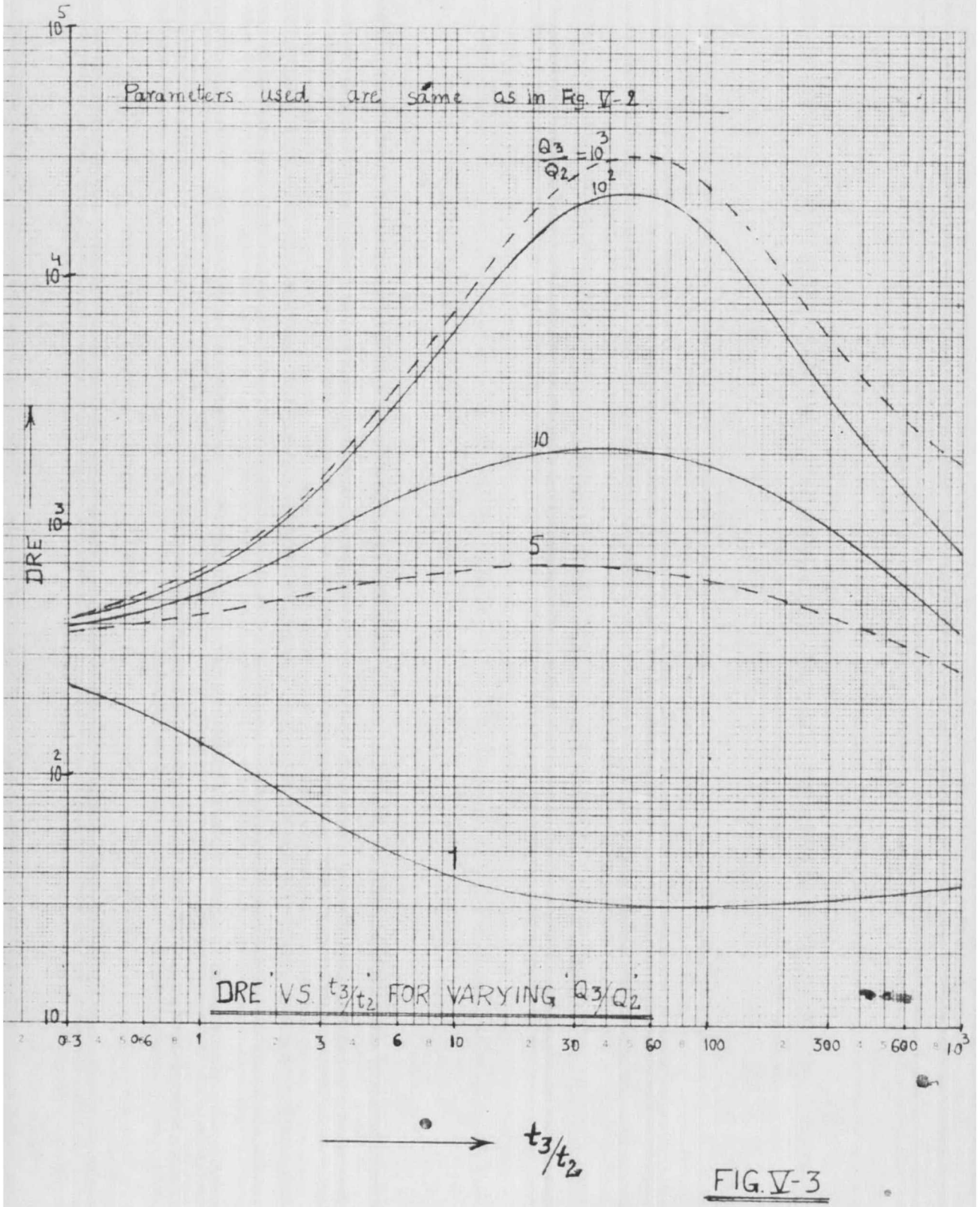

DRE VS t_3/t_2 FOR VARYING Q_3/Q_2

FIG. V-3

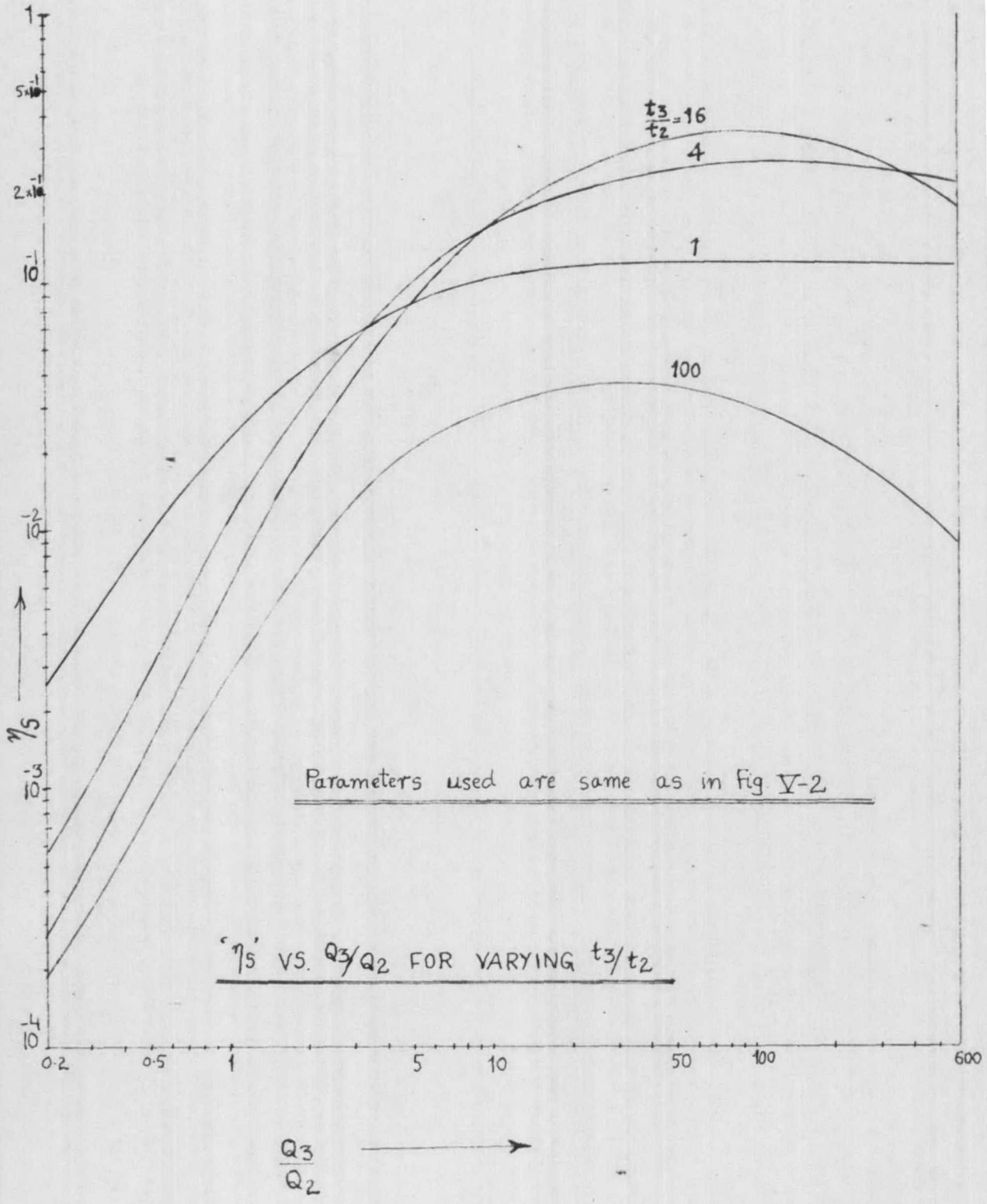

Parameters used are same as in Fig. V-2

'η_s' VS. Q_3/Q_2 FOR VARYING t_3/t_2

FIG. V-4

should be $\geq 10 \frac{G_2}{t_2}$. It may be seen that for the situation given in Fig. V-4, for optimum damping, the corresponding factor has the values given as under.

$\frac{t_3}{t_2}$		$\frac{G_3}{t_3} \Big/ \frac{G_2}{t_2}$
1	.....	20
4	.....	25
16	.....	6
100	.....	0.3

(ii): Figs. V-5 to V-8 are drawn for η_s and DRE against $\phi_{2.4}$, the shear parameter involving G_2, E_4, t_4 and $\frac{n\pi}{L}$. These are drawn for various values of $\frac{G_3}{G_2}$ when both layers 2 and 3 are the damping layers. It may be seen from Figs. V-5 and V-6 that the curves for higher ratios of $\frac{G_3}{G_2}$ are much flatter than those with low values of the ratio, e.g. in Fig. V-5, η_s is above the value of 0.1, for a considerably larger range of $\phi_{2.4}$, when $\frac{G_3}{G_2} = 1000$ than when $\frac{G_3}{G_2} = 10$. In practice, if the shear parameter $\phi_{2.4}$ changes due to a change of modal number 'n', i.e. for various modes of vibration or due to change of G_2 because of temperature or frequency change, a flatter curve which implies better frequency response, should be preferable. The ratio $\frac{G_3}{G_2}$ should remain high for all values of frequency and temperature encountered. The reasons for flatter curves at

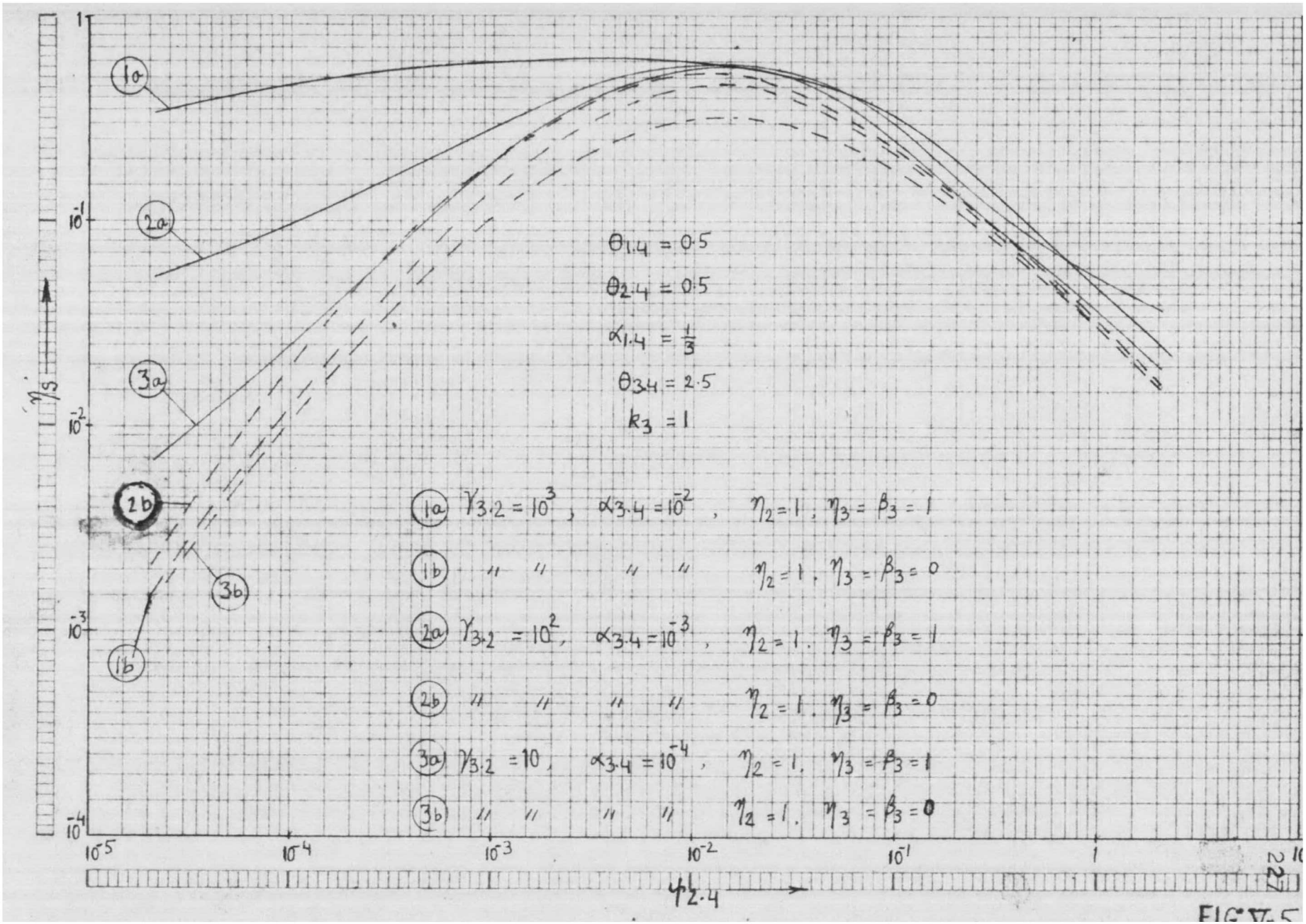
1a
2a
3a
2b
3b
1b
η_s
$\theta_{1.4} = 0.5$
$\theta_{2.4} = 0.5$
$\alpha_{1.4} = \frac{1}{3}$
$\theta_{3.4} = 2.5$
$k_3 = 1$
1a $\gamma_{3.2} = 10^3$, $\alpha_{3.4} = 10^{-2}$, $\eta_2 = 1$, $\eta_3 = \beta_3 = 1$
1b " " " " $\eta_2 = 1$, $\eta_3 = \beta_3 = 0$
2a $\gamma_{3.2} = 10^2$, $\alpha_{3.4} = 10^{-3}$, $\eta_2 = 1$, $\eta_3 = \beta_3 = 1$
2b " " " " $\eta_2 = 1$, $\eta_3 = \beta_3 = 0$
3a $\gamma_{3.2} = 10$, $\alpha_{3.4} = 10^{-4}$, $\eta_2 = 1$, $\eta_3 = \beta_3 = 1$
3b " " " " $\eta_2 = 1$, $\eta_3 = \beta_3 = 0$
1
10^{-1}
10^{-2}
10^{-3}
10^{-4}
10^{-5}
10^{-4}
10^{-3}
10^{-2}
10^{-1}
1
$\psi_{2.4}$

FIG V-5

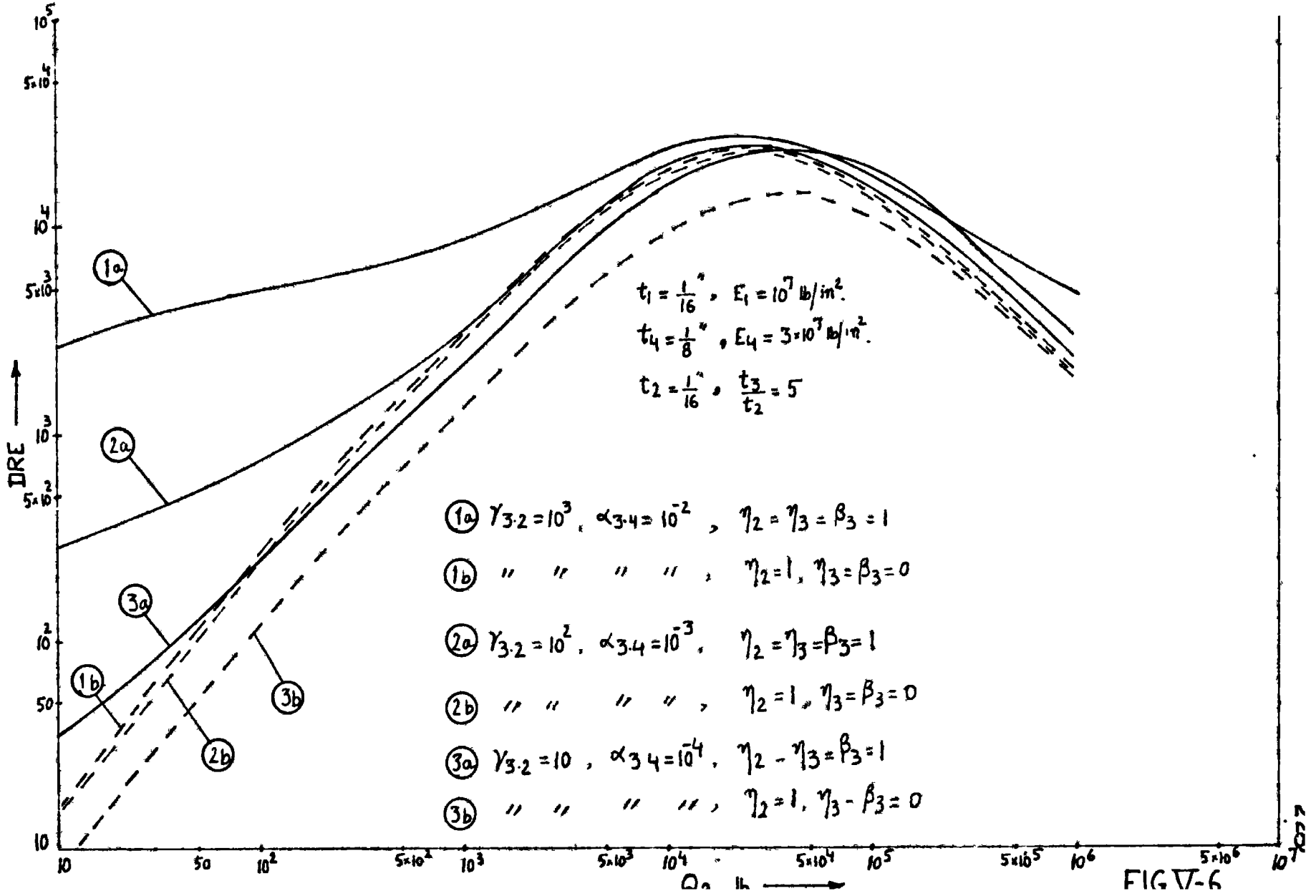
DRE
10^5
5×10^4
10^4
5×10^3
10^3
5×10^2
10^2
50
10
1a
2a
3a
1b
2b
3b
$t_1 = \frac{1}{16}$", $E_1 = 10^7$ lb/in^2.
$t_4 = \frac{1}{8}$", $E_4 = 3\times10^7$ lb/in^2.
$t_2 = \frac{1}{16}$", $\frac{t_3}{t_2} = 5$
1a $\gamma_{3\cdot2} = 10^3$, $\alpha_{3\cdot4} = 10^{-2}$, $\eta_2 = \eta_3 = \beta_3 = 1$
1b " " " ", $\eta_2 = 1$, $\eta_3 = \beta_3 = 0$
2a $\gamma_{3\cdot2} = 10^2$, $\alpha_{3\cdot4} = 10^{-3}$, $\eta_2 = \eta_3 = \beta_3 = 1$
2b " " " ", $\eta_2 = 1$, $\eta_3 = \beta_3 = 0$
3a $\gamma_{3\cdot2} = 10$, $\alpha_{3\cdot4} = 10^{-4}$, $\eta_2 = \eta_3 = \beta_3 = 1$
3b " " " ", $\eta_2 = 1$, $\eta_3 = \beta_3 = 0$
10
50
10^2
5×10^2
10^3
5×10^3
10^4
5×10^4
10^5
5×10^5
10^6
5×10^6
10^7
Ω_n in ⟶

FIG V-6

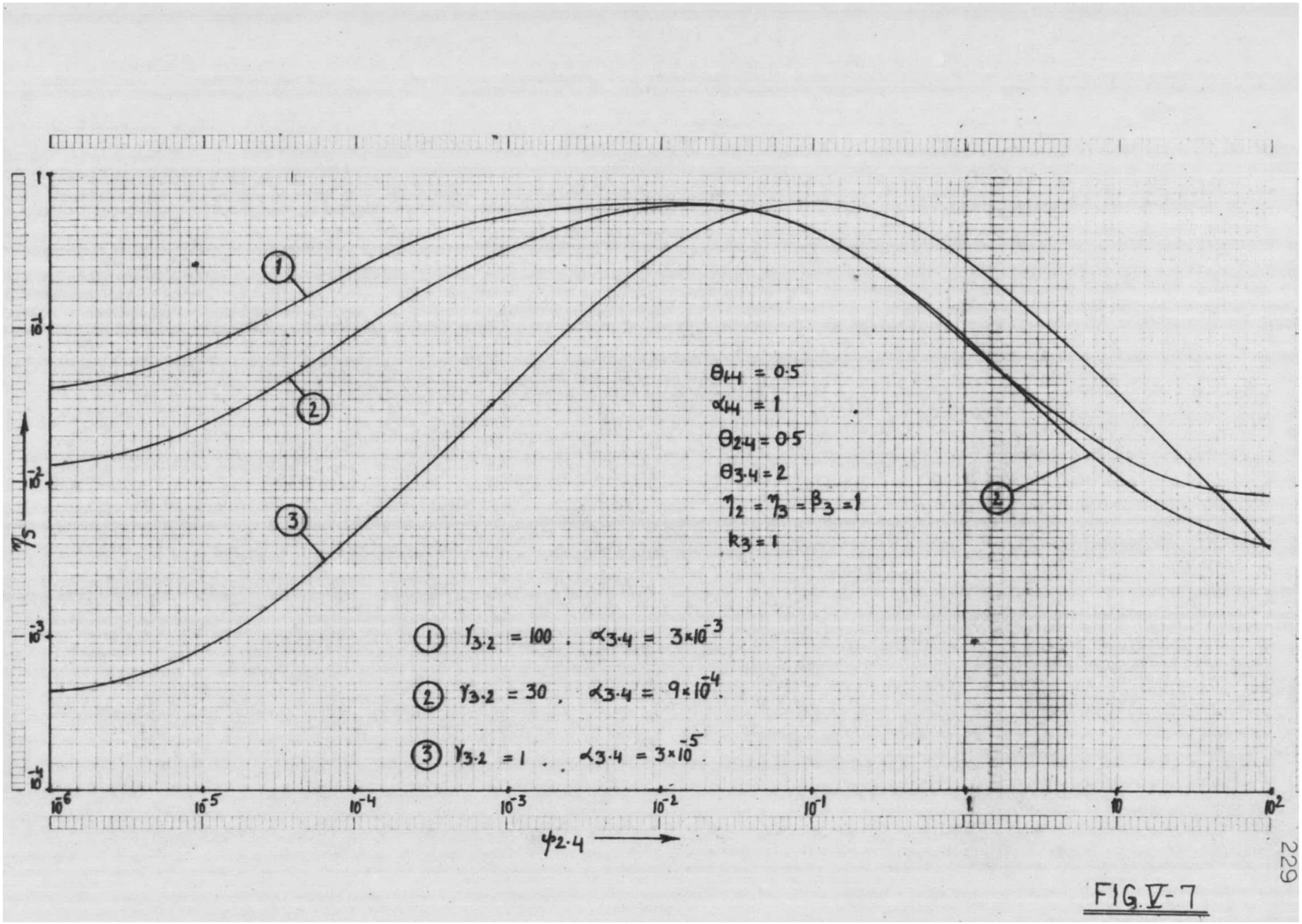
1
10^{-1}
10^{-2}
10^{-3}
10^{-4}
$\eta_{3.4}$
$\theta_{4.4} = 0.5$
$\alpha_{4.4} = 1$
$\theta_{2.4} = 0.5$
$\theta_{3.4} = 2$
$\eta_2 = \eta_3 = \beta_3 = 1$
$k_3 = 1$
① $\gamma_{3.2} = 100$. $\alpha_{3.4} = 3\times10^{-3}$
② $\gamma_{3.2} = 30$. $\alpha_{3.4} = 9\times10^{-4}$.
③ $\gamma_{3.2} = 1$. $\alpha_{3.4} = 3\times10^{-5}$.
10^{-6}
10^{-5}
10^{-4}
10^{-3}
10^{-2}
10^{-1}
1
10
10^{2}
$\psi_{2.4}$

FIG. V-7

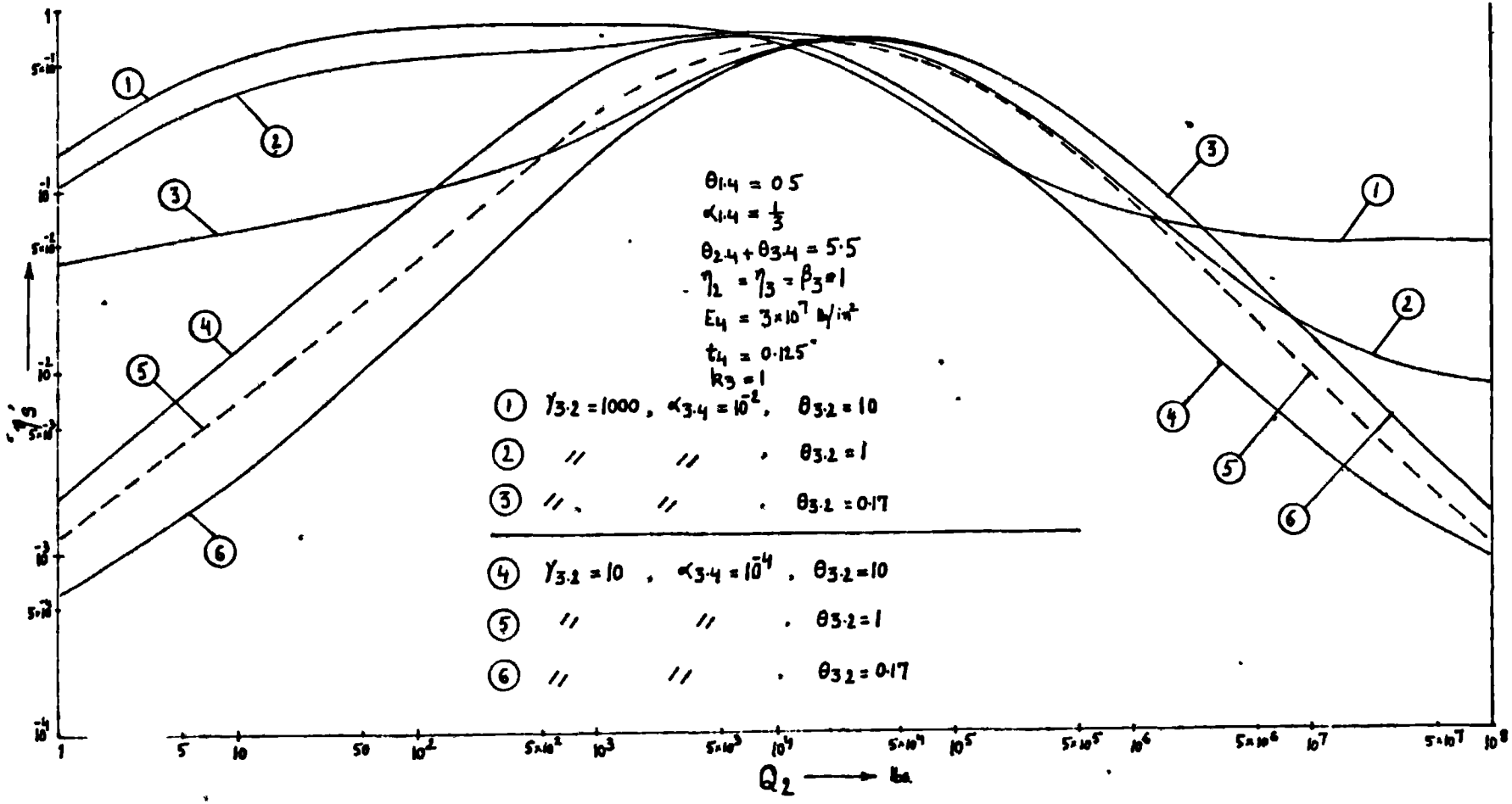
θ1.4 = 0.5
α1.4 = 1/3
θ2.4 + θ3.4 = 5.5
η2 = η3 = β3 = 1
E4 = 3×10^7 lb/in^2
t4 = 0.125"
k3 = 1
① γ3.2 = 1000, α3.4 = 10^-2, θ3.2 = 10
② // // , θ3.2 = 1
③ // // , θ3.2 = 0.17
④ γ3.2 = 10, α3.4 = 10^-4, θ3.2 = 10
⑤ // // , θ3.2 = 1
⑥ // // , θ3.2 = 0.17
Q2 ⟶ lbs.

FIG. V-8

higher ratios of G_3/G_2 are:

a) At higher values of the shear parameter, the damping in the system is due to shear in layer 2, the effect is enhanced by the rigid layer 3.

b) Because of increased stiffness and thickness of layer 3, extensional damping contributes significantly to the total damping of the system. This is especially true at lower values of the shear parameter. In Figs. V-5 and V-6, the dotted graphs are drawn by taking into account the damping due to layer 2 only. For higher ratios of $\frac{Q_3}{Q_2}$, the contribution of damping due to layer 3 is evident, resulting in flatter damping graphs.

Fig.V-7 illustrates the same points as in Figs. V-5 and V-6, but for different values of system parameters. In Fig. V-8, various graphs are shown for same total thickness of viscoelastic layers (i.e. t_2+t_3) but the ratio $\frac{t_3}{t_2}$ is varied. For the same total thickness, a higher ratio $\frac{t_3}{t_2}$ is seen to be preferable, from point of view of increased damping at most values of $\psi_{2.4}$, when a higher value of $\gamma_{3.2}$ (i.e. G_3/G_2) is used. In case of low values of $\gamma_{3.2}$, the effect of using different ratios $\frac{t_3}{t_2}$, keeping the total thickness same, is merely to shift the position of peak in the damping graph.

(iii): In Fig. V-9, a comparison is done between a 3 layered and a 4 layered arrangement, layer 2 is same in both cases

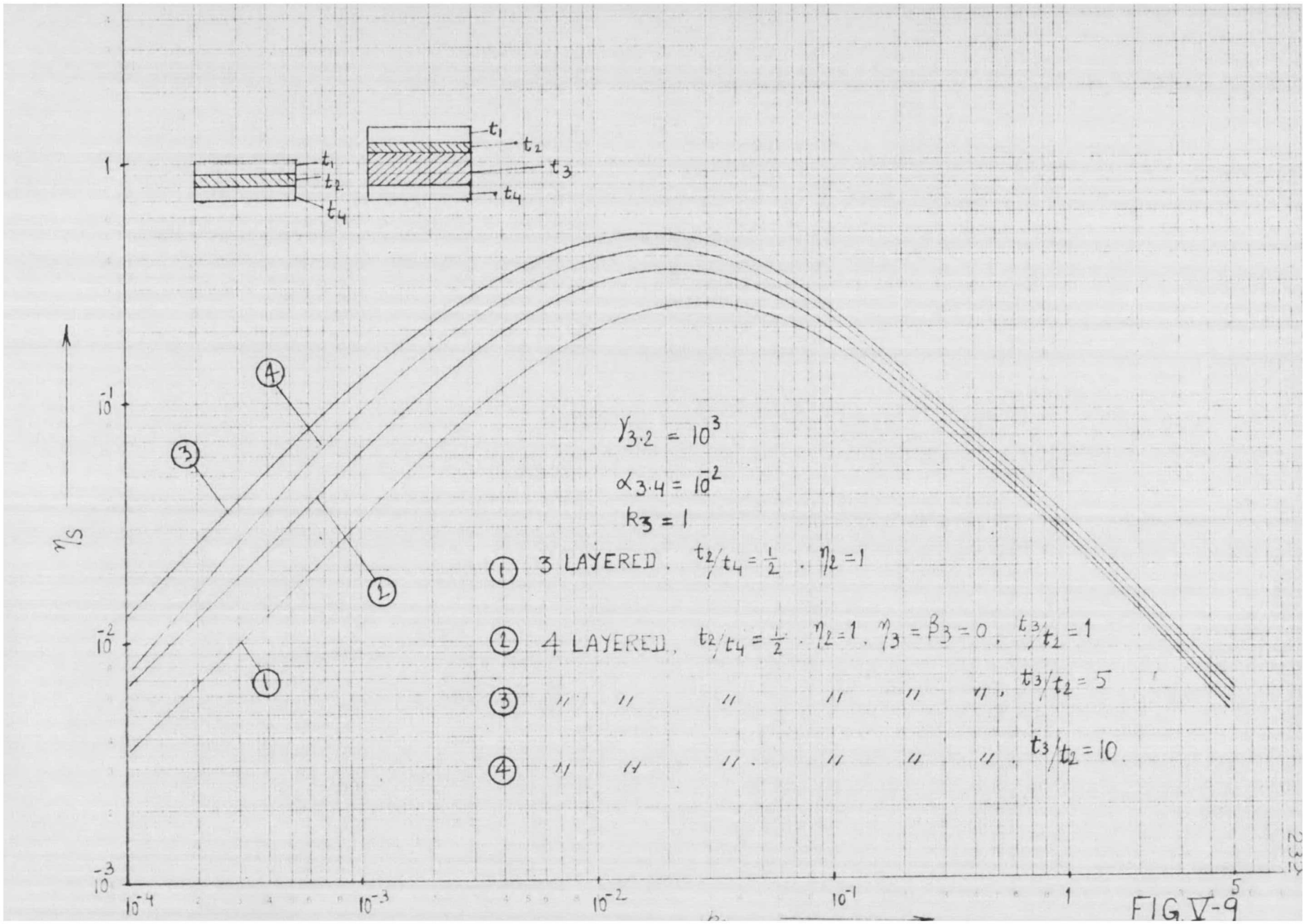
t_1
t_2
t_4
t_1
t_2
t_3
t_4
η_s
1
10^{-1}
10^{-2}
10^{-3}
10^{-4}
10^{-3}
10^{-2}
10^{-1}
1
5
$\gamma_{3\cdot2} = 10^3$
$\alpha_{3\cdot4} = 10^{-2}$
$k_3 = 1$
① 3 LAYERED. $t_2/t_4 = \frac{1}{2}$. $\eta_2 = 1$
② 4 LAYERED. $t_2/t_4 = \frac{1}{2}$. $\eta_2 = 1$. $\eta_3 = \beta_3 = 0$. $t_3/t_2 = 1$
③ // // // // // // . $t_3/t_2 = 5$
④ // // // . // // // . $t_3/t_2 = 10$.

FIG. V-9

and damping in layer 3 is assumed to be negligible. Layer 3 is more rigid than layer 2 in shear. This may be regarded as a comparison of the two configurations with and without a spacer. The maximum damping is increased by the addition of layer 3, even though its material loss factor is zero. Also, the frequency response is better in the 4 layered case (i.e. there is higher damping for a larger range of $\phi_{2.4}$, which involves 'n', the modal number). However, as shown in Fig.V-9, for optimum damping the ratio $\frac{t_3}{t_2}$ has to be chosen suitably, depending on the remaining system parameters.

(iv): In Fig. V-10, a comparison between the performance of 2, 3 and 4 layered configurations is done. The configurations chosen are such that the total thickness of viscoelastic materials used is same, as shown on the Fig. It may be seen that, for the situation considered, a rigid layer '3' gives high damping in 2 and 4 layered cases. For the 2 layered case, η_s has been calculated from [60], the damping in the system being due to extensional effect. For most values of G_3 (except very high values), 4 layered case is superior to the 2 layered one. From practical viewpoint, the 4 layered configuation is preferable to the 2 layered one since in the former, the viscoelastic layers are concealed and not exposed to outside environments.

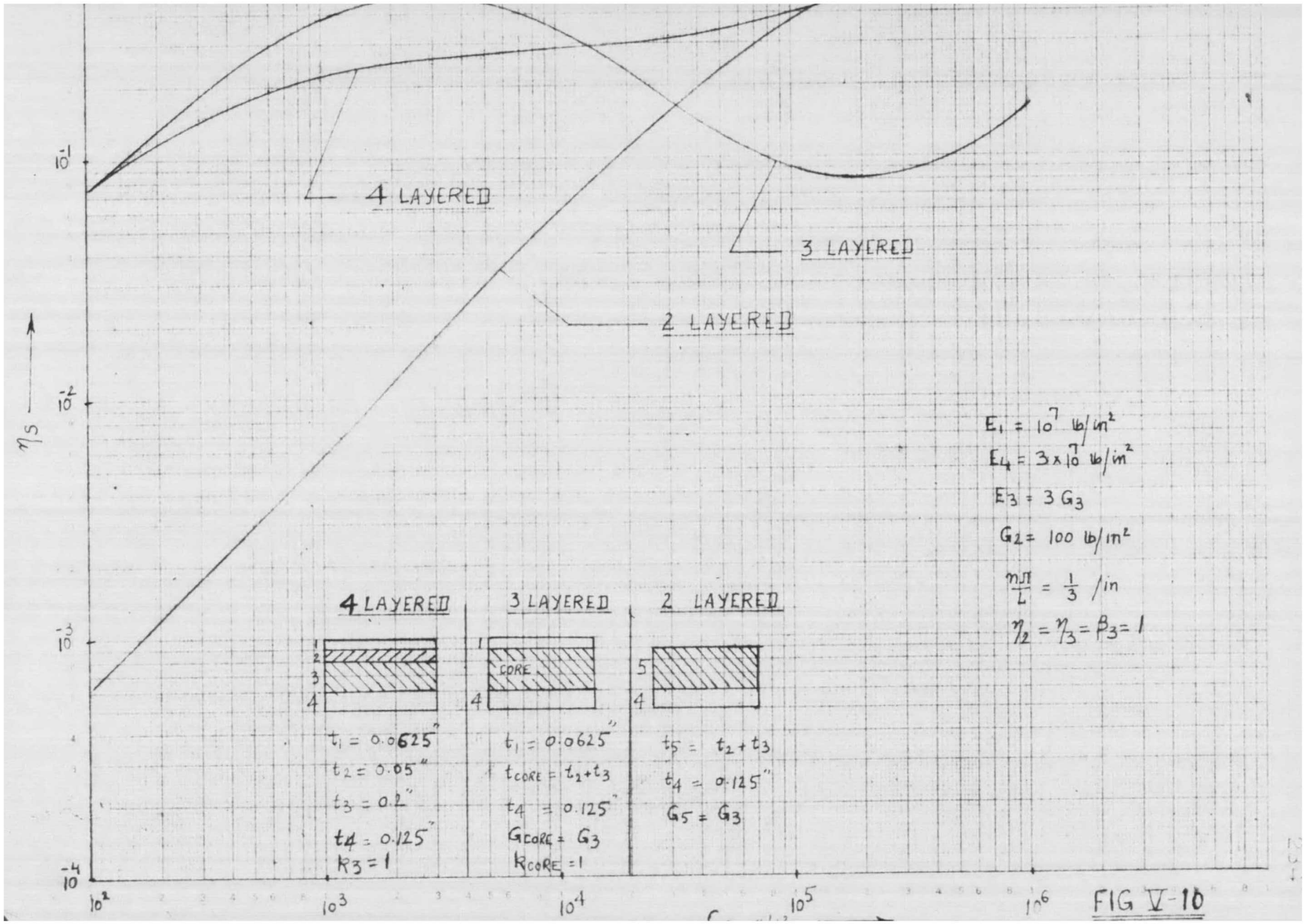
4 LAYERED
3 LAYERED
2 LAYERED
η_s
10^{-1}
10^{-2}
10^{-3}
10^{-4}
10^2
10^3
10^4
10^5
10^6
$E_1 = 10^7$ lb/in^2
$E_4 = 3 \times 10^7$ lb/in^2
$E_3 = 3 G_3$
$G_2 = 100$ lb/in^2
$\frac{n\pi}{L} = \frac{1}{3}$ /in
$\eta_2 = \eta_3 = \beta_3 = 1$
4 LAYERED
3 LAYERED
2 LAYERED
CORE
$t_1 = 0.0625"$
$t_2 = 0.05"$
$t_3 = 0.2"$
$t_4 = 0.125"$
$K_3 = 1$
$t_1 = 0.0625"$
$t_{CORE} = t_2 + t_3$
$t_4 = 0.125"$
$G_{CORE} = G_3$
$K_{CORE} = 1$
$t_5 = t_2 + t_3$
$t_4 = 0.125"$
$G_5 = G_3$

FIG V-10

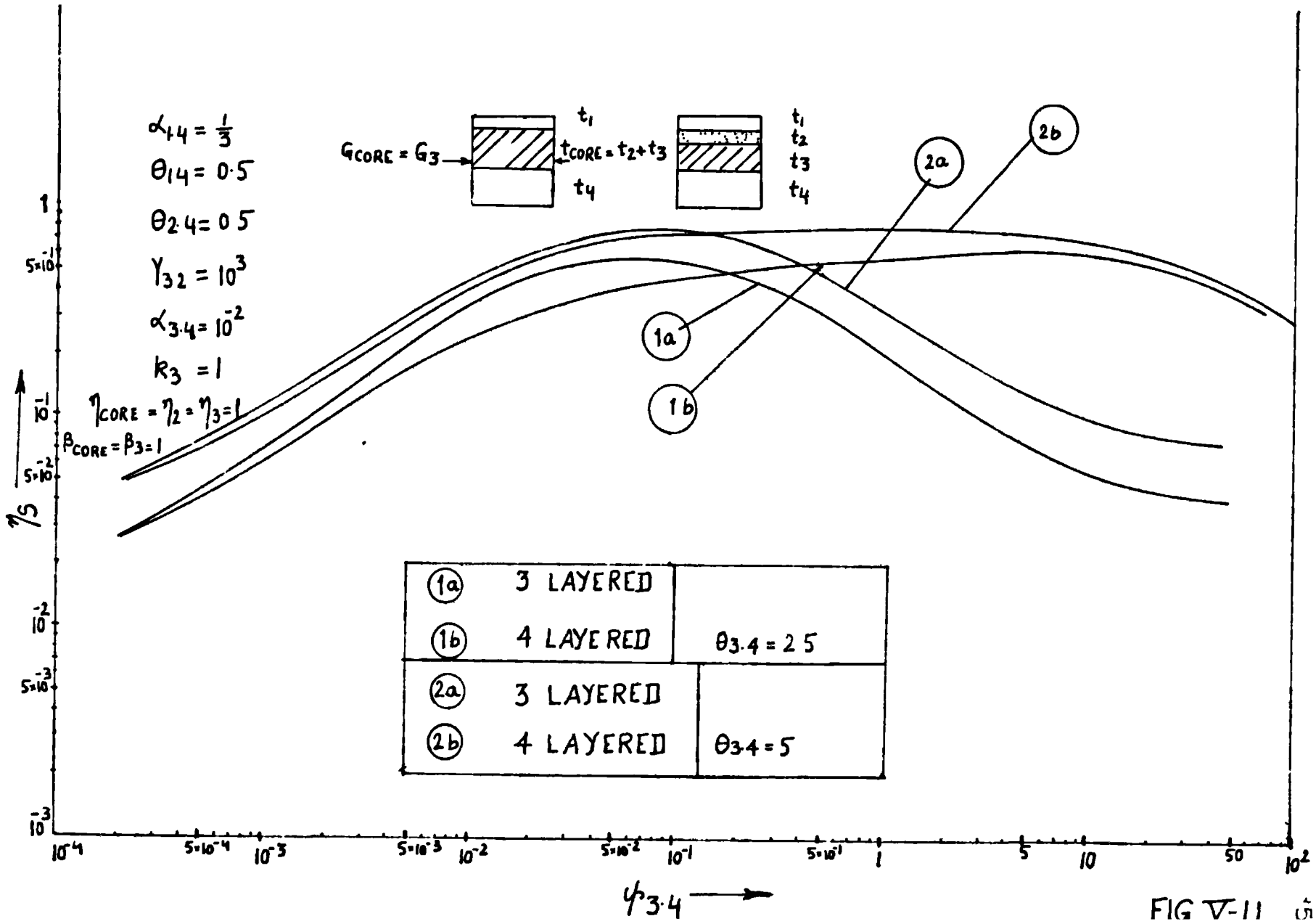
$\alpha_{1,4} = \frac{1}{3}$
$\theta_{1,4} = 0.5$
$\theta_{2,4} = 0.5$
$\gamma_{3,2} = 10^{3}$
$\alpha_{3,4} = 10^{-2}$
$k_3 = 1$
$\eta_{CORE} = \eta_2 = \eta_3 = 1$
$\beta_{CORE} = \beta_3 = 1$
$G_{CORE} = G_3$
$t_{CORE} = t_2 + t_3$
t_1
t_2
t_3
t_4
1a
1b
2a
2b
η_S
$\psi_{3,4}$
1 5×10^{-1} 10^{-1} 5×10^{-2} 10^{-2} 5×10^{-3} 10^{-3}
10^{-4} 5×10^{-4} 10^{-3} 5×10^{-3} 10^{-2} 5×10^{-2} 10^{-1} 5×10^{-1} 1 5 10 50 10^{2}
1a 3 LAYERED
1b 4 LAYERED
$\theta_{3,4} = 2.5$
2a 3 LAYERED
2b 4 LAYERED
$\theta_{3,4} = 5$

FIG V-11

(v): In Fig.V-11, the performance of 3 and 4 layered configurations is compared, the outer metal layers being same and the total thickness of viscoelastic materials used being equal in the two configurations. Results for 'η_s' are plotted against dimensionless shear parameter $\Phi_{3.4}$, which involves 'n', the modal number, in addition to other parameters and thus the graph gives the behaviour at various modes of vibration. The 4 layered configuration gives a flatter curve than that obtained for the 3 layered one.

V.B.1 5 Layered Multicored Configuration

Equations of Motion: The configuration is shown in Fig. V-1(b). The outer layers or faces are of metal while the inner layers are made of viscoelastic materials. A symmetrical case will be analysed in this section.

The assumptions made for derivation are almost similar to those of Section V.A.1, except that, here all the viscoelastic layers take up only shear, being much less rigid than the metal layers. As before, assumptions 3, 4, 5, 7 and 8 of IV.A.1 hold. The outer metal layers are assumed to bend like Bernoulli-Euler beams.

The longitudinal displacements vary with slopes of $\bar{\alpha}$, $\bar{\beta}$ and ξ through the thickness of layers 2, 3 and 1 respectively.

$\xi = w'$, according to our assumption of no shear in the

outer layers, w being the transverse displacement.

Shear strain in layer 2 = $\bar{\alpha}$ -w', while that in layer 3 - $\bar{\beta}$ -w'.

The longitudinal displacement of middle fibre of layer 1 is $= \frac{\bar{\beta} t_3}{2} + \bar{\alpha} t_2 + \xi \frac{t_1}{2}$.

Total strain energy 'U' =

$$q_3 \int_o^L (\bar{\beta}-w')^2 dx + q_2 \int_o^L (\bar{\alpha}-w')^2 dx + r_1 \left[\int_o^L \left\{\bar{\beta}' \frac{t_3}{2} + \bar{\alpha}' t_2 + w'' \frac{t_1}{2}\right)^2 + w''^2 \frac{t_1^2}{12} \right\} dx\right] \quad (V.12)$$

where
$$q_3 = \frac{bt_3G_3}{2}$$

$$q_2 = bt_2G_2 \quad (V.13)$$

$$r_1 = bt_1E_1$$

$$\text{Kinetic Energy 'T'} = \tfrac{1}{2} \rho \int_o^L (\dot{w})^2 \, dx \quad (V.14)$$

ρ being the mass density of the sandwich per unit length.

Potential Energy 'V' due to loading of intensity f(x)g(t)

$$= g(t) \int_o^L f(x) w \, dx \quad (V.15)$$

Application of Hamilton s principle gives the following equations of motion and boundary conditions. Details are given in Appendix 7.

$$2q_3(\bar{\beta}-w') - t_3 r_1 \left(\bar{\beta}'' \frac{t_3}{2} + \bar{\alpha}'' t_2 + w''' \frac{t_1}{2}\right) = 0 \quad (V.16)$$

$$2q_2(\bar{\alpha}-w')-2t_2r_1(\bar{\beta}''\frac{t_3}{2}+\bar{\alpha}''t_2+w'''\frac{t_1}{2}) = 0 \qquad (V.17)$$

$$2q_3(\bar{\beta}'-w'')+2q_2(\bar{\alpha}'-w'')+r_1t_1(\bar{\beta}'''\frac{t_3}{2}+\bar{\alpha}'''t_2+w''''\frac{t_1}{2})$$
$$+\frac{r_1t_1^2}{6}w'''' - - \rho\ddot{w}^{\circ}+g(t)f(x) \qquad (V.18)$$

Boundary conditions for both ends simply supported are:

At $x - 0, L,$

$$\left.\begin{aligned} w &= w'' = 0 \\ \bar{\alpha} &= \bar{\beta}' = 0 \end{aligned}\right| \qquad (V.19$$

V.B.2: Solution

As before, the solution will be assumed in the form of series as below, for sinusoidal excitation.

$$\left.\begin{aligned} w &- \sum_{n}^{\infty}{}_1 w_n \sin\frac{n\pi x}{L} \sin pt \\ \bar{\alpha}_n &\quad \sum_{n}^{\infty}{}_1 \bar{\alpha}_n \cos\frac{n\pi x}{L} \sin pt \\ \bar{\beta}_n &- \sum_{n=1}^{\infty} \bar{\beta}_n \cos\frac{n\pi x}{L} \sin pt \end{aligned}\right| \qquad (V.20)$$

Also expanding $f(x) \sin pt \quad \sum_{n=1}^{\infty} f_n \sin\frac{n\pi x}{L} \sin pt.$

With the above solution, the boundary conditions for simply supported ends are satisfied and equations (V.16) to (V.18) are reduced to algebraic equations:

$$\left.\begin{aligned} \bar{\alpha}_n A + \bar{\beta}_n B + w_n C &= 0 \\ \bar{\alpha}_n D + \bar{\beta}_n A + w_n F &= 0 \\ \bar{\alpha}_n F + \bar{\beta}_n C + w_n [H - \rho p^2] &= f_n \end{aligned}\right| \qquad \text{(V.21)}$$

where

$$A = \left(\frac{n\pi}{L}\right)^2 E_1 t_1^3 \{\theta_{3.1}\theta_{2.1}\}$$

$$B = \left(\frac{n\pi}{L}\right)^2 E_1 t_1^3 \{\phi_{3.1}\theta_{3.1} + \tfrac{1}{2}\theta^2_{3.1}\}$$

$$C = \left(\frac{n\pi}{L}\right)^3 E_1 t_1^3 \{-\phi_{3.1}\theta_{3.1} + \tfrac{1}{2}\theta_{3.1}\}$$

$$D = \left(\frac{n\pi}{L}\right)^2 E_1 t_1^3 \{2\phi_{2.1}\theta_{2.1}\ 2\theta^2_{2.1}\}$$

$$F = \left(\frac{n\pi}{L}\right)^3 E_1 t_1^3 \{-2\phi_{2.1}\theta_{2.1} + \theta_{2.1}\}$$

$$H = \left(\frac{n\pi}{L}\right)^4 E_1 t_1^3 \{\phi_{3.1}\theta_{3.1} + 2\phi_{2.1}\theta_{2.1} + \tfrac{2}{3}\}$$

$$\theta_{j.1} = \frac{t_j}{t_1}\ ;\ j=2,3 \quad \text{and} \quad \phi_{j.1} = \frac{G_j}{E_1 t_1^2 \left(\frac{n\pi}{L}\right)^2}\ ;\ j=2,3$$

In order to get theequations for the viscoelastic case, the elastic moduli G_2 and G_3 have to be replaced by complex ones, viz. $G_2(1+i\eta_2)$ and $G_3(1+i\eta_3)$ respectively. The solution is obtained by solving simultaneously eqns. (V.21), with the various coefficients A, B etc. being complex.

After elimination and simplification, it is possible to get a single equation in 'w_n' as follows.

$$b\left(\frac{n\pi}{L}\right)^4 E_1 t_1^3 [Z_{rn} + iZ_{in}] - \rho p^2 w_n = f_n \qquad (V.22)$$

ρ being $= bt_1(2\rho_1+2\rho_2\theta_{2.1}+\rho_3\theta_{3.1})$

ρ_1, ρ_2 and ρ_3 are the mass densities per unit volume, of layers 1, 2 and 3 respectively.

Expressions for Z_{rn} and Z_{in} are not given here but may be obtained by the algebraic procedure of elimination and simplification from eqn. (V.21).

Eqn. (V.22) may be written in the form

$$w_n[Z'_{rn}+iZ'_{in}-\rho p^2] = f_n \qquad (V.23)$$

where $Z'_{rn} = b\left(\frac{n\pi}{L}\right)^4 E_1 t_1^3 (Z_{rn})$

$Z'_{in} = b\left(\frac{n\pi}{L}\right)^4 E_1 t_1^3 (Z_{in})$

As in Section V.A.2,

$$'\eta_s' \text{ for nth mode} = \frac{Z'_{in}}{Z'_{rn}} \qquad (V.24)$$

$$k\eta_s = \frac{Z'_{in}}{b\left(\frac{n\pi}{L}\right)^4 \frac{E_s t_s^3}{12}}$$

$$= \frac{E_1 t_1^3 (Z_{in})}{\frac{E_s t_s^3}{12}} \qquad (V.25)$$

E_s and t_s are the parameters of a solid beam which might be chosen for comparison with the dynamic rigidity of the sandwich. In the next section, only the numerator in eqn. (V.25) is designated as DRE (Displacement response effectiveness) and evaluated.

Again, because of similarity of eqns. (V.23) and (IV.11), the displacement response of the beam, due to ends of the beam being excited by similar harmonic displacement, may be determined using eqns. (IV.12) and (IV.13).

V.B.3 : Effect of various system parameters on damping effectiveness and comparisons with other arrangements

(i) Figs. V-12 and V-13 may be regarded as graphs of the system damping for various modes of the system. As for a 3 layered configuration, involving a single core, the system damping is optimum at one value of modal number 'n'

The use of various values of Q_3/Q_2 appears to cause only a shift in the position of the peak, with the maximum damping remaining unchanged.

In Fig.V-13, graphs are plotted both for single cored and multicored configurations, the total thickness of the viscoelastic materials used, remaining the same. The curves are seen to be similar in each case, except that the optimum value of η_s occurs at different values of 'n'. In practice, if it is desired to have the optimum damping conditions for a specified value of 'n', it is possible to attain these conditions by suitably choosing the core shear modulus in a 3 layered case, as given in Section III.A. However, it may not be possible to get a material having exactly the desired value of shear modulus, at the frequency of the mode under consideration. In this case, as seen

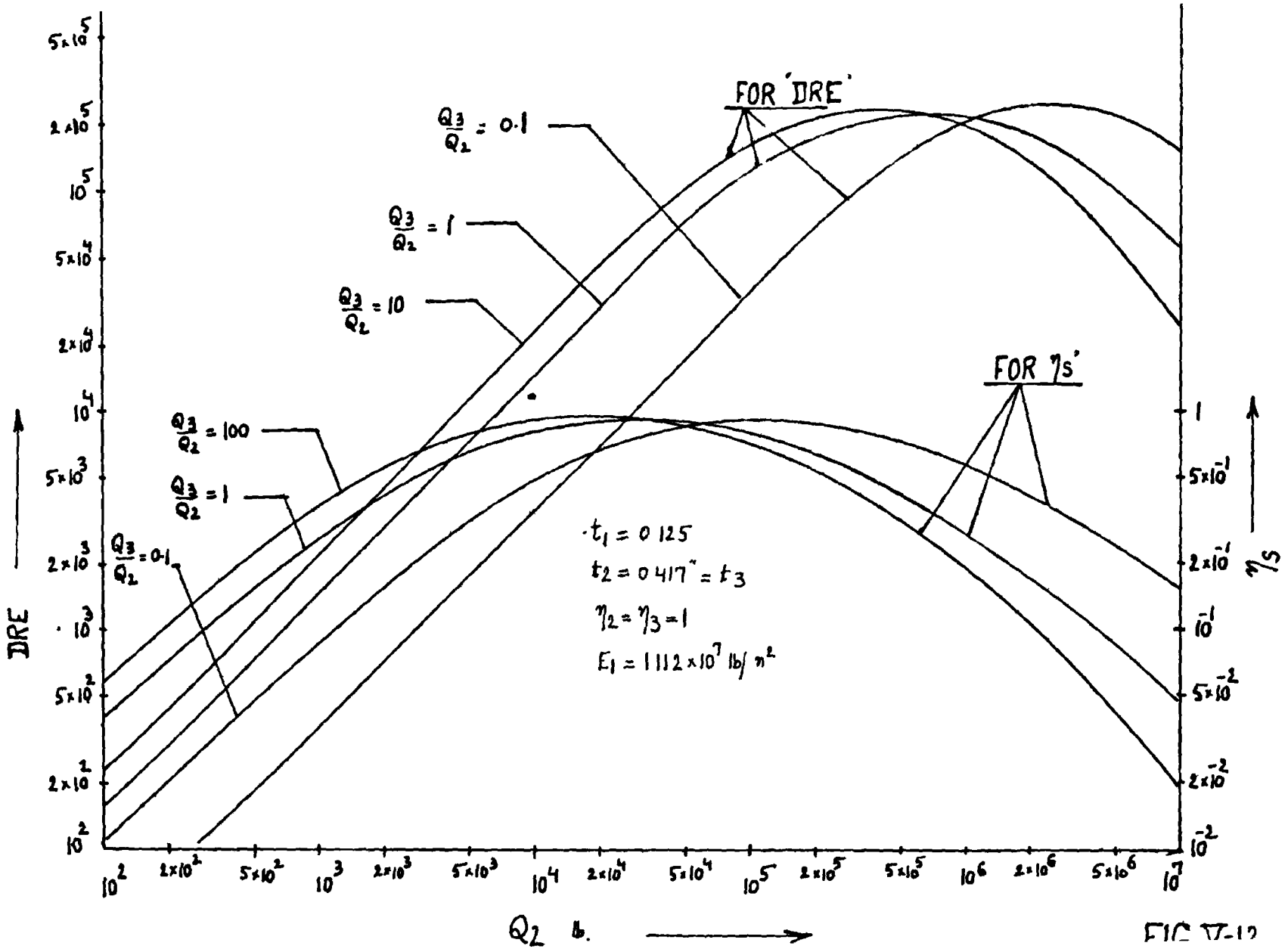
FOR 'DRE'
FOR 'ηs'
$\frac{Q_3}{Q_2} = 0.1$
$\frac{Q_3}{Q_2} = 1$
$\frac{Q_3}{Q_2} = 10$
$\frac{Q_3}{Q_2} = 100$
$\frac{Q_3}{Q_2} = 1$
$\frac{Q_3}{Q_2} = 0.1$
$t_1 = 0.125$
$t_2 = 0.417 = t_3$
$\eta_2 = \eta_3 = 1$
$E_1 = 1.112 \times 10^7$ lb/in²
DRE
ηs
Q_2 lb.
5×10^5 2×10^5 10^5 5×10^4 2×10^4 10^4 5×10^3 2×10^3 10^3 5×10^2 2×10^2 10^2
1 5×10^{-1} 2×10^{-1} 10^{-1} 5×10^{-2} 2×10^{-2} 10^{-2}
10^2 2×10^2 5×10^2 10^3 2×10^3 5×10^3 10^4 2×10^4 5×10^4 10^5 2×10^5 5×10^5 10^6 2×10^6 5×10^6 10^7

FIG IV-12

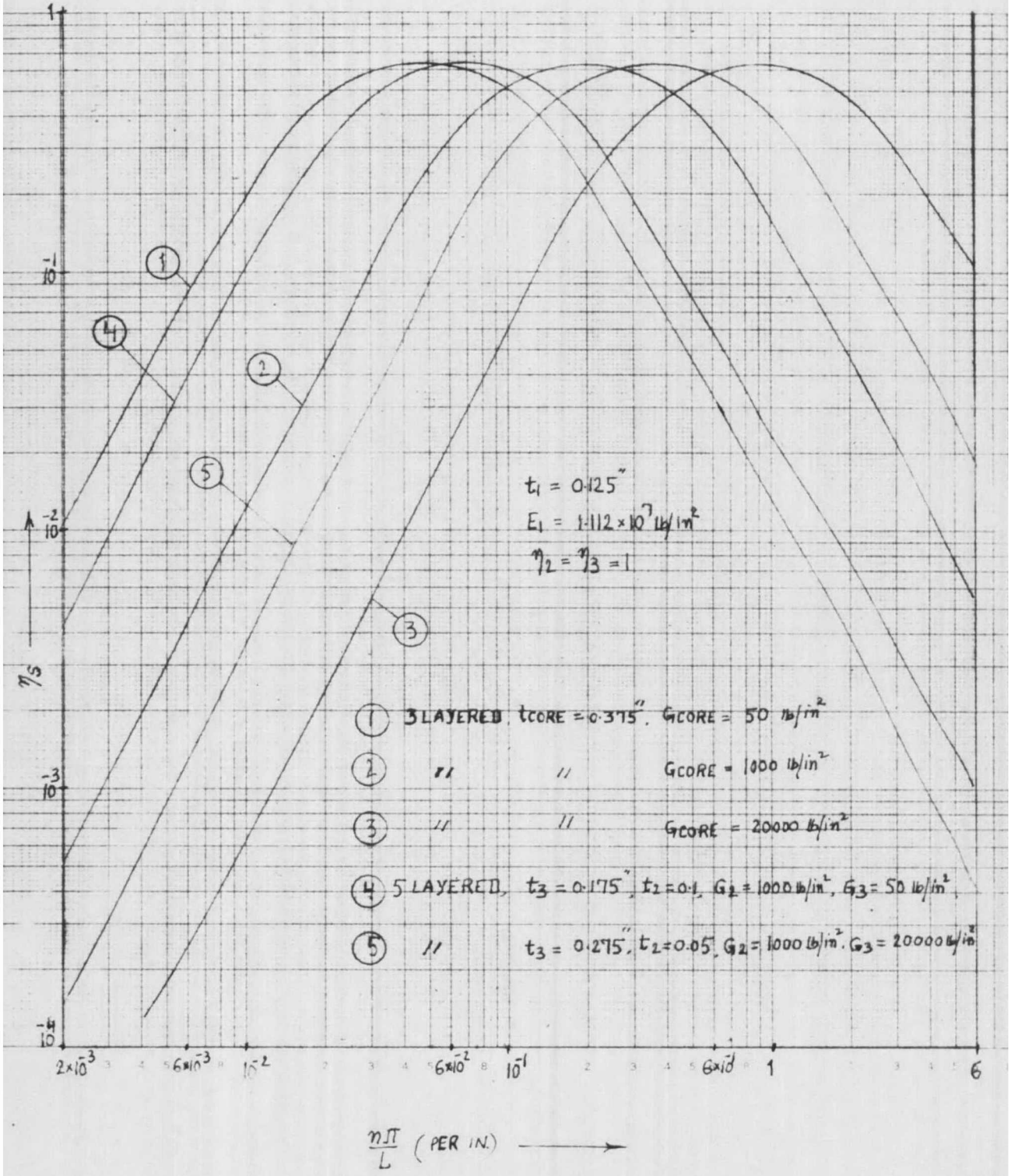
1
10^{-1}
10^{-2}
10^{-3}
10^{-4}
η_s
$t_1 = 0.125''$
$E_1 = 1.112 \times 10^7$ lb/in^2
$\eta_2 = \eta_3 = 1$
① 3 LAYERED, $t_{CORE} = 0.375''$, $G_{CORE} = 50$ lb/in^2
② // // $G_{CORE} = 1000$ lb/in^2
③ // // $G_{CORE} = 20000$ lb/in^2
④ 5 LAYERED, $t_3 = 0.175''$, $t_2 = 0.1$, $G_2 = 1000$ lb/in^2, $G_3 = 50$ lb/in^2
⑤ // $t_3 = 0.275''$, $t_2 = 0.05$, $G_2 = 1000$ lb/in^2, $G_3 = 20000$ lb/in^2
2×10^{-3}
6×10^{-3}
10^{-2}
6×10^{-2}
10^{-1}
6×10^{-1}
1
6
$\frac{n\pi}{L}$ (PER IN.) ⟶

FIG. V-13

from Fig.V-13, the use of a multicored sandwich, employing viscoelastic materials with different shear moduli and the same total thickness of core as in the 3 layered case, would assist in attaining optimum damping conditions. The thickness ratio of the two viscoelastic materials used would have to be suitably chosen.

(ii) Fig. V-14 shows a comparison of a 3 layered case with a multicored 5 layered one, the former configuration may be obtained from the latter by eliminating the central core '3'. For varying values of t_3/t_2, η_3 is chosen equal to 1 and 0. Since, the graph is drawn against Q_2, it may be regarded as representing the behaviour of the sandwich beam at various modes i.e. the frequency response. In Fig.V-14, which is drawn for $\frac{Q_3}{Q_2} = 100$, the multicored configurations, (both when $\eta_3 = 1$ and 0) show improved frequency response, when compared to the 3 layered case. It may be seen that layer 3 need not have a high material loss factor for the chosen parameters, i.e. when $\frac{Q_3}{Q_2} = 100$. For $\frac{Q_3}{Q_2} - 1$ in Fig. V-15, the introduction of an undamped core 3 in the 3 layered case, makes the frequency response worse.

Fig. V-16 is drawn for $\frac{Q_3}{Q_2} = 20$ for 2 multicored cases with different '$\frac{t_3}{t_2}$', having the same total thickness. The 3 layered case used for comparison has its core thickness - $2t_2$ as in Figs. V-14 and V-15. As before, the multicored

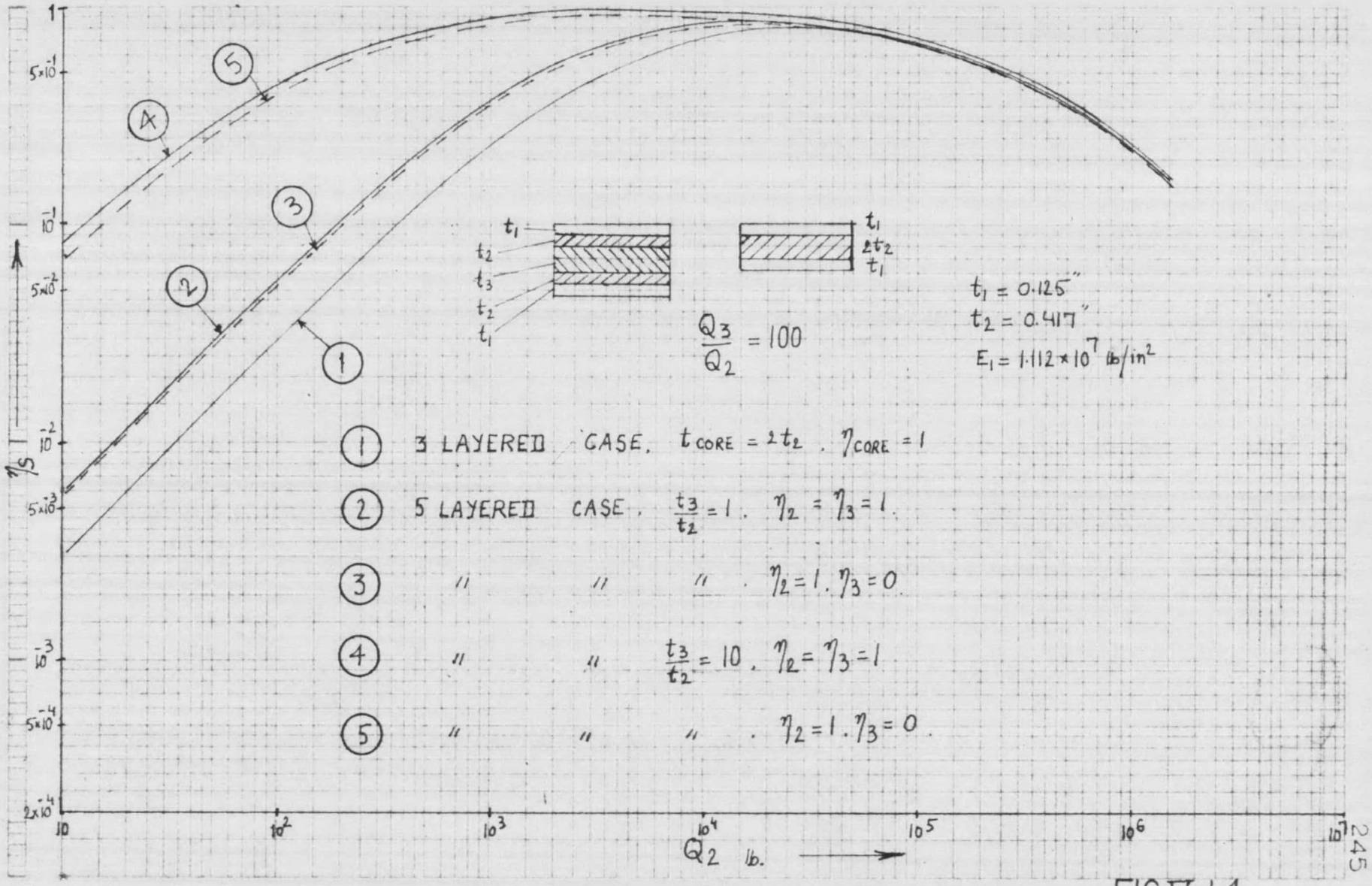
1
5×10⁻¹
10⁻¹
5×10⁻²
10⁻²
5×10⁻³
10⁻³
5×10⁻⁴
2×10⁻⁴
η/s
10
10²
10³
10⁴
10⁵
10⁶
10⁷
Q2 lb.
A
1
2
3
5
t1
t2
t3
t2
t1
t1
2t2
t1
Q3/Q2 = 100
t1 = 0.125"
t2 = 0.417"
E1 = 1.112×10⁷ lb/in²
(1) 3 LAYERED CASE. t CORE = 2t2 . η CORE = 1
(2) 5 LAYERED CASE. t3/t2 = 1 . η2 = η3 = 1.
(3) // // // . η2 = 1 . η3 = 0
(4) // // t3/t2 = 10 . η2 = η3 = 1
(5) // // // . η2 = 1 . η3 = 0

FIG. V-14

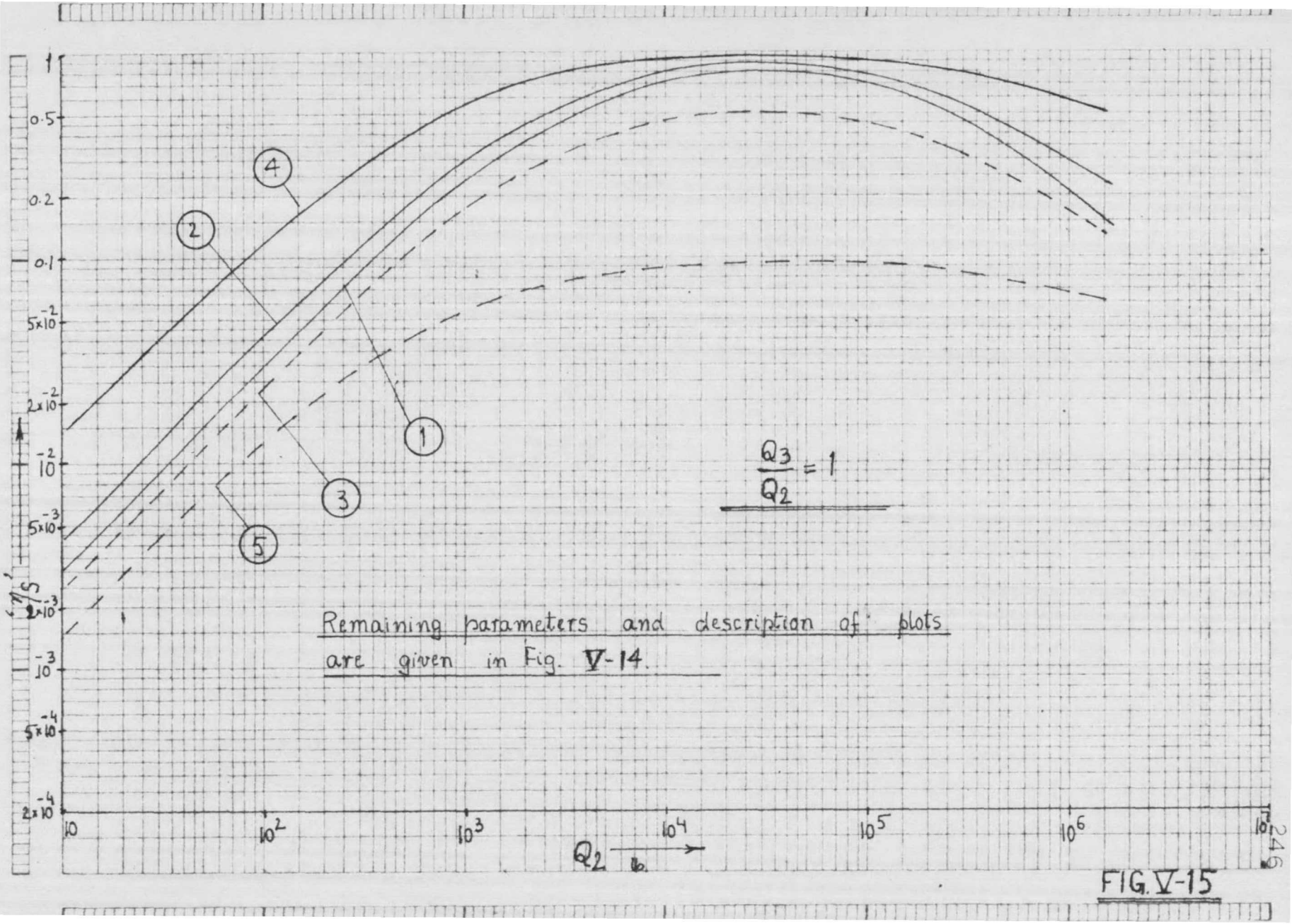
1
0.5
0.2
0.1
5×10⁻²
2×10⁻²
10⁻²
5×10⁻³
2×10⁻³
10⁻³
5×10⁻⁴
2×10⁻⁴
η/S
10
10²
10³
10⁴
10⁵
10⁶
Q2
4
2
1
3
5
Q3/Q2 = 1
Remaining parameters and description of plots are given in Fig. V-14.

FIG. V-15

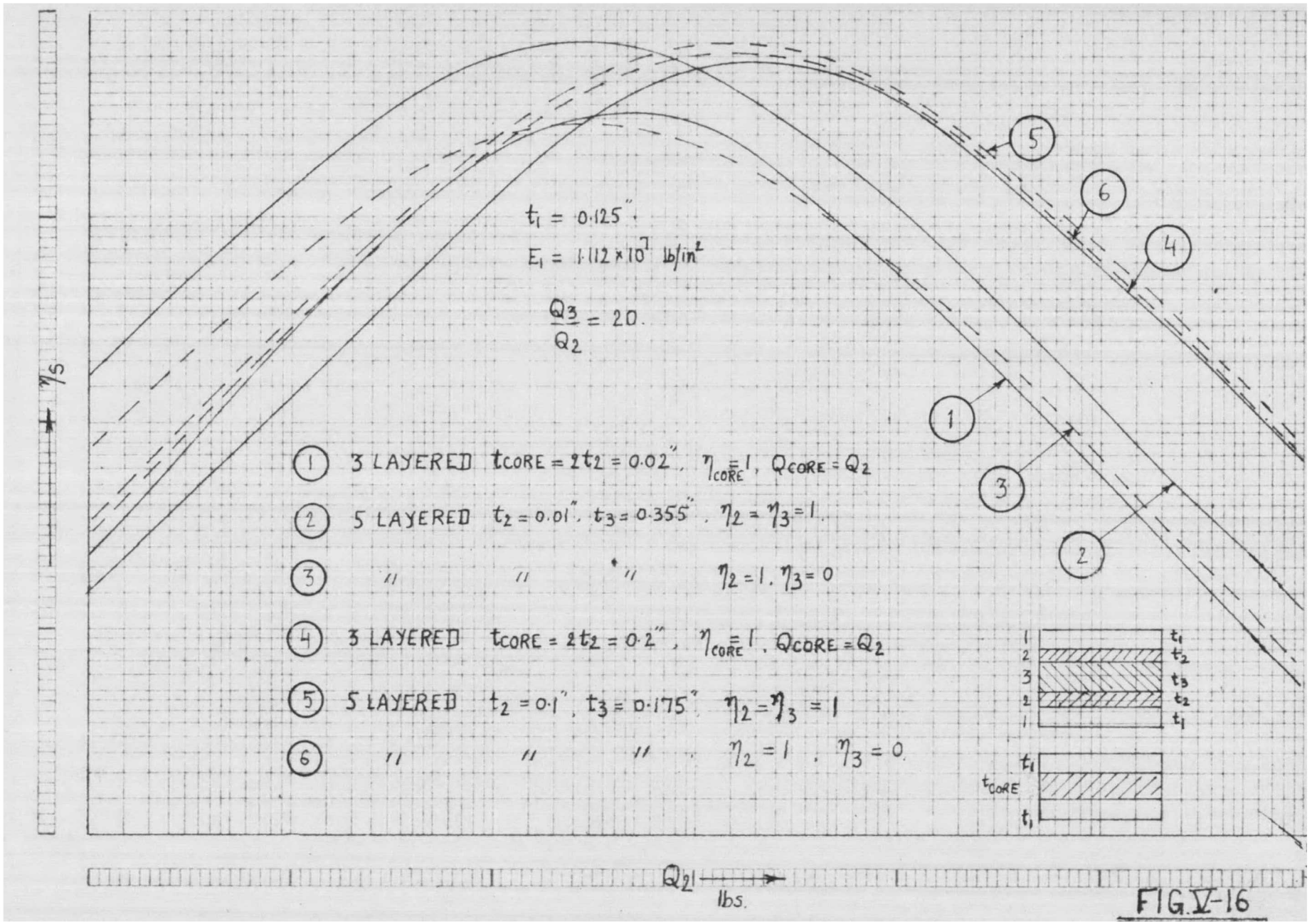
$t_1 = 0.125''$
$E_1 = 1.112 \times 10^7$ lb/in^2
$\frac{Q_3}{Q_2} = 20.$
1 3 LAYERED $t_{CORE} = 2t_2 = 0.02''$, $\eta_{CORE} = 1$, $Q_{CORE} = Q_2$
2 5 LAYERED $t_2 = 0.01''$, $t_3 = 0.355''$, $\eta_2 = \eta_3 = 1$
3 " " " $\eta_2 = 1$, $\eta_3 = 0$
4 3 LAYERED $t_{CORE} = 2t_2 = 0.2''$, $\eta_{CORE} = 1$, $Q_{CORE} = Q_2$
5 5 LAYERED $t_2 = 0.1''$, $t_3 = 0.175''$ $\eta_2 = \eta_3 = 1$
6 " " " $\eta_2 = 1$, $\eta_3 = 0$
η_S
Q_2
lbs.
t_{CORE}

FIG. V-16

configurations h ve better frequency response than the 3 layered ones. Also it is evident that if $\frac{t_2}{t_3}$ in the multi-cored case is increased beyond a certain value, the material loss factor of layer 3 i.e. η_3 has little effect on the system damping. This has also been seen to hold when $\frac{Q_3}{Q_2}$ is high.

(iii) Fig. V-17 is drawn for a multicored configuration, in which 't_2' is very small. It is seen that if $\frac{Q_3}{Q_2}$ is high i.e. layer 2 has low shear modulus compared to that of layer 3, the maximum damping achieved in the system is considerably reduced if the material loss factor of layer '2' i.e. η_2 is less, as in curve No.4 in Fig. V-17. So, if in a 3 layered case, one uses a soft adhesive which has comparatively less damping, the maximum damping which can be otherwise obtained (say by using a rigid adhesive) is considerably reduced.

(iv) From Fig. V-18, it is seen that the maximum damping obtainable from a thin layer 3 may be increased by the use of layers '2', which are more rigid, even though the material loss factor of the latter is negligible. The rigid layers 2 amplify the shearing motion induced in the thin and soft viscoelastic layer 3. For a given total thickness of the sandwich, the increase is more pronounced for smaller value of $\frac{t_2}{t_3}$.

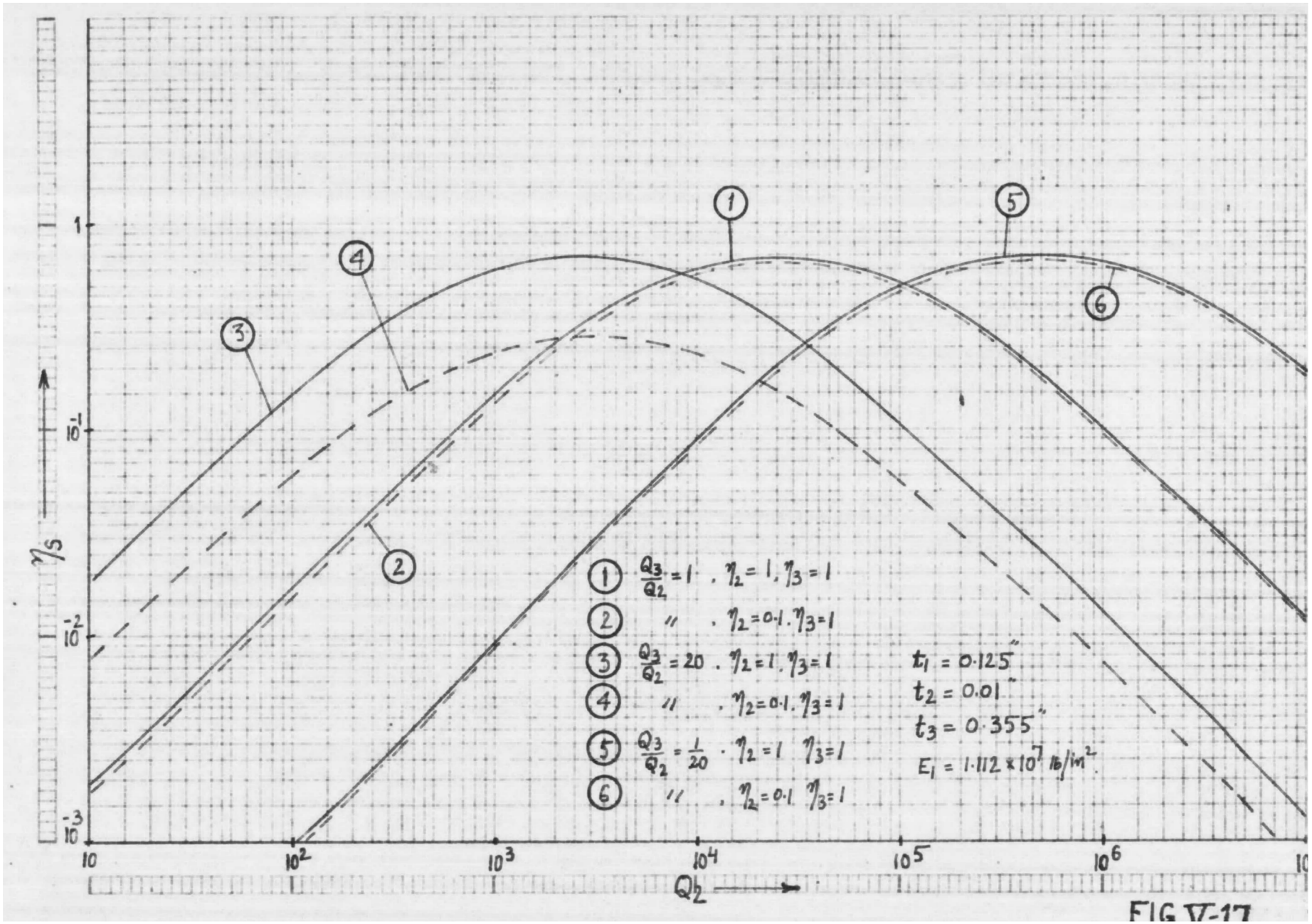
1
10⁻¹
10⁻²
10⁻³
η_S
10
10²
10³
10⁴
10⁵
10⁶
Q₂
1
2
3
4
5
6
① Q₃/Q₂ = 1 . η₂ = 1, η₃ = 1
② " . η₂ = 0.1 . η₃ = 1
③ Q₃/Q₂ = 20 . η₂ = 1 . η₃ = 1
④ " . η₂ = 0.1 . η₃ = 1
⑤ Q₃/Q₂ = 1/20 . η₂ = 1 η₃ = 1
⑥ " . η₂ = 0.1 η₃ = 1
t₁ = 0.125"
t₂ = 0.01"
t₃ = 0.355"
E₁ = 1.112 × 10⁷ lb/in²

FIG V-17

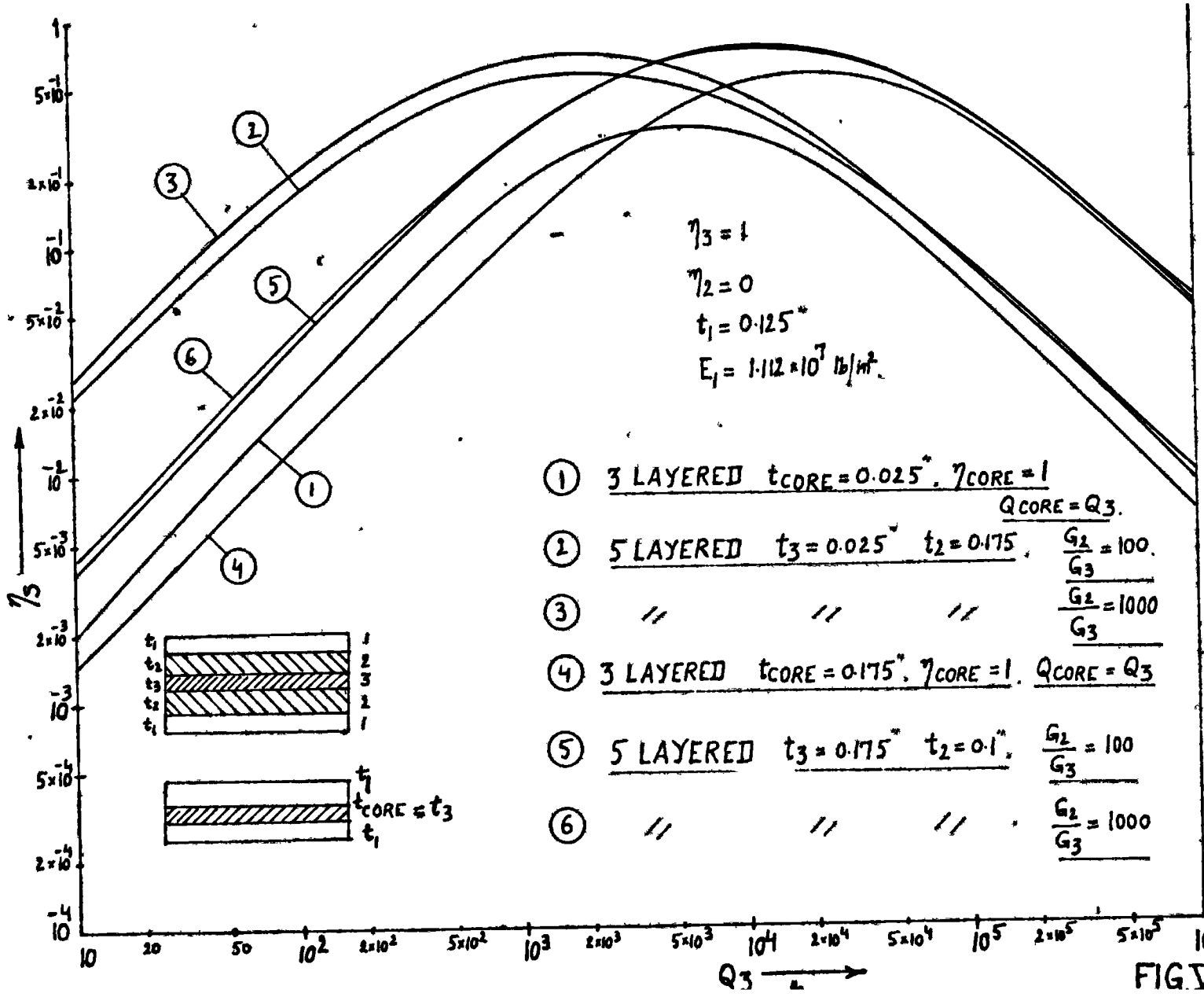
$\eta_3 = 1$
$\eta_2 = 0$
$t_1 = 0.125"$
$E_1 = 1.112 \times 10^7$ lb/in²
① 3 LAYERED $t_{CORE} = 0.025"$, $\eta_{CORE} = 1$, $Q_{CORE} = Q_3$.
② 5 LAYERED $t_3 = 0.025"$ $t_2 = 0.175"$, $\frac{G_2}{G_3} = 100$.
③ // // // $\frac{G_2}{G_3} = 1000$
④ 3 LAYERED $t_{CORE} = 0.175"$, $\eta_{CORE} = 1$, $Q_{CORE} = Q_3$
⑤ 5 LAYERED $t_3 = 0.175"$ $t_2 = 0.1"$, $\frac{G_2}{G_3} = 100$
⑥ // // // $\frac{G_2}{G_3} = 1000$
η_3
Q_3
$t_{CORE} = t_3$

FIG. V-18

CHAPTER VI : EXPERIMENTAL WORK

This is divided into two sections. Firstly, the dynamic properties in shear were measured for a number of viscoelastic materials. Next, dynamic response tests were carried out on a few multilayered beams, of different types. These laminated beams employed some of the viscoelastic materials tested earlier.

VI.A: Determining Dynamic Properties of Viscoelastic Materials

The dynamic properties of viscoelastic materials in shear, will be denoted by the values of in-phase shear modulus and loss factor. If a viscoelastic material is in pure shear varying sinusoidally, then there is a phase difference between the shearing force and strain, the tangent of which is denoted by the term loss factor. In-phase shear modulus is the ratio of shear stress in phase with the strain, to the value of the strain amplitude. These values will be determined for a few viscoelastic materials, in dynamic shear test.

VI.A.1 : Description of Set-Up

The set-up used for determining dynamic shear properties of viscoelastic materials was developed earlier [59] at the Department of Mechanical Engineering, Imperial College, London and was used with minor alterations. Complete

details are given in [59]. However, a brief description will be given below:

In this arrangement, two similar rectangular viscoelastic specimens are subjected to sinusoidal shearing force, which is applied by an electromagnetic exciter through a push rod. One side of each specimen is glued to the moving block by an adhesive and the other side of each is glued to rectangular blocks, which are fixed to a base plate, which in turn is attached to the body of the exciter, as shown in the Photograph. In [59], the set-up was designed for mounting on the Goodman exciter, which could deliver a maximum thrust of around 15 lbs. In the present work, it was modified for use on a Derritron Exciter (Model VP5), delivering a maximum thrust of 50 lbs so that stiff viscoelastic materials can be tested and also higher strain amplitudes may be employed. This necessitated changes in base plate dimensions, from point of view of its stiffness and the geometrical dimensions of the exciter. Also, the rectangular blocks were reduced in size for correct assembly, according to the new dimensions of the base-plate.

The force amplitude was measured by bonding strain gauges on to the push rod, the latter being screwed into the moving block. The strain in viscoelastic material was obtained from the displacement of the push rod. The instrumentation used for testing is shown in Fig. VI-1 and

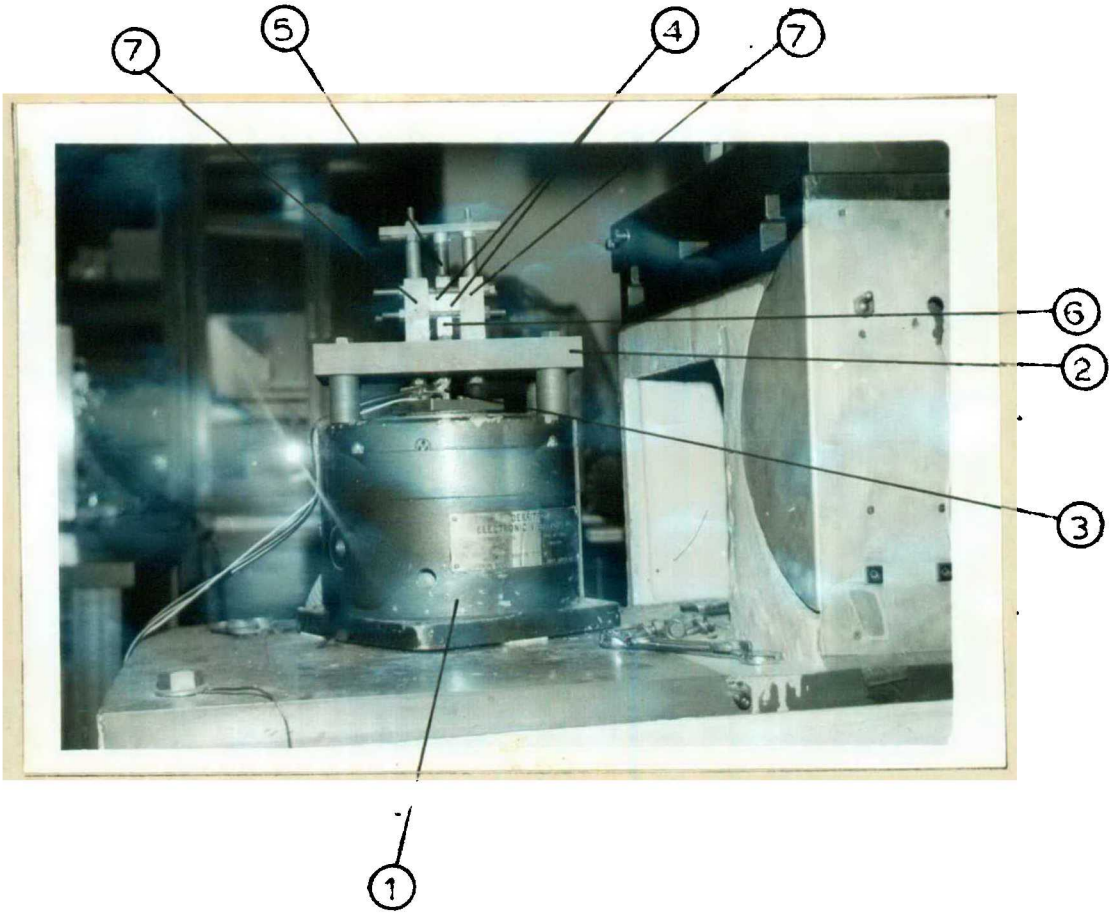

1 Vibrator.

2 Base-plate.

3 Push rod with strain gauge.

4 Viscoelastic specimens.

5 Inductance pick up for displacement signal.

6 Moving block - screwed on to the push rod.

7 Fixed rectangular blocks - bolted to the base plate

Set-up for measuring dynamic properties of viscoelastic materials in shear

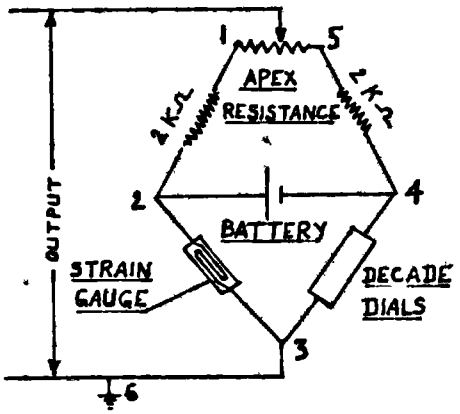

DETAILS OF
STRAIN GAUGE BRIDGE

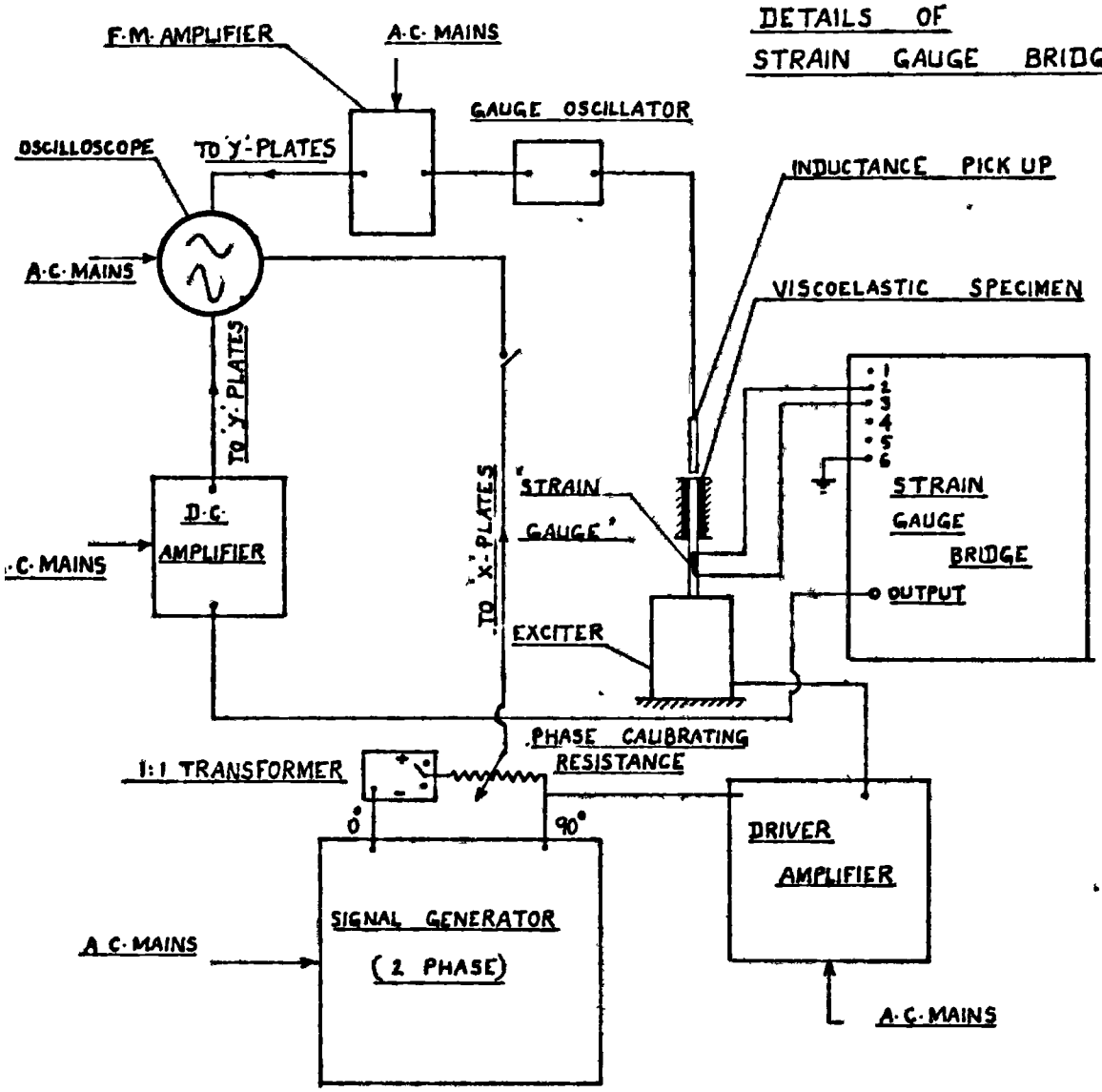

DYNAMIC PROPERTIES OF VISCOELASTIC MATERIALS

BLOCK DIAGRAM OF TESTING EQUIPMENT

FIG VI-1

described below.

Muirhead 2 phase L.F. decade oscillator (Model 880-A) was used to drive the Derritron Electromagnetic vibrator (Model VP5) through a 250 W.L.F. power amplifier. For measuring the sinusoidal displacement of the push rod, proximity vibration pick up of inductance type (G.211-Southern Instruments Ltd.) was employed. This is of mutual inductance type and signal is proportional to displacement. The signal was passed through a radio frequency gauge oscillator (Model M 700 L - Southern Instruments Ltd.), which in turn was connected to an F.M. amplifier (Southern Instruments Ltd.). The signal from the F.M. amplifier was fed to one channel of a double beam oscilloscope. For measuring sinusoidal stress, the strain gauge formed one of the arms of a strain gauge bridge (Model MR 353 Resistance gauge bridge - Southern Instruments Ltd.). The output from the bridge was amplified by D.C. amplifiers (Type MR 514 - Southern Instruments Ltd.) or Fenlow transistor amplifiers and then fed to the second channel of the oscilloscope.

IV.A.2 : Experimental Procedure

Firstly, the specimens were glued to the moving block and fixed rectangular blocks, using adhesives like Araldite (Resin AV 100 together with hardener HV 100) and allowing these to set. Before gluing, the surfaces had to be thoroughly cleaned, degreased and roughened by sand blasting

and etching. The etching agent used for steel was 2% Nitric acid and for aluminium alloy was 5% Hydrofluoric acid. The degreasing chemicals used were carbon tetrachloride and acetone.

During assembly of the set-up, care had to be taken to ensure that the push rod moved vertically up and down, without bending and causing only pure shearing in the specimens. Since the material properties are dependent on temperature, frequency and strain amplitude, the experimental procedure had to take account of all these factors. During the experiment, only one of these factors was varied, while others were kept constant, e.g. in order to get frequency dependence, temperature and strain amplitudes were kept constant, and readings were taken for different frequencies. The quantities to be measured were: Temperature, amplitude of direct force in push rod, displacement amplitude of the rod and phase difference between the force and displacement signals.

Measurement of Force. The direct force amplitude in the push rod was measured by strain gauges fixed on to it. Two similar strain gauges in series were fixed, one on each side of the push rod, so that any bending of push rod does not cause any error in force measurement. These formed one arm of a strain gauge bridge, as shown in Fig. VI-1. Initial balancing of the bridge was obtained by changing the resistance of one of the arms, having decade

dials. When the push rod was subjected to a direct strain due to the force exerted by the vibrator, a change in the resistance of strain gauge caused unbalance in the bridge circuit and the output signal was displayed on the oscilloscope, after being amplified. The calibration for strain gauge was done statically and the values were checked dynamically too. In each case, the calibrating factor was obtained in terms of the change in apex resistance in the bridge, which is a 10 turn helical potentiometer, each divided into 100 divisions. Application of a known direct load to the push rod, changed the strain gauge resistance and caused unbalance in an initially balanced bridge. By changing the apex resistance by a known value, the circuit could be balanced again, thus giving a calibrating factor as force per unit division of the apex resistance scale. For static calibration, the load was applied directly to the push rod by hanging it freely. For dynamic calibration, the push rod carrying a known weight was screwed on to the exciter. The inertia force at any frequency may be easily computed, knowing the amplitude of vibration of the known weight.

During actual experimentation while measuring the properties of viscoelastic samples, for a given setting on the oscilloscope, a known change in apex resistance could be related to the shift on the oscilloscope. Since the calibrating factor is known, the shift on the oscilloscope

is thus related to the force applied.

Measurement of Displacement: The sinusoidally varying displacement of the push rod was measured, using an inductance pick-up together with a gauge oscillator and an F.M. amplifier. The principle of operation is frequency modulation of the oscillator, which runs at about 2 m.c.p.s. and has in its tuned circuit, the variable inductance gauge performing the measurement. Due to change of inductance, the frequency of oscillator is altered. The radio frequency signal is transmitted back to the amplifier, passes through an amplifying stage and is applied to a frequency discriminator circuit, before being fed to the oscilloscope. Calibration of the displacement signal was done by a reading microscope, provided with the objectives of various magnifications. The microscope for any setting was itself calibrated against a standard scale, supplied with the microscope. For very stiff viscoelastic materials, the displacement signal was very small and the calibration was carried out statically by dial gauge type attachment supplied with the inductance pick-up, which could read up to 10^{-4} in displacement.

Measurement of Phase: The phase angle between sinusoidal displacement and sinusoidal stress signals was obtained by one of the two methods described below. In the first one, the phase angle was got directly from the ellipse

obtained by feeding one signal to Y plates of oscilloscope and the other one to X plates. In the other method, the 2 phase supply from the signal generator was used, one signal lagging beyond the other by 90^{o}. In order to vary the phase from 0 to 180^{o}, a 1 : 1 transformer having two equal secondary windings, connected in opposition was used on one of the ends, as shown in Fig. VI-1. This provided signals of the same amplitude but opposite phase. The two ends of a calibrating resistance were connected to the supply terminals of the signal generators, one end being connected through the transformer, the supply to the ends being adjusted to the same voltage. It resulted in the phase drop from 0 to $+90^{o}$ from one end of resistance to the other end for one setting of the transformer and 90^{o} to 180^{o} for the other setting. The resistance was calibrated for phase angle, using a Beckman Universal Eput Timer (Model 8360 HW), in which smallest unit of time measured is one microsecond. The phase was calculated, knowing time difference between the two signals and their frequency. The calibration was done at different frequencies, for each setting of the transformer.

During the actual use of the above arrangement for measuring the phase angle between the displacement and force signals, these signals were fed to the Y plates of a double beam oscilloscope and the supply from a variable point in the calibrating resistance was fed to X plates, the voltage

to each end of the resistance being adjusted to the same value. Two ellipses were obtained, The variable point on the calibrating resistance was moved till each ellipse in turn appeared as a straight line and the reading of phase angle on the calibrated resistance was noted in each case, along with the corresponding setting of the transformer. With this, the relative phase between the two signals could be easily computed. This method appeared to be more convenient and accurate than direct calculation from a plotted ellipse.

Temperature Measurement: The temperature of the visco-elastic material, during testing, was measured by using copper-constantan thermocouples, the hot end being embedded in the material and the cold end kept at $0^{\circ}C$. The voltage was measured by using an accurate portable potentiometer (Type 3184 D, H. Tinsley & Co., Ltd.) and reference tables used for calculation of temperature were B.S. 1828: 1961 for copper constantan thermocouples. Checks were made on these values, using an accurate thermometer in which the smallest division on the scale was $0.2^{\circ}C$.

VI.A.3 : Calculation of Material Properties

The quantities measured experimentally are

Amplitude of sinusoidal displacement of push rod say 'a_o', amplitude of sinusoidal force transmitted by the rod

(a)

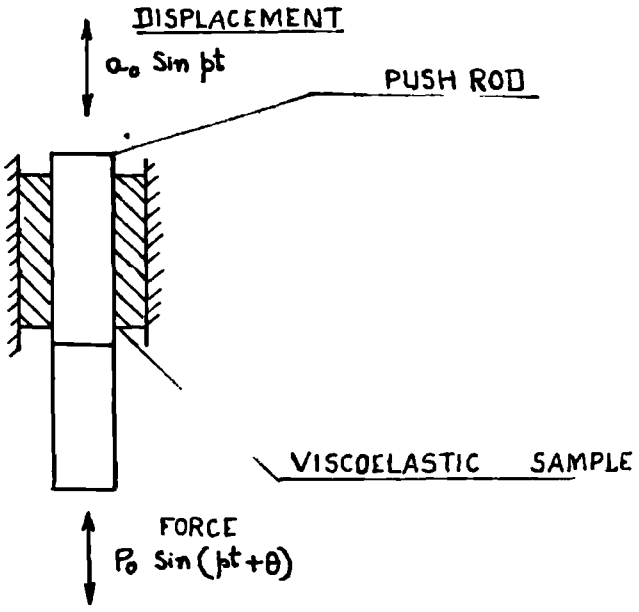
DISPLACEMENT
$a_0 \sin pt$
PUSH ROD
VISCOELASTIC SAMPLE
FORCE
$P_0 \sin(pt+\theta)$

(b)

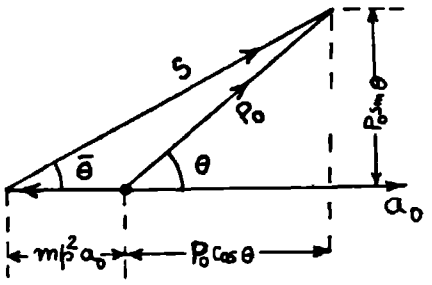
S
P_0
$P_0 \sin\theta$
$\bar{\theta}$
θ
a_0
$mp^2 a_0$
$P_0 \cos\theta$

FIG VI-2

'P_o' and the phase difference between the two signals 'θ' (Fig. VI-2a).

If 'm' is the mass of the push rod and specimen width, length and thickness are W, D and h respectively, then shear strain amplitude $\gamma_o = \frac{a_o}{h}$.

If 'S' is the amplitude of the in-phase component of force, resisting shear in the specimens, then

$S = P_o \cos\theta + mp^2 a_o$ (Fig. VI-2b), p being the circular frequency of oscillation. The term $mp^2 a_o$ is due to the inertia force of the push rod and the moving block. Inertia effect of the specimen is neglected since it is expected to be very small.

The out of phase component of force = $P_o \sin\theta$

G_i or in phase shear modulus = $\dfrac{P_o \cos\theta + mp^2 a_o}{2WD\gamma_o}$

Area in shear being = 2WD

Material loss factor $\eta_i = \dfrac{P_o \sin\theta}{P_o \cos\theta + mp^2 a_o}$

VI.A.4 : Experimental Results for Materials Tested

Experimental values for the in-phase shear modulus and the loss factor of the following viscoelastic materials, were determined.

a) Velbex P.V.C. Formula 629/0900, made by B.X.Plastics Ltd., was tested at 3 values of temperatures, at a constant shear strain amplitude for various frequencies and also

effect of shear strain amplitude was determined at a number of frequencies. The results are given in Figs. VI-3 and VI-4. The in-phase shear modulus and loss factor increase with frequency and are seen to decrease with temperature. The shear strain amplitude appears to have no effect on material loss factor but an increase in the strain amplitude decreases the in-phase shear modulus, the effect being more pronounced at higher frequencies. Sheet B of the above material was tested and results were found to be different from those of another sheet (designated as sheet A in the present work) given in [59] by up to 35%. Sheet A was also tested and results were found to be almost similar to those in [59] and hence are not given in the present work.

Properties of Velbex P.V.C. for any strain, temperature and frequency were determined from Figs. VI-3 and VI-4, using the following procedure. From Fig. VI-3, a graph of in-phase shear modulus 'G_i' and material loss factor 'η_i' vs. temperature, was drawn for a number of frequencies (shown only for 50 and 200 c.p.s. in Fig. VI-5) and the values of these properties were read by interpolation from these graphs for a number of values of temperature and these values are plotted in Fig. VI-6. The variation of in-phase shear modulus during each interval of temperature shown in Fig. VI-6 was assumed linear, in order to determine

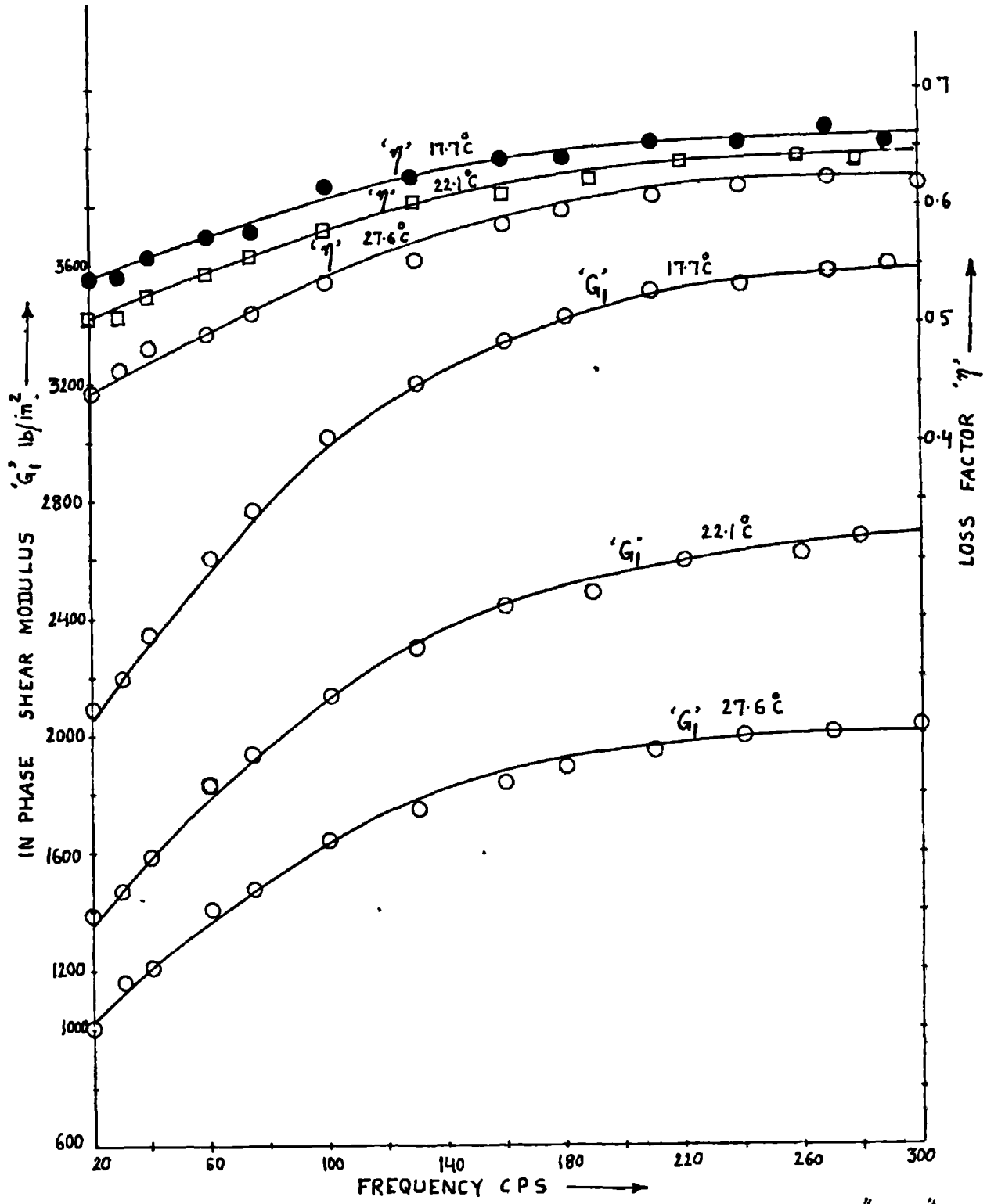

SPECIMEN 1·04" x 0·49" 0·127" THICK

VELBEX P.V.C. (SHEET B)

FORMULA 629/0900

SHEAR STRAIN AMPLITUDE = $3{\cdot}18 \times 10^{-3}$

FIG VII-3

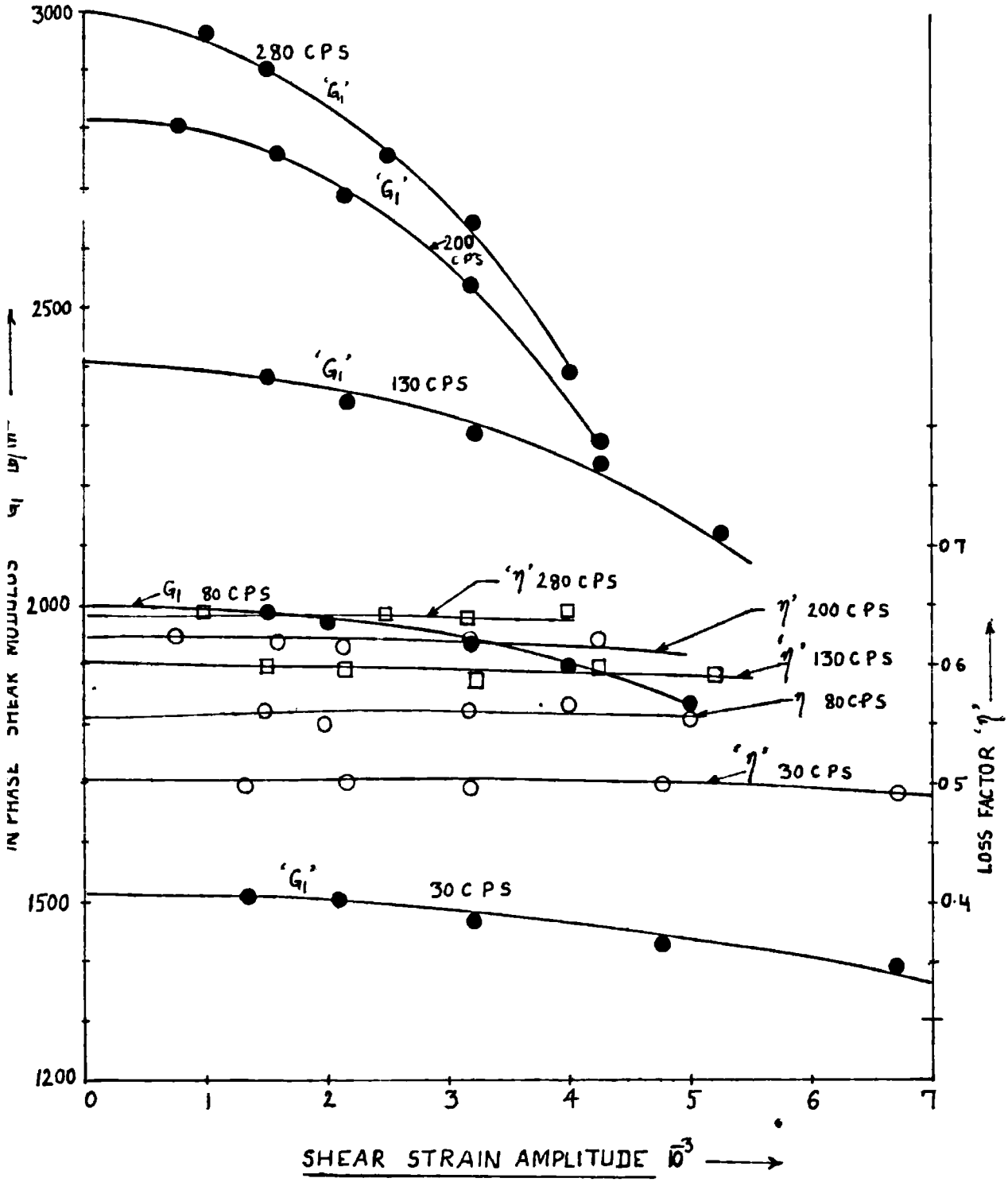

FORMULA 621.0900

SPECIMEN : 1.04" × 0.49"
0.127" THICK

VELBEX PVC (SHEET B)

TEMPERATURE - 22.4°C

FIG. VI-4

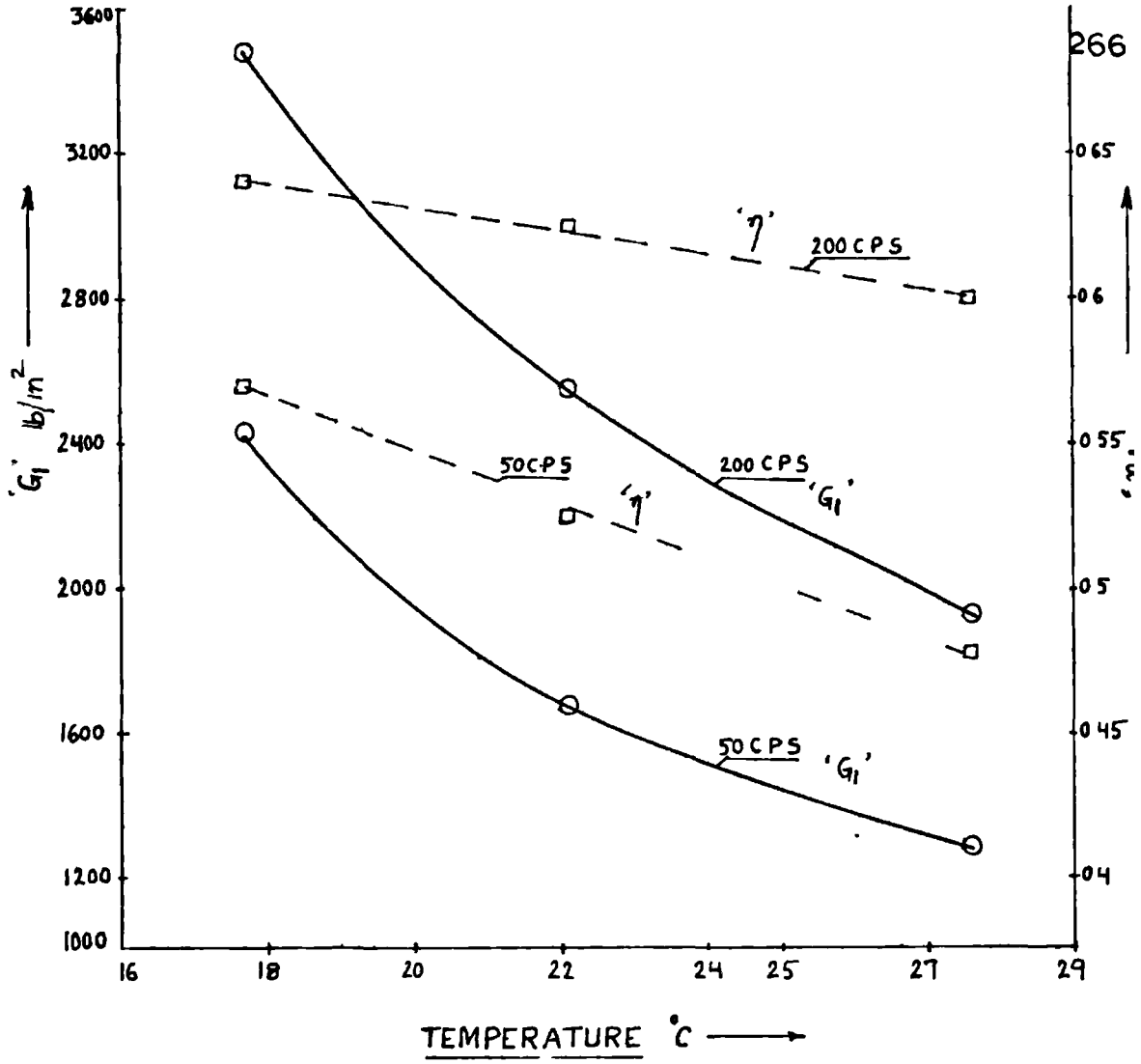

VELBEX P.V.C.

(SHEET B)

FIG. VI-5

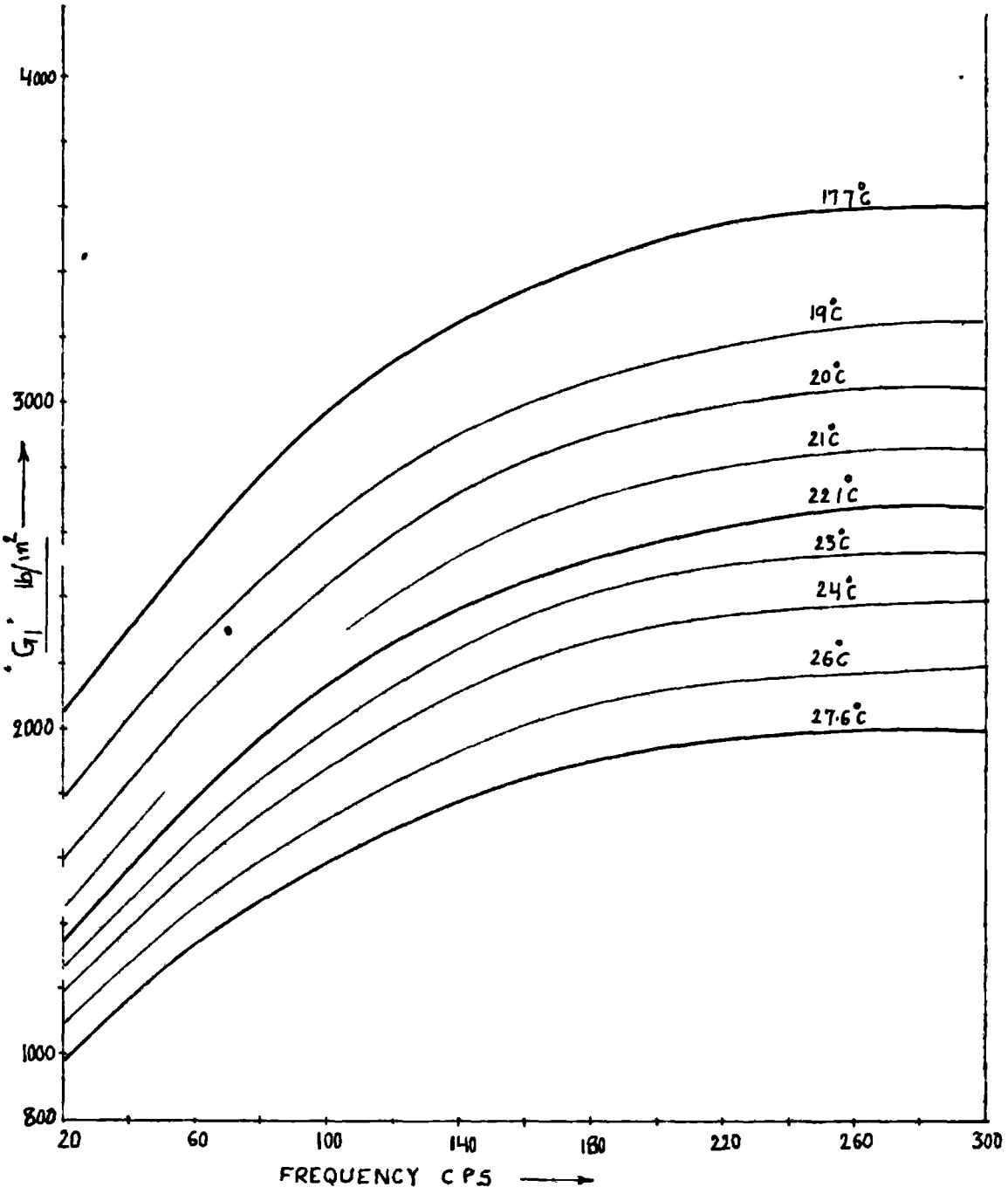

VELBEX P.V.C. (SHEET B)

SHEAR STRAIN AMPLITUDE - 3.18×10^{-3}

FIG VI-6

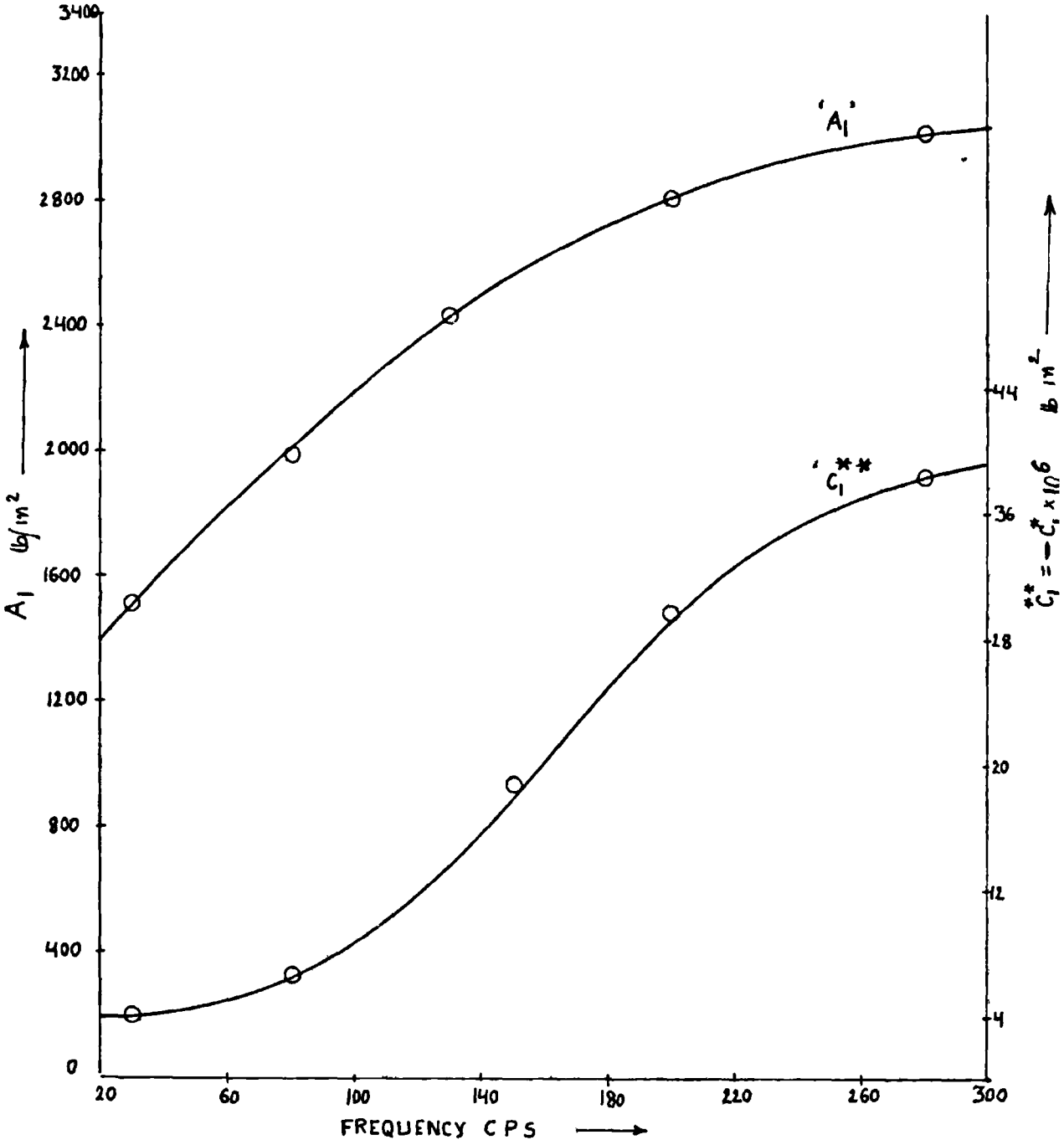

VELBEX PVC (SHEET B)

TEMPERATURE - 22.4°C

FIG VI 7

its value at any temperature. From Fig.VI-5, the loss factor is seen to vary linearly over a wide interval and so its value at any temperature, within the range of temperatures employed, could be directly obtained from Fig. VI-3. All these values correspond to $\gamma_o = 3.18 \times 10^{-3}$.

In Fig. VI-4, graphs of G_i and η_i against γ_o are given. η_i is seen to be strain independent while G_i decreases with strain γ_o. Relation $G_i = A_1 + C_1^* \gamma_o^2$ was employed for each frequency, to represent the variation of G_i with γ_o and was seen to hold within an accuracy of 4%. The values of A_1 and C_1^* thus determined are given in Fig.VI-7. Using these values, G_i at $\gamma_o = 3.18 \times 10^{-3}$ was evaluated and was found to check reasonably with the values of Fig. VI-3, at all frequencies. Since experimental results in Fig. VI-4 are obtained only for a temperature of 22.4°C, it was taken that the variation of G_i with 'γ_o' is similar at all temperatures at a constant frequency or C_1^* was taken to be independent of temperature. With this assumption, it is possible to determine A_1 at any temperature since G_i corresponding to any temperature at γ_o 3.18×10^{-3} is known from Fig. VI-6.

b) Properties of Velbex P.V.C. (Formula 521/2127), Admiralty Plastic Yellow compound and Butakon 40:60 modified with carbon black (40% of Butadiene Acrylonitrile Copolymer and 60% of P.V.C. blended with carbon black) were

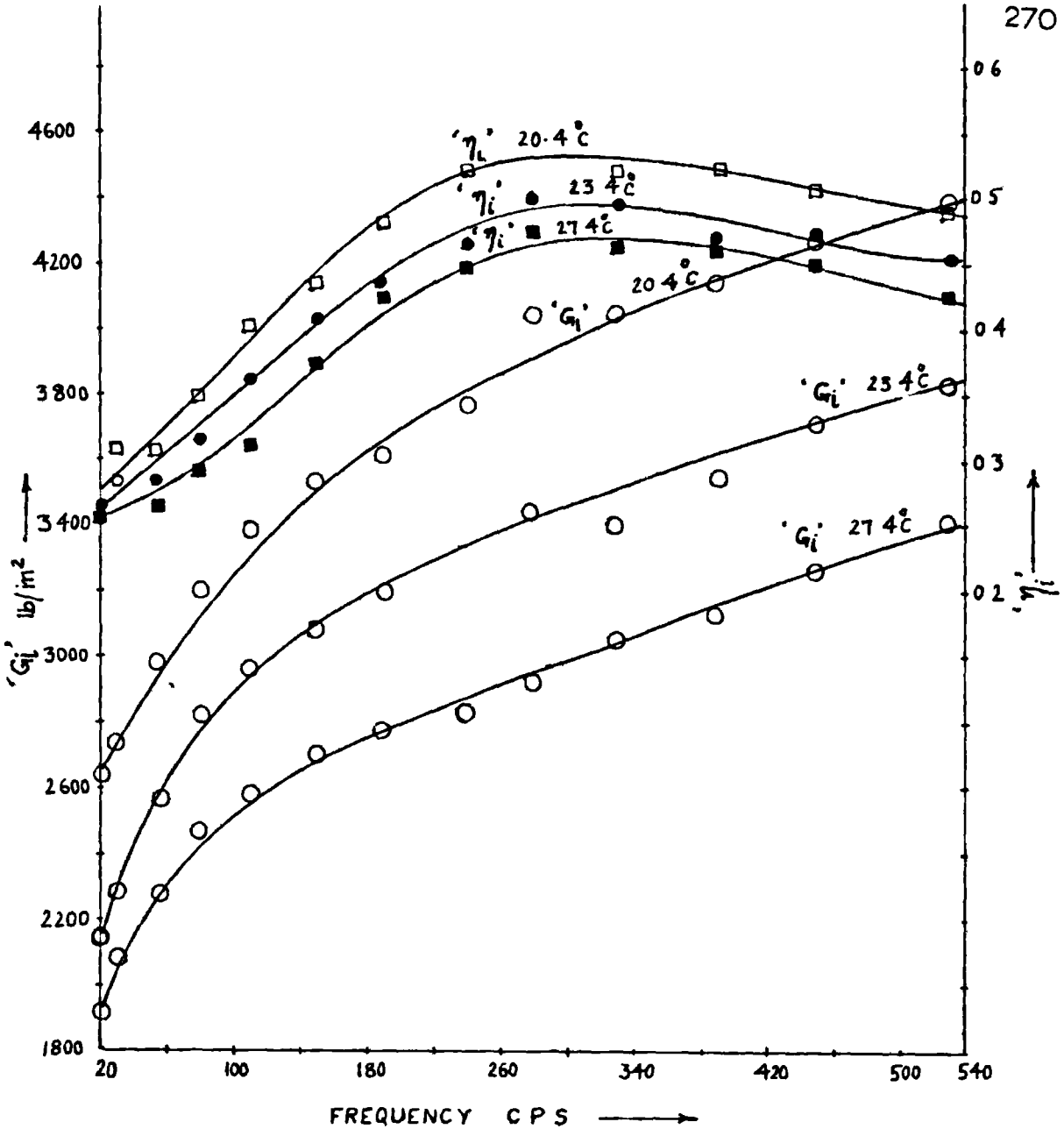

VELBEX PV·C·
(FORMULA 521/2127)

SPECIMEN 0·495" × 0·49"
0·02 THICK

SHEAR STRAIN AMPLITUDE = 11.5×10^{-3}

FIG VI-8

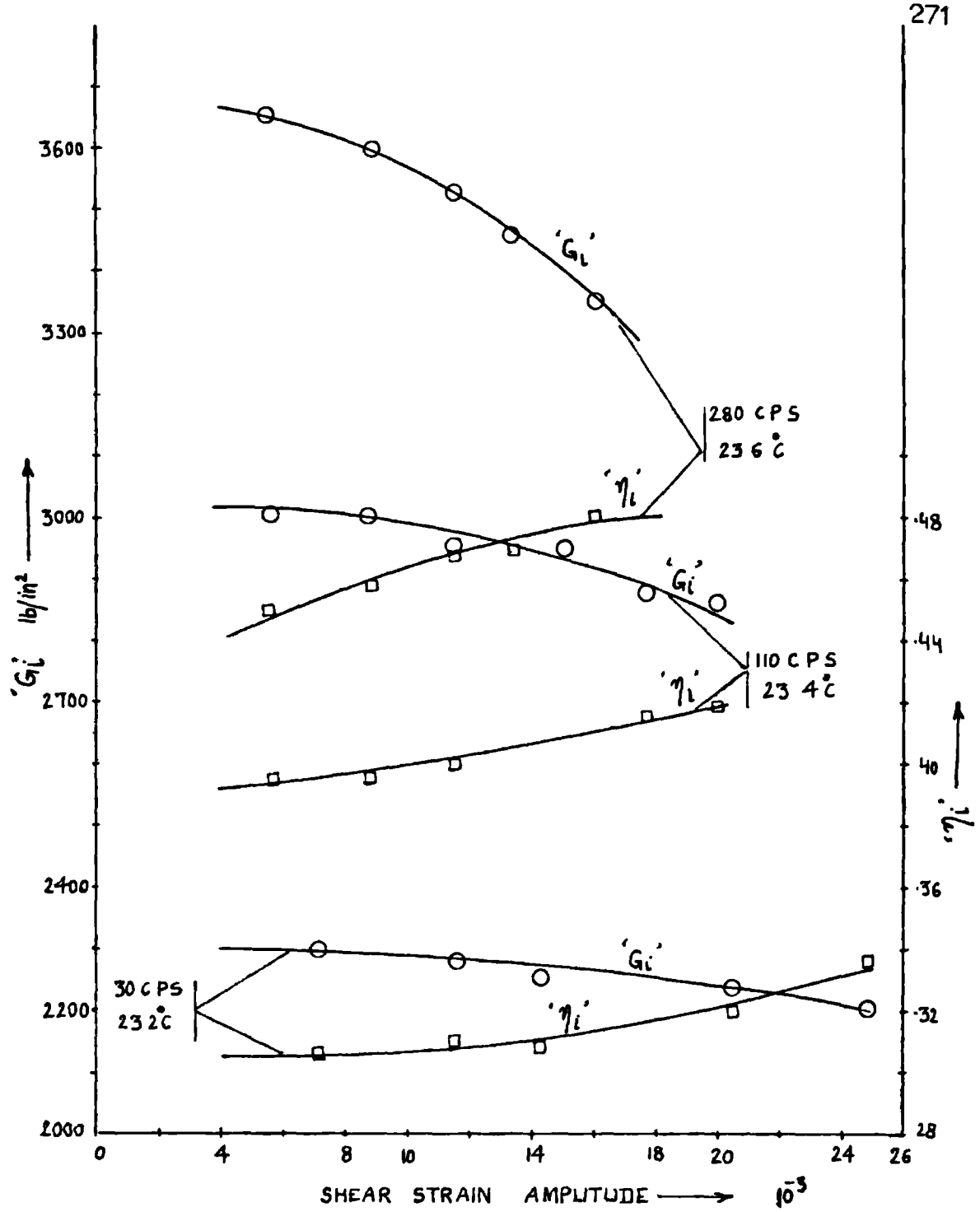

VELBEX P.V.C.
(FORMULA 521/2127)

SPECIMEN 0·495 × 0·49'
0·02 THICK

FIG. VI-9

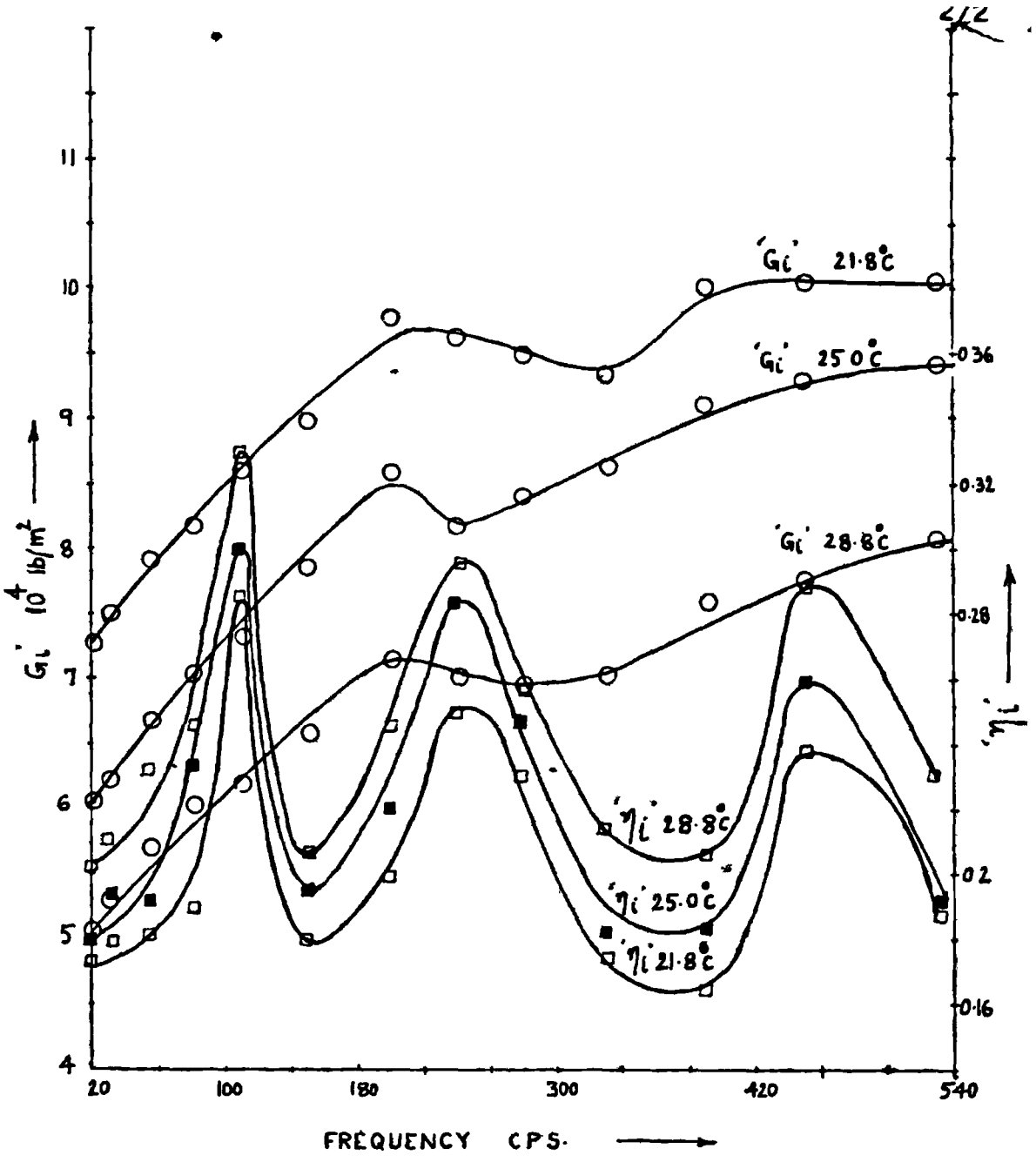

MODIFIED BUTAKON 40/60

SHEAR STRAIN AMPLITUDE = 0.707×10^{-3}

SPECIMEN : 0·495 × 0·365
0·197" THICK

FIG VI-10

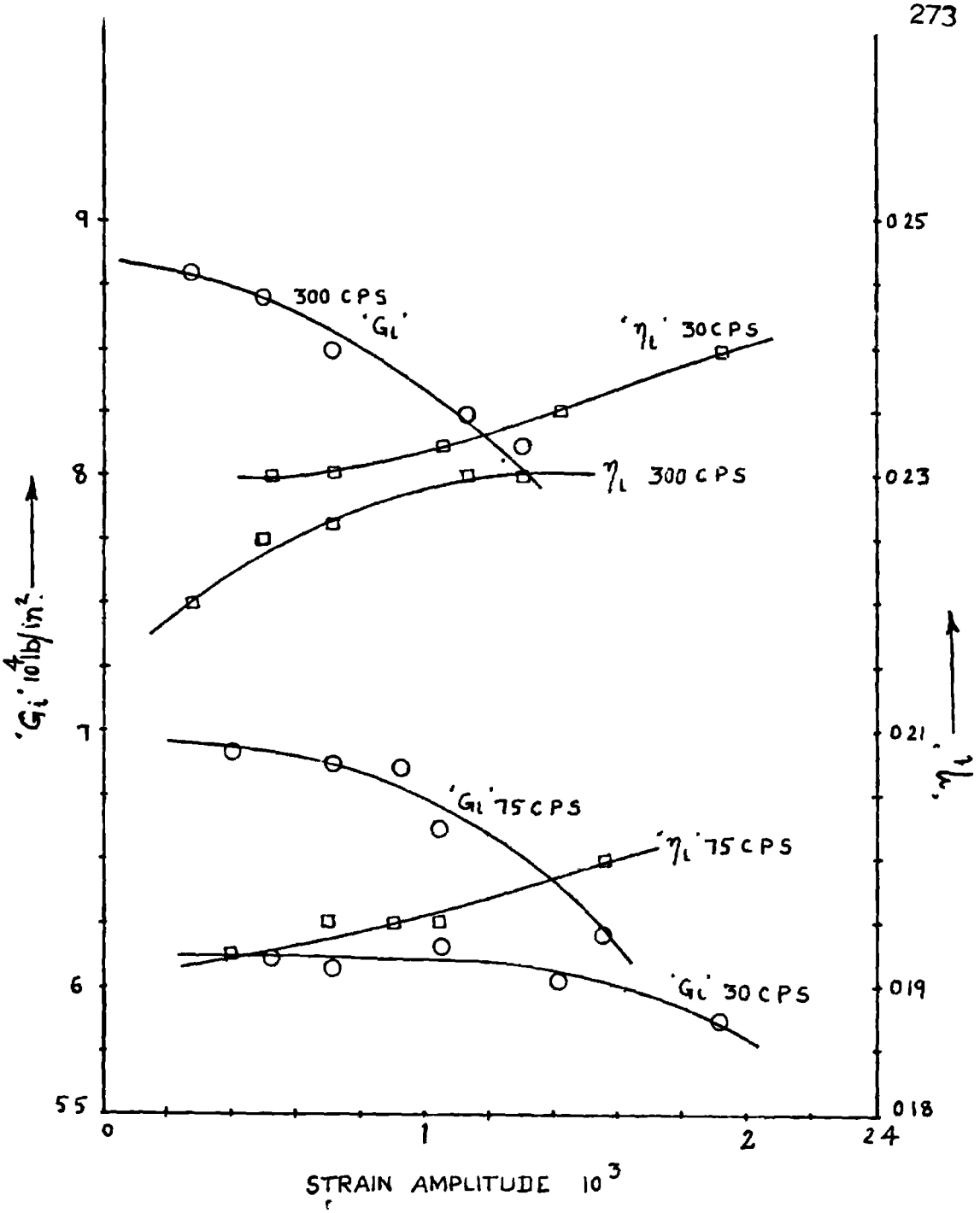

MODIFIED BUTAKON 40/60

TEMPERATURE 25·0°C

SPECIMEN 0·495 × 0·365
0·197" THICK

FIG VI 11

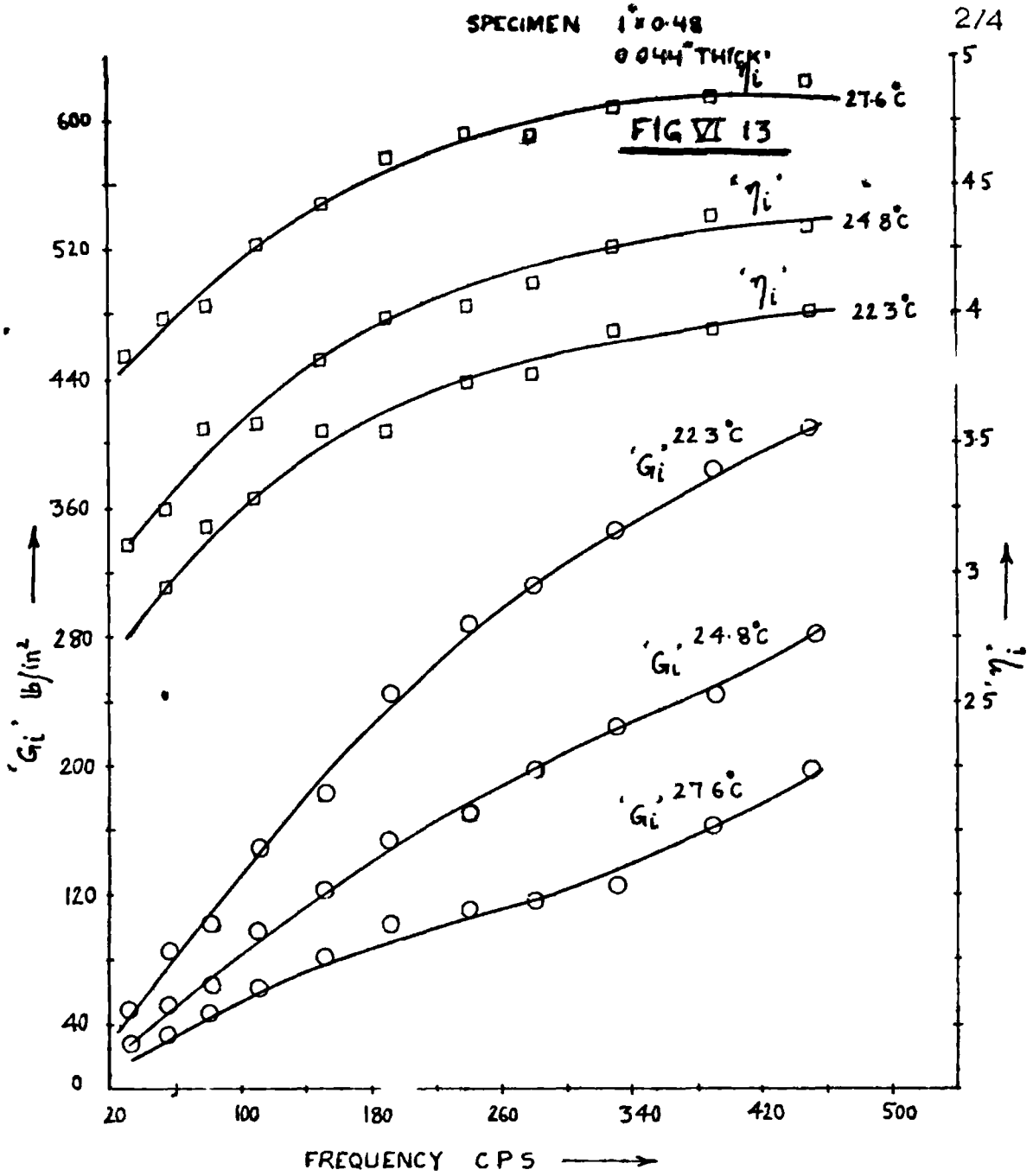

ADMIRALTY PLASTIC YELLOW COMPOUND

SPECIMEN 1"×0·48
0·044 THICK.

SHEAR STRAIN AMPLITUDE - 6.82×10^{-3}

FIG VI-12

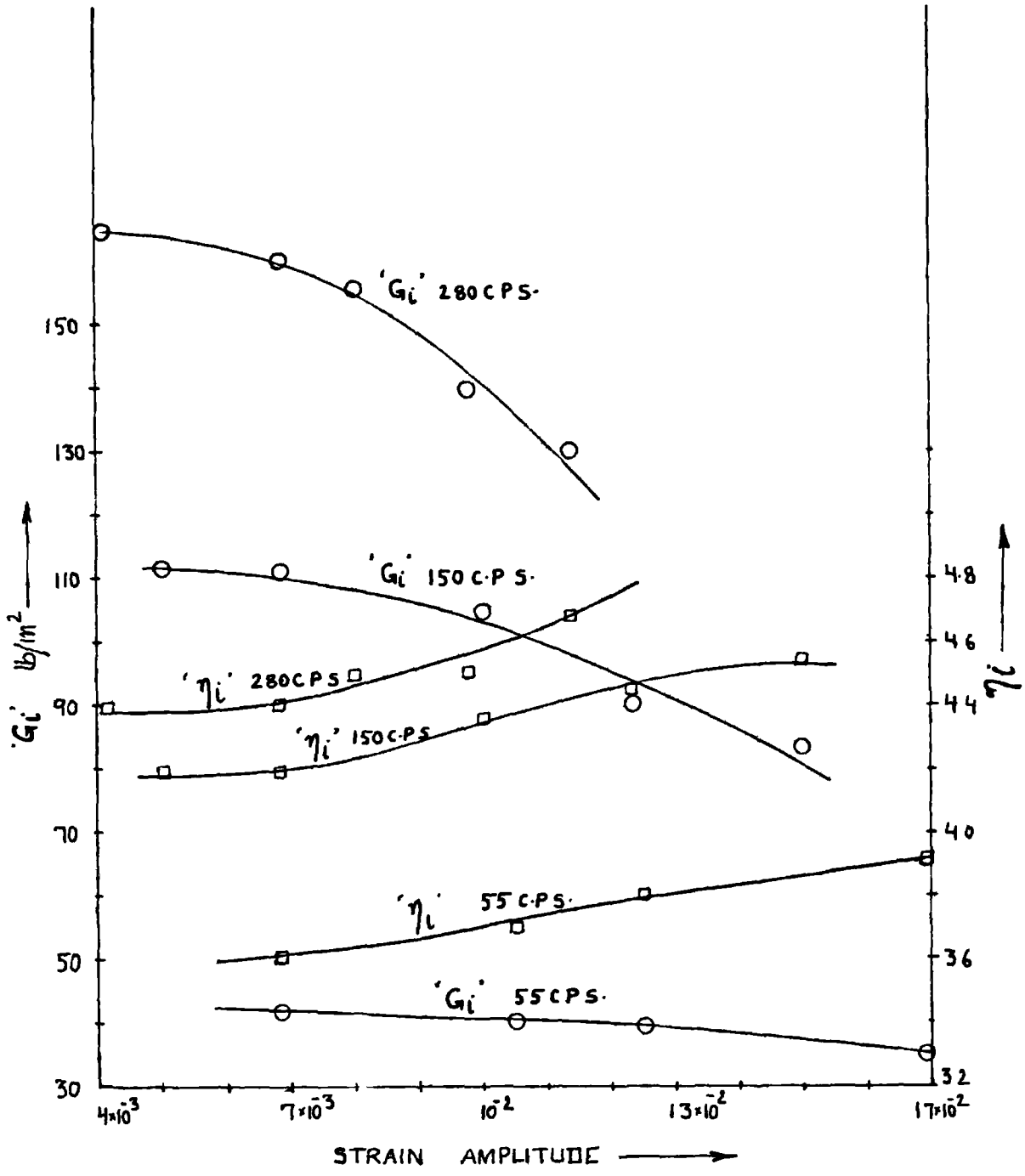

ADMIRALTY PLASTIC YELLOW COMPOUND

TEMPERATURE 26.3°C
SPECIMEN 1'×0.48'
0.044" THICK

FIG. VI 13

determined experimentally and are given in Figs. VI-8 to VI-13. Velbex P.V.C. (formula 521/2127), made by B.X. Plastics Ltd. was found to be somewhat stiffer and to have less damping than the earlier variety (i.e. formulae 629/0900). Admiralty Plastic Yellow Compound, made by A.E.I. Ltd., has very high damping and is very soft. Modified Butakon 40:60, supplied by I.C.I. is a very stiff damping material.

c) In order to find the suitability of certain visco-elastic materials for use in the dynamic response tests on sandwich beams, the dynamic properties of these materials were determined and are given in Appendix 8. The materials are Butakon 80/20, 60/40 and 40/60. With the increase of the percentage of Butadiene-Acrylonitrile in the mixture, 'G_i' decreases and so it may be seen that a suitably chosen variety may give any desired properties. The difference in results of the two samples of Butakon 40/60 given in Figs. AP8-3 and AP8-4 might be due to different thermal history of the samples during manufacture.

Vibrating reed tests, a theory of which is given in [66], were carried out on samples of Velbex P.V.C. (formula 629/0900), modified Butakon 40/60 and Butakon 40/60 and results for dynamic Young's modulus E_i and loss factor β_i were determined. Taking $G_i = E_i/3$ as for an incompressible material and $\eta_i = \beta_i$, the values were checked with those

obtained during shear test and were found to be in agreement within 10%. Limitations of the vibrating reed method are discussed in Section VI.C.

VI.B : Vibration Response Tests on Laminated Beams

VI.B.1 : Introduction

The object of dynamic response tests on various configurations of laminated beams, is to compare the results obtained from actual tests, with those obtained from the theoretical analysis of previous chapters, under experimental conditions. The theoretical analysis is based on several assumptions and hence a comparison with experimental work is desirable, in order to confirm their validity.

As given under 'Literature Survey' in Chapter I, experiments were done on simply supported symmetrical 3 layered sandwich beams in [52], where the modal loss factor and dynamic stiffness were determined experimentally, for comparison with the theoretical values. In [59], experiments on multilayered symmetrical cantilevers have been carried out, in order to measure the displacement response at various frequencies, by subjecting the root of cantilever beams to sinusoidal motion and comparisons were done with the theoretical values. In the present work, experiments have been carried out on simply supported

multilayered configurations - 3 layered unsymmetrical, 5 layered unsymmetrical and 4 layered double cored types. The ends of the beam were subjected to sinusoidal displacements of same amplitude and phase and frequency response of the beam was determined, for comparison with theoretical values. The dynamic properties of viscoelastic materials employed in making laminated beams, have been determined earlier in Section VI.A.

For comparison of theoretical and experimental results, the values used are the displacement response (both amplitude and phase) at the middle of the beam over as wide a frequency range as possible and the distribution of the displacement response over the length of the beam at a frequency close to the peak displacement frequency. Alternatively, the Kennedy-Pancu polar graphs [95, 96] could have been employed to determine the modal loss factor from experimental results and compared with theoretical values. This has not been done in the present work since the excitation chosen being a single one, is unlikely to excite a generalized mode only especially a higher one in a heavily damped system. Because of the contribution of off resonant modes at a resonance and the variation of viscoelastic material properties with frequency, an error is likely to occur in results, obtained from such graphs. Another factor which is likely to affect the results obtained from polar graphs is the accuracy with which

a circle may be made to pass through experimental points. These points are illustrated later in Appendix 10.

VI.B.2 : Development of Test-Rig

The test-rig consist of an arrangement for applying sinusoidal displacement excitation of same magnitude and phase to each end of a simply supported sandwich beam and to measure the amplitude and phase of transverse motion of any point on the beam at various frequencies of excitation.

Excitation Arrangement. A possible approach to give same motion at each end of the beam is to use two similar exciters, one at each end. For such a case, one can anticipate the difficulty of getting the two end displacements exactly in phase at all frequencies since in practice no two exciters are likely to be exactly identical. Also, such an arrangement would be cumbersome to work with during the response tests. So this arrangement was not employed. Instead, a single exciter was used to drive at the middle of a rigid I-beam, on which the specimen sandwich was mounted.

The Aluminium alloy I-beam was chosen because of its light weight and high stiffness. The dimensions of the I-beam were suitable chosen so that the motion imparted to the I-beam was sufficient enough to be measured accurately. This was found out from the maximum thrust of the exciter which was equated to the total inertia force of the beam.

A check was made to see that the I-beam was stiff enough so that the frequency corresponding to its own fundamental mode of bending vibrations is much higher than the high frequency limit of the tests intended. This was seen to hold good if the I-beam was treated as a free free beam or a double cantilever with root at the middle.

The section chosen for the I-beam was 4" x 2" and the length was taken slightly more than that of the specimen length. The specimen length was fixed at 30" and width at $1\frac{1}{2}$". The total weight of the arrangement was around 6 lbs. This weight could not be carried directly by the mounting table of the 50 lb thrust Derritron VP 5 exciter and hence the I-beam was supported on very soft spring cords at each end and driven at its middle by the exciter through a drive rod. The arrangement is shown in the photograph, without the exciter. Later, when the 250 lb thrust Derritron VP 25 exciter became available, the I-beam was directly mounted at its middle on to the exciter, since its weight could be carried by the exciter table. Specimens D_1 and D_2, the details of which are given in Table T-13 were tested on the latter arrangement which was used till 400 c.p.s. while the remaining specimens were tested on the earlier one, which was employed till 300 c.p.s.

Obtaining desired end-supports The end supports desired are the simply supported ones, i.e. when transverse displace-

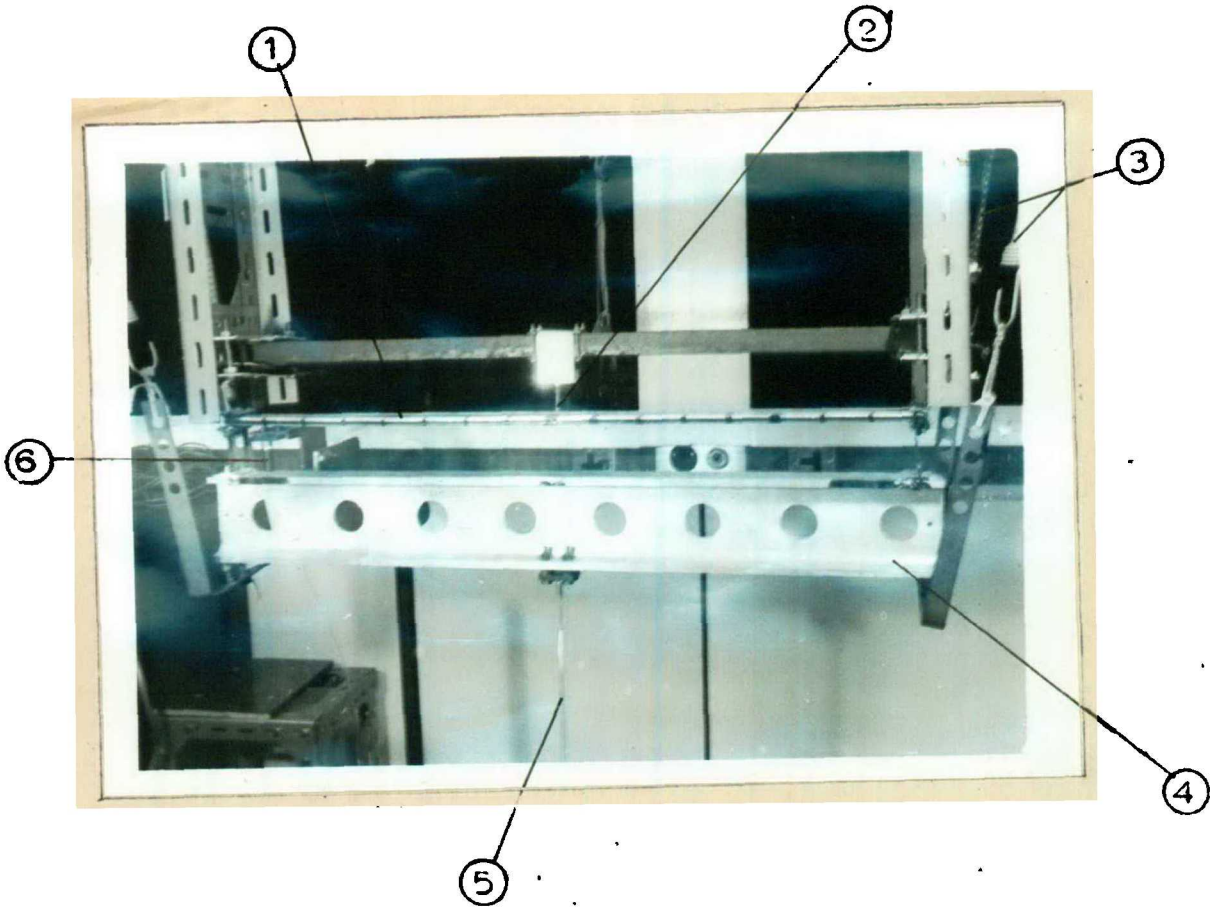

1 Laminated beam specimen.

2 Inductance pick up.

3 Soft spring cords.

4 Aluminium alloy I-beam.

5 Drive rod.

6 Inductance pick up.

Arrangement for vibration response test - using 50 lb. thrust vibrator

ment is zero and there is no constraint at the ends, the ends being free to rotate. In order to achieve conditions as close as possible to the above mentioned ones, the sandwich test beam was mounted on spring steel strips, which were attached to the I-beam, as shown in Fig.VI-14. The other ends of these strips were connected to Aluminium Tee sections, having a Vee groove at the top. An M.S. $\frac{1}{8}$" square rod fits in the Vee grooves and presses against the sandwich beam, both at the top and bottom of the beam, tightening being done by B.A. bolts, as shown in the figure. There is line contact at the ends of the sandwich beam specimen, due to the square rods and anti-clastic bending is prevented.

In order to provide least restraint at the ends, the spring steel strips chosen were as flexible as possible and consistent with other static and dynamic requirements. Two types of strips (thickness .0108" and .015") were tried, the higher thickness being used for heavy specimens. For chosen dimensions of a strip, approximate calculations were carried out as described below in order to check that the effects due to rotational inertia of ends and flexibility of supports were not of any significant consequence. For a few sandwich specimens intended to be supported by the strips, calculations were done in order to determine the natural frequencies of vibrations of spring steel strips,

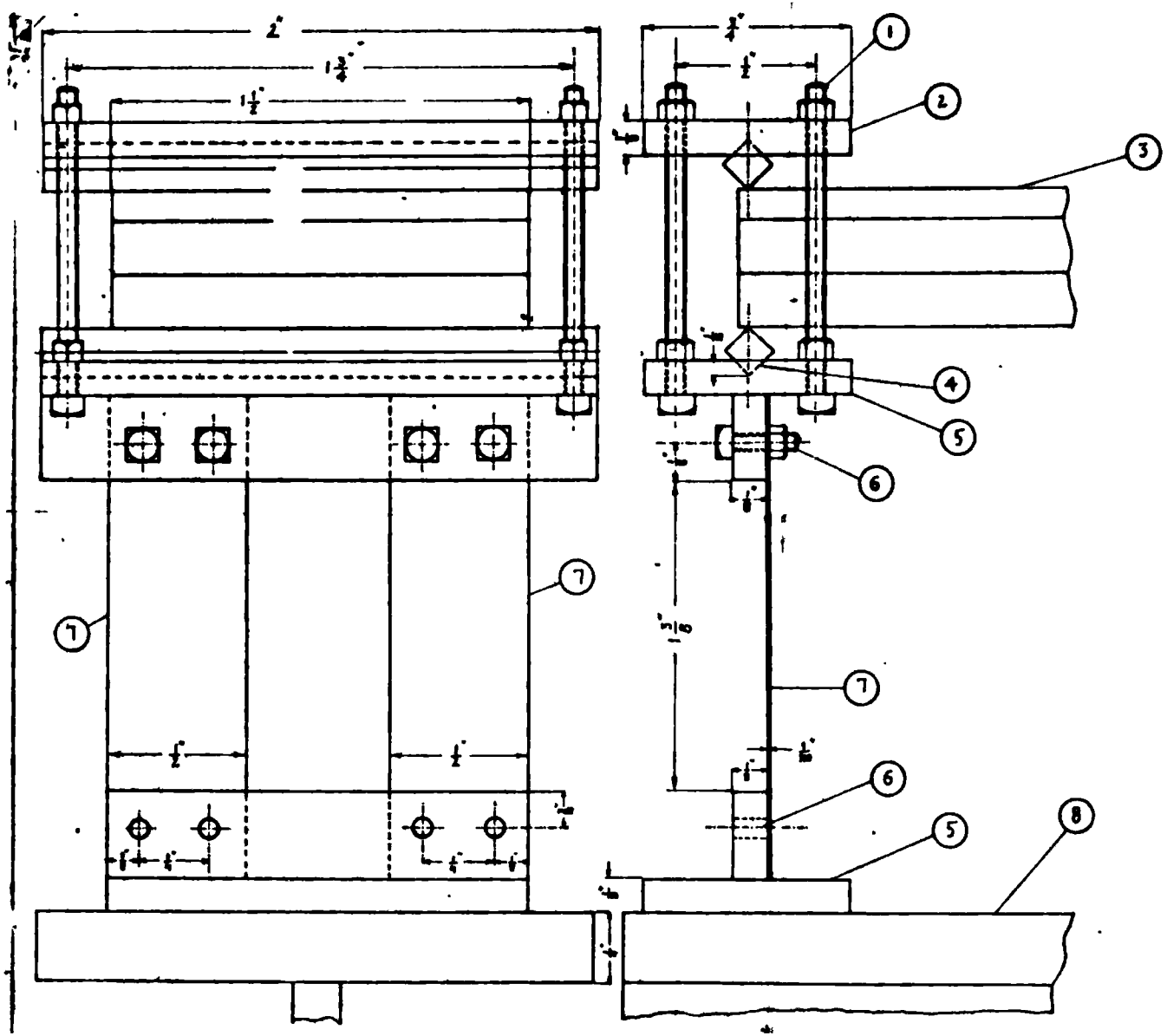

S.NO	PART	NO OFF	REMARKS
8	I SECTION	1	4"·2"·36" AL. ALLOY
7	SHEET	2	SPRING STEEL
6	BOLTS	8	NO 8 B.A.
5	TEE SECTION 3/4" · 3/8"	2	BRACED TO PART NO 8 AL. ALLOY
4	BAR	2	GROUND M.S.
3	SANDWICH BEAM	1	36" LONG
2	PLATE	1	AL. ALLOY
1	BOLTS	4	NO 9 B.A.

END SUPPORT

FIG II.14

the fundamental frequency in transverse direction of strips was below 15 c.p.s. The vibrations along the longitudinal directions of strips were not of any consequence below 2000 c.p.s., so that the motion of each end of the sandwich beam could be taken as equal to that of the I-beam for frequencies below this value. Taking the rotation of the strips to be the same as that of beam ends, the stresses induced in the spring steel strips were checked to be below the elastic limit of the material, at resonance for a given sandwich specimen. Further, the rotational moment due to the inertia of end supports, was computed for high frequencies, taking the expected value of end roation of a chosen specimen by the application of maximum thrust of the exciter. The rotational moment so obtained was seen to be less than 1% of the maximum bending moment at the middle of the beam specimens under those conditions.

In order to check whether the ends actually corresponded to the simply supported ones as desired, the natural frequencies of vibrations of a solid aluminium beam were experimentally determined and compared with the theoretical values. The results are given in table T-12 and there is seen to be good agreement between the theoretical and experimental values of natural frequencies. Also, high values of Q factors obtained, indicated that damping due to

possible friction at the ends was negligible. It was also checked whether any extraneous vibrations due to flexibility of drive rod, or soft spring cord supporting arrangement of the I-beam etc., existed. Either these existed below or above the frequency range of testing or these occurred at frequencies (e.g. at 100 c.p.s.) at which resonances of sandwich specimens were not likely to occur. It was also checked whether both the sandwich beam ends receive the same motion at various frequencies. This motion was seen to be same as that of the I-beam ends in the frequency ranges considered.

TABLE T-12

Resonant Frequencies of Aluminium Alloy Bar

Size: 30" x 1½" x 0.1875"

Theoretical values	18.55 c.p.s.	166.5	462.5
Experimental values	18.70	166.6	456.7
Percentage difference of experimental values over theoretical ones	+0.809	+0.0601	-1.252

i) Q-factor: at 18.70 c.p.s. = 936 approximately.

ii) Q-factor: at 166.6 c.p.s. = 1150 approximately.

N.B.:- The Q factor was very high and hence an exact value was rather difficult to determine.

VI.B.3 : Preparation of Specimens

In the multilayered sandwich configurations, the various elastic and viscoelastic layers were joined together by using adhesives. Araldite (AV 100 together with hardener HV 100) was used for this purpose. Before applying the adhesives, the layers were thoroughly cleaned, and degreased by using Acetone and carbon tetrachloride. The metal layers were roughened by sand blasting and etching. The etching agents were same as given in Section VI.A.2. After applying the layer of adhesive on each layer, these were joined and the sandwich specimen was kept under load, uniformly distributed along its length for 24 hours, allowing the adhesive to set. The load was applied by placing the sandwich under a thick 1" steel bar and using a Denison universal machine for loading or by using 'C' clamps and dead weights. During loading, slipping of layers started to occur, because of the slippery adhesive. This was prevented by locating the various layers with respect to one another by using guiding metal pins or strips at each end. The ends of a few thermocouples were inserted in the viscoelastic layer so that these remained in position after the setting of the adhesive.

VI.B.4 : Testing Procedure

Vibration response tests on sandwich beams involved

the following measurements at various frequencies of excitation.

1) End displacement amplitude of the sandwich beam.

2) Absolute values of displacement amplitudes at various locations on the sandwich beam.

3) Phase difference between motion at any point of the beam and that at the ends.

4) Measurement of temperature of the viscoelastic layers.

A block diagram of the testing equipment is shown in Fig. VI-15. A Muirhead 2 phase decade oscillator was used to drive the Derritron vibrator through a power amplifier. A 250 w. power amplifier was used for 50 lb. thrust exciter and 1 Kw one for the 250 lb. thrust exciter in the alternative arrangement. The instrumentation used for the measurement of displacement amplitude was same as in Section VI.A, viz. inductance pick up, along with the gauge oscillator and F.M. amplifier. A description of these is given in SectionsVI.A.1 and VI.A.2. The calibration for these pick ups was done optically by the use of reading microscopes. The phase measurement between the two displacement signals, was done by the use of the phase calibrated resistance or directly from an ellipse, as described in Section VI.A.2. The temperature was measured as described in Section VI.A.2 by the use of copper constantan thermocouples.

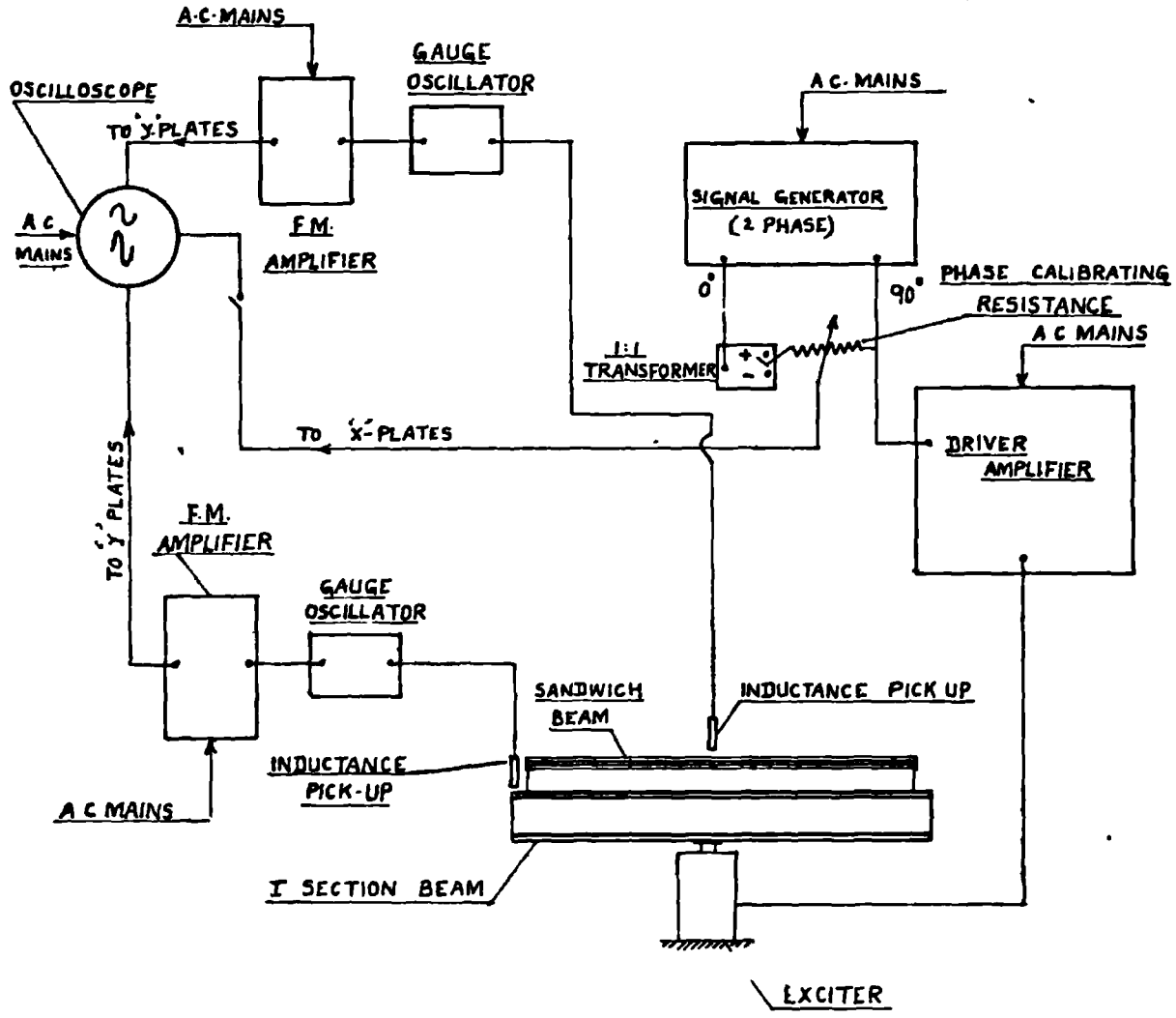

SANDWICH BEAM - DYNAMIC RESPONSE TEST

BLOCK DIAGRAM OF TESTING EQUIPMENT

FIG VI-15

The tests were carried out by first calibrating the inductance pick ups for the given setting of the gap between the pick up and vibrating object. A given height of signal on the oscilloscope was calibrated against the reading on a reading microscope. Next, the resonant frequency corresponding to a mode was approximately detected. Near this frequency, the change in phase between the end displacement and any other point on the beam say the middle of the beam, was rapid. This was seen to occur around a phase angle of 90^{o} in most specimens. Around this frequency, the frequency was varied in small steps and the end displacement amplitude was kept constant at each. The absolute value of the amplitude of vibration of middle of the beam and the phase angle relative to the ends were measured. Near each resonant frequency (i.e. when the amplitude at middle of beam was maximum), the amplitudes of various points on the beam were measured by shifting the central pick up. The temperatures of the viscoelastic layers were measured along the length of the beam at every step.

VI.B.5 : Test results on Specimens

The details of various specimens tested are given in Table T-13. The specimens were chosen in such a way that all the layers were different from one another and the

parameters were different in the various specimens. Also, the system damping expected at resonances of the specimens was checked in order to ensure that it was the optimum in some cases while far from the optimum in the others. Three layered specimens S_3, S_4 and S_5 have nearly the same total thickness but different layer thicknesses. Specimen M_2 was made from specimen S_2 by adding 2 layers, one being viscoleastic and the other being elastic. 5 three layered, 2 five layered and 2 four layered specimens have been tested experimentally.

The experimental results for 3 layered specimens S_1 to S_5 are given in Figs. VI-16 to Fig. VI-20, for 5 layered specimens M_1 and M_2 in Figs. VI-21 and VI-22 and for 4 layered specimens D_1 and D_2 in Figs. VI-24 and VI-25. For each specimen, the results corresponding to first two resonances have been given. Since the excitation is of symmetrical type, resonances corresponding to only odd numbered modes (i.e. n=1,3) were excited. The results are given in the form of resonance graphs, i.e. graphs of ratio T^A of the amplitude of vibration of middle of beam to the end amplitude against frequency and its phase $(\theta^A)M$ with respect to beam ends. Also, the amplitude distribution along the beam length at a frequency close to the peak displacement frequency, are plotted. The experimental results are plotted as points in the above mentioned Figs.,

TABLE T-13

Details of Specimens

Specimen No.	Layer No.	Layer Thickness (in.) and Material	Remarks
S_1	1	0.099 Al.Alloy	i) The layer arrangement for specimen S_1 to S_5 corresponds to that in Fig.II-2(a), for M_1 and M_2 to Fig. IV-1(a), and for D_1 and D_2 to Fig. V-1(a).
	2	0.1424 PVC-Sheet A	
	3	0.1875 Al. Alloy	
S_2	1	0.065 M.S.	
	2	0.131 PVC-Sheet A	
	3	0.127 Al. Alloy	
S_3	1	0.099 M.S.	
	2	0.126 PVC-Sheet B	
	3	0.125 Al. Alloy	
S_4	1	0.035 Al. Alloy	ii) Al. Alloy used is SiC $\frac{1}{2}$H.
	2	0.13 PVC-Sheet B	
	3	0.1875 Al. Alloy	
S_5	1	0.099 Al. Alloy	iii) PVC-Sheets A and B are made of Velbex PVC formula 629/0900. Material properties for sheet B are given in section VI.A while those for sheet A, which are somewhat different, are taken from [59].
	2	0.130 PVC-Sheet B	
	3	0.125 Al. Alloy	
M_1	1	0.099 M.S.	
	2	0.13 PVC-Sheet B	
	3	0.099 M.S.	
	4	0.13 PVC-Sheet B	
	5	0.099 Al. Alloy	
M_2	1	0.065 M.S.	
	2	0.131 PVC-Sheet A	
	3	0.127 Al. Alloy	
	4	0.130 PVC-Sheet B	
	5	0.035 Al. Alloy	
D_1	1	0.064 Al. Alloy	iv) Length of each specimen = 30" Breadth = $1\frac{1}{2}$"
	2	0.027 Admiralty Yellow Compound	
	3	0.189 Modified Butakon 40:60	
	4	0.188 Al. Alloy	
D_2	1	0.128 Al. Alloy	
	2	0.02 Velbex PVC (formulae 521/2127)	
	3	0.191 Modified Butakon 40:60	
	4	0.064 Al. Alloy	

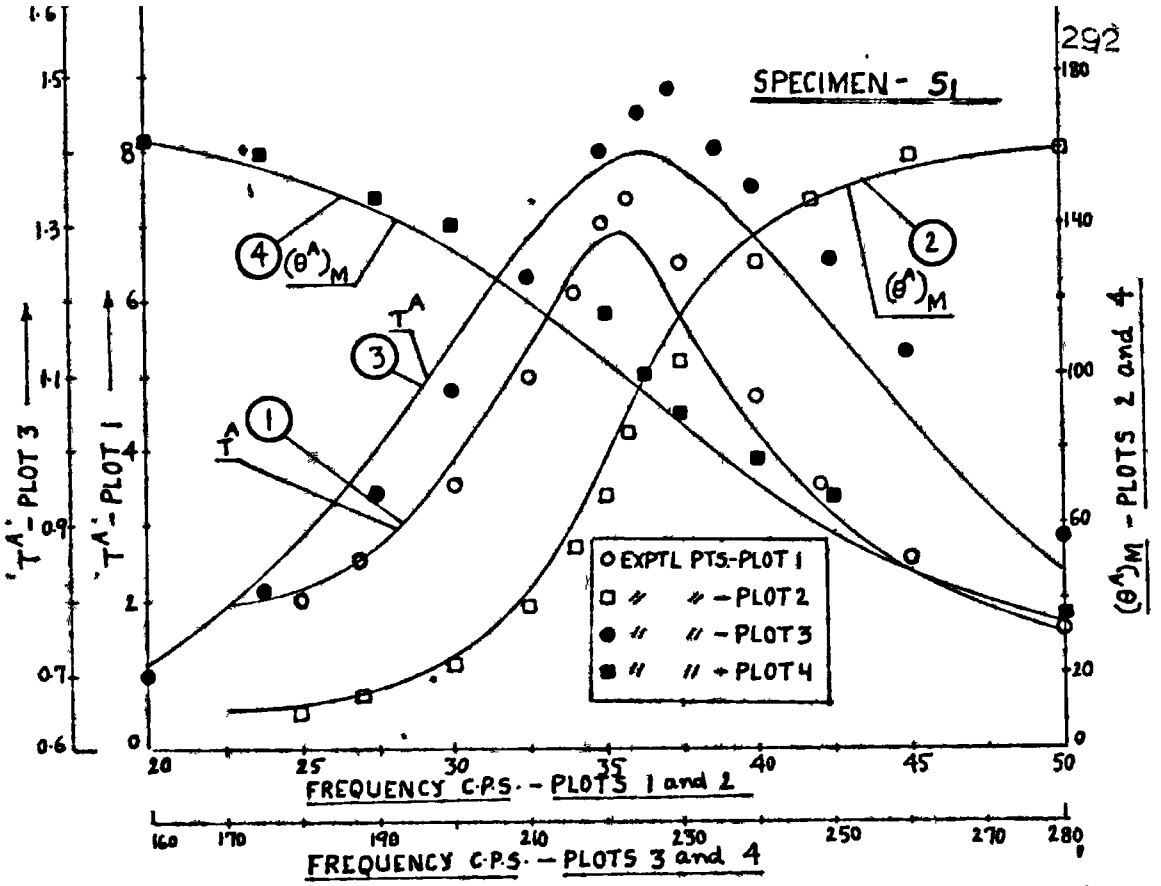
SPECIMEN - S1
(θ^A)M
T^A
EXPTL PTS-PLOT 1
// // - PLOT 2
// // - PLOT 3
// // - PLOT 4
T^A - PLOT 3
T^A - PLOT 1
(θ^A)M - PLOTS 2 and 4
FREQUENCY C.P.S. - PLOTS 1 and 2
FREQUENCY C.P.S. - PLOTS 3 and 4

FIG. VI-16 (a)

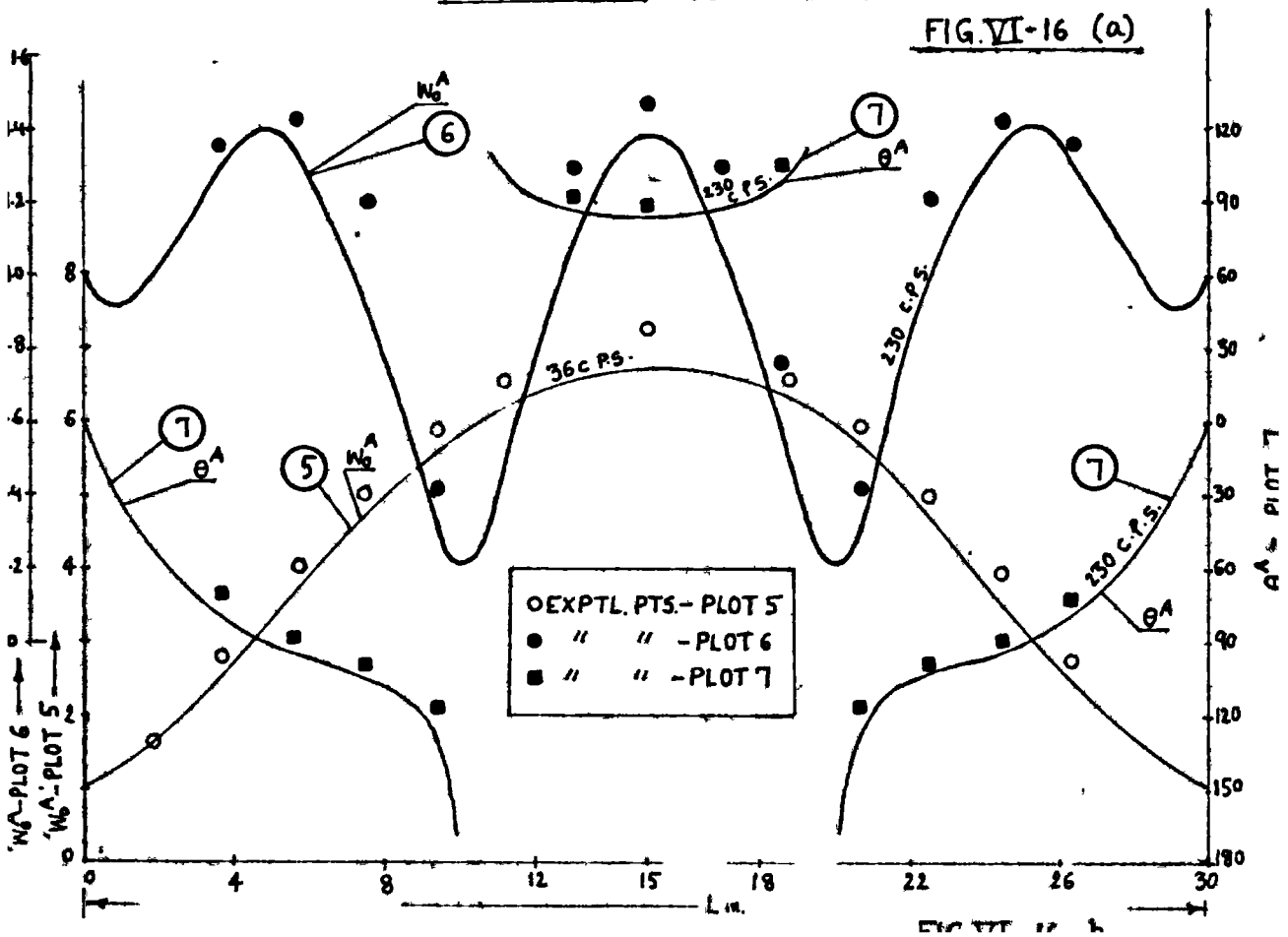
W0^A
θ^A
230 C.P.S.
36C P.S.
EXPTL. PTS.- PLOT 5
// // - PLOT 6
// // - PLOT 7
W0^A - PLOT 6
W0^A - PLOT 5
θ^A - PLOT 7
L in.

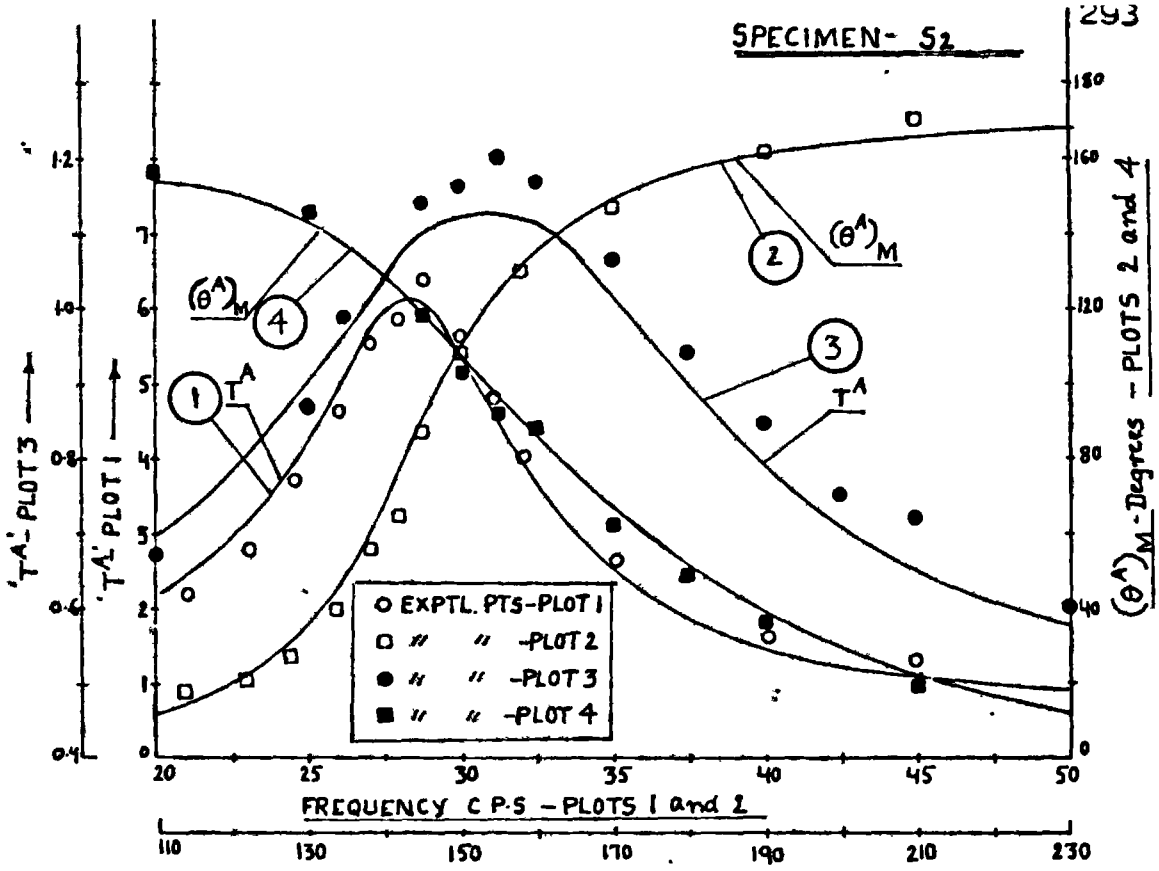

FIG. VI-17 (a)

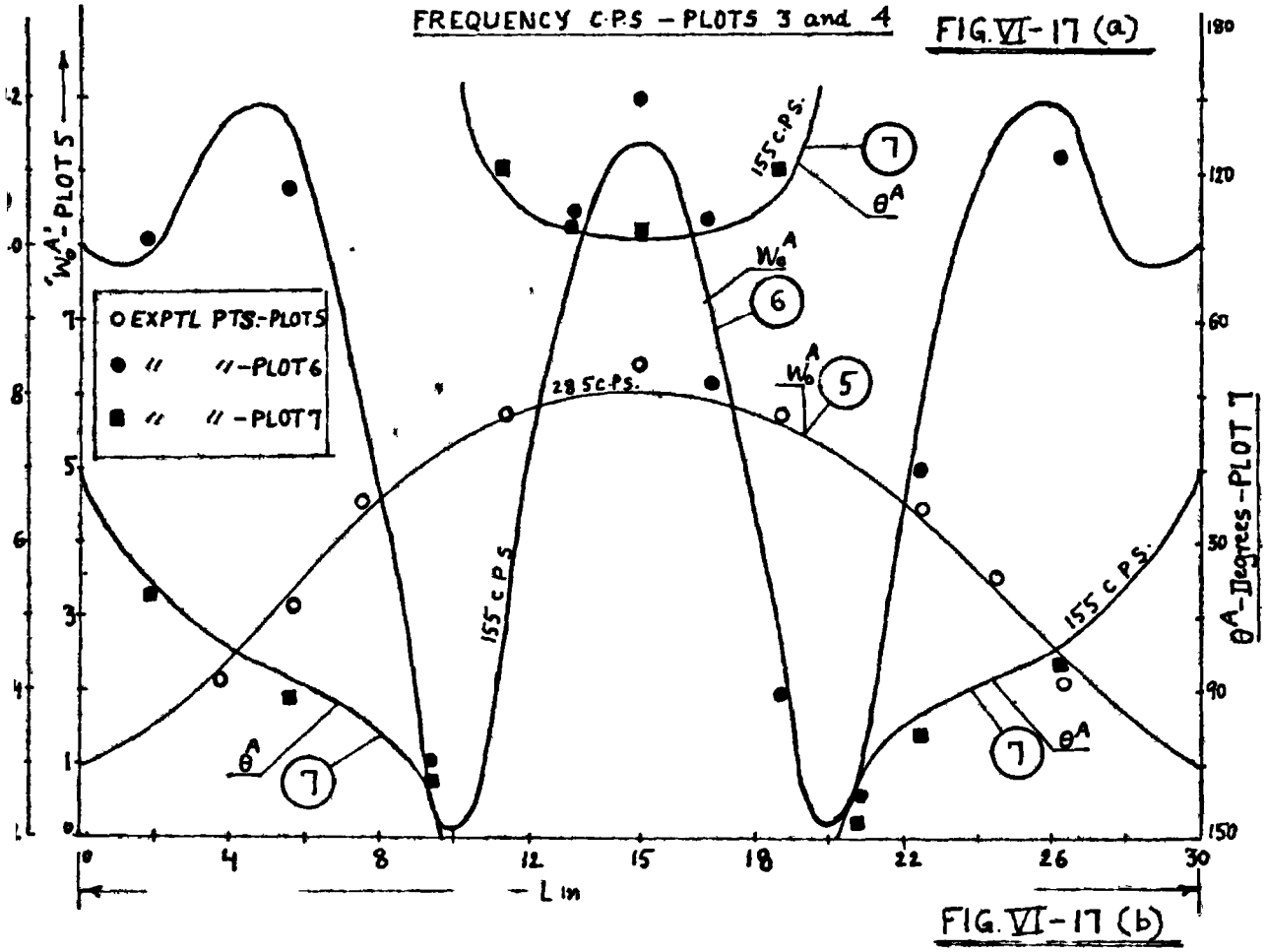

FIG. VI-17 (b)

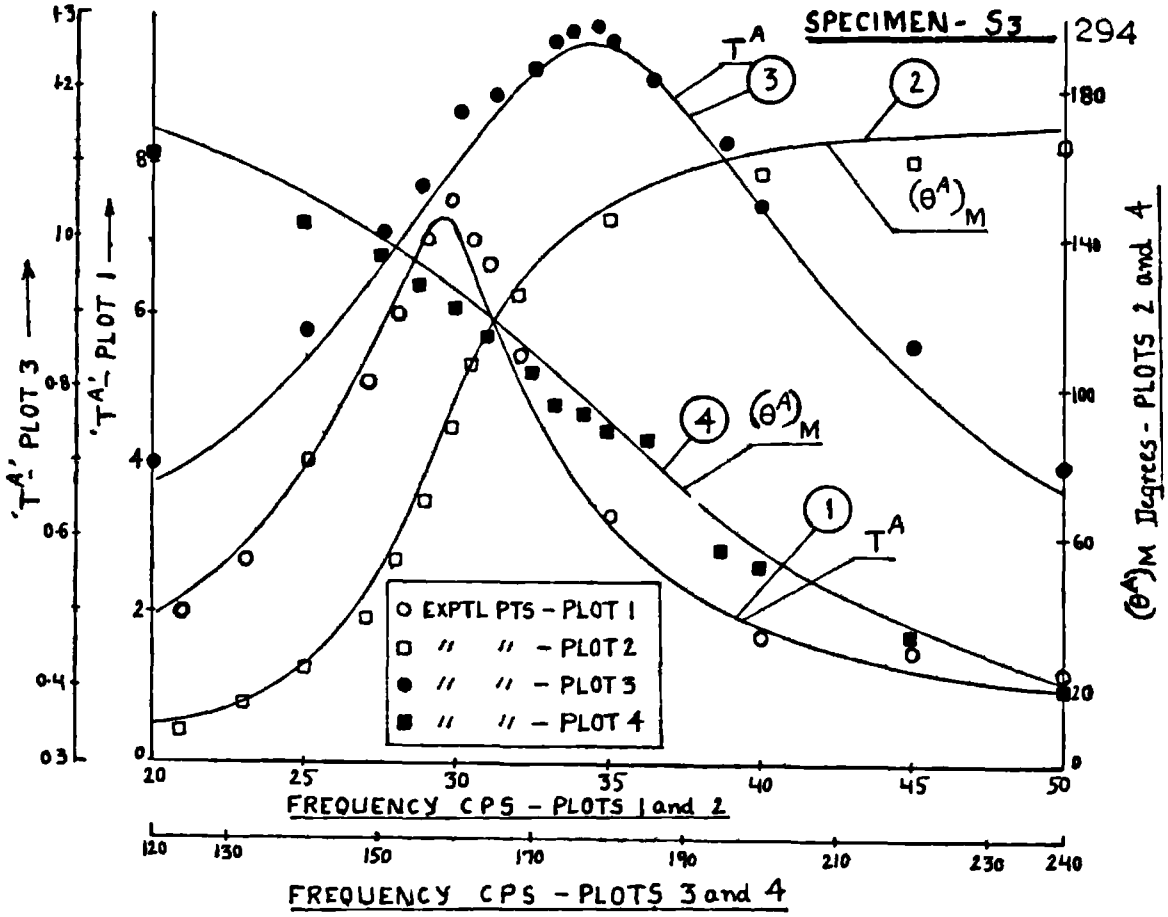

FIG. VI - 18 (a)

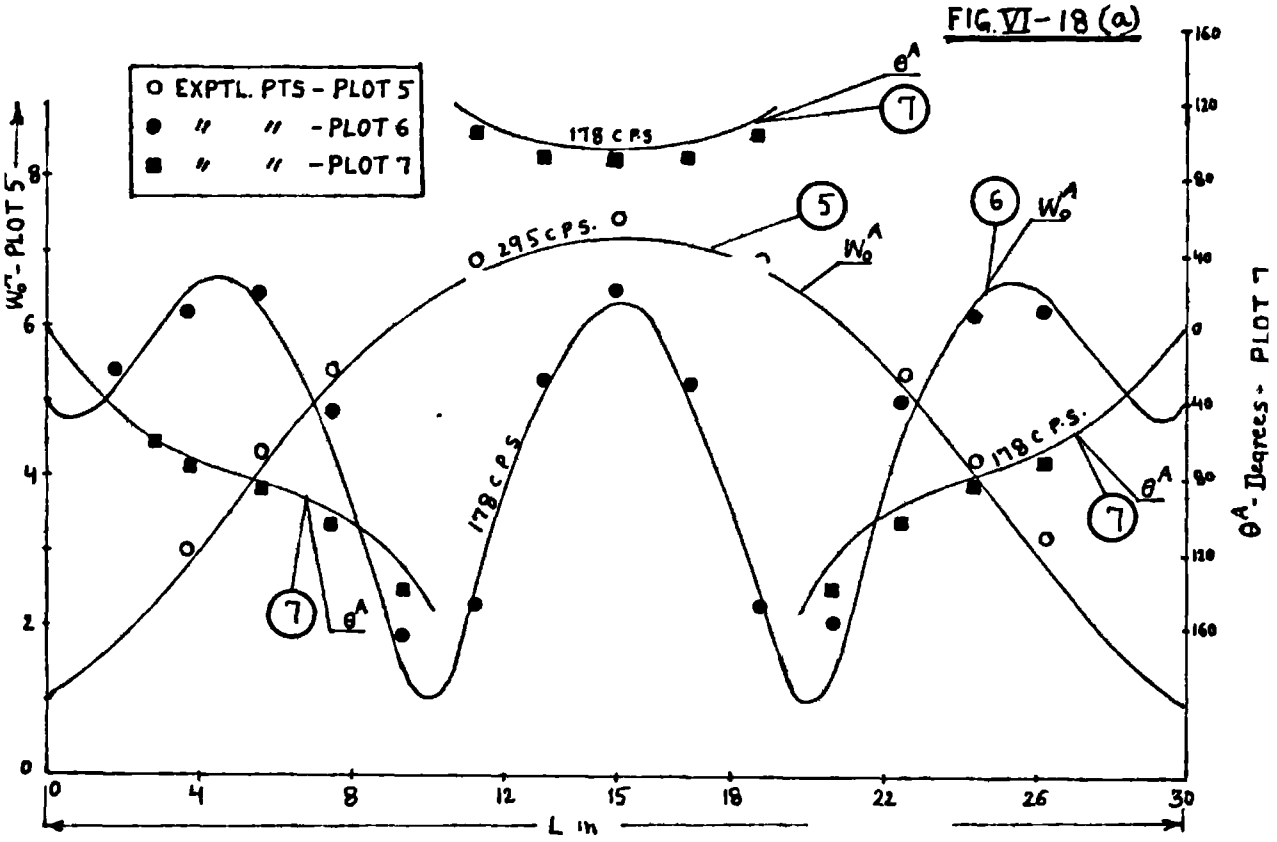

FIG. VI - 18 (b)

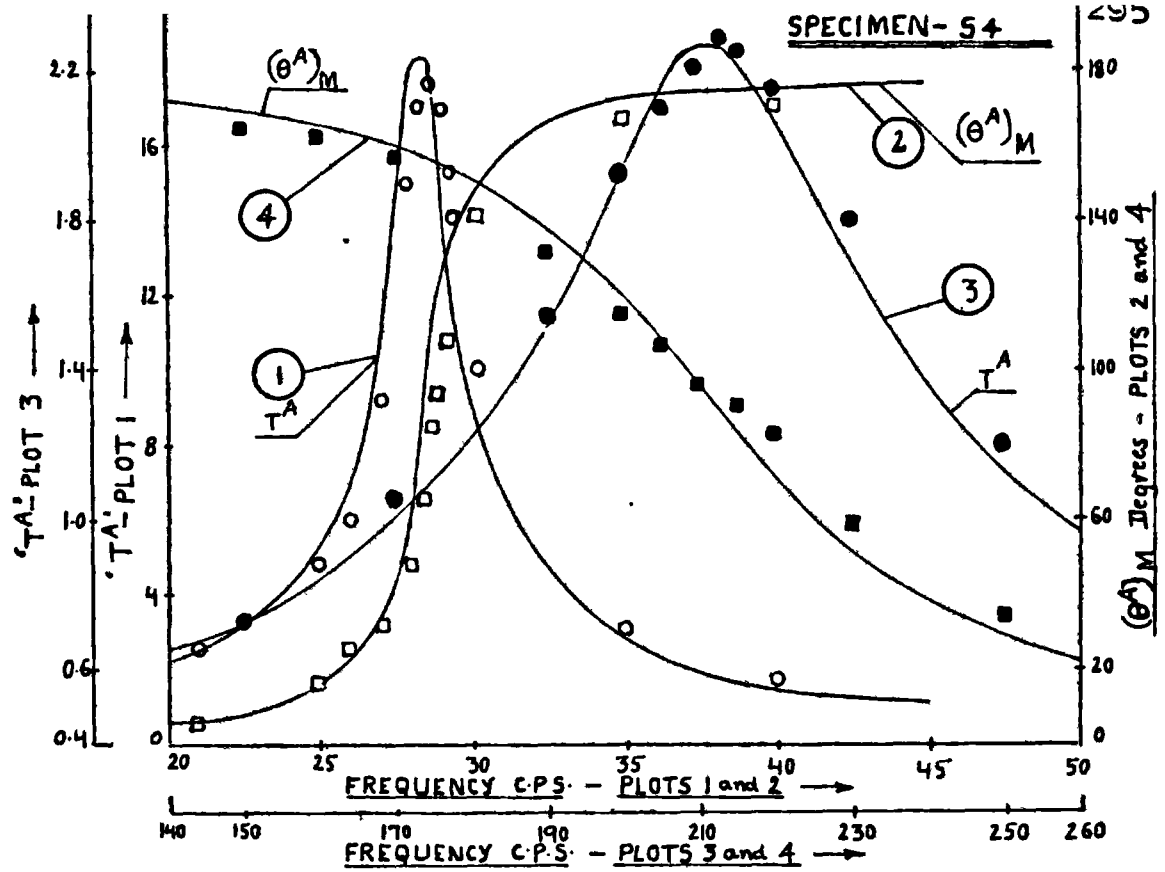

FIG. VI- 19 (a)

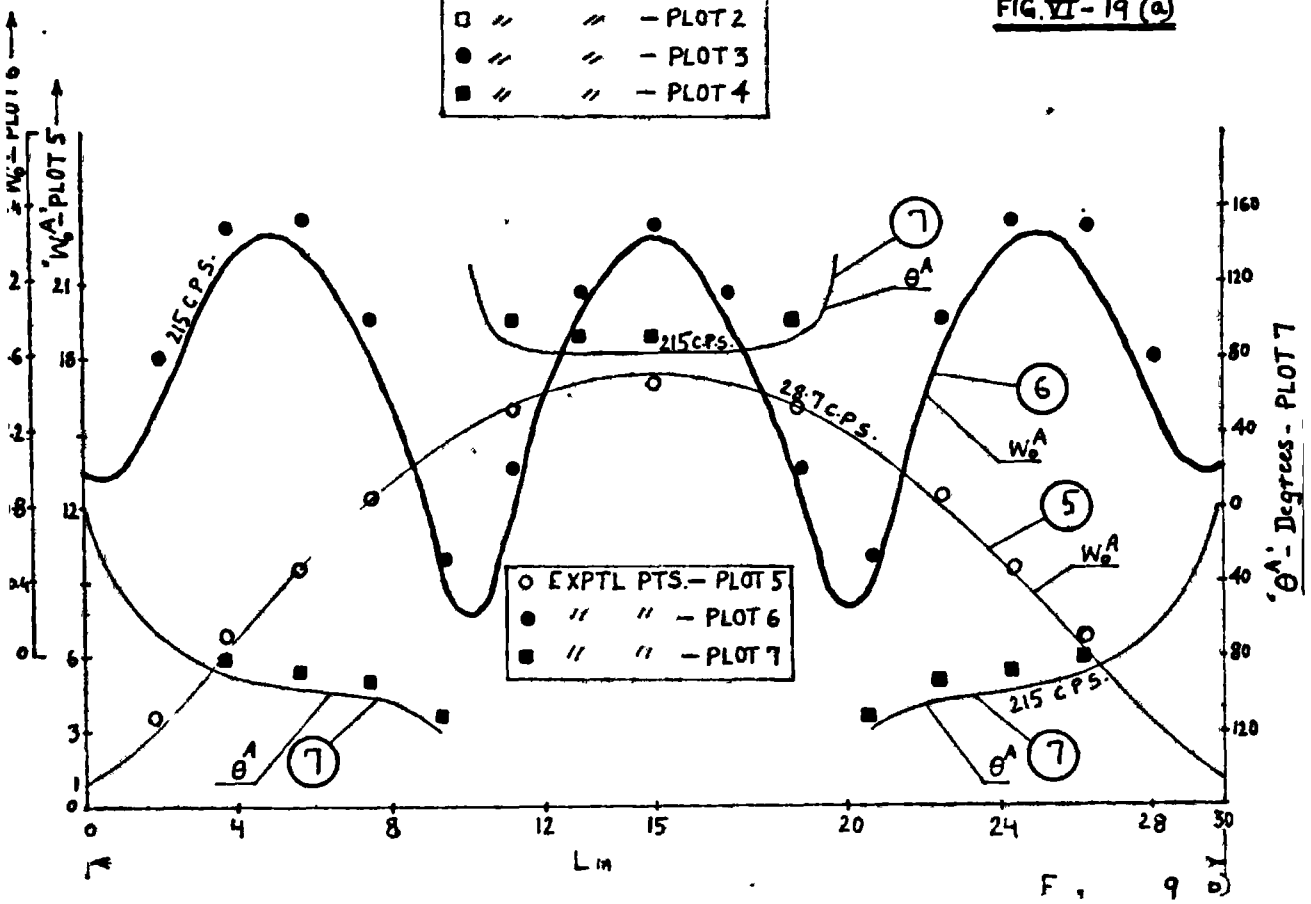

F. 9 b)

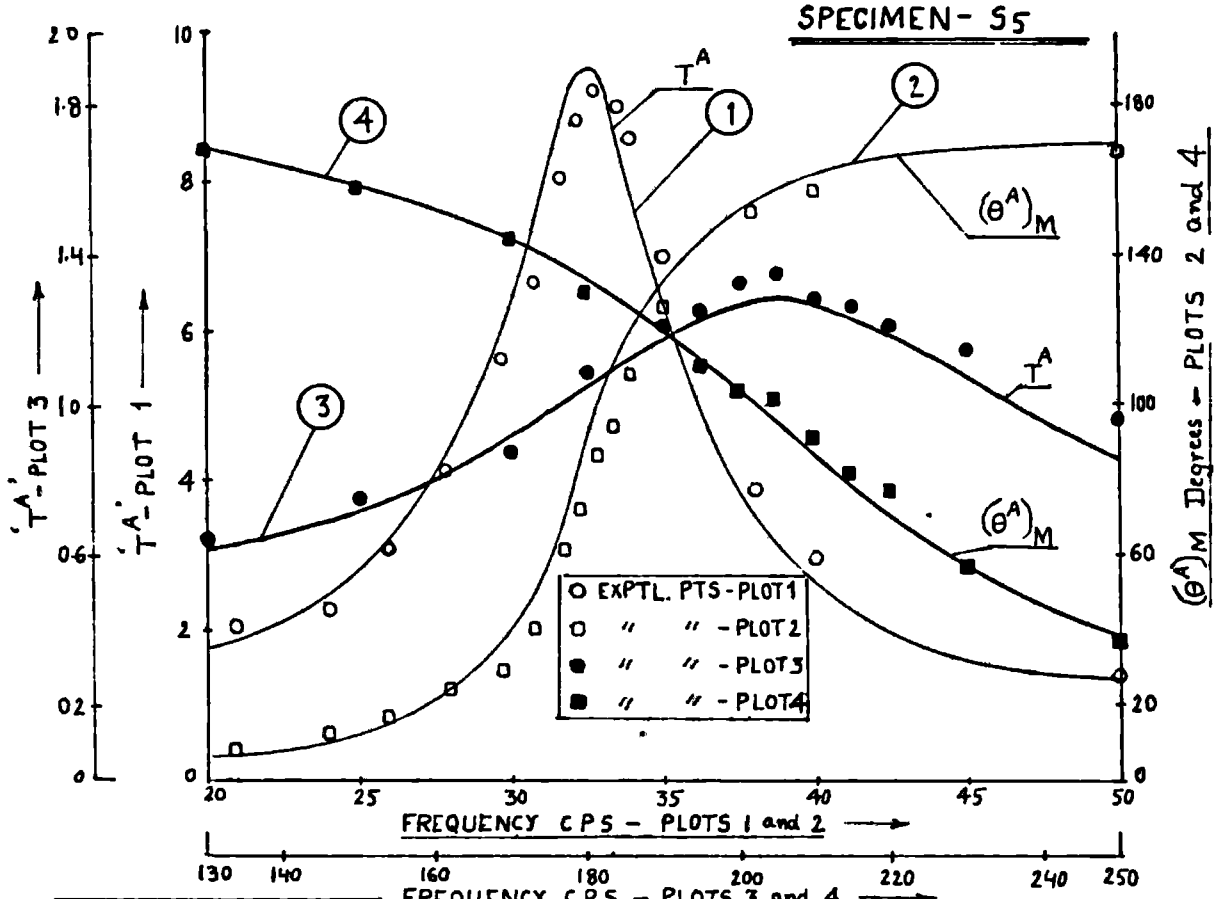

FIG. VI-20(a)

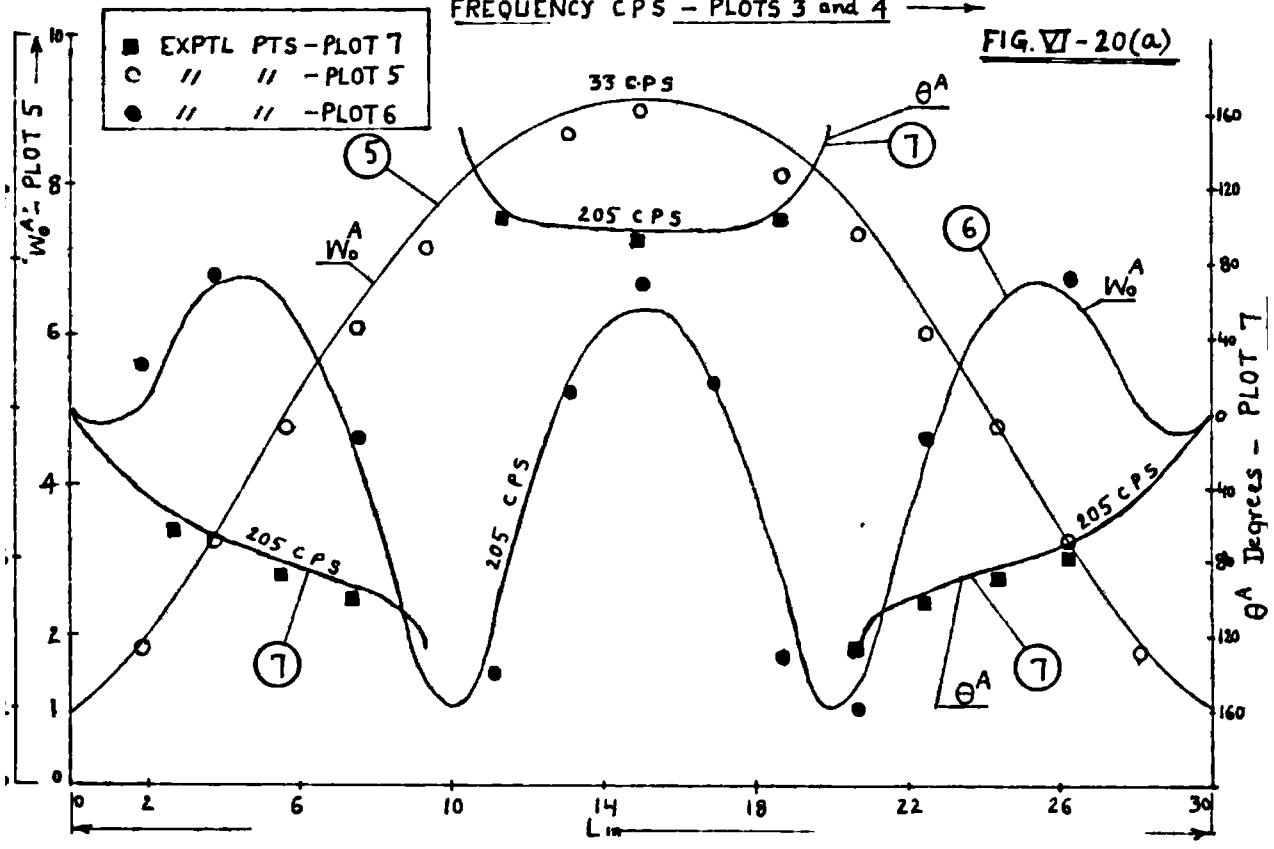

FIG. VI-20(b)

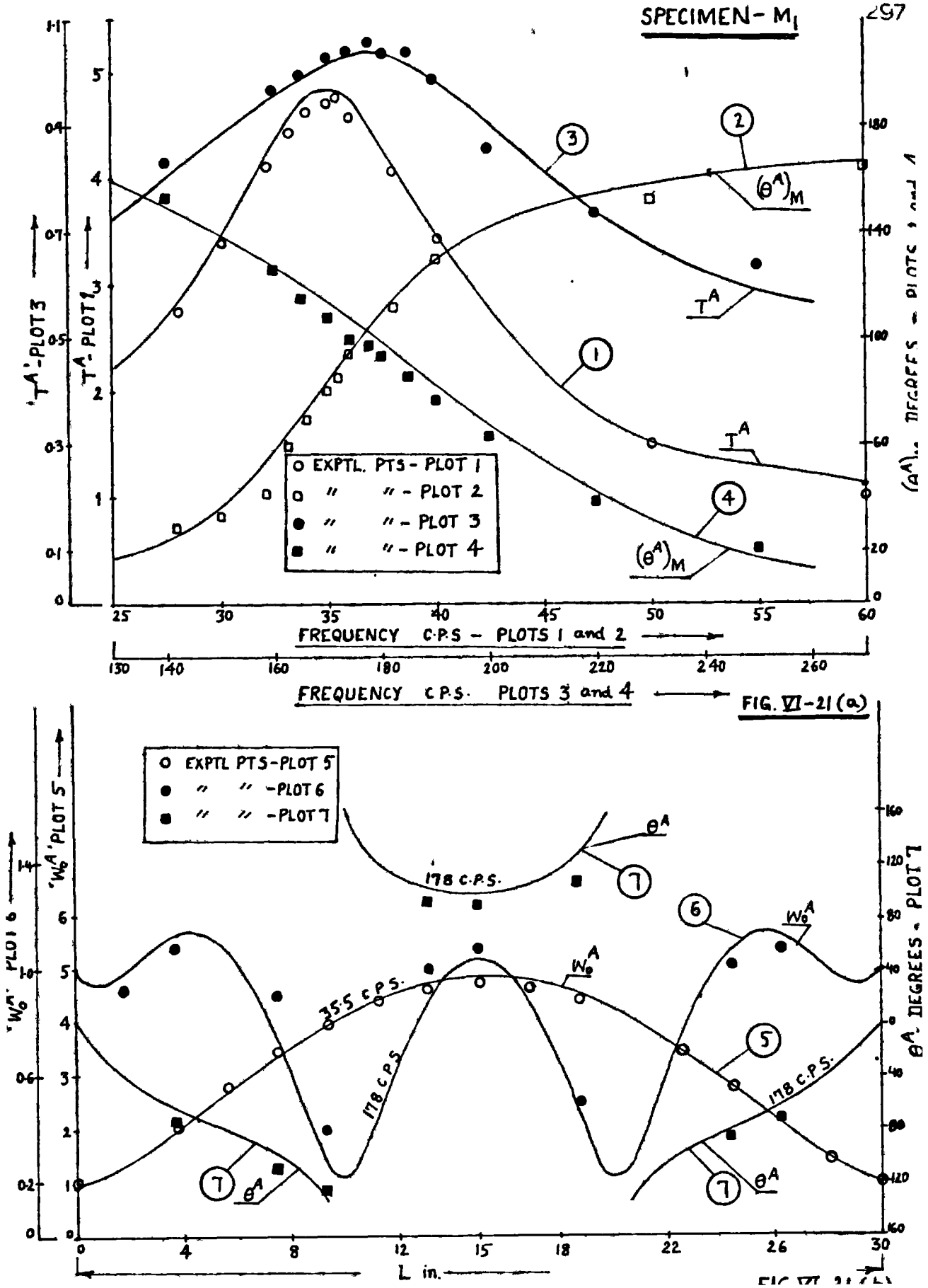
SPECIMEN - M1
EXPTL. PTS - PLOT 1
" " - PLOT 2
" " - PLOT 3
" " - PLOT 4
FREQUENCY C.P.S - PLOTS 1 and 2
FREQUENCY C.P.S. PLOTS 3 and 4
EXPTL PTS - PLOT 5
" " - PLOT 6
" " - PLOT 7
178 C.P.S.
35.5 C.P.S.
L in.

FIG. VI-21 (a)

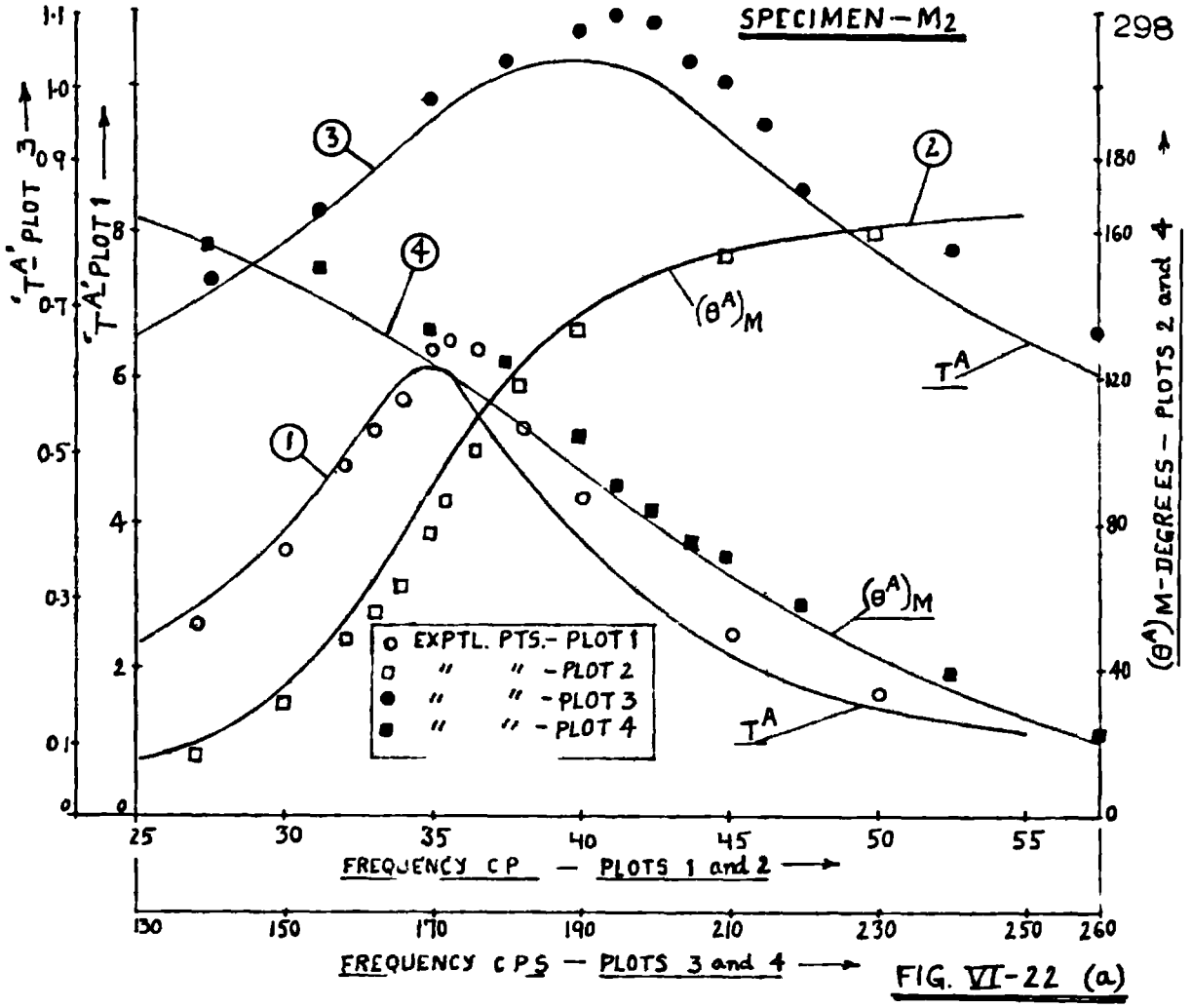
SPECIMEN – M2
298
'T^A' PLOT 3
'T^A' PLOT 1
(θ^A)M – DEGREES – PLOTS 2 and 4
EXPTL. PTS.- PLOT 1
" " - PLOT 2
" " - PLOT 3
" " - PLOT 4
(θ^A)M
T^A
FREQUENCY CPS – PLOTS 1 and 2
FREQUENCY CPS – PLOTS 3 and 4

FIG. VI-22 (a)

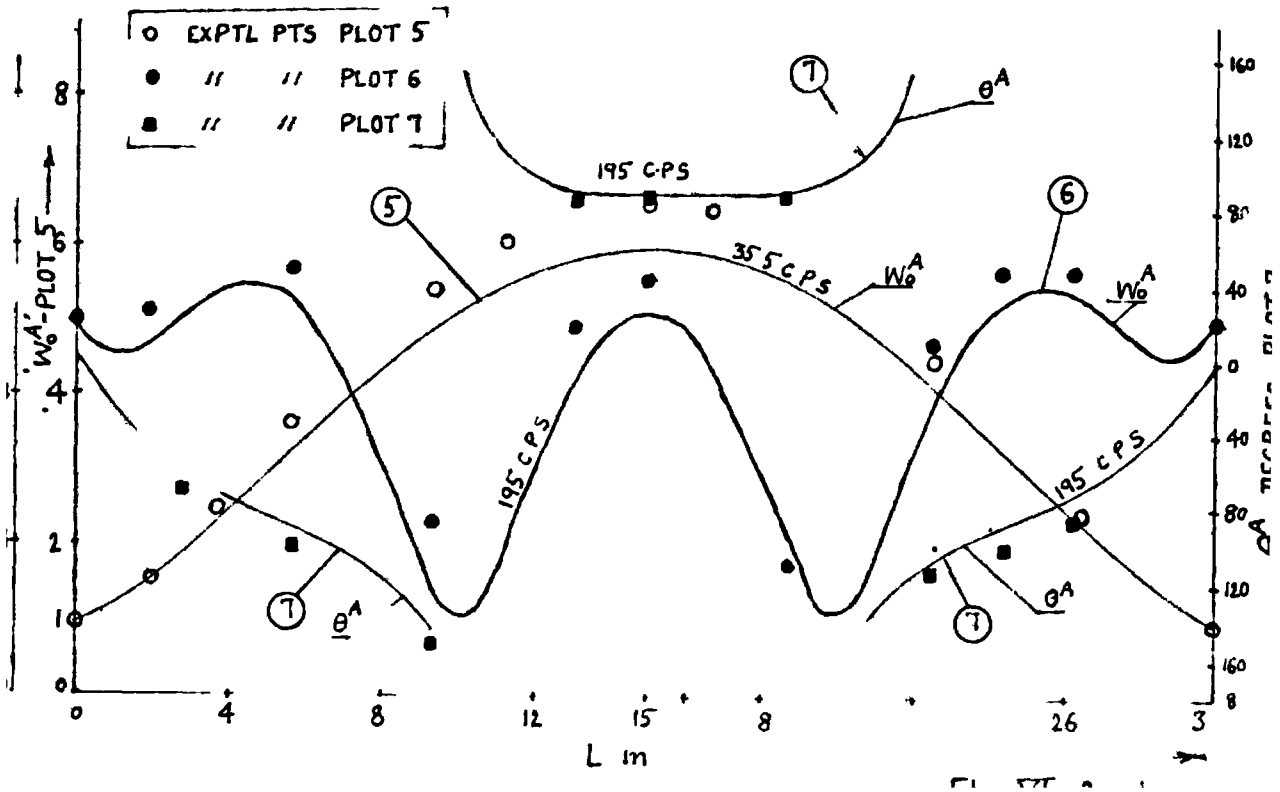
EXPTL PTS PLOT 5
" " PLOT 6
" " PLOT 7
'W0^A' PLOT 5
195 C.P.S
355 C.P.S
W0^A
θ^A
L in

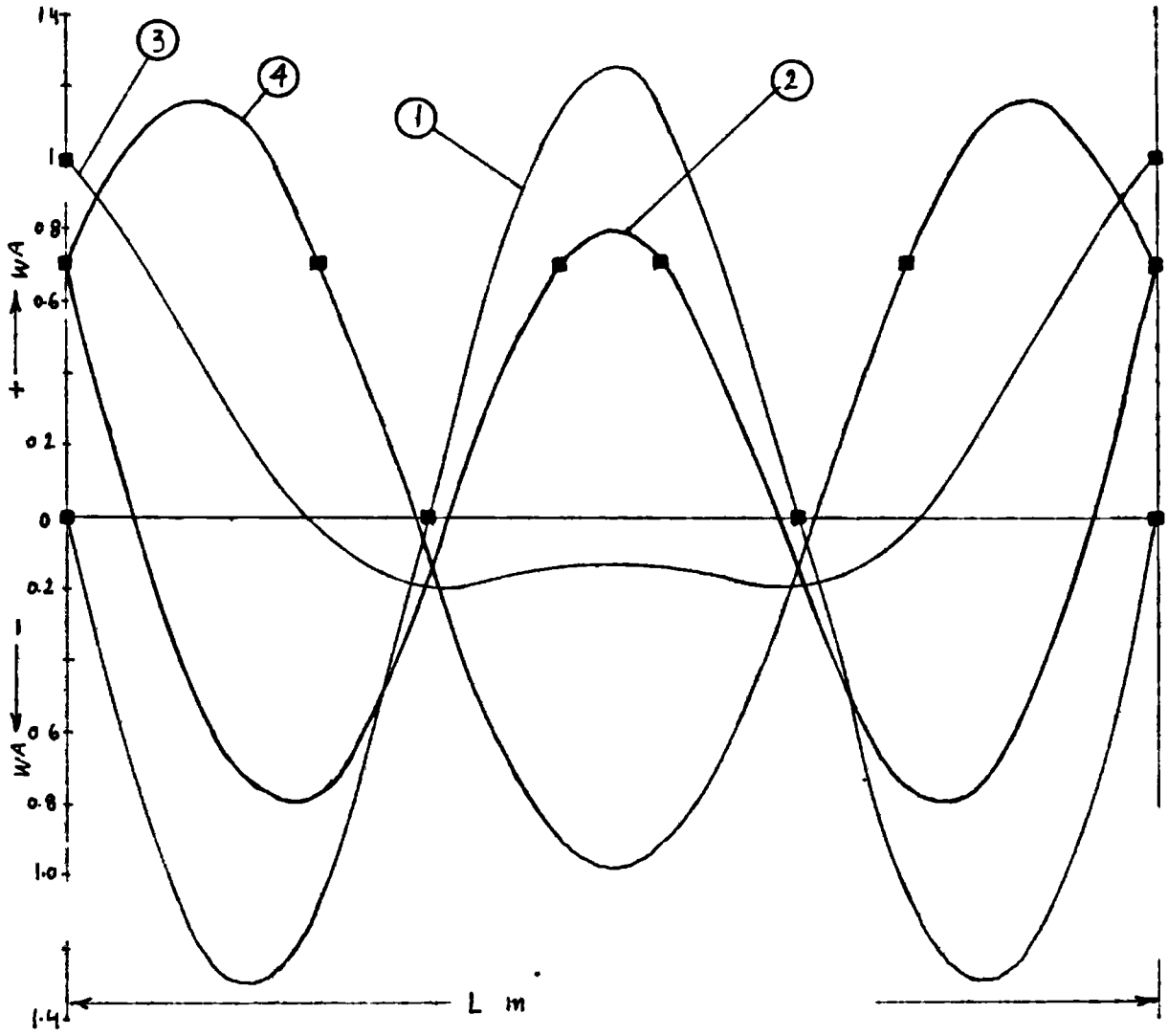

(1) MOTION AT INSTANT 'T_1

(2) // // // T_2

(3) // // // T_3

(4) // // // T_4

■ NODE

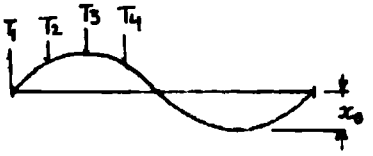

END EXCITATION

$x_0 = 1$

FREQUENCY- 178 CPS

SPECIMEN - S3

FIG. VI-23

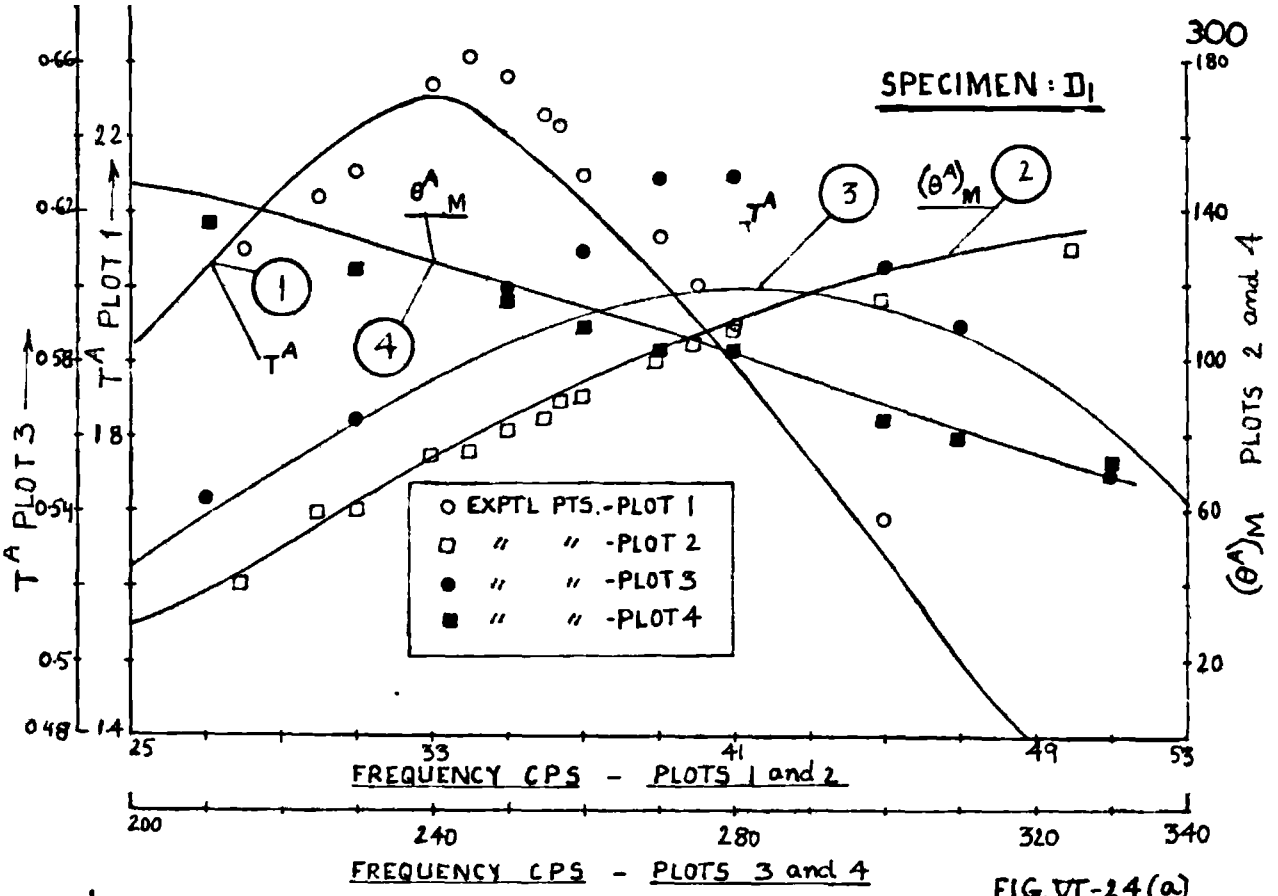

FIG. VI-24 (a)

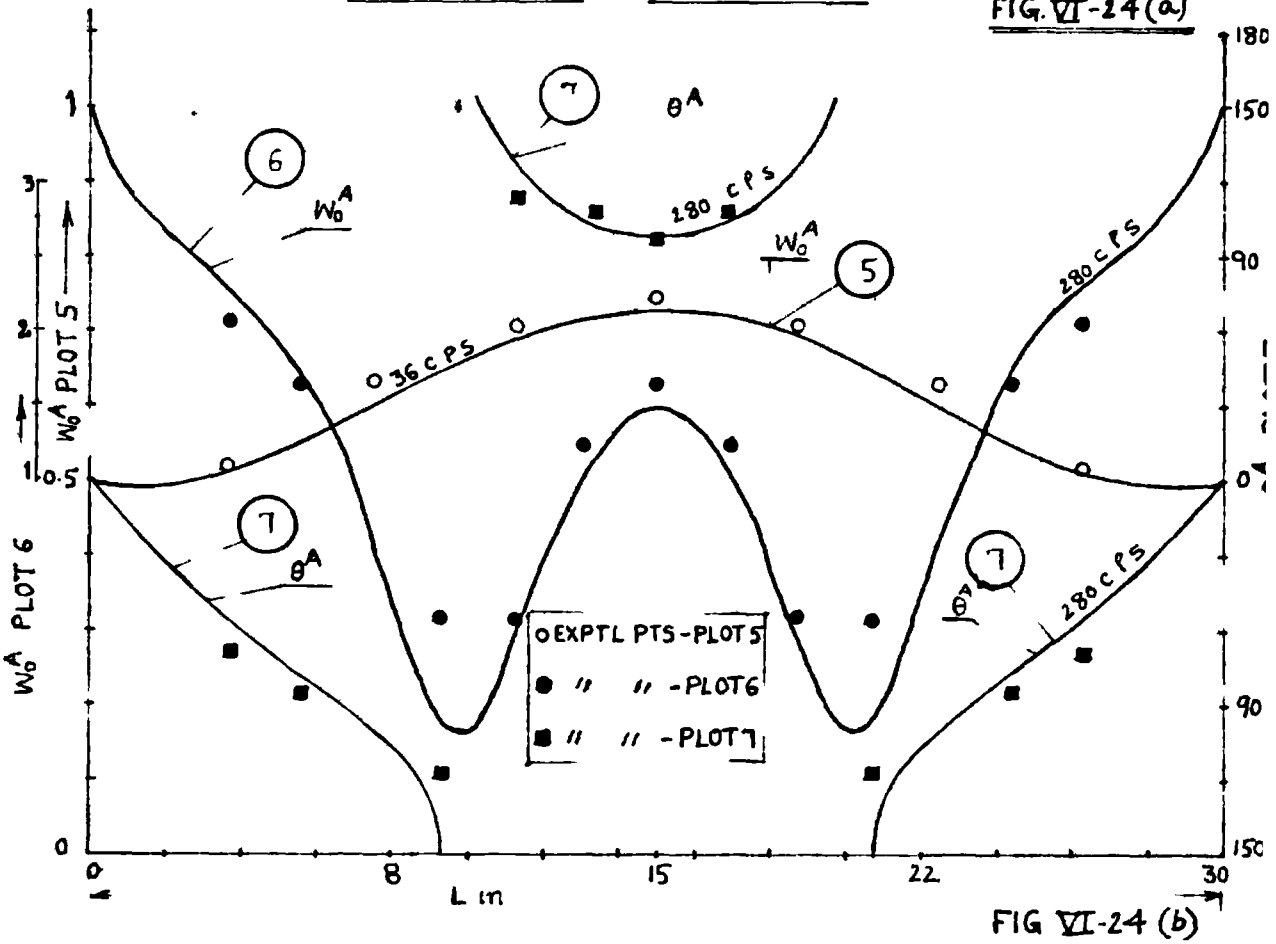

FIG VI-24 (b)

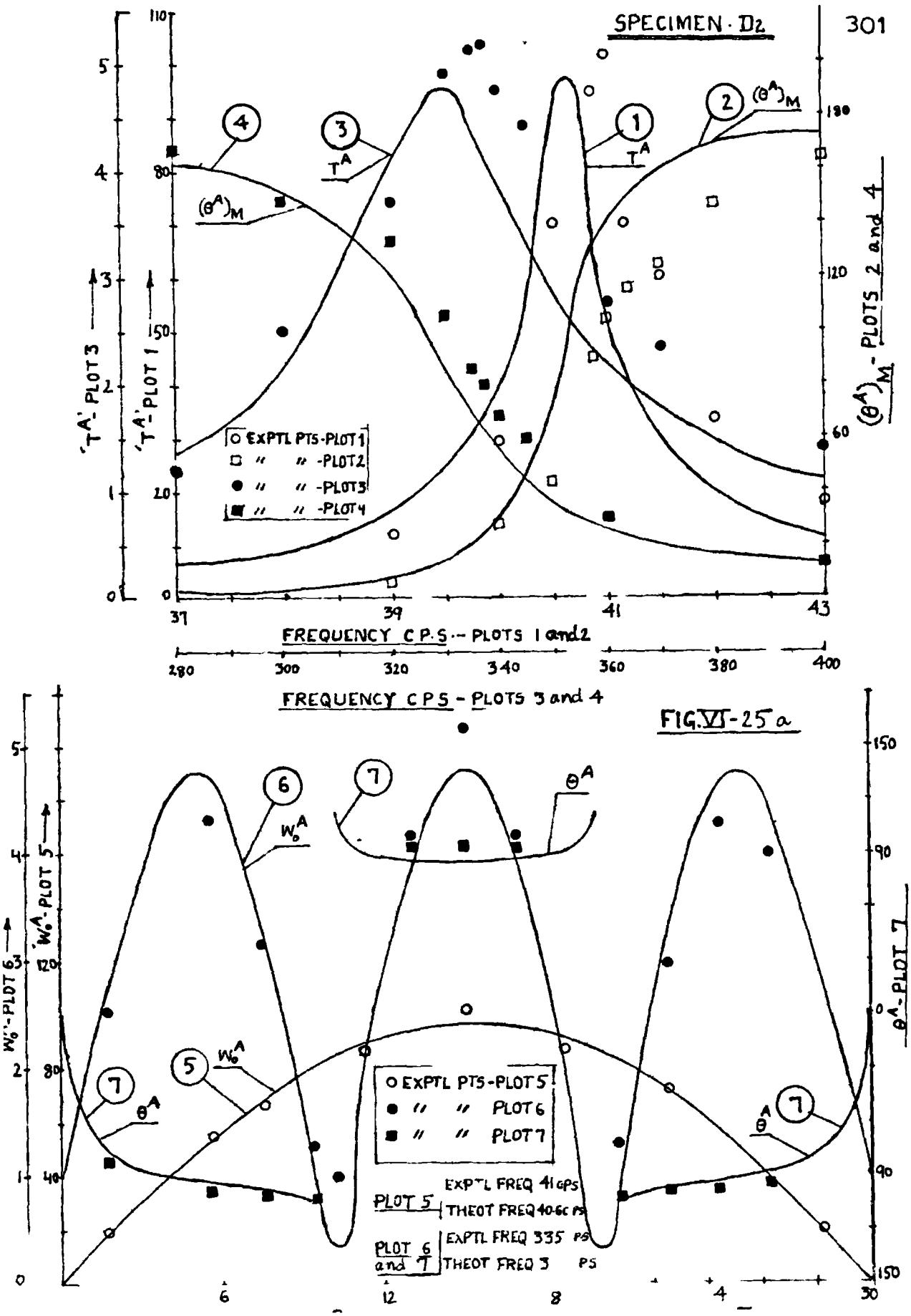
SPECIMEN · D2
'T^A'- PLOT 3
'T^A'- PLOT 1
(θ^A)_M - PLOTS 2 and 4
EXPTL PTS-PLOT 1
// // -PLOT 2
// // -PLOT 3
// // -PLOT 4
FREQUENCY C P S -- PLOTS 1 and 2
FREQUENCY C P S - PLOTS 3 and 4
W_o^A - PLOT 6
'W_o^A'- PLOT 5
θ^A - PLOT 7
EXPTL PTS-PLOT 5
// // PLOT 6
// // PLOT 7
PLOT 5 EXPTL FREQ 41 CPS THEOT FREQ 40·6 CPS
PLOT 6 and 7 EXPTL FREQ 335 PS THEOT FREQ 3 PS

FIG. VI-25 a

for comparison with theoretical values, which are plotted as continuous curves.

Further experimental testing details regarding 'x_o' and temperature at each resonance are given in Table T-16 in Appendix 9.

VI.B.6 : Calculations of Theoretical Values and Comparison with Experimental Results

After carrying out experimental test on each specimen, the corresponding theoretical values were computed on the Atlas digital computer, using equations of previous Chapters. These values were plotted in Figs. VI-16 to VI-25. Corresponding to the temperature of testing, as given in Appendix 9, and each frequency, the properties of viscoelastic layers used, were read from the properties graphs given in Section VI.A. Using these properties and equations of previous Chapters, the displacement amplitude and phase angle at the middle of the beam at various frequencies were computed. Also, the amplitudes of vibration of various points along the beam length at frequencies close to the peak displacement frequencies were calculated. These frequencies generally were taken to be the experimental frequencies, at which measurements were taken during the response tests. However for specimen D_2, a slight shift in the frequencies near the peak displacements, changed the displacement amplitudes considerably

because of low system damping and hence frequencies employed for theoretical computation of amplitude distribution along the beam length were taken to be different from the corresponding experimental frequencies. Similarly, the distribution of phase along the beam length was plotted but this was done only for the higher resonance, since at the first resonance, there was no appreciable change in phase along the beam length except in the vicinity of the ends.

For 3 layered beams, equations given in Section III.D corresponding to analysis I were used, for 5 layered ones, equations of Section IV.A.2 and for 4 layered specimens, equations of Section V.A.2 were employed for the theoretical computations.

It may be observed from the graphs of the material properties of the viscoelastic materials tested that these materials are reasonably linear exeept at higher frequencies. In most theoretical computations, the linear theory was employed wherein the stress strain law is taken as linear or amplitude independent. This appeared to be reasonable, since in the experimental testing, the end displacement amplitudes involved were small and resulted in small shearing strains. This could be checked quantitatively for the specimens. The properties graphs are seen to be reasonably flat in the region of small strains.

At higher frequencies especially, the maximum shear strain amplitude in the viscoelastic layers were found to be small since end displacement amplitude 'x_o' is small. In general, the procedure adopted was as follows: Values of material shear modulus and loss factor corresponding to $\gamma_o = 0$ were read in at various frequencies and temperature, according to the experimental conditions. After computing theoretically for the sandwich specimen, the maximum shear strain at beam ends was noted. The properties corresponding to an average value (half the maximum) were finally used for the theoretical computations. In most cases, this value of strain was found to lie in the flat portion of the properties graphs.

The values of Young s modulus for metal layers were determined on a Universal testing machine using Huggenberger Extensometer 5027. The values were found to be as under:

For Aluminium alloy sheet, $E_i = 0.99 \times 10^7$ lb/in^2

For M.S. sheet, $E_i = 2.995 \times 10^7$ lb/in^2

For viscoelastic materials, the value of E_i was taken $= 3G_i$, as for an incompressible material and loss factor in extension β_i, was taken equal to that in shear η_i.

A comparison of theoretical and experimental values in Figs. VI-16 to VI-25, in general shows reasonable agreement between the two. The difference between the peak displacement amplitudes is less than 10 percent and for

the corresponding frequencies, it is around 1-2 percent. Moreover, both the resonance plots for the middle of the beam and amplitude distribution along the length at frequencies close to peak amplitudes, are seen to be similar. This appears to be reasonably satisfactory agreement, keeping in view the various sources of error, which are possible in the experimental testing.

In most cases, the experimental points for maximum T^A, i.e. the amplitude ratio at middle of beam, are above the theoretical points, except in low frequency resonance of specimens S_4, S_5 and M_1, and the experimental resonant frequencies are higher than the theoretical ones. The specimens made by gluing various layers together, if not perfectly made, as assumed in the theory, may result in less damping actually than theoretically anticipated and may account for the experimental points to be above the theoretical ones. Since the damping due to end-supports was found to be negligible, as discussed in Section VI.B.2, the error at low frequency resonance of specimens S_4, S_5 and M_1 may be due to some other reasons discussed later.

The experimental resonant frequencies may be expected to be higher than the corresponding theoretical values, because of possible end restraint. A shift in frequency might also occur if the oscillator scale shows wrong readings or the temperature has not been accurately measured,

by the use of thermocouples. The oscillator frequency was checked by measuring time period accurately up to 10^{-6} second on a Beckman Digital Counter. The thermocouple readings were checked by an accurate thermometer, which could read up to $0.2^{o}C$. Both these were found to be satisfactory.

For very low displacement amplitudes below $0.5x10^{-3}$ in., the optical calibration may be in error by up to 5%. Also, the accuracy with which the viscoelastic material properties have been determined in the shear test, will also be reflected in the comparisons between experimental and theoretical values of virbation response. Table T-14 shows the effect of changing G_2 and η_2 separately by $\pm$ 10% from the standard values, for one of the specimens. The percentage change in the peak value of T^A and corresponding frequency are given. In fact, an appreciable change in peak T^A occurs due to change in η_2 and frequency F_p is affected considerably by a change in G_2.

The non-linearity in viscoelastic material propetties can be a source of error, though in the present case, as discussed earlier, the results for vibration response are not expected to be affected significantly. This was checked for the low frequency resonance of specimen S_3 and results are given in Table T-15. The theoretical results of Section III.G were employed and the non-linear constants

TABLE T-14

Effect of change of G_2 and $_2$ in Specimen S_3

	S.No.	G_2 lb/in^2	$\eta_2 = \beta_2$	Frequency F_p' corresponding to Peak Displacement (T^A)- c.p.s.	Peak T^A	% Change in frequency 'F_p' from Values in (1)	% Change in peak T^A from values in (1)	Remarks
First Resonance	1	1560	0.528	29.5	7.2907			Standard value for comparison
	2	1716	0.528	29.9	7.708	+1.355	+5.73	10% increase in G_2
	3	1404	0.528	28.8	6.895	-2.37	-5.42	10% decrease in G_2
	4	1560	0.581	29.55	6.827	+0.17	-6.35	10% increase in η_2
	5	1560	0.475	29.23	7.908	-0.915	+8.47	10% decrease in η_2

TABLE T-14 (Cont.)

Second Resonance	1	2820	0.629	178	1.2674			Standard value for comparison
	2	3100	0.629	183.3	1.2738	+2.98	+0.506	10% increase in G_2
	3	2540	0.629	172.4	1.2642	-3.144	-0.253	10% decrease in G_2
	4	2820	0.692	179.4	1.1675	+0.786	-7.89	10% increase in η_2
	5	2820	0.566	177	1.3905	-0.562	+9.72	10% decrease in η_2

TABLE T-15

Comparison of Non-linear and Linear Solutions for Specimen S_3

Frequency c.p.s.	Linear solution		Non-linear solution	
	w_o^A at middle of beam	θ^A degrees	w_o^A at middle of beam	θ^A degrees
28	1.244×10^{-2}	53.527	1.247×10^{-2}	53.80
29	1.414×10^{-2}	71.862	1.417×10^{-2}	72.379
30	1.424×10^{-2}	94.41	1.421×10^{-2}	95.01
30.5	1.358×10^{-2}	104.668	1.353×10^{-2}	105.189
31	1.267×10^{-2}	113.401	1.262×10^{-2}	113.817

N.B. 1 In above, x_o 1.94×10^{-3} in.

2) For linear solution, properties corresponding to $\gamma_o = 0$ have been used.

3) θ^A is the phase difference between motion at the middle of the beam and the end motion.

for Velbex P.V.C. were taken from Fig. VI.7. It is seen from Table T-15, that the results for the amplitude and the phase obtained from non-linear theory are different from the linear solution by less than 1 percent.

In actual specimens, the adhesive for joining various layers, has finite thickness and might have an effect on experimental results. This effect is expected to be more pronounced for specimens M_1, M_2, D_1 and D_2, in which more layers are involved.

VI.C: Discussion

It may be seen from the foregoing sections that the theoretical results of previous Chapters, for vibration response of 3 layered, 5 and 4 layered unsymmetrical beam configurations, have been in reasonable agreement with experimental tests, which were carried out at low frequencies. The properties of the various viscoelastic materials were separately determined in shear in the frequency range of interest, taking due account of frequency, temperature and strain. These properties were subsequently employed in the theoretical evaluation of vibration response under experimental conditions of vibration response tests.

The properties of the viscoelastic materials are very susceptible to change, by a variation in the thermal history

of the materials, during manufacture, as could be seen by the difference in results of sheets A and B of Velbex P.V.C. and 2 samples of Butakon 40/60. A factor which could not be taken account of in the present work, is the size effect of the specimens. The viscoelastic samples used in the properties test were smaller than those used in making the sandwich beams.

The shear set up is reasonably convenient to work with and accurate for common viscoelastic materials but for very stiff and low damping ones, it tends to be difficult to obtain very accurate results, because of the difficulty in measuring very small displacement amplitudes and very low values of phase difference between displacement and force signals, to the desired accuracy. A further limitation is at the higher frequencies when the material tends to be considerably stiff and a large force is required to cause shear in the specimens. Under these conditions, it becomes difficult to keep the fixing device for the fixed end of the specimens perfectly stationary, because of its flexibility. In such cases, some other method of measuring properties like the vibrating reed method may be employed. The vibrating reed method does not require as elaborate a testing equipment as is required in the shear test but has its own limitations. It is not possible to specify the strain dependence of material

properties since the strain varies throughout the sample of the vibrating reed. Also, it cannot be used for very soft materials. The calculation procedure is tedious as given in [66]. Error might occur in the resonant frequency of the sample because of the practical difficulty of obtaining a fixed root for the cantilever specimens. For materials with heavy damping, it is difficult to detect the resonant frequency exactly and determine the damping. The use of a number of specimens of different lengths, giving properties at resonance frequency of each is tedious and likely to give scatter in results.

The vibration response tests on laminated beams were intended for comparison of theoretical and experimental results of displacement response. Although the specimens were selected so that the various physical parameters were different and the system damping could be varied from optimum to non-optimum conditions, the variation was restricted due to the practical difficulty of obtaining viscoelastic materials of any desired properties. The set-up for vibration response test was used between 20 to 400 c.p.s. For higher frequencies, the thrust required to vibrate the I-beam with measurable amplitudes, is large. The supporting spring steel strips have to be designed accordingly to carry a large thrust. This may necessitate the use of thicker springs, which may cause large end restraint

In the present work, only odd numbered resonances were encountered since the excitation was a symmetrical one. By moving the ends in antiphase, it will be possible to excite the even numbered resonances. But that would require changes in the arrangement of the present set-up. Only the first two odd numbered resonances were included in testing the specimens since the higher ones occurred at higher frequencies, at which properties of viscoelastic materials were not known.

For various specimens, the graphs of amplitude distribution along beam length for the first and second resonance (corresponding to n=1 and 3 respectively) have been drawn. For the higher resonance, there are rapid changes in the values of amplitude and phase along beam length and phase changes from leading to lagging at some points along the length, and hence the curves for phase angle are shown discontinuous in the various graphs.

At various locations on the beam, the maximum values of displacements occur at different instants, because of high damping in each system. The theoretical values of instantaneous displacements at various instants for specimen S_3 were plotted in Fig.VI-23, for the second resonance in order to indicate the nodes in the beam. Taking the node as the point having same motion as the beam ends, the number of nodes in the beam is seen to vary from instant to instant.

CHAPTER VII

VII.A : General Discussion and Conclusions

3 layered configuration: The equations describing the flexural vibrations of 3 layered rectangular sandwich beams, with the parameters of each layer different from those of other layers, have been derived in Chapter II. These equations may be employed for determining the dynamic response of any 3 layered sandwich beam, with a viscoelastic core. The solution has been determined for simply supported end conditions and the procedure is outlined for beams with other types of boundary conditions. Different assumptions have been employed for analysis I and II, the outer faces in analysis I being taken to bend like Bernoulli-Euler beams, while analysis II is more general. For sinusoidal vibrations, the solution for analysis II may be used for a layered beam in which any of the three layers may be viscoelastic, by taking the appropriate elastic moduli as complex. In each analysis, there is no limitation on the stiffness of the core and longitudinal and rotary inertia effects have been included, in addition to the transverse inertia effect.

The above mentioned equations have been used in Chapter III for studying the dynamic behaviour of the 3 layered configuration. The damping effectiveness of the

configuration has been analysed by studying the influence of various parameters of the system. The damping is seen to be optimum only at a certain value of the shear parameter, which is a dimensionless parameter involving core shear modulus, modal number of vibrations and physical parameters of one of the faces. The shear parameter has been defined from the point of view of convenience, so that the parameters of each layer could be separated and their influence studied separately. The optimum value of shear parameter, as given in Section III.A.2 depends on the core thickness ratio ($\theta_{2.3}$), face thickness ratio ($\theta_{1.3}$), ratio of Young s modulus of the faces ($\alpha_{1.3}$) and core material loss factor (η_2). In practice, the damping of the system might vary considerably due to change in the value of shear modulus, because of frequency dependence and also at various modes of vibration due to changes in the modal number n'. The curves of modal damping against the shear parameter are useful in the choice of core viscoelastic material, and in indicating the range of effective damping for a chosen design of sandwich beam, under specified environmental conditions of frequency of excitation and temperature. Suitable choice of relative thickness and stiffness of the outer layers might also be done in order to satisfy the static requirements and also to achieve reasonable damping under dynamic conditions. It might also be possible to specify

the frequency dependence of viscoelastic material required to keep the system damping unchanged at all modes, which are likely to be excited. Assuming, for instance that η_2 does not vary with frequency, it is seen that 'G_2' should vary linearly with frequency, in order to achieve constant system damping at all modes.

There are different criteria for minimising displacement, acceleration or stress response etc in the system and the choice depends upon the application intended. If the amplitude of the exciting force is constant with frequency, the displacement response depends on '$k\eta_s$' whilst if the amplitude of the exciting force is proportional to the square of frequency, it is 'η_s' which determines the displacement response effectiveness. The various criteria for damping effectiveness are meant to designate the damping at a generalized mode. Depending on the space distribution of excitation, the peak system response may not occur at the frequency corresponding to a generalized mode, this being due to high damping in the system. Due to the same reasons, the change in a system parameter may not influence the peak response in the same way as indicated by the damping effectiveness criteria. In such a situation, the graphs of peak response and corresponding frequencies are desirable. This was not found to be necessary for the type of loading

employed in the present work viz. the end displacement excitation.

In a 3 layered sandwich beam with viscoelastic core, the shear effect is generally predominant in the core. But for a stiff and thick core, the extensional effect becomes significant, especially in an unsymmetrical sandwich beam. At high frequencies, the stress response is considerably affected by the inclusion of longitudinal and rotary inertia terms in the equations of motion. This is due to the fact that for each modal number, a family of modes exists due to the inclusion of rotary and longitudinal inertia terms. Some of these modes are of the thickness shear type and occur at very high frequencies for a homogeneous beam but may occur at intermediate frequencies for a sandwich beam. This was illustrated by an example for which the effect of longitudinal and rotary inertia terms became pronounced at frequencies around 1400 c.p.s.

To take account of non-linearity in stress strain relations, which is exhibited by some viscoelastic materials, an approximate solution has been developed using the Ritz method, resulting in non-linear algebraic equations. An alternative approach is to solve the equations of motion by finite difference technique, which is expected to be highly tedious and time consuming, because of large number of high order differential equations.

The method given in the present work is simpler for low frequencies but is likely to be tedious as well, for higher frequencies, because of a large number of terms required in the assumed series which would increase the number of simultaneous algebraic equations. As indicated in the illustration given in Section III.G, it is possible to estimate the effect of non-linearity on the peak response and corresponding frequency, by the use of linear solution. Since the shear strain in the viscoelastic core varies from zero to maximum along the beam length, a linear solution employing viscoelastic material, with properties corresponding to an intermediate value of shear strain, might give nearly the same results as obtained from the solution based on a non-linear stress strain law. This is seen to be true for the illustration given. It might be seen that the effect of the non-linearity in stress strain relations, has not been taken account of, in the various curves of damping against the shear parameter in the present work, since these plots are not drawn for any specified material.

Configurations with higher number of layers.

The work described in Chapters IV and V is devoted to further multilayered configurations - 5 and 7 layered ones with alternate elastic and viscoelastic layers and 4 and 5 layered multicored sandwich configurations, with

different viscoelastic layers placed adjacent to each other. The use of increased number of viscoelastic layers, with different properties is attempted in order to increase the system damping at a number of modes. In each case, it has been possible to define a shear parameter, in a manner similar to that in the 3 layered configuration. The various damping effectiveness criteria as employed for the 3 layered case have also been applied in all those configurations. In Chapter IV, an analysis of the two possible arrangements in 5 layered configuration employing different viscoelastic materials, shows that two peaks in the curve of damping against shear parameter occur - a situation which is to be preferred. A single peak would occur if both the viscoelastic layers are of the same material. The value of the shear parameter at which each of the two peaks in a 5 layered sandwich beam employing two layers of different viscoelastic materials, occurs is approximately the same at which a single peak would occur if both the layers were of the same material. However, in the former case (of layers of different viscoelastic materials), the maximum value of damping corresponding to each peak is less than the maximum value of the peak in the latter case.

Further studies on the 5 layered configuration in Chapter IV indicate the need of determining the correct

ratio of stiffness of the two viscoelastic layers used, in a given situation, for optimum damping. Mostly, the damping results due to shear in this arrangement but decrease of constraining effect on one of the layers, would result in the contribution of extensional damping to the system damping. In such a case, the system damping does not vary appreciably for various modes. Thick and stiff viscoelastic layers are required for attaining these conditions.

The 7 layered configuration analysed in Chapter IV employs 3 viscoelastic layers or it might also be taken to correspond to a conventional honey-comb sandwich, damped by two viscoelastic layers, one on each side. In this configuration too, the use of suitably chosen different viscoelastic layers gives increased damping over a wider range of shear parameter values than would otherwise be possible if only one type of viscoelastic material is employed either in a 3 layered or 7 layered configuration.

In the 4 layered double cored configuration analysed in Chapter V, one of the viscoelastic layers is taken to be considerably stiffer than the other one. A particularly useful result is the fact that the graphs of system loss factor or displacement response effectiveness against the shear parameter, are considerably flatter than those obtained from a 3 layered sandwich employing a single

core. Since the shear parameter involves the modal number and the shear modulus amongst other parameters, a change of modal number, frequency and temperature value, would not be as detrimental in a suitably designed 4 layered configuration, as in a 3 layered one. At lower modes, the system damping is mostly due to shearing in the softer viscoelastic layer while at higher modes, the extensional damping due to the stiffer layer is seen to play an important role. The arrangement is particularly useful if the stiff layer is at least 100 times as stiff as the other viscoelastic layer. The 4 layered arrangement may also be taken to correspond to the one, employing a viscoelastic layer over a 'spacer' layer.

By the analysis of a 5 layered multicored configuration, it has been observed that the desired characteristics of a sandwich beam may be attained by a proper choice of the relative thickness of the viscoelastic layers. Also, only one of the viscoelastic layers need have a high material loss factor if a suitable stiffness ratio is maintained between the two viscoelastic materials, It may be seen from the results of this analysis that the adhesive joining the metal to viscoelastic layer in a 3 layered configuration should be of the rigid type.

The behaviour of the above mentioned configurations, has been indicated by studying the effect of certain

important parameters. A complete study of the influence of all the parameters in a sandwich employing a large number of layers is highly tedious and has not been attempted. It is suggested that the curves of modal damping effectiveness against shear parameter, might be used at the design stage to give an idea of the damping expected over a specified frequency range. Once a design has been chosen, an accurate response analysis may be done by using the solution to the equations of motion, with the actual space distribution of excitation.

Experimental Work: The vibration response tests on laminated beams were meant for verifying the results obtained from the theoretical analysis. In order to compute the theoretical values of vibration response corresponding to the experimental conditions of vibration response tests, the dynamic properties of the viscoelastic layer materials were required to be known accurately in advance. So, the viscoelastic materials were tested in shear at various values of frequency, temperature and strain amplitudes and the shear apparatus was found to be useful for the purpose. The results of vibration response experiments on a few specimens of 3 layered, 5 layered (alternate elastic and viscoelastic layers) and 4 layered double cored configurations have shown reasonable agreement with the theoretical results.

The maximum difference between the theoretical and experimental values of the peak amplitudes was around 10 percent and that between the values of frequencies corresponding to the peak amplitudes was 1-2 percent. Details of these comparisons and the sources of error are discussed in Section VI.B.6. A detailed discussion of experimental work is given in Section VI.C and is not repeated here.

It may be expected that the analysis of the remaining configurations for which experimental verification has not been attempted, is also likely to hold since it is based on assumptions which are similar to those for the analysis of the configurations which have been tested experimentally.

Finally, it appears that a careful consideration of various factors involved, would make it possible to achieve suitable design of laminated structures, involving viscoelastic layers, for use in severe vibration environments in a wide frequency range and to satisfy both the dynamic and static requirements. The use of a digital computer is necessary for the theoretical analysis. The development of new high damping viscoelastic materials in wide range of stiffness values with the properties not appreciably affected by temperature and other environments, is desirable. Also the development of suitable adhesives

for joining various layers is of importance.

VII.B: Further Work

The present work has been confined to the harmonic vibrations of a few types of sandwich beam configurations and the results are analysed for simply supported end conditions. Though the equations are stated for other boundary conditions, further work is desirable for solving these numerically for application to sandwich beams with other types of end conditions for various configurations. The adequacy of approximate methods e.g. the variational ones, has to be verified for beams with various end conditions, by comparing the results obtained with those obtained from an exact solution.

In the present work, a limited number of graphs relating to optimum damping have been drawn for illustration. Since these are useful at the design stage, further work is required in order to draw complete set of these graphs, with the various system parameters chosen in a wide range so as to include any sandwich beam parameters, likely to be encountered. Of course, this is expected to be tedious especially when the number of layers is high and all layers are different from one another. In addition, detailed investigations are necessary, to be of ready use at design stage regarding the

choice of any particular configuration viz. the number of layers and their properties, to be effectively useful under dynamic and static conditions.

Further analysis might deal with other types of structures, viz. sandwich plates, circular bars, shells and with structures carrying concentrated masses.

The effectiveness of damping in a sandwich structure employing viscoelastic layers and subjected to impact excitation, may be different from that determined for sinusoidal excitation conditions. This is due to the fact that the operating stress strain law is different in the two cases. Theoretical and experimental work is desirable on the analysis during and after an application of impact and the part played by viscoelastic damping. Work on the random vibration of sandwich structures, with viscoelastic damping was initiated in [52] and subsequent work would be of interest.

Further experimental work is required at high frequencies, both for the measurement of dynamic properties of damping materials and also for stress and displacement response measurements on sandwich specimens, the latter being meant for comparison with theoretical results. Experimental work on sandwich structures employing highly non-linear materials, will also be of interest and in such cases, analytical solution for higher modes has to be derived.

REFERENCES:

1. Plunkett R. "Vibration damping". Applied Mechanics Reviews Vol.6 July 1953.

2. Ruzicka J.E. (Ed.). "Structural damping". Papers presented at the Colloquium on Structural Damping, A.S.M.E., December 1959.

3. Henderson J.P. "New techniques and materials for damping". Paper No.64-MD-22, A.S.M.E., Design Engineering Conference Chicago, May 11-14, 1964.

4. Mentel T.J. "Viscoelastic boundary damping of beams and plates". J. Applied Mechanics, Vol.31, March 1964.

5. Rosen H. and Veilleux E.D. "Designing damping into laminated structures". Machine Design Vol.32, No.4, 4th February 1960, p.24.

6. Ungar E.E. "Damping tapes for vibration control" Product Engineering vol.31, January 25, 1960, p.57.

7. Ruzicka J.E. "Increased reliability of aviation and missile electronics by use of damped structures" S.A.E. Paper No.100Y, S.A.E. National Aeronautic Meeting, October 1959.

8. "Wide band vibration dampers in sheets, hats, angles". Machine Design, vol.32, 1960 March 17, p.34.

9. Bland D.R. "Theory of linear viscoelasticity" Pergamon Press, 1960.

10. Nowacki W. "Dynamics of elastic systems". Chapman and Hall Publication, 1963.

11. Gross B. "Mathematical structure of the theories of viscoelasticity". Herrman and Cie, Paris 1953.

12. Lockett F.J. "The practical applications of the mathematical theory of linear viscoelasticity", Arm.Res. and Dev. Est. Report (B) 2/61, Fort Halstead, Kent, 1961.

13. Gehman S.D. "Dynamic properties of elastomers", Rubber Chemistry and Technology, Vol.30, 1957,p.1203.

14. Dietz Albert G.H. (Edit.) "Engineering Laminates" Wiley Publications 1949.

15. Habip L.M. "A survey of modern developments in the analysis of sandwich structures", Applied Mechanics Reviews, Vol.18, No.2, February, 1965.

16. Hoff N.J. "Bending and buckling of rectangular sandwich plates", N.A.C.A. Tech. Note 2225, 1950.

17. Hoff N.J. "Analysis of structures", Wiley Publications 1956.

18. Kimel W.R., Raville M.E., Kirmser P.G. and Patel M.P. "Natural frequencies of simply supported sandwich beams", Proc. 4th Midwestern Conference on Solid Mechanics, 1959.

19. Raville M.E., En-Shiuh Ueng, Ming-Min Lei "Natural frequencies of fixed fixed sandwich beams" J. Applied Mechanics, September, 1961, p.367.

20. Yu Yi Yuan "A new theory of elastic sandwich plates - one dimensional case". J. Applied Mechanics, September, 1959.

21. Yu Yi Yuan. "Simple thickness shear modes of vibrations of infinite sandwich plates". J. Applied Mechanics, December 1959, p.679.

22. Yu Yi Yuan "Flexural vibrations of elastic sandwich plates". J. Aero-Space Sciences, Vol.27, No.4, April 1960.

23. Yu Yi Yuan. "Simplified vibration analysis of elastic sandwich plates" J. Aero-Space Sciences, Vol.27, No.12, December, 1960.

24. Yu Yi Yuan. "Forced flexural vibrations of sandwich plates in plane strain". J. Applied Mechanics, Vol.27, 1960, p.535.

25. Yu Yi Yuan. "Non-linear flexural vibrations of sandwich plates". J. Acoustical Society of America, Vol.34, No.9, 1962, p.1176.

26. Frankland . "Discussion to paper by Yu Yi Yuan, published in J. Applied Mechanics, September, 1959" J. Applied Mechanics, Vol.27, 1960.

27. Bolotin V.V. "Vibrations of layered elastic plates" Review given in Applied Mechanics Reviews, January 1965, No.181, Published in Proceeding Vibrations Problems. Polska Akad. Nauk, Inst. Podstawowych Problemow Tech. Vol.4, No.4, 1963, p.331.

28. Chang and Fang. "Transient and periodic response of a loaded sandwich panel", J. Aero-Space Sciences, Vol.28, May 1961, p.382.

29. Bieniek and Freudenthal: "Frequency response of orthotropic sandwich plates". J. Aero-Space Sciences, Vol.28, 1961, p.732.

30. Oberst H. "Ueber die Dämpfung der Biegeschwingungen dünner Bleche durch fest haftende Beläge", Part I: Acustica Vol.2, 1952, Part II: Acustica Vol.4,1954.

31. Lie'nard P. "Etude d'une Méthode de Mesure du Frottement Intérieur de Revetements Plastiques Travaillant en Flexion". La Recherche Aéronautique Vol.20, 1951, p.11.

32. Itterbeck von and Myncke H. "Vibration of plates covered with a damping layer". Acustica Vol.3, 1953, p.207.

33. Mead D.J. "The effect of a damping compound on Jet Efflux excited vibrations". a) Part I: Aircraft Engineering Vol.32, March 1960. b) Part II: Aircraft Engineering Vol.32, April 1960.

34. Schwarzl. "Forced bending and extensional vibrations of a 2 layer compound linear viscoelastic beam". Acustica Vol.8, 1958, p.164.

35. Oberst H. "Werkstoffe mit extreme hoher inner dämpfung", Acustica Vol.6, 1956, p.144.

36. Plass H.J. "Damping of vibrations in elastic rods and sandwich structures by incorporation of additional viscoelastic materials". Proceedings of 3rd Midwestern Conference on Solid Mechanics, April 1957, p.48.

37. Kerwin E.M. "Damping of flexural waves by a constrained visco-elastic layer". J. Acoustical Society of America, Vol.31, July 1959.

38. Ross Donald, Kerwin E.M. and Dyer Ira. "Flexural vibration damping of multi-layer plates", B.B.N. Report 564, June 26, 1958.

39. Ross Donald and Kerwin E.M. "Damping of flexural vibrations in plates by free and constrained visco-elastic layers" B.B.N. Report 632, May 28, 1959.

40. Ungar E.E. and Ross D. "Damping of flexural vibrations by alternate viscoelastic and elastic layers", Proc. 4th Midwestern Conference on Solid Mechanics, 1959.

41. Kerwin E.M. "Ideal spaced damping treatment for flexural waves". Contributed at 57th Meeting of Acoustical Society of America, May 1959 (Abstract given in J. Acoustical Society of America, Vol.31, 1959, p.846.

42. Kerwin E.M. "Damping of flexural waves in plates by spaced damping treatments having spacers of finite stiffness" - Paper Presented at 3rd International Congress on Acoustics, Stuttgart, September 1959.

43. Kerwin E.M. and McQuillan R.J. "Plate damping by a constrained viscoelastic layer: partial coverage and boundary effects" Bolt, Beranek and Newman Inc. Report No.760, June 1960.

44. Kerwin E.M. and Ross, Donald. "A comparison of the effectiveness of homogeneous layers and constrained layers of visco-elastic materials in damping flexural waves in plates". Paper Presented at 3rd International Congress on Acoustics, Stuttgart, September 1959.

45. Ungar E.E. and Kerwin E.M. "Loss factors of visco-elastic systems in terms of energy concepts". J.Acoustical Society of America, Vol.34, No.7, July 1962, p.954.

46. Ungar E.E. "Loss factors of viscoelastically damped beam structures", J. Acoustical Society of America, Vol.34, No.8, August 1962, p.1082.

47. Whittier J.S. "Effect of configurational additions, using viscoelastic interfaces on damping of a cantilever beam", W.A.D.C.Report 58-568, May 1959.

48. Yu Yi Yuan: "Damping of flexural vibrations of sandwich plates". J. Aero-Space Sciences, Vol.29, No.7, July 1962.

49. Mead, D.J. "Criteria for comparing effectiveness of damping treatments" - Noise Control Vol.7, No.3, 1961, p.27.

50. Skudrzyk :"Vibrations of a system with finite or infinite number of resonances". J. Acoustical Society of America, Vol.3, No.12, 1958, p.1140.

51. Mead D.J. "The double skin damping configuration" -

University of Southampton, A.A.S.U. Report No.160, April 1962.

52. Mead D.J. "The effect of certain damping treatments on the response of idealised aeroplane structures excited by noise", Ph.D. Thesis, University of Southampton, 1963.

53. Kurtze and Watters : "New wall design for high transmission loss or high damping", J. Acoustical Society of America, Vol.31, 1959, p.739.

54. Kurtze G. "Bending wave propagation in multilayer plates" J. Acoustical Society of America, Vol.31, September 1959, p.1183.

55. Ruzicka : "Damping structural resonances using viscoelastic shear damping mechanisms". Parts I and II. J. of Engineering for Industry, Vol.83, November 1961, p.403.

56. Parfitt and Lambeth. "Damping of structural vibrations", A.R.C. C.P.596, 1962.

57. Yildiza : "On the damping of a multilayer plate", J. Acoustical Society of America, Vol.34, 1962, p.353.

58. R.A. Di Taranto: "Theory of vibratory bending for elastic and viscoelastic layered finite-length beams", J. Applied Mechanics, Vol.32, No.4, December 1965.

59. Agbasiere J. "Flexural vibrations of multilayered beams with viscoelastic damping". 1966. Ph.D.Thesis, University of London.

60. Ross Donald, Ungar E.E. and Kerwin E.M. "Damping of plate flexural vibrations by means of viscoelastic laminae". - Section 3 of "Structural Damping" (Reference 2).

61. Harris and Crede : "Handbook of Shock and Vibrations", 1961, Chapters 35-37.

62. Neumark : "Concept of complex stiffness applied to problems of oscillations with viscous and hysteretic damping", A.R.C., R&M 3269, 1957.

63. Markovitz H. "Free vibration experiments in the theory of linear visco-elasticity", J.Applied Physics, Vol.34, No.1, January 1963, p.21.

64. Tschoegl N.W. "Equations of motion of the torsion pendulum and the complex modulus", J.Applied Physics, Vol.32, 1961, p.1794.

65. Lee H.C. "Forced lateral vibrations of a uniform cantilever beam with internal and external damping". J.Applied Mechanics, Vol.27, 1960, p.551.

66. Bland and Lee : "Calculation of complex modulus from vibrating reed tests". J. Applied Physics, 1955, p.1497.

67. Hunter S.C. "Viscoelastic waves". Chapter 1 of Progress in Solid Mechanics, Vol.1, 1960 (Eds. Sneddon and Hill): North Holland Publishing Co., Amsterdam.

68. Williams M.L. "Structural analysis of viscoelastic materials". A.I.A.A.Journal,Vol.2,No.5,May 1964,p.785.

69. Mindlin R.D. "An introduction to mathematical theory of vibrations of elastic plates", Monograph prepared for U.S.Army Signal Corps. Engineering Laboratories, Forth Monmouth, 1955.

70. Mindlin and Deresiewicz F "Timoshenko s shear coefficient for flexural vibration of beams", Proc. II U.S. National Congress on Applied Mechanics, June 1954, p.175.

71. "Dynamic mechanical properties of materials for noise and vibration control" - Chesapeake Instrument Corporation - Technical Report Vol.2, July 1962.

72. Nolle A.W. "Methods for measuring dynamic mechanical properties of rubber-like materials". J. Applied Physics, Vol.19, 1948, p.753.

73. Ungar and Hatch "Selection guide to high damping materials" - Product Engineering, Vol.32, No.16, April 17, 1961, p.44.

74. Biezieno and Grammel : "Engineering Dynamics", Vol.1. Blackie & Son, Ltd.

75. Budiansky and Hu : "The Lagrangian multiplier method of finding upper and lower limits to critical stresses in clamped plates", N.A.C.A. Report No.848, 1946.

76. Kantrovich and Krylov : "Approximate methods of higher analysis" Noordhoff Ltd. Groningen, 1958.

77. Singer J. "A note on the choice of coordinate functions for Rayleigh-Ritz method". J.Royal Aeronautical Society, 1961, p.765.

78. Weinstock R. "Calculus of variations" McGraw Hill Publication. 1952.

79. Langhaar H.L. "Energy methods in applied mechanics", Wiley Publications. 1962.

80. Crandall S.H. "Engineering analysis". McGraw Hill Publication. 1956.

81. Jacobsen L.S. and Ayre R.S. "Engineering vibrations" McGraw Hill Publication. 1958.

82. Milne R.D. "The steady state response of continuous dissipative systems with small non-linearity" Quarterly Journal of Mechanics and Applied Mathematics Vol.14, 1961, p.229.

83. Sethna : "Free vibrations of beams with non-linear viscoelastic material properties". Proc. 4th U.S. National Congress of Applied Mechanics, Vol.2, 1962, p.1103.

84. Silverman I.K. "On forced pseudo-harmonic vibrations" J. Franklin Institute, 1934, p.743.

85. Klotter K. "Non-linear vibration problem treated by the averaging method of W.Ritz". Proc. I U.S. National Congress on Applied Mechanics 1951, p.125.

86. Timoshenko S. "Advanced Dynamics" McGraw Hill Co. Publication.

87. Booth A.D. "Numerical Methods" Butterworth Scientific Publication 1955.

88. Householder A.S. "Principles of numerical analysis",

89. Payne A.R. "Dynamic mechanical properties of filler loaded vulcanisates", Rubber and Plastic Age, Vol. 42, 1961, p.963.

90. Davey A.B. and Payne A.R. "Rubber in Engineering Practice", MacLaren and Sons Ltd., 1964.

91. Payne A.R. and Scott J.R. "Engineering design with rubber", MacLaren and Sons Ltd. 1960.

92. Timoshenko S. and Goodier J.N. "Theory of elasticity", McGraw Hill Publication, 1951.

93. Mikhlin S.G. "Variational methods in mathematical physics" Pergamon Press, 1964.

94. Payne A.R. "Properties and Uses of Viscoelastic Materials", Society of Environmental Engineers - Symposium Part II, 1963 March.

95. Kennedy and Puncu. "Use of vector plots in vibration measurement and analysis". J. Aeronautical Sciences, Vol.14, No.11, 1947, p.403.

96. Bishop and Gladwell "The theory of resonance testing", Phil. Trans. Royal Society of London, Series A, Vol.255, 1963, p.241.

97. Fox L. "The numerical solution of two-point boundary problems in ordinary differential equations", Oxford, Clarendon Press, 1957.

98. Li W.H. "Engineering analysis". Prentice Hall, 1960.

99. Von Kármán T. and Biot M.A. "Mathematical methods in science and engineering". McGraw Hill Co. 1940.

100. Pipes L.A. "Applied mathematics for engineers and physicists". McGraw Hill Co., 1958.

APPENDIX 1 Details of derivation in II.C.1

The details involed in obtaining equations of motion and boundary conditions in section II.C are given here.

The variations of U, the strain energy, T, the kinetic energy and V, the potential energy expressions are carried out and the derivatives of δw, δu_1, and δu_3 are eliminated, giving:

$$\delta U = \frac{2s}{t_2}\int_o^L \left(\frac{u_1-u_3}{t_2} - \frac{w'a}{t_2}\right)\delta u_1 dx + \left[2r_1u_1' + 2c_2u_1' + c_2u_3' + c_2\left(\frac{t_3}{2} - t_1\right)w''\right]\delta u_1 \Big|_o^L$$

$$- \int_o^L \left[2r_1u_1'' + 2c_2u_1'' + c_2u_3'' + c_2\left(\frac{t_3}{2} - t_1\right)w'''\right]\delta u_1\, dx$$

$$- \frac{2s}{t_2}\int_o^L \left(\frac{u_1-u_3}{t_2} - \frac{w'a}{t_2}\right)\delta u_3 dx + \left[2r_3u_3' + 2c_2u_3' + c_2u_1' + c_2\left(t_3 - \frac{t_1}{2}\right)w''\right]\delta u_3 \Big|_o^L$$

$$- \int_o^L \left[2r_3u_3'' + 2c_2u_3'' + c_2u_1'' + c_2\left(t_3 - \frac{t_1}{2}\right)w'''\right]\delta u_3\, dx$$

$$+ \frac{2sa}{t_2}\int_o^L \left(\frac{u_1' - u_3'}{t_2} - \frac{w''a}{t_2}\delta w dx - \frac{2sa}{t_2}\left\{\frac{u_1-u_3}{t_2} - \frac{w'a}{t_2}\right\}\delta w \Big|_o^L\right.$$

$$+ \left[2q_1w'' + 2q_3w'' + \frac{c_2}{2}(t_1^2 + t_3^2 - t_1t_3)w'' + c_2\left(\frac{t_3}{2} - t_1\right)u_1' + c_2\left(t_3 - \frac{t_1}{2}\right)u_3'\right]\delta w' \Big|_o^L$$

$$- \left[2q_1w''' + 2q_3w''' + \frac{c_2}{2}(t_1^2 + t_3^2 - t_1t_3)w''' + c_2\left(\frac{t_3}{2} - t_1\right)u_1'' + c_2\left(t_3 - \frac{t_1}{2}\right)u_3''\right]\delta w \Big|_o^L$$

$$+\int_o^L \{2q_1 w''''+2q_3 w''''+\frac{c_2}{2}(t_1^2+t_3^2-t_1t_3)w''''+c_2(\frac{t_3}{2}-t_1)u_1'''$$

$$+ c_2(t_3-\frac{t_1}{2})u_3'''\}\delta w\, dx.$$

$$\delta T = \int_o^L \rho\dot{w}\delta\dot{w}dx + \int_o^L \{b\rho_1 t_1\dot{u}_1 + \frac{b\rho_2 t_2}{2}(\frac{\dot{u}_1+\dot{u}_3}{2}+\dot{w}'\varepsilon_1)+$$

$$+\frac{b\rho_2 t_2}{12}(\dot{u}_1-\dot{u}_3-\dot{w}'\varepsilon_2)\}\delta\dot{u}_1 dx$$

$$+\int_o^L\Big[\{b\rho_3 t_3\dot{u}_3+\frac{b\rho_2 t_2}{2}\{\frac{\dot{u}_1+\dot{u}_3}{2}+\dot{w}'\varepsilon_1\}-\frac{b\rho_2 t_2}{12}\{\dot{u}_1-\dot{u}_3-\dot{w}'\varepsilon_2\}\Big]\delta\dot{u}_3 dx$$

$$-\int_o^L\Big[b\{\frac{\rho_1 t_1^3+\rho_3 t_3^3}{12}\dot{w}''+\rho_2 t_2\varepsilon_1(\frac{\dot{u}_1'+\dot{u}_3'}{2}+\dot{w}''\varepsilon_1)\frac{\rho_2 t_2}{12}\varepsilon_2$$

$$(\dot{u}_1'-\dot{u}_3'-\dot{w}''\varepsilon_2)\}\Big]\delta\dot{w}dx$$

$$+b\{\frac{\rho_1 t_1^3+\rho_3 t_3^3}{12}\dot{w}'+\rho_2 t_2\varepsilon_1(\frac{\dot{u}_1+\dot{u}_3}{2}+\dot{w}'\varepsilon_1)\frac{\rho_2 t_2\varepsilon_2}{12}$$

$$(\dot{u}_1-\dot{u}_3-\dot{w}'\varepsilon_2)\}\delta\dot{w}\Big|_o^L$$

$$\delta V = \int_o^L f(x)g(t)\delta w dx.$$

Applying Hamilton's Principle and noting that

$$\int_{t_1}^{t_2}\int_o^L \dot{w}\,\delta\dot{w}\,dxdt = \int_o^L[\dot{w}\delta w\Big|_{t_1}^{t_2} - \int_{t_1}^{t_2}\int_o^L \dot{w}'\delta w dxdt$$

virtual displacement δw vanishes for $t=t_1$ and $t=t_2$ [86]

Hence, above $= -\int_{t_1}^{t_2}\dot{w}'\,\delta w dxdt$

Also applying this for u_1 and u_3, we get the equations of motion, and the terminal point conditions. The equations of motion are:

$$[2q_1+2q_2+c_2(\frac{t_1^2+t_3^2-t_1t_3}{2})]w''''-2s(\frac{a}{t_2})^2\ w''+\frac{2sa}{t_2^2}\ u_1'$$

$$+\ c_2(\frac{t_3}{2}-t_1)u_1'''-\frac{2sa}{t_2^2}\ u_3'+c_2(t_3-\frac{t_1}{2})u_3'''$$

$$=\ f(x)g(t)-\rho\ddot{w}+b\rho_2t_2(t_3-\frac{2t_1}{12})\ddot{u}_1'+\frac{2t_3-t_1}{12}\ddot{u}_3'\rho_2t_2b+$$

$$+\ddot{w}''b\ [\frac{\rho_1t_1^3+\rho_3t_3^3}{12}+\rho_2t_2\epsilon_1^2+\frac{\rho_2t_2}{12}\epsilon_2^2]$$

$$-\frac{2sa}{t_2^2}\ w'-c_2(\frac{t_3}{2}-t_1)w'''+\frac{2s}{t_2^2}\ u_1-u_1''\ (2r_1+2c_2)$$

$$-\frac{2s}{t_2^2}\ u_3-c_2u_3''=-b[\rho_1t_1\ddot{u}_1+\rho_2t_2(\frac{\ddot{u}_1}{3}+\frac{\ddot{u}_3}{6}+\ddot{w}'(\frac{t_3-2t_1}{12})]]$$

$$\frac{2sa}{t_2^2}\ w'-c_2(t_3-\frac{t_1}{2})w'''-\frac{2s}{t_2^2}\ u_1-c_2u_1''+\frac{2s}{t_2^2}\ u_3$$

$$-u_3''\ (2r_3+2c_2)=-b[\rho_3t_3\ddot{u}_3+\rho_2t_2(\frac{\ddot{u}_1}{6}+\frac{\ddot{u}_3}{3}+\ddot{w}'(\frac{2t_3-t_1}{12})]]$$

The terminal point conditions are:

<u>For simply supported ends</u>: $W = 0$

$W''= 0$

$U_1'= 0$

$U_3'= 0$

<u>For fixed ends</u>: $W = 0$

$W'= 0$

$U_1= 0$

$U_3= 0$

For free end:

$$W'' = 0$$

$$U_1' = 0$$

$$U_3' = 0$$

$$-\frac{2sa}{t_2}\left(\frac{u_1-u_3}{t_2}-\frac{w'a}{t_2}\right)-2q_1w'''-2q_3w'''\frac{c_2}{2}(t_1^2+t_3^2-t_1t_3)w'''$$

$$-c_2\left(\frac{t_3}{2}-t_1\right)u_1''-c_2\left(t_3-\frac{t_1}{2}\right)u_3''+b\,\frac{\rho_1t_1^3+\rho_3t_3^3}{12}\,\dot{w}''+$$

$$+b\,\rho_2t_2\varepsilon_1\left(\frac{\dot{u}_1+\dot{u}_3}{2}+\dot{w}''\varepsilon_1\right)-b\frac{\rho_2t_2\varepsilon_2}{12}(\dot{u}_1-\dot{u}_3-\dot{w}''\varepsilon_2)=0$$

APPENDIX 2 Details of derivation in II.D.1

The total strain energy U of the sandwich, after eliminating u_1, u_3, w_1 and w_3 as explained in II.D.1 is

$$
\begin{aligned}
= \int_o^L \Big[& \frac{E_1^*}{2}\Big\{t_1\Big(u_2'^2+\bar{w}_2'^2\frac{t_2^2}{4}+\bar{u}_1'^2\frac{t_1^2}{4}-u_2'\bar{u}_2't_2-u_2'\bar{u}_1't_1+\bar{u}_1'\bar{u}_2'\frac{t_1t_2}{2}\Big)\Big] \\
& +\bar{u}_1'^2\frac{t_1^3}{12}+\bar{w}_1^2t_1\Big\}+z_1\Big(u_2'-\bar{u}_2'\frac{t_2}{2}-\bar{u}_1'\frac{t_1}{2}\Big)\bar{w}_1t_1 \\
& +k_1\frac{G_1}{2}\Big\{\bar{u}_1^2t_1+\bar{w}_1'\frac{t_1^3}{12}+2\bar{u}_1t_1\Big(w_2'-\bar{w}_2'\frac{t_2}{2}-\bar{w}_1'\frac{t_1}{2}\Big) \\
& +t_1\Big(w_2'^2+\bar{w}_2'\frac{t_2^2}{4}+\bar{w}_1'^2\frac{t_1^2}{4}-w_2'\bar{w}_2't_2-w_2'\bar{w}_1't_1+\bar{w}_1'\bar{w}_2'\frac{t_1t_2}{2}\Big)\Big] \ dx \\
& +\int_o^L \Big[\frac{E_3^*}{2}\Big\{t_3\Big(u_2'+\bar{u}_2'\frac{t_2}{2}+\bar{u}_3'\frac{t_3}{2}\Big)^2+\bar{u}_3'^2\frac{t_3^3}{12}+\bar{w}_3^2t_3\Big\} \\
& z_3\Big(u_2'+\bar{u}_2'\frac{t_2}{2}+\bar{u}_3'\frac{t_3}{2}\Big)\bar{w}_3t_3 \\
& +k_3\frac{G_3}{2}\Big\{\bar{u}_3^2t_3+t_3\Big(w_2'+\bar{w}_2'\frac{t_2}{2}+\bar{w}_3'\frac{t_3}{2}\Big)^2+\bar{w}_3'^2\frac{t_3^3}{12} \\
& +2\bar{u}_3t_3\Big(w_2'+\bar{w}_2'\frac{t_2}{2}+\bar{w}_3'\frac{t_3}{2}\Big)\Big\}\Big] \ dx \\
& +\int_o^L \Big\{\frac{E_2^*}{2}\Big(u_2'^2t_2+\bar{u}_2'^2\frac{t_2^3}{12}+\bar{w}_2^2t_2\Big)+z_2\Big(u_2'\bar{w}_2t_2\Big) \\
& +k_2\frac{G_2}{2}\Big(\bar{u}_2^2t_2+w_2'^2t_2+\bar{w}_2'^2\frac{t_2^3}{12}+2\bar{u}_2w_2't_2\Big)\Big\} \ dx
\end{aligned}
$$

Total Kinetic Energy 'T' of the sandwich, after eliminating u_1, u_3, w_1 and w_3 as explained in II.D.1 is given as.

$$T = \int_o^L [\frac{\rho_1}{2}\{t_1(\dot{u}_2^2+\dot{\bar{u}}_2^2\frac{t_2^2}{4}+\dot{\bar{u}}_1^2\frac{t_1^2}{4}-\dot{u}_2\dot{\bar{u}}_2t_2-\dot{u}_2\dot{\bar{u}}_1t_1$$
$$+\dot{\bar{u}}_1\dot{\bar{u}}_2\frac{t_1t_2}{2}) + \dot{\bar{u}}_1^2\frac{t_1^3}{12} + \dot{\bar{w}}_1\frac{t_1^3}{12}$$
$$+t_1(\dot{w}_2^2+\dot{\bar{w}}_2^2\frac{t_2^2}{4} + \dot{\bar{w}}_1^2\frac{t_1^2}{4} -\dot{w}_2\dot{\bar{w}}_2t_2-\dot{w}_2\dot{\bar{w}}_1t_1+\dot{\bar{w}}_1\dot{\bar{w}}_2\frac{t_1t_2}{2})\}$$
$$+\frac{\rho_3}{2}\{t_3(\dot{u}_2^2+\dot{\bar{u}}_2^2\frac{t_2^2}{4}+\dot{\bar{u}}_3\frac{t_3^2}{4}+\dot{u}_2\dot{\bar{u}}_2t_2+\dot{u}_2\dot{\bar{u}}_3t_3+\dot{\bar{u}}_2\dot{\bar{u}}_3\frac{t_2t_3}{2})$$
$$+\dot{\bar{u}}_3\frac{t_3^3}{12} + \dot{\bar{w}}_3^2\frac{t_3^3}{12}$$
$$+t_3(\dot{w}_2^2+\dot{\bar{w}}_2^2\frac{t_2^2}{4}+\dot{\bar{w}}_3^2\frac{t_3^2}{4}+\dot{w}_2\dot{\bar{w}}_2t_2+\dot{w}_2\dot{\bar{w}}_3t_3+\dot{\bar{w}}_2\dot{\bar{w}}_3\frac{t_2t_3}{2})\}$$
$$+\frac{\rho_2}{2}\{\dot{u}_2^2t_2+\dot{\bar{u}}_2^2\frac{t_2^3}{12}+\dot{w}_2^2t_2+\dot{\bar{w}}_2^2\frac{t_2^3}{12}\}] \, bdx.$$

$$V = g(t)\int_o^L f(x)\,(w_1-\bar{w}_1\frac{t_1}{2})dx.$$

Substituting $w_1 = w_2-\bar{w}_2\frac{t_2}{2} - \bar{w}_1\frac{t_1}{2}$

$$V = g(t)\int_o^L f(x)\,[w_2 - \bar{w}_2\frac{t_2}{2} -\bar{w}_1t_1]\, b\, dx.$$

In order to apply Hamilton's principle, variations of U, V, T have to be carried out as done in Appendix I. Following the same procedure, we get the following equations of motion.

$$\frac{bE_1^*}{2}(\frac{2}{3}t_1^3\bar{u}_1'' - t_1^2u_2'' + \frac{t_1^2t_2}{2}\bar{u}_2'') - \frac{bx_1}{2}t_1^2\bar{w}_1'$$
$$- bG_1k_1(t_1\bar{u}_1 + t_1w_2 - \frac{t_1t_2}{2}\bar{w}_2' - \frac{t_1^2}{2}\bar{w}_1')$$

$$= \frac{\rho_1 b}{2}[\ddot{\bar{u}}_1 \frac{t_1^3}{2} - \ddot{u}_2 t_1^2 + \frac{t_1^2 t_2}{2} \ddot{\bar{u}}_2 + \frac{t_1^3}{6} \ddot{\bar{u}}_1]$$

$$\frac{bE_1^*}{2}(2t_1 u_2'' - t_1 t_2 \bar{u}_2'' - t_1^2 \bar{u}_1'') + bz_1(t_1 \bar{w}_1')$$

$$+ \frac{bE_3^*}{2}(2t_3 u_2'' + t_2 t_3 \bar{u}_2'' + t_3^2 \bar{u}_3'') + bz_3(t_3 \bar{w}_3')$$

$$+ \frac{bE_2^*}{2}(2u_2'' t_2) + bz_2(t_2 \bar{w}_2')$$

$$= \frac{b\rho_1}{2}[2t_1 \dot{u}_2 - t_1 t_2 \ddot{\bar{u}}_2 - t_1^2 \ddot{\bar{u}}_1] + \frac{6\rho_3}{2}[2t_3 \dot{u}_2 + t_3 t_2 \ddot{\bar{u}}_2 + t_3^2 \ddot{\bar{u}}_3]$$

$$+ \frac{b\rho_2}{2}[2t_2 \dot{u}_2]$$

$$\frac{bE_1^*}{2}[\frac{t_1 t_2^2}{2} \bar{u}_2'' - t_1 t_2 u_2'' + \frac{t_1^2 t_2}{2} \bar{u}_1''] - bz_1 \frac{t_1 t_2}{2} \bar{w}_1'$$

$$+ \frac{bE_3^*}{2}(\frac{t_3 t_2^2}{2} \bar{u}_2'' + t_2 t_3 u_2'' + \frac{t_3^2 t_2}{2} \bar{u}_3'') + bz_3 \frac{t_2 t_3}{2} \bar{w}_3'$$

$$+ \frac{bE_2^*}{2}(\frac{t_2^3}{6} \bar{u}_2'') - bG_2 t_2 k_2(w_2' + \bar{u}_2)$$

$$= \frac{b\rho_1}{2}[\ddot{\bar{u}}_2 \frac{t_1 t_2^2}{2} - t_1 t_2 \dot{u}_2 + \frac{t_1^2 t_2}{2} \ddot{\bar{u}}_1] + \frac{b\rho_3}{2}[\frac{t_3 t_2^2}{2} \ddot{\bar{u}}_2 + t_3 t_2 \dot{u}_2 + \frac{t_2 t_3^2}{2} \ddot{\bar{u}}_3]$$

$$+ \frac{b\rho_2}{2}[\ddot{\bar{u}}_2 \frac{t_2^3}{6}]$$

$$\frac{bE_3^*}{2}(\frac{2}{3} t_3^3 \bar{u}_3'' + t_3^2 u_2'' + \frac{t_2 t_3^2}{2} \bar{u}_2'') + bz_3(\frac{t_3^2}{2} \bar{w}_3')$$

$$- \frac{bG_3 k_3}{2}(2t_3 \bar{u}_3 + 2t_3 w_2' + t_2 t_3 \ddot{\bar{w}}_2' + t_3^2 \bar{w}_3')$$

$$= \frac{b\rho_3}{2}[\frac{t_3^3}{2} \ddot{\bar{u}}_3 + t_3^2 \dot{u}_2 + \frac{t_2 t_3^2}{2} \ddot{\bar{u}}_2 + \frac{t_3^3}{6} \ddot{\bar{u}}_3]$$

$$- \frac{bE_1^*}{2}(2t_1\bar{w}_1) - b\bar{z}_1(u_2' - \bar{u}_2' \frac{t_2}{2} - \bar{u}_1' \frac{t_1}{2})t_1$$

$$+ \frac{bG_1k_1}{2}(\frac{t_1^3}{6}\bar{w}_1'' - \bar{u}_1' t_1^2 + \frac{t_1^3}{2}\bar{w}_1'' - t_1^2 w_2'' + \frac{t_1^2 t_2}{2}\bar{w}_2'')$$

$$= \frac{b\rho_1}{2}[\frac{t_1^3}{2}\ddot{\bar{w}}_1 - t_1^2\ddot{w}_2 + \frac{t_1^2 t_2}{2}\ddot{\bar{w}}_2 + \frac{t_1^3}{6}\ddot{\bar{w}}_1] + t_1\, g(t)\, f(x)$$

$$\frac{bG_1k_1}{2}(2\bar{u}_1' t_1 + 2t_1 w_2'' - t_1 t_2 \bar{w}_2'' - t_1^2 \bar{w}_1'')$$

$$+ \frac{bG_3k_3}{2}(2\bar{u}_3' t_3 + 2t_3 w_2'' + t_2 t_3 \bar{w}_2'' + t_3^2 \bar{w}_3'')$$

$$+ \frac{bG_2k_2}{2}(2t_2 w_2'' + 2t_2 \bar{u}_2) = \frac{b\rho_1}{2}(2t_1\ddot{w}_2 - t_1 t_2 \ddot{\bar{w}}_2 - t_1^2 \ddot{\bar{w}}_1)$$

$$+ \frac{b\rho_3}{2}(2t_3\ddot{w}_2 + t_2 t_3 \ddot{\bar{w}}_2 + t_3^2 \ddot{\bar{w}}_3) + \frac{b\rho_2}{2}(2t_2\ddot{w}_2) - g(t)\, f(x)$$

$$\frac{bG_1k_1}{2}[-t_1 t_2 \bar{u}_1' + \frac{t_2^2 t_1}{2}\bar{w}_2'' - t_1 t_2 w_2'' + \frac{t_1^2 t_2}{2}\bar{w}_1'']$$

$$- \frac{bE_2^*}{2}(2t_2\bar{w}_2)$$

$$+ \frac{bG_3k_3}{2}(t_2 t_3 \bar{u}_3' + \frac{t_3 t_2^2}{2}\bar{w}_2'' + t_2 t_3 w_2'' + \frac{t_2 t_3^2}{2}\bar{w}_3'')$$

$$- b\bar{z}_2(t_2 u_2') + \frac{bG_2k_2}{2}(\frac{t_2^3}{6}\bar{w}_2'')$$

$$= \frac{b\rho_1}{2}(\frac{t_1 t_2^2}{2}\ddot{\bar{w}}_2 - t_1 t_2 \ddot{w}_2 + \frac{t_1^2 t_2}{2}\ddot{\bar{w}}_1)$$

$$+ \frac{b\rho_3}{2}(\frac{t_3 t_2^2}{2}\ddot{\bar{w}}_2 + t_2 t_3 \ddot{w}_2 + \frac{t_2 t_3^2}{2}\ddot{\bar{w}}_3) + \frac{b\rho_2}{2}(\frac{t_2^3}{6}\ddot{\bar{w}}_2)$$

$$+ g(t)\, f(x)\, \frac{t_2}{2}$$

$$- \frac{bE_3^*}{2}(2t_3\bar{w}_3) - bt_3 z_3 (u_2' + \bar{u}_2' \frac{t_2}{2} + \bar{u}_3' \frac{t_3}{2})$$

$$+ \frac{bG_3 k_3}{2} \left(\frac{t_3^3}{6}\bar{w}_3'' + t_3^2 \bar{u}_3' + \frac{t_3^3}{2}\bar{w}_3'' + t_3^2 w_2'' + \frac{t_2 t_3^2}{2}\bar{w}_2'' \right)$$

$$= \frac{b\rho_3}{2}\left(\frac{t_3^3}{2}\ddot{\bar{w}}_3 + t_3^2 \ddot{w}_2 + \frac{t_2 t_3^2}{2}\ddot{\bar{w}}_2 + \frac{t_3^3}{6}\ddot{w}_3 \right)$$

The terminal point conditions obtained are:

$$\frac{E_1^*}{2}\left(\frac{2}{3}t_1^3\bar{u}_1' - t_1^2 u_2' + \frac{t_1^2 t_2}{2}\bar{u}_2'\right) + z_1\left(-\frac{t_1^2}{2}\bar{w}_1\right) \Bigg|_0^L = 0 \quad \text{or} \quad \bar{u}_1 \Big|_0^L = 0$$

$$\frac{E_1^*}{2}(2t_1 u_2' - t_1 t_2 \bar{u}_2' - t_1^2 \bar{u}_1') + z_1(t_1\bar{w}_1) + \frac{E_3^*}{2}(2t_3 u_2' + t_2 t_3 \bar{u}_2' + t_3^2 \bar{u}_3') + z_3(t_3\bar{w}_3) + \frac{E_2^*}{2}(2t_2 u_2') + z_2(t_2\bar{w}_2) \Bigg|_0^L = 0 \quad \text{or} \quad u_2 \Big|_0^L = 0$$

$$\frac{E_1^*}{2}\left(\frac{t_1 t_2^2}{2}\bar{u}_2' - t_1 t_2 u_2' + \frac{t_1^2 t_2}{2}\bar{u}_1'\right) - z_1\frac{t_1 t_2}{2}\bar{w}_1 + \frac{E_3^*}{2}\left(\frac{t_3 t_2^2}{2}\bar{u}_2' + t_2 t_3 u_2' + \frac{t_3^2 t_2}{2}\bar{u}_3'\right) + z_3\frac{t_3 t_2}{2}\bar{w}_3 + \frac{E_2^*}{2}\left(\frac{t_2^3}{6}\bar{u}_2'\right) \Bigg|_0^L = 0 \quad \text{or} \quad \bar{u}_2 \Big|_0^L = 0$$

$$\frac{E_3^*}{2}\left[\frac{2}{3}t_3^3\bar{u}_3' + t_3^2 u_2' + \frac{t_2 t_3^2}{2}\bar{u}_2'\right] + z_3\left[\bar{w}_3\frac{t_3^2}{2}\right] \Bigg|_0^L = 0 \quad \text{or} \quad \bar{u}_3 \Big|_0^L = 0$$

$$\left. \begin{aligned} & k_1\frac{G_1}{2}(2\bar{u}_1 t_1 + 2t_1 w_2' - t_1 t_2 \bar{w}_2 \ldots \bar{w}_1' \\ & + \frac{G_3 k_3}{2}(2\bar{u}_3 t_3 + 2t_3 w_2' + t_2 t_3 \bar{w}_2' + t_3^2 \bar{w}_3') \\ & + \frac{G_2 k_2}{2}(2t_2 w_2' + 2t_2 \bar{u}_2) \end{aligned} \right|_0^L = 0 \quad \text{or} \quad w_2 \Big|_0^L = 0$$

$$\left. \frac{t_1^3}{6}\bar{w}_1' - \bar{u}_1 t_1^2 + \frac{t_1^3}{2}\bar{w}_1' - t_1^2 w_2' + \frac{t_1^2 t_2}{2}\bar{w}_2' \right|_0^L = 0 \quad \text{or} \quad \bar{w}_1 \Big|_0^L = 0$$

$$\left. \begin{aligned} & k_1\frac{G_1}{2}\left(-t_1 t_2 \bar{u}_1 + \frac{t_2^2 t_1}{2}\bar{w}_2' - t_1 t_2 w_2' + \frac{t_1^2 t_2}{2}\bar{w}_1'\right) \\ & + \frac{G_3 k_3}{2}\left(t_2 t_3 \bar{u}_3 + \frac{t_3 t_2^2}{2}\bar{w}_2' + t_2 t_3 w_2' + \frac{t_2 t_3^2}{2}\bar{w}_3'\right) \\ & + \frac{G_2 k_2}{2}\left(\frac{t_2^3}{6}\bar{w}_2'\right) \end{aligned} \right|_0^L = 0 \quad \text{or} \quad \bar{w}_2 \Big|_0^L = 0$$

$$\left. \frac{t_3^3}{6}\bar{w}_3' + t_3^2 \bar{u}_3 + \frac{t_3^3}{2}\bar{w}_3' + t_3^2 w_2' + \frac{t_2 t_3^2}{2}\bar{w}_2' \right|_0^L = 0 \quad \text{or} \quad \bar{w}_3 \Big|_0^L = 0$$

For simply supported ends, the boundary conditions deduced from above are:

$$w_2 = \bar{w}_1 = \bar{w}_2 = \bar{w}_3 = 0$$

$$\bar{u}_1' = \bar{u}_3' = \bar{u}_2' = u_2' = 0$$

APPENDIX 3 Details of derivation in IV.A.1

The details involved for obtaining Equations of motion and boundary conditions from energy integrals in section IV.A.1 for 5 layered case are given here.

From section IV.A.1, expression for δU can be written, for small displacements as:

$$\delta U = q_2 \int_o^L 2(\bar{\alpha} - w')(\delta\bar{\alpha} - \delta w')dx + 2q_4 \int_o^L (\bar{\beta} - w')(\delta\bar{\beta} - \delta w')dx$$

$$+ 2r_1 \int_o^L [u' + \bar{\alpha}' t_2 + w'' \frac{t_1+t_3}{2}](\delta u' + \delta\bar{\alpha}' t_2 + \delta w'' \frac{t_1+t_3}{2})dx$$

$$+ 2r_1 \int_o^L w'' \frac{t_1^2}{12} \delta w'' dx + 2r_3 \int_o^L u' \delta u' dx + 2r_3 \int_o^L w'' \frac{t_3^2}{12} \delta w'' dx$$

$$+ 2r_4 \int_o^L [u' - \bar{\beta}' \frac{t_4}{2} - w'' \frac{t_3}{2}](\delta u' - \delta\bar{\beta}' \frac{t_4}{2} - \delta w'' \frac{t_3}{2})dx$$

$$+ 2r_4 \int_o^L \bar{\beta}' \delta\bar{\beta}' \frac{t_4^2}{12} dx + 2r_5 \int_o^L w'' \frac{t_5^2}{12} \delta w'' dx$$

$$+ 2r_5 \int_o^L [u' - \bar{\beta}' t_4 - w''(\frac{t_3+t_5}{2})](\delta u' - \delta\bar{\beta}' t_4 - \delta w'' \frac{t_3+t_5}{2})dx$$

$$\delta \int_{t_1}^{t_2} \int_o^L T dx dt = \rho \int_{t_1}^{t_2} \int_o^L \dot{w}\, \delta\dot{w}\, dx\, dt$$

$$= - \int_{t_1}^{t_2} \int_o^L \rho \ddot{w}\, \delta w\, dx\, dt$$

(as in Appendix 1)

$$\delta V = \int_o^L f(x)g(t)\, \delta w\, dx.$$

Eliminating derivatives of δw, $\delta\bar{\alpha}$ etc. in expression for δU by integration by parts and applying Hamilton's

Principle, $\int_{t_1}^{t_2} (\delta T - \delta U - \delta V)dt = 0$.

gives equations of motion viz. eqns. (IV.1) to (IV.4).

The terminal point conditions are obtained as.

i) $\{2r_1(u' + \bar{\alpha}\, t_2 + w''\frac{t_1+t_3}{2}) + 2r_3 u' + 2r_4(u' - \bar{\beta}'\frac{t_4}{2} - w''\frac{t_3}{2})$

$+2r_5(u' - \bar{\beta}' t_4 - w''\frac{t_3+t_5}{2})\}\, \delta U \Big|_o^L = 0$

ii) $\{2r_1 t_2(u' + \bar{\alpha}' t_2 + w''\frac{t_1+t_3}{2})\}\delta\bar{\alpha} \Big|_o^L = 0$

iii) $\{r_4\bar{\beta}'\frac{t_4^2}{6} - r_4 t_4(u' - \bar{\beta}'\frac{t_4}{2} - w''\frac{t_3}{2}) - 2r_5 t_4(u' - \bar{\beta}' t_4 - w''\frac{t_3+t_5}{2})\}\delta\bar{\beta}\Big|_o^L$

$= 0$

iv) $\{-2q_2(\bar{\alpha} - w') - 2q_4(\bar{\beta} - w') - r_1(t_1+t_3)(u'' \bar{\alpha}'' t_2 + w''\frac{t_1+t_3}{2})$

$- \frac{r_1 t_1^2 w'''}{6} - \frac{r_3 t_3^2}{6} w''' + r_4 t_3(u'' - \bar{\beta}''\frac{t_4}{2} - w'''\frac{t_3}{2}) - \frac{r_5 t_5^2}{6} w'''$

$+r_5(t_3+t_5)(u'' - \bar{\beta}'' t_4 - w'''\frac{t_3+t_5}{2})\}\, \delta W \Big|_o^L = 0$

v) $\{2r_1(u' + \bar{\alpha}' t_2 + w''\frac{t_1+t_3}{2})\frac{t_1+t_3}{2} + \frac{r_1}{6} w'' t_1^2 + \frac{r_3}{6} t_3^2 w''$

$-r_4 t_3(u' - \bar{\beta}'\frac{t_4}{2} - w''\frac{t_3}{2}) + \frac{r_5 t_5^2}{6} w''$

$-r_5(t_3+t_5)(u' - \bar{\beta}' t_4 - w''\frac{t_3+t_5}{2})\}\, \delta w' \Big|_o^L = 0$

From these, the boundary conditions for various ends may be written down as below:

For simply supported end, boundary conditions are:

$$w = 0$$

$$w'' = \bar{\alpha}' = \bar{\beta}' = u' = 0$$

For fixed end, boundary conditions are:

$$w = 0 = \bar{\alpha} = \bar{\beta} = u = w'$$

For free end, $\bar{\alpha}' = \bar{\beta}' = u' = w'' = 0$

and the term included in parenthesis{ } in (iv) above = 0.

APPENDIX 4 Details of derivation in IV.B.1

The details involved for obtaining equations of motion and boundary conditions from energy integrals in section IV.B.1 for 7 layered case are given here.

U can be written from section IV.B.1, for small displacements as

$$
\begin{aligned}
= \; & 2q_2 \int_o^L (\bar{\alpha}-w')\delta\bar{\alpha}\, dx + 2q_4 \int_o^L (\bar{\beta}-w')\,\delta\bar{\beta}\, dx \\
& + 2q_6 \int_o^L (\bar{\gamma}-w')\,\delta\bar{\gamma}\, dx \\
& - \int_o^L [2q_2(\bar{\alpha}-w') + 2q_4(\bar{\beta}-w') + 2q_6(\bar{\gamma}-w')]\,\delta w'\, dx \\
& + \int_o^L 2r_1 t_2 (u' + \bar{\beta}'\frac{t_4}{2} + \bar{\alpha}' t_2 + w'' t_{31})\delta\bar{\alpha}'\, dx \\
& + \int_o^L [r_3 t_4 (u' + \bar{\beta}'\frac{t_4}{2} + w''\frac{t_3}{2}) - r_5 t_4 (u' - \bar{\beta}'\frac{t_4}{2} - w''\frac{t_5}{2}) \\
& \quad + r_1 t_4 (u' + \bar{\beta}'\frac{t_4}{2} + \bar{\alpha}' t_2 + w'' t_{31}) \\
& \quad - r_7 t_4 (u' - \bar{\beta}'\frac{t_4}{2} - \bar{\gamma}' t_6 - w'' t_{57})]\delta\bar{\beta}'\, dx \\
& - \int_o^L 2r_7 t_6 (u' - \bar{\beta}'\frac{t_4}{2} - \bar{\gamma}' t_6 - w'' t_{57})\delta\bar{\gamma}'\, dx \\
& + \int_o^L [2r_3 (u' + \bar{\beta}'\frac{t_4}{2} + w''\frac{t_3}{2}) + 2r_5 (u' - \bar{\beta}'\frac{t_4}{2} - w''\frac{t_5}{2}) \\
& \quad + 2r_1 (u' + \bar{\beta}'\frac{t_4}{2} + \bar{\alpha}' t_2 + w'' t_{31}) + 2r_7 (u' - \bar{\beta}'\frac{t_4}{2} - \bar{\gamma}' t_6 - w'' t_{57})]\delta u'\, dx \\
& + \int_o^L [r_3 t_3 (u' + \bar{\beta}'\frac{t_4}{2} + w''\frac{t_3}{2}) \quad \frac{r_3 t_3^2 + r_1 t_1^2 + r_5 t_5^2 + r_7 t_7^2}{6} w''
\end{aligned}
$$

$$-r_5 t_5(u' - \bar{\beta}'\frac{t_4}{2} - w''\frac{t_5}{2}) + 2r_1 t_{13}(u' + \bar{\beta}'\frac{t_4}{2} + \bar{\alpha}' t_2 + w'' t_{31})$$

$$-2r_7 t_{57}(u' - \bar{\beta}'\frac{t_4}{2} - \bar{\gamma}' t_6 - w'' t_{57})] \, \delta w'' dx$$

δT and δV are same as in Appendix 3.

Eliminating derivatives of $\delta w, \delta\bar{\alpha}$ etc. by integration by parts and applying Hamilton's Principle gives equations of motion (IV.14) to (IV.18).

The terminal point conditions are:

i) $$\{2r_1 t_2(u' + \bar{\beta}'\frac{t_4}{2} + \bar{\alpha}' t_2 + w'' t_{31})\} \, \delta\bar{\alpha}\Big|_0^L = 0$$

ii) $$\{r_3 t_4(u' + \bar{\beta}'\frac{t_4}{2} + w''\frac{t_3}{2}) - r_5 t_4(u' - \bar{\beta}'\frac{t_4}{2} - w''\frac{t_5}{2}) + r_1 t_4(u' + \bar{\beta}'\frac{t_4}{2} + \bar{\alpha}' t_2 + w'' t_{31}) - r_7 t_4(u' - \bar{\beta}'\frac{t_4}{2} - \bar{\gamma}' t_6 - w'' t_{57})\} \delta\bar{\beta} \Big|_0^L = 0$$

iii) $$\{(u' - \bar{\beta}'\frac{t_4}{2} - \bar{\gamma}' t_6 - w'' t_{57})\} \, \delta\bar{\gamma}\Big|_0^L = 0$$

iv) $$\{2r_3(u' + \bar{\beta}'\frac{t_4}{2} + w''\frac{t_3}{2}) + 2r_5(u' - \bar{\beta}'\frac{t_4}{2} - w''\frac{t_5}{2}) + 2r_1(u' + \bar{\beta}'\frac{t_4}{2} + \bar{\alpha}' t_2 + w'' t_{31}) + 2r_7(u' - \bar{\beta}'\frac{t_4}{2} - \bar{\gamma}' t_6 - w'' t_{57})\} \delta u \Big|_0^L = 0$$

v) $$\{r_3 t_3(u' + \bar{\beta}'\frac{t_4}{2} + w''\frac{t_3}{2}) + \frac{r_3 t_3^2 + r_1 t_1^2 + r_5 t_5^2 + r_7 t_7^2}{6} w'' - r_5 t_5(u' - \bar{\beta}'\frac{t_4}{2} - w''\frac{t_5}{2}) + 2r_1 t_{13}(u' + \bar{\beta}'\frac{t_4}{2} + \bar{\alpha}' t_2 + w'' t_{31}) - 2r_7 t_{57}(u' - \bar{\beta}'\frac{t_4}{2} - \bar{\gamma}' t_6 - w'' t_{57})\} \delta w' \Big|_0^L = 0$$

vi) $$\Big[-2q_2(\bar{\alpha}-w')-2q_4(\bar{\beta}-w')-2q_6(\bar{\gamma}-w')$$

$$-r_3t_3(u''-\bar{\beta}''\frac{t_4}{2}-w'''\frac{t_3}{2})-\frac{r_3t_3^2+r_1t_1^2+r_5t_5^2+r_7t_7^2}{6}w'''$$

$$+r_5t_5(u''-\bar{\beta}''\frac{t_4}{2}-w'''\frac{t_5}{2})-2r_1t_{31}(u''+\bar{\beta}''\frac{t_4}{2}+\bar{\alpha}''t_2+w'''t_{13})$$

$$+2r_7t_{57}(u''-\bar{\beta}''\frac{t_4}{2}-\bar{\gamma}''t_6-w'''t_{57})\ \delta w\Big]\Big|_o^L = 0$$

For <u>simply supported</u> end, boundary conditions are seen to be

$$\bar{\gamma}' = u' = \bar{\beta}' = \bar{\alpha}' = w'' = 0$$

$$w = 0$$

For <u>fixed</u> end,

$$\bar{\gamma} = u = \bar{\beta} = \bar{\alpha} = w' = w = 0$$

For <u>free</u> end,

$$\bar{\gamma}' = u' = \bar{\beta}' = \bar{\alpha}' = w'' = 0$$

and terms enclosed in parenthesis [ ] in (vi) above = 0.

APPENDIX 5 Details of derivation in V.A.1

In this, the details for obtaining equations of motion and boundary conditions in section V.A.1 for 4 layered unsymmetrical case are given.

From section V.A.1, δU can be written as below, for small displacements.

$$\delta U = 2q_2 \int_o^L (\bar{\alpha} - w')^2 \delta\bar{\alpha}\, dx + 2q_3 \int_o^L (\bar{\beta} - w')^2 \delta\bar{\beta}\, dx$$

$$-2q_2 \int_o^L (\bar{\alpha} - w')\delta w'\, dx - 2q_3 \int_o^L (\bar{\beta} - w')\delta w'\, dx$$

$$+ \int_o^L [2r_1(u' + \bar{\alpha}' t_2 + w'' \frac{t_1}{2}) + 2r_4(u' - \bar{\beta}' t_3 - w'' \frac{t_4}{2})$$

$$+ 2r_3(u' - \bar{\beta}' \frac{t_3}{2})]\delta u'$$

$$+ \int_o^L [2r_1 t_2 (u' + \bar{\alpha}' t_2 + w'' \frac{t_1}{2})]\delta\bar{\alpha}'\, dx$$

$$- \int_o^L [2r_4 t_3 (u' - \bar{\beta}' t_3 - w'' \frac{t_4}{2}) + r_3 t_3 (u' - \bar{\beta}' \frac{t_3}{2})$$

$$- \frac{r_3 t_3^2}{6} \bar{\beta}']\delta\bar{\beta}'\, dx$$

$$+ \int_o^L [r_1 t_1 (u' + \bar{\alpha}' t_2 + w'' \frac{t_1}{2}) + \frac{r_1 t_1^2}{6} w'' + \frac{r_4 t_4^2}{6} w''$$

$$- r_4 t_4 (u' - \bar{\beta}' t_3 - w'' \frac{t_4}{2})]\delta w''$$

Expressions for δV and δT are similar to those in Appendix 3.

Eliminating derivatives of δw, $\delta\bar{\alpha}$ etc. in expression for δu, by integration by parts and applying Hamilton's

Principle, equations of motion and terminal point conditions are obtained. Equations of motion are written as eqns. (V.1) to (V.4).

The terminal point conditions are:

i) $$\left\{\begin{matrix} 2r_1(u'+\bar{\alpha}'t_2+w''\frac{t_1}{2})+2r_4(u'-\bar{\beta}'t_3-w''\frac{t_4}{2} \\ +2r_3(u'-\bar{\beta}'\frac{t_3}{2}) \end{matrix}\right\} \quad \delta u \Big|_o^L = 0$$

ii) $$\{u'+\bar{\alpha}'t_2+w''\frac{t_1}{2}\}\ \delta\bar{\alpha}\Big|_o^L = 0$$

iii) $$\{2r_4t_3(u'-\bar{\beta}'t_3-w''\frac{t_4}{2})+r_3t_3(u'-\bar{\beta}'\frac{t_3}{2})-\frac{r_3t_3^2}{6}\bar{\beta}'\}\delta\bar{\beta}\Big|_o^L = 0$$

iv) $$\left\{\begin{matrix} r_1t_1(u'+\bar{\alpha}'t_2+w''\frac{t_1}{2})+\frac{r_1t_1^2}{6}w''+\frac{r_4t_4^2}{6}w'' \\ -r_4t_4(u'-\bar{\beta}'t_3-w''\frac{t_4}{2}) \end{matrix}\right\} \delta w' \Big|_o^L = 0$$

v) $$\Big[-2q_2(\bar{\alpha}-w')-2q_3(\bar{\beta}-w')-r_1t_1(u''+\bar{\alpha}''t_2+w'''\frac{t_1}{2})$$
$$\frac{r_1t_1^2}{6}w'''-\frac{r_4t_4^2}{6}w'''+r_4t_4(u''-\bar{\beta}''t_3-w'''\frac{t_4}{2})\,\delta w\Big]\Big|_o^L = 0$$

For simply supported end, the boundary conditions are seen to be: $w=w''=\bar{\alpha}'=\bar{\beta}'=u'=0$

For fixed end, $w=w'=\bar{\alpha}-\bar{\beta}=u=0$

For free end, $w''=\bar{\alpha}'=\bar{\beta}'=u'=0$

and expression enclosed in parenthesis { } in (v) in above = 0.

APPENDIX 6: Shear Coefficient 'k_3' in 4 layered configuration

In the derivation given in section V.A.1 for 4 layered case, both shear and extensional effects of layer 3 are included. This makes the shear coefficient 'k_3' for that layer, to have a value different from unity. Its expression may be derived in a manner similar to that for 3 layered case, given in section II.D.3. Fig.V-1(a) gives a sketch of the 4 layered configuration, with z_o and z_3 as the dummy coordinates in layer 3. The shear stress τ_{zx} at any distance say 'z_3' from the interface of layers 2 and 3, is got by equilibrium of forces in 'x' direction for an element of length dx, comprising layer 4 and part of layer 3 of thickness (t_3-z_3).

$$\tau_{zx}\, b\,dx = bE_4t_4\left[u''-\bar{\beta}''t_3-w'''\frac{t_4}{2}\right]dx + bE_3\,dx\int_{z_3}^{t_3}(u''-z_o\bar{\beta}'')\,dz_o$$

$$\tau_{zx} = E_4t_4\left[u''-\bar{\beta}''t_3-w'''\frac{t_4}{2}\right] + E_3\left[u''(t_3-z_3)-\frac{\bar{\beta}''}{2}(t_3^2-z_3^2)\right]$$

Taking shear force due to layer '3' as

$$Q_3 = b\int_o^{t_3}\tau_{zx}\,dz_3$$

$$\text{and}\quad k_3 = \frac{Q_3}{bt_3(\tau_{zx})\text{ at middle of layer 3}}$$

we get

$$k_3 = \frac{E_4\left[t_4 t_3 (u''-\bar{\beta}''t_3-w'''\frac{t_4}{2})\right]+E_3\left[u''\frac{t_3^2}{2}-\frac{\bar{\beta}''}{3}t_3^3\right]}{E_4\left[t_4 t_3 (u''-\bar{\beta}''t_3-w'''\frac{t_4}{2})\right]+E_3\left[\left[u''\frac{t_3^2}{2}\right]-\frac{3}{8}\bar{\beta}''t_3^3\right]}$$

The solution given by eqn. (V.6) may be substituted in above. The value of k_3 in any given situation may be determined by initially taking it equal to unity and then determining the solution from Chapter V. This may be substituted in the above expression for k_3. This new value may be used again and the procedure repeated till two consecutive values of k_3 obtained, are nearly same.

For a given 4 layered sandwich, the following values of k_3 were obtained. These are nearly equal to unity except when layer 3 is thick and rigid.

Parameters used:

$E_1 = 10^7$ lb/in^2 , $G_2 = 100$ lb/in^2

$E_4 = 3 \times 10^7$ lb/in^2 , $E_3 = 3G_3$

$t_1 = 0.0625"$, $t_4 = 0.125"$

$\frac{m\pi}{L} = 0.05$ per in.

G_3/G_2	t_3/t_2	'k_3'
1	1	1
	4	1
	10	0.99999
10	1	1.000001
	4	1.000016
	10	1.00015
100	1	1.00001
	4	1.000238
	10	1.0433
1000	1	1.0001
	4	1.00255
	10	0.9052

APPENDIX 7 Details of derivation in V.B.1

In this, the details of derivation of equations of motion and boundary conditions for 5 layered, multi-cored case analysed in section V.B.1, will be given.

δU is got from eqn. (V.12), for small displacement as

$$- \int_o^L 2q_3(\bar{\beta} - w')\, \delta\bar{\beta}\, dx + \int_o^L 2q_2(\bar{\alpha} - w')\, \delta\bar{\alpha}\, dx$$

$$+ \int_o^L 2r_1 t_2 \left(\bar{\beta}' \frac{t_3}{2} + \bar{\alpha}' t_2 + w'' \frac{t_1}{2}\right) \delta\bar{\alpha}'\, dx$$

$$+ \int_o^L r_1 t_3 \left(\bar{\beta}' \frac{t_3}{2} + \bar{\alpha}' t_2 + w'' \frac{t_1}{2}\right) \delta\bar{\beta}'\, dx$$

$$- \int_o^L \{2q_3(\bar{\beta} - w') + 2q_2(\bar{\alpha} - w')\}\, \delta w'\, dx$$

$$+ \int_o^L \left\{r_1 t_1 \left(\bar{\beta}' \frac{t_3}{2} + \bar{\alpha}' t_2 + w'' \frac{t_1}{2}\right) + \frac{r_1 t_1^2}{6} w''\right\} \delta w''$$

Expressions for δT and δV are same as in Appendix 3. Eliminating derivatives of $\delta w, \delta\bar{\alpha}$ etc. in above expression, by integrating by parts and applying Hamilton's principle,

$$\int_{t_1}^{t_2} (\delta T - \delta U - \delta V)\, dt = 0 \ ,$$

Equations of motion are obtained and are given as equations V.16 to V.18.

The terminal point conditions are obtained as:

i) $$2r_1 t_2 \left\{\bar{\beta}' \frac{t_3}{2} + \bar{\alpha}' t_2 + w'' \frac{t_1}{2}\right\} \delta\bar{\alpha} \Big|_o^L = 0$$

ii) $$r_1 \int \{\bar{\beta}'\frac{t_3}{2} + \bar{\alpha}' t_2 + w''\frac{t_1}{2}\}\,\delta\bar{\beta}\Big|_o^L = 0$$

iii) $$\{r_1 t_1(\bar{\beta}'\frac{t_3}{2} + \bar{\alpha}' t_2 + w''\frac{t_1}{2}) + \frac{r_1 t_1^2}{6} w''\}\,\delta w'\Big|_o^L = 0$$

iv) $$\{-2q_2(\bar{\alpha} - w') - 2q_3(\bar{\beta} - w') - r_1 t_1(\bar{\beta}''\frac{t_3}{2} + \bar{\alpha}'' t_2 + w'''\frac{t_1}{2}) - \frac{r_1 t_1^2}{6} w'''\}\,\delta w\Big|_o^L = 0$$

From above, the boundary conditions for various types of end conditions are:

For simply supported: $w = \bar{\alpha}' = \bar{\beta}' = w'' = 0$

For fixed end: $w = w' = \bar{\alpha} = \bar{\beta} = 0$

For free end: $\bar{\alpha}' = \bar{\beta}' = w'' = 0$

and expression enclosed in $\{\}$ in (iv) above = 0.

Appendix 8 Dynamic shear properties of a few varieties of Butakon.

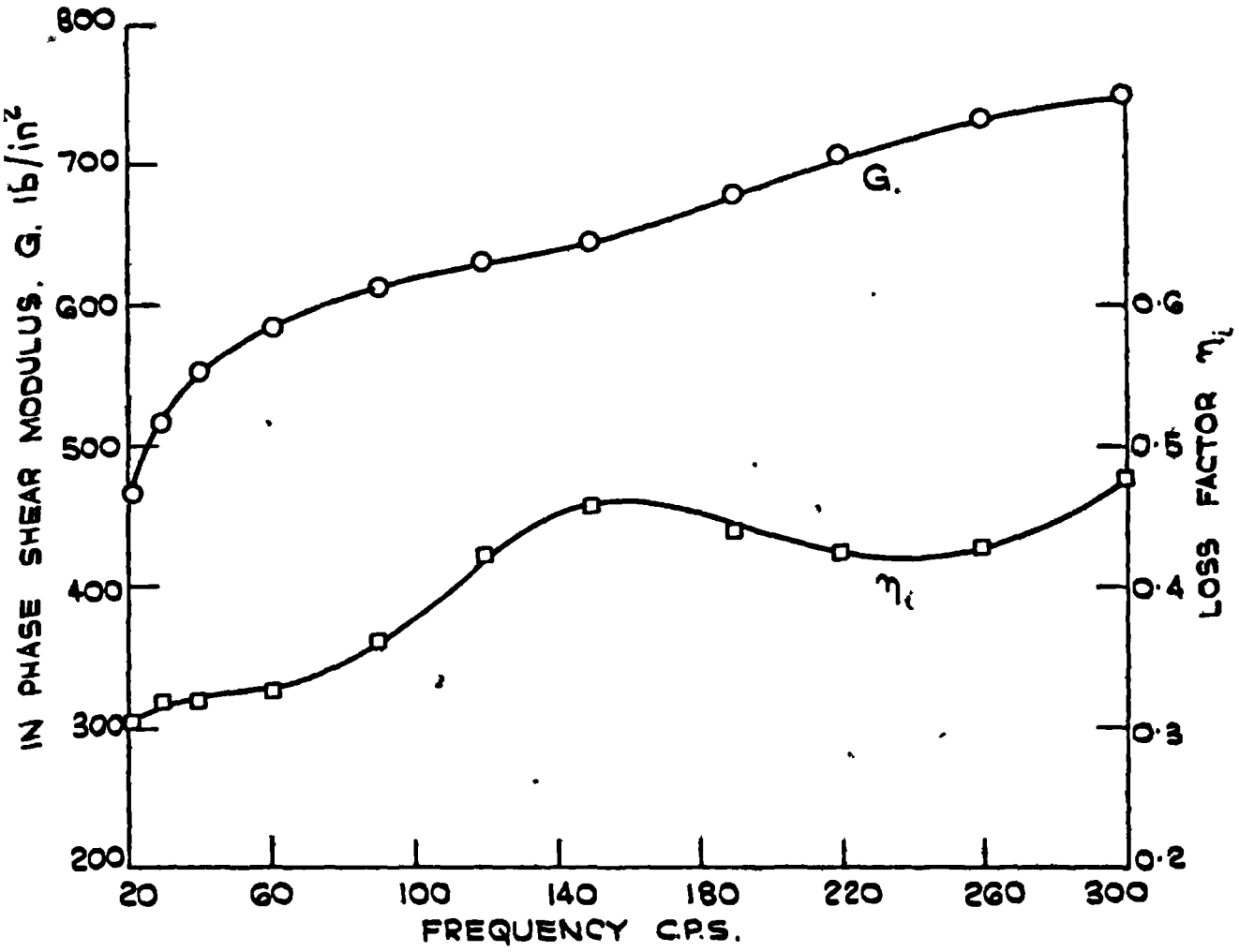

BUTAKON. 80/20

(COPOLYMER/PVC.)

TEMPERATURE :- 21·8 °C.

SHEAR STRAIN AMPLITUDE :- 6·6 x 10^{-3}

SPECIMEN 1" x 0·508"

0·107" THK.

FIG. AP8-1

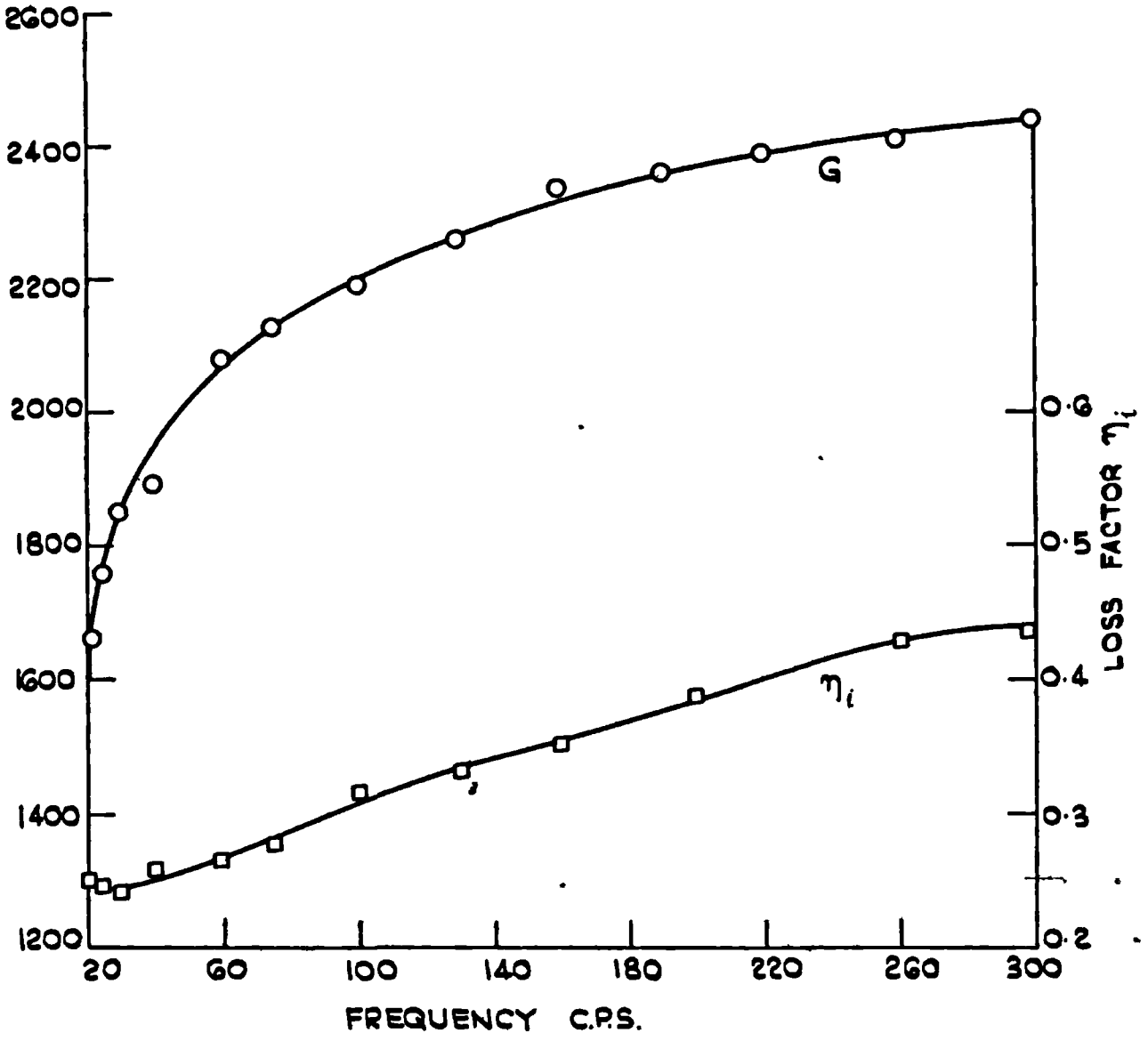

BUTAKON 60/40

(COPOLYMER / PVC BLEND.)

TEMPERATURE :- 21·0°C.

SHEAR STRAIN AMPLITUDE :- $3{\cdot}1 \times 10^{-3}$

SPECIMEN 1·07" x 0·505"

0·109" THK.

FIG. AP8-2

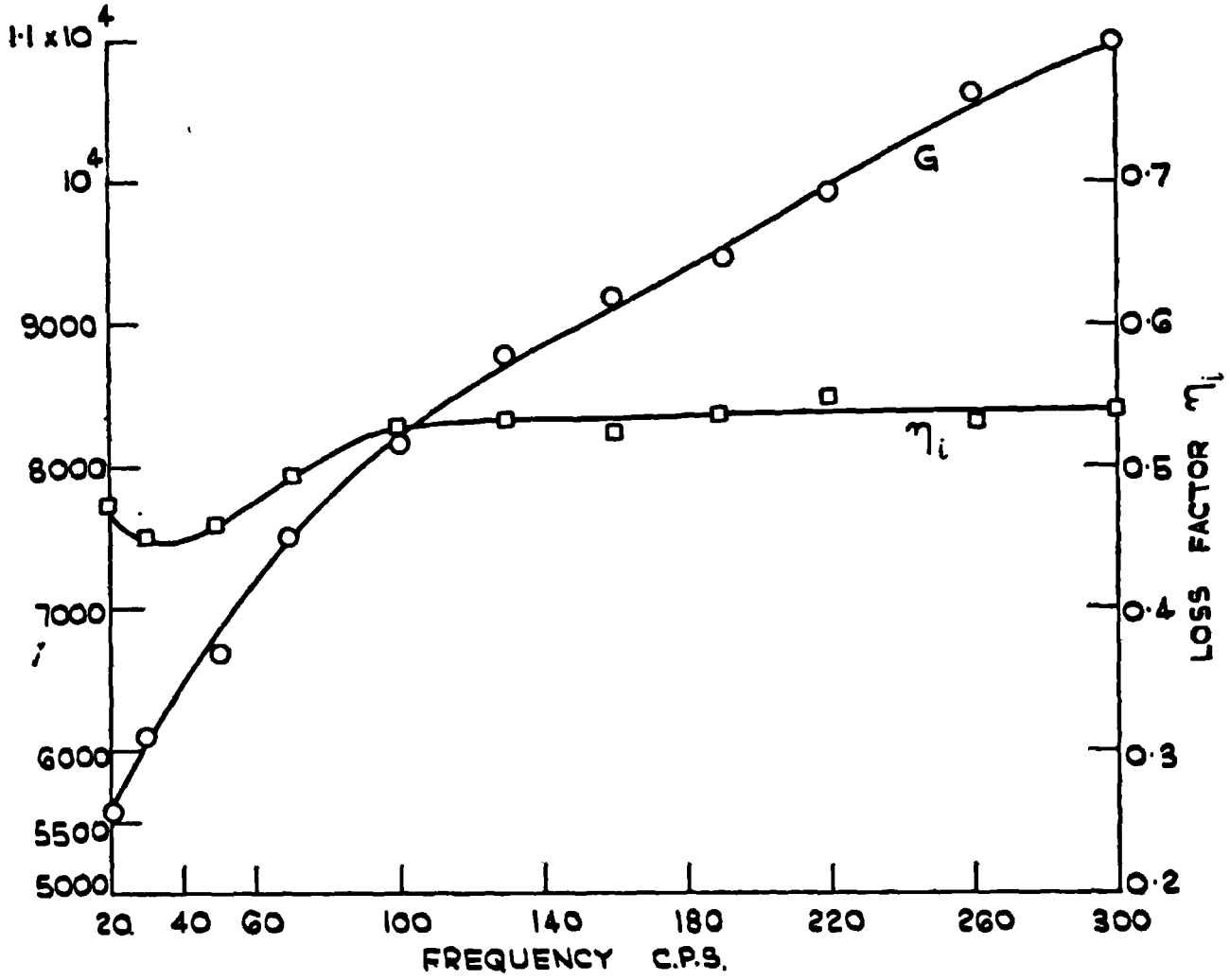

BUTAKON 40/60
(COPOLYMER / PVC BLEND)

SAMPLE : 1

TEMPERATURE :- 25·0 °C.

SHEAR STRAIN AMPLITUDE :- $2{\cdot}28 \times 10^{-3}$

SPECIMEN :- 0·57" x ·487"
0·108" THK.

FIG. AP 8-3

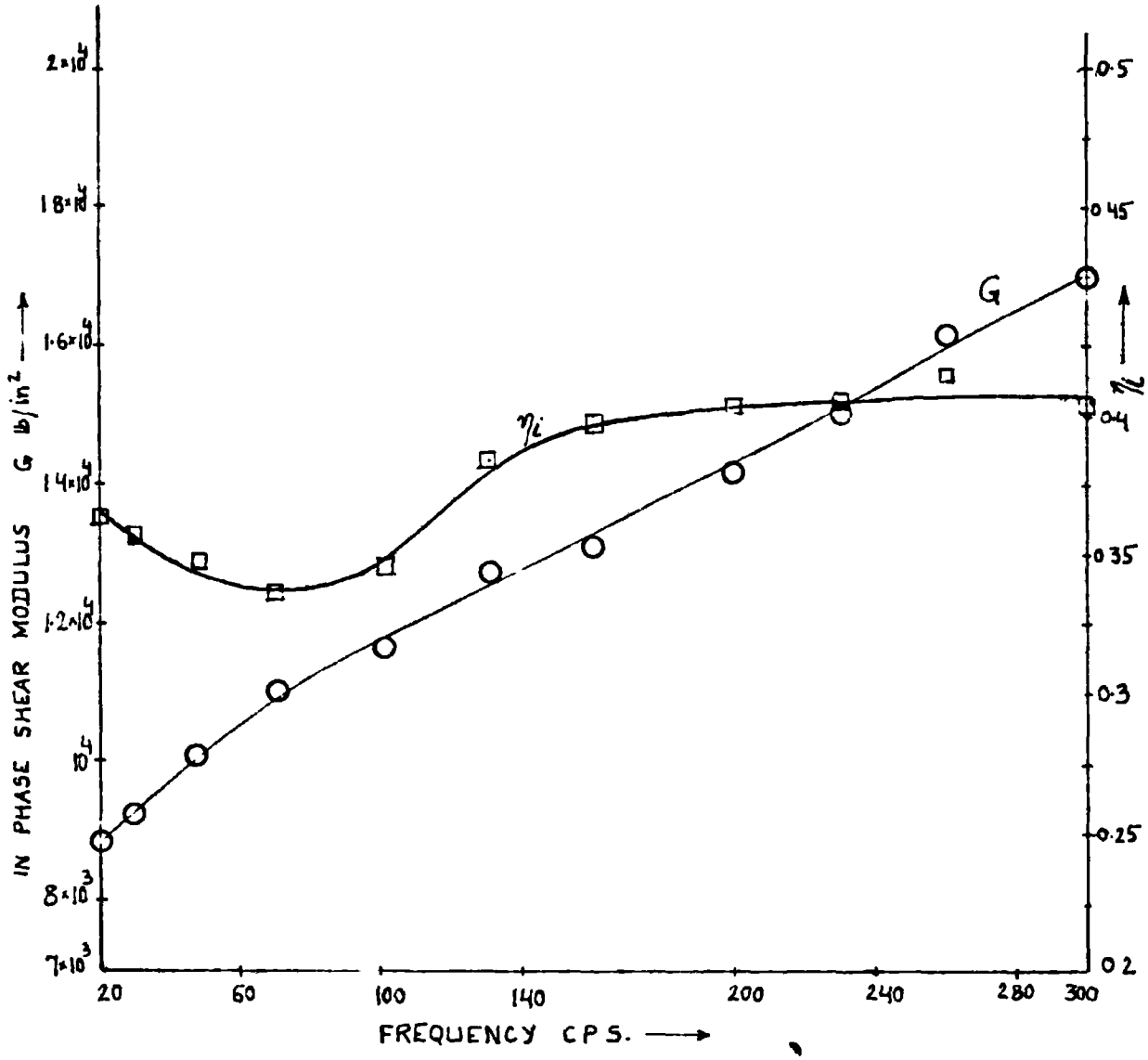

BUTAKON 40/60 (COPOLYMER/PVC)

SAMPLE : 2

TEMPERATURE : 23·5°C

SHEAR STRAIN AMPLITUDE . 2.47×10^{-3}

SPECIMEN 0·496" × 0·412"
0·081" THICK

FIG. AP8-4

APPENDIX 9

Table T-16

Experimental testing details

Specimen	"x_o"x10^3 in. Beam end displacement amplitude		Average Temperature ^oC		Remarks
	First Resonance	Second Resonance	First Resonance	Second Resonance	
S_1	2.4	0.634	22.3	21.7	Specimens S_1 to S_5 and M_1, M_2 were tested using the 50 lb thrust exciter, while specimens D_1 and D_2 were tested on the 250 lb thrust exciter.
S_2	1.488	0.718	21.1	22.9	
S_3	1.94	0.661	21.0	21.0	
S_4	0.57	0.485	21.9	21.8	
S_5	1.21	0.52	20.9	20.8	
M_1	2.77	0.547	20.8	21.6	
M_2	2.79	0.557	20.5	21.8	
D_1	1.701	2.05	23.6	25.1	
D_2	0.45	1.498	23.8	25.3	

APPENDIX 10: Polar plots for specimen S_5

Polar plots will be drawn for two resonances (corresponding to n=1 and 3) for the experimental results of vibration response, obtained for specimen S_5.

An examination of eqn. (III.22) indicates that the expression for contribution of nth term in the series to T_R/p^2 resembles that of a single degree freedom system, the polar plot of which is a circle. The value of the system loss factor may be determined using eqn. III.23. As explained in [95 and 96], the polar plots for a continuous system may also be expected to be a circle near any resonance, if near the resonant frequency, the contribution of off resonant modes is negligible or effectively constant. For specimen S_5, the values of T^A and its phase angle have been determined experimentally from which value of T^R and corresponding phase were calculated by subtracting x_o (equal to unity) vectorially. The values of T_R/p^2 and corresponding phase angle have been plotted here.

In Fig. AP.10-a, the values corresponding to n=1 (i.e. first resonance) have been plotted and a circle is made to pass through the experimental points. A reasonably accurate value for system loss factor η_s is obtained, when compared with the theoretical value. However, for the plot of Fig. AP.10-2, which corresponds

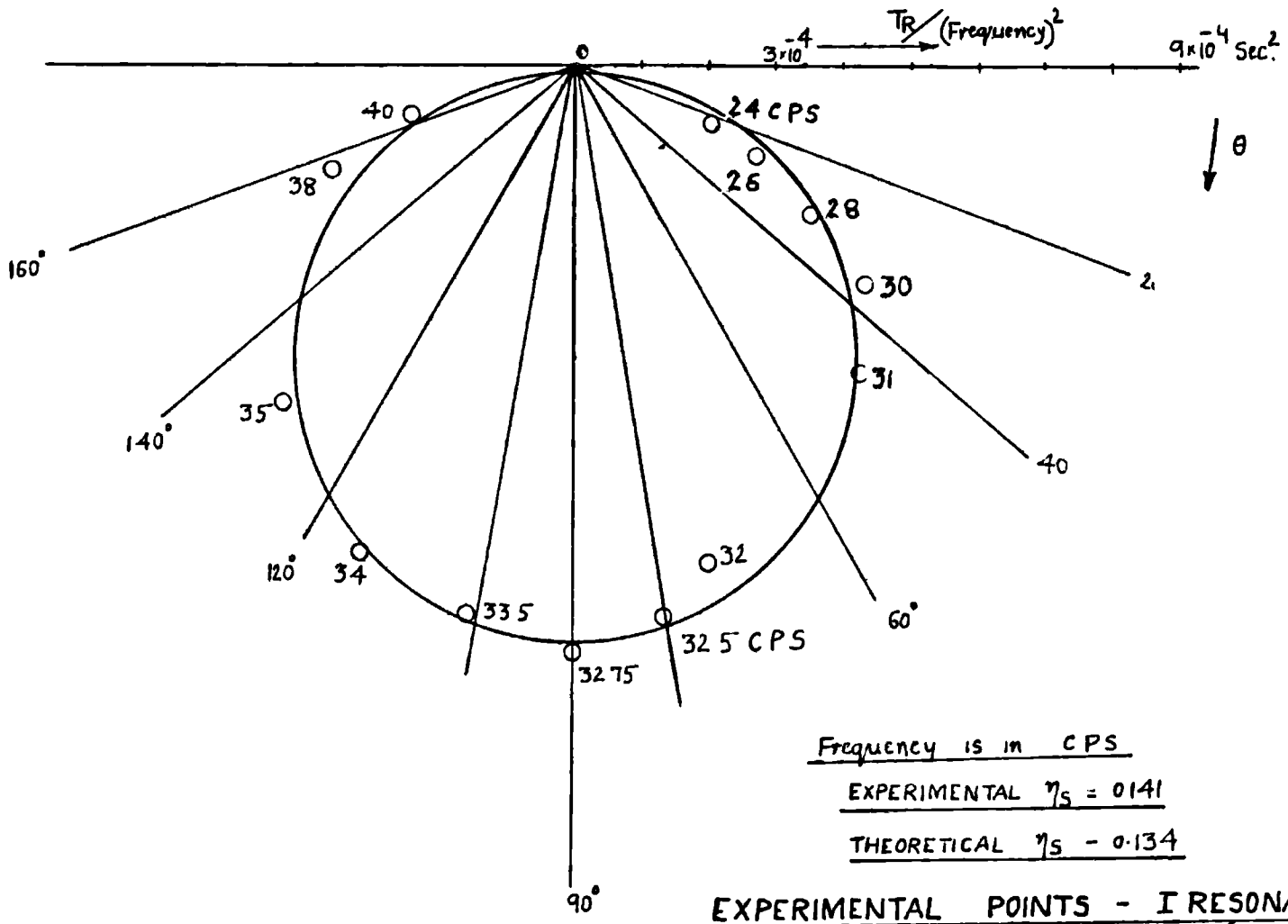

Frequency is in CPS

EXPERIMENTAL η_S = 0141

THEORETICAL η_S - 0·134

EXPERIMENTAL POINTS - I RESONANCE (n=1)

FIG. AP10-1

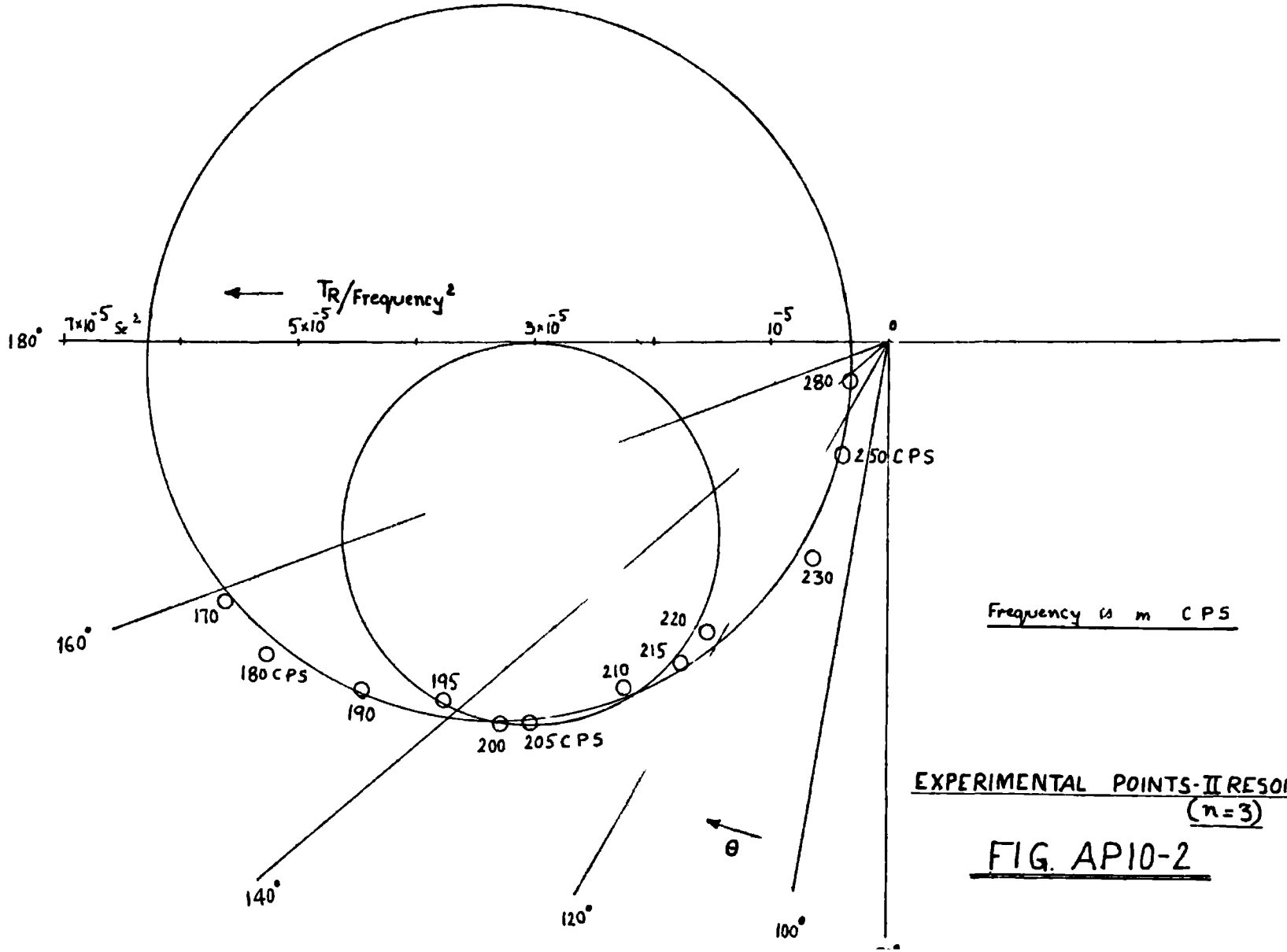

Frequency in m CPS

EXPERIMENTAL POINTS-II RESONANC (n=3)

FIG. AP10-2

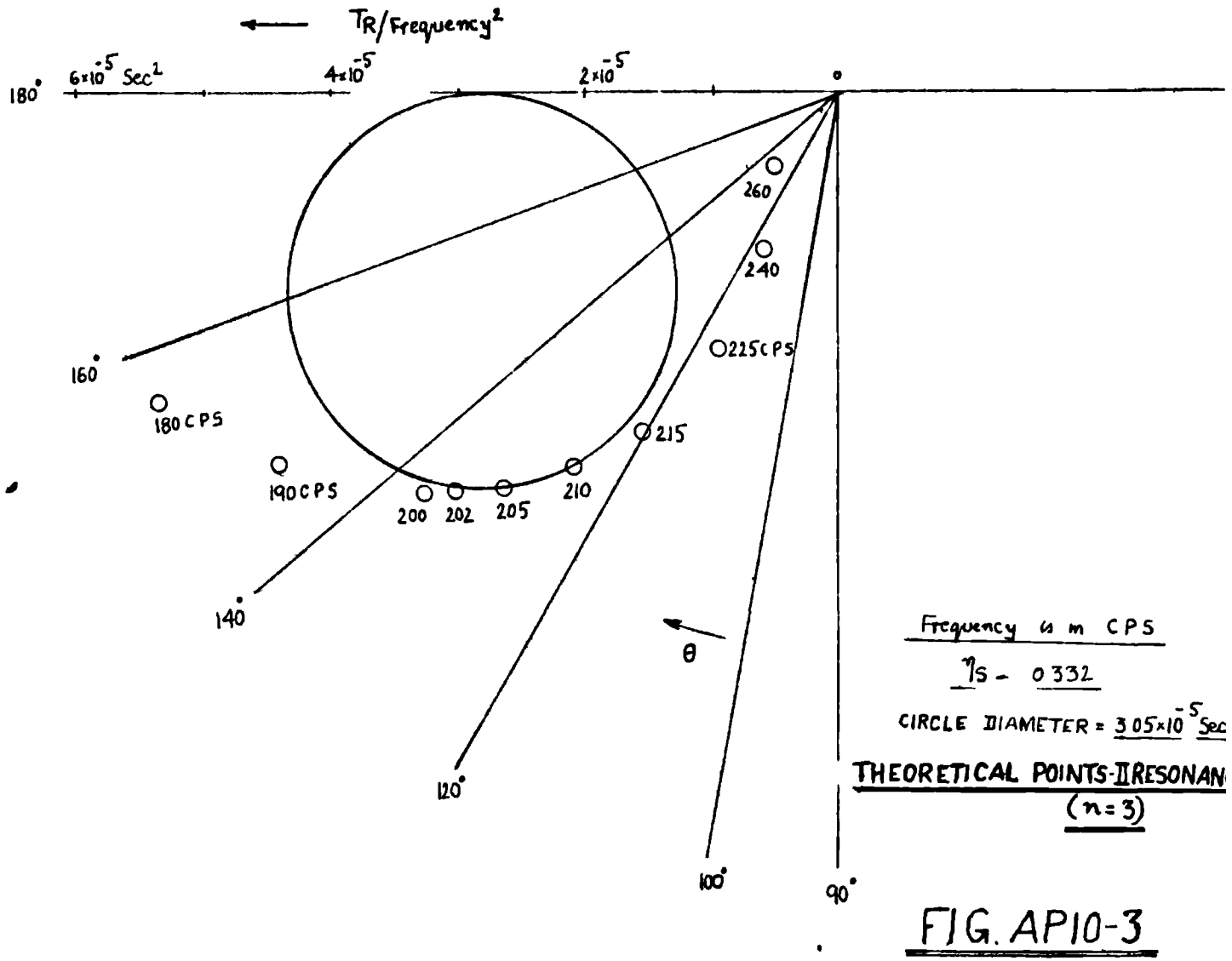

Frequency is m CPS

η_S - 0.332

CIRCLE DIAMETER = 3.05×10^{-5} Sec

THEORETICAL POINTS-II RESONANCE
(n = 3)

FIG. AP10-3

to the second resonance, it is found difficult to determine in advance about the best circle to pass through the experimental points in order to obtain η_s corresponding to n=3. Two of the possible circles are shown in the Fig. A check is made by using the reverse procedure. In Fig. AP.10-3, the corresponding theoretical points for the specimen for higher resonance, have been plotted. From the theoretical value of 'η_s' corresponding to n=3, the diameter of the circle is determined and the circle is made to pass through the theoretical points. It is seen that the points somewhat away from the resonant frequency do not lie on the circle and it would have been difficult to foresee such a circle from the points plotted. This may be due to the fact that the system is highly damped and the excitation employed involves very high contribution of off resonant modes near this resonance, and this contribution varies considerably at frequencies on either side of the resonant frequency. Also, the variation in viscoelastic material properties with frequency would distort the circular plot expected. Thus the limitation of the use of polar plots for higher modes becomes apparent in the case analysed.